Novel Modulators of Rho Transcriptional Signaling in Cancer

by

Jessica L. Bell

A dissertation submitted in partial fulfillment
of the requirements for the degree of
Doctor of Philosophy
(Medicinal Chemistry)
in the University of Michigan
2012

Research Professor Scott D. Larsen, Co-Chair
Professor Richard R. Neubig, Co-Chair
Associate Professor George A. Garcia
Associate Professor Jason E. Gestwicki
Assistant Professor Matthew B. Soellner

To my mom, whose hard work, dedication, and unwavering love and support have helped make me the woman I am today.

Acknowledgements

First and foremost, I want to thank my husband and best friend Matt Bell. I could not have done this without all of your love and encouragement. I'm eternally grateful and so lucky to have you in my life. I can't wait to see what the future holds for us both.

Thank you to my parents Michelle McDonald and Jack Miklovich and my step-parents Wayne McDonald and Sherry Miklovich for their love, support, and encouragement. To my sisters Katie and Kim, I love you, and I hope that I've been a good role model for you both. To my stepsisters Carmin, Jake, and Michelle and their families, thanks for all of the crazy times. To Ken and Michele Bell and my Bell siblings Nick, Michelle, Liz, Brandon, Katie, and Luke and to the extended Bell family, thank you for welcoming me into your family and loving me like I was your own.

A big thanks to all of my Med Chem friends, but especially to my friend Elizabeth Girnys. I would never have been able to survive grad school without you. Thank you for being such a caring and giving person and for teaching me how to become a more generous person. I'll miss all of our outings, especially the happy hours!

To my lab mates Bryan Yestrepsky and Scott Barraza—thanks for all of the silly videos, drawings, and for all the laughs. To my lab and cubby mate Janice Sindac, thanks for the coffee breaks, lunches, pie breaks, encouragement, and of course all of our "conspiracies." Also, a big thank you to Michael Wilson for his patience, chemistry knowledge, and mentorship, and to Jenny Ryu who synthesized the initial compounds for our project and trained me when I first entered the lab.

I would also like to acknowledge members of the Neubig lab—former member Dr. Chris Evelyn and current member Susan Wade for testing all of my compounds. Thank you to Andrew Haak for all your tireless hard work and excitement for the project. A huge thank you to Martha Larsen in the Center for Chemical Genomics and to Paul Kirchhoff for performing our high-throughput screens and triages. A major thanks to all of the labs that borrowed me chemicals and allowed me to use their equipment, especially

the Mosberg lab. Thank you for allowing me to use the LC/MS, and thanks to Elizabeth Girnys for repeatedly assisting me with it, even when you probably had other things to do. Thank you to the Showalter lab for your constant supply of chemicals, advice, and feedback.

Finally, I would like to acknowledge my committee members, Drs. Richard Neubig, George Garcia, Jason Gestwicki, Matthew Soellner, and especially my advisor Scott Larsen. Thank you for agreeing to serve on my committee and for your invaluable advice and feedback. Finally, I would like to extend a world of thanks to Dr. Larsen, who was always willing to share his enthusiasm for drug discovery and his vast chemistry knowledge. Thank you for being a great mentor.

Table of Contents

List of Figures

List of Tables

List of Schemes

List of Equations

Chapter 1
Introduction

G Protein-Coupled Receptors (GPCRs)

The G Protein-Coupled-Receptors comprise a superfamily of integral membrane proteins of which there are more than 1,000 known.[1] GPCRs are essential components of cellular communication, conveying extracellular messages through interaction with cytokines, hormones, odorants, peptides, small molecules, and neurotransmitters just to name a few.[1, 2] Their multitude and diversity make them highly-desirable targets for the pharmaceutical industry, capturing almost 50% of the current therapeutics market.[3, 4] However, despite their diversity, all GPCRs are composed of seven transmembrane helices that contain an extracellular N-terminal tail and an intracellular C-terminal tail and are connected by three extracellular and three intracellular loops. The GPCRs are coupled to a heterotrimeric intracellular G protein composed of α, β, and γ subunits. Following receptor activation, guanosine diphosphate (GDP) of the inactive G-protein is exchanged for guanosine triphosphate (GTP), thus activating the G protein. After exchange, the α, and βγ subunits dissociate and interact with their downstream effectors, producing a myriad of signaling events resulting in physiological processes such as inflammatory response, cellular differentiation, and neurotransmission.[5]

The downstream effectors activated by a GPCR are dependent on the heterotrimeric G protein it is coupled to. The large variety of α, β, and γ subunits provide a multitude of possibilities, often leading to a simplified categorization based on the type of Gα subunit it couples to.[3] The G proteins include four subfamilies: $G\alpha_s$, $G\alpha_i$, $G\alpha_q$, and $G\alpha_{12/13}$[6] that are classified based on the signaling pathway controlling second messenger production and gene expression they activate (or inactivate). $G\alpha_s$ and $G\alpha_i$ affect adenylyl cyclase (AC) production, which in turn affects cyclic adenosine 3′,5′-monophosphate (cAMP) levels. $G\alpha_s$ stimulates AC production and which increases cAMP levels, whereas $G\alpha_i$ inhibits AC production, thus decreasing cAMP. Stimulation and inhibition of AC

regulates Ca^{2+} and K^+ ion channels. $G\alpha_q$ activation results in the stimulation of phospholipase Cβ (PLCβ), an enzyme that cleaves phosphatidylinositol 4,5-bisphosphate (PIP_2) to afford messengers inositol 1,4,5-triphospate (IP_3) and diacylglycerol (DAG). Lastly, the $G\alpha_{12}$ protein family, which includes $G\alpha_{12}$ and $G\alpha_{13}$, regulate the small GTPase RhoA subfamily[7], which includes RhoA, B, and C, and is the focus of the work contained in this dissertation.

At least 25 receptors have been implicated in coupling with the $G\alpha_{12}$ family, either with $G\alpha_{12}$, $G\alpha_{13}$, or both. These receptors have also been found to couple with other G proteins such as $G\alpha_i$ and $G\alpha_q$.[8] This finding, in conjunction with their ubiquity in almost all tissues, allows the receptors to regulate multiple biological processes such as cellular growth, proliferation, cell-cell adhesion, apoptosis, migration, and invasion, just to name a few.[6]

GPCRs and Cancer

As G protein Coupled Receptors exert control over a variety of cellular processes, especially those related to growth, proliferation, migration, invasion, and apoptosis, several have been shown to play a significant role in cancer and metastasis. One such example is the protease-activated receptors (PARs), which are activated by thrombin.[4] Even-Ram, *et al.* demonstrated that highly invasive breast cancer carcinoma cell lines MDA-435 and MDA 231 correlated with the level of overexpression of thrombin receptor, a member of the PAR family.[9] A study by Chay, *et al.* confirmed that both VCaP, a bone-derived prostate cancer cell line, as well as PC-3 prostate cancer cells, maintain increased expression of PAR1.[10] Additionally, studies have demonstrated that increased expression of PAR1 is found in aggressive and metastatic prostate cancers, potentially leading to resistance to apoptotic signals, stimulation of angiogenic factors, and promotion of invasion. Thrombin has also been shown to promote this invasion in a Rho-dependent fashion.[11]

A second GPCR family that has been linked to cancer progression is bombesin, which includes receptor types BB_1, BB_2, and BB_3. Findings by Cuttitta, *et al.* show that human small-cell lung cancer (SCLC) produces bombesin-like proteins (BLP) that can function as autocrine growth factors for SCLC tumors.[12] Corral and colleagues observed that bombesin stimulation of poorly aggressive colon carcinoma (Caco-2) cells leads to

swift induction of Cox-2 as well as enhancement of the invasiveness of Caco-2 cells.[13] Bombesin has also been shown to enhance migration and invasion of prostate cancer cells in a RhoA-dependent fashion.[14] Finally, while bombesin has been shown to be a growth factor for tumors, it has also been shown to promote angiogenesis in SK-N-SH neuroblastoma cells[15] in addition to metastatic prostate cancer.[16]

A third GPCR family with a well-established role in cancer is the lysophosphatidic acid (LPA) receptors, which include LPA_1, LPA_2, and LPA_3. It has been determined that LPA takes on many roles in ovarian cancer, including enhancement of the migration of SK-OV3 cells[17] and as a major tumor-promoting factor in ovarian cancer.[4, 18] Recent evidence using human MDA-B02 breast carcinoma cells points to the role of LPA in promoting the secretion of cytokines and growth factors, leading to the establishment and progression of bone metastases.[19] Finally, LPA has also been observed to enhance the migration of Caov-3[20] and invasiveness of PC-3 prostate cancer cells[21] using a RhoA-dependent mechanism.

Rho GTPases

The Rho family of GTPases is a subset of the Ras superfamily and is comprised of more than 20 signaling proteins.[22-24] Of these greater than 20 proteins, the most thoroughly investigated members are RhoA (consisting of isoforms RhoA, RhoB, and RhoC), Cdc42, and Rac.[25] Rho GTPases are ubiquitously expressed and are responsible for the dynamic rearrangement of the actin cytoskeleton. Such rearrangement is necessary for biological processes including cell motility, migration, proliferation, etc. RhoA, Cdc42, and Rac form stress fibers; filopodia; and lamellipodia in addition to membrane ruffling, respectively[22, 26], which are crucial for these processes.

Rho GTPases function as molecular switches for signal transduction that originate extracellularly through the activation of many processes, including activation of GPCR by ligands such as LPA[26], thrombin[4], and bombesin.[12, 15] Their activation is tightly controlled using spatio-temporal regulation.[27] These switches cycle between a guanosine diphosphate (GDP)-bound inactive state and a guanosine triphosphate (GTP)-bound active state.[28-31] The tight regulation is afforded through regulator proteins that include (1) guanine nucleotide exchange factors (GEFs); (2) GTPase activating proteins (GAPs)[24, 26, 32]; and (3) guanine nucleotide dissociation inhibitors (GDIs).[23, 25] A

schematic of the basic RhoGTPase cycle can be found in Figure 1.1.[33] RhoGEFs catalyze the exchange of GDP for GTP, therefore activating the cycle. GAPs enhance the hydrolysis of GTP to GDP, thereby accelerating inactivation and terminating the signaling pathway. GDIs sequester the GTPases in the cytoplasm to prevent their activation and plasma membrane association.

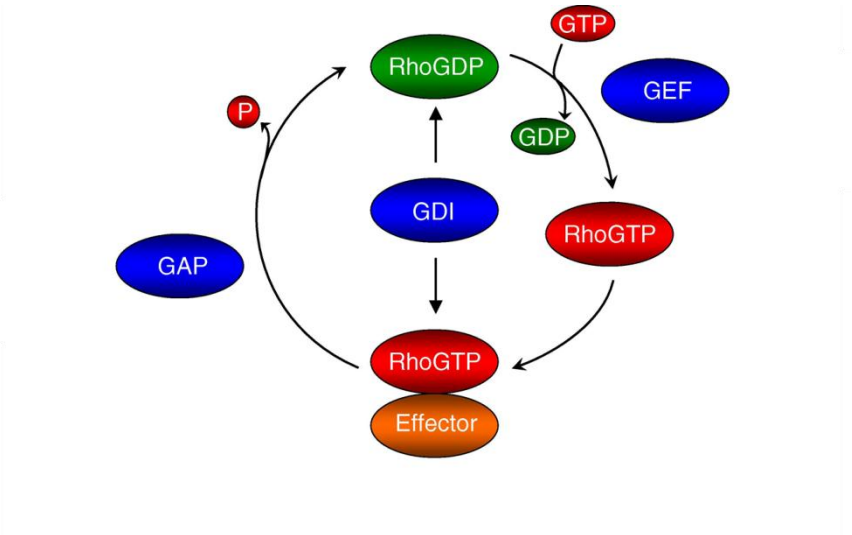

Figure 1.1. Basic Rho GTPase Cycle

Activation of the RhoGTPase cycle is dependent on RhoGEFs, and greater than 70 have been identified in humans.[34] A vast majority of the GEFs are composed of a Dbl homology (DH) domain and a plekstrin homology (PH) domain that catalyze GDP/GTP exchange and therefore activation. While PH domains boost the catalytic activity of the DH domains, additional evidence shows that the PH domain may facilitate localization of the DH domain to the plasma membrane.[35] Aside from the traditional DH and PH domains, GEFs that initiate RhoA activation through the $G\alpha_{12}$ coupled GPCRs also contain regulator of G protein signaling (RGS) domains, known as RGS homology (RH) domains. Four members comprise this family, including PDZ-RhoGEF, p115-RhoGEF, lymphoid blast crisis (Lbc)-RhoGEF, and leukemia-associated RhoGEF (LARG)[36, 37], which has been the primary focus of the work performed in the Neubig laboratory.[38]

RhoA Transcriptional Signaling Pathway

In addition to the well-documented effects on the actin cytoskeleton, RhoGTPases also activate signaling pathways that maintain transcriptional regulation.[25] Figure 1.2

shows a cartoon depiction of the RhoA-initiated MKL1/SRF transcriptional regulation pathway.[39] The pathway is initiated by the binding of a ligand to its respective GPCR, thus activating the $G\alpha_{12}$ family of proteins, which continue on to activate GEFs such as LARG. LARG catalyzes the exchange of GDP for GTP, thus activating Rho, which acts on downstream effectors such as Rho-kinase (ROCK) and mammalian homologue of the Drosophila gene *Diaphanous1* (mDia1).[40] These effectors contribute to the polymerization of monomeric, free G-actin into polymeric F-actin through inhibition of actin disassembly and catalysis of polymerization, respectively. The decrease in free G-actin due to polymerization releases transcriptional co-activator megakaryoblastic leukemia 1 (MKL1, MAL, MRTF-A), which translocates into the nucleus. In concert with serum response factor (SRF), MKL1 can induce serum response factor (SRF)-mediated gene transcription through interaction with the serum response element (SRE) promoter.

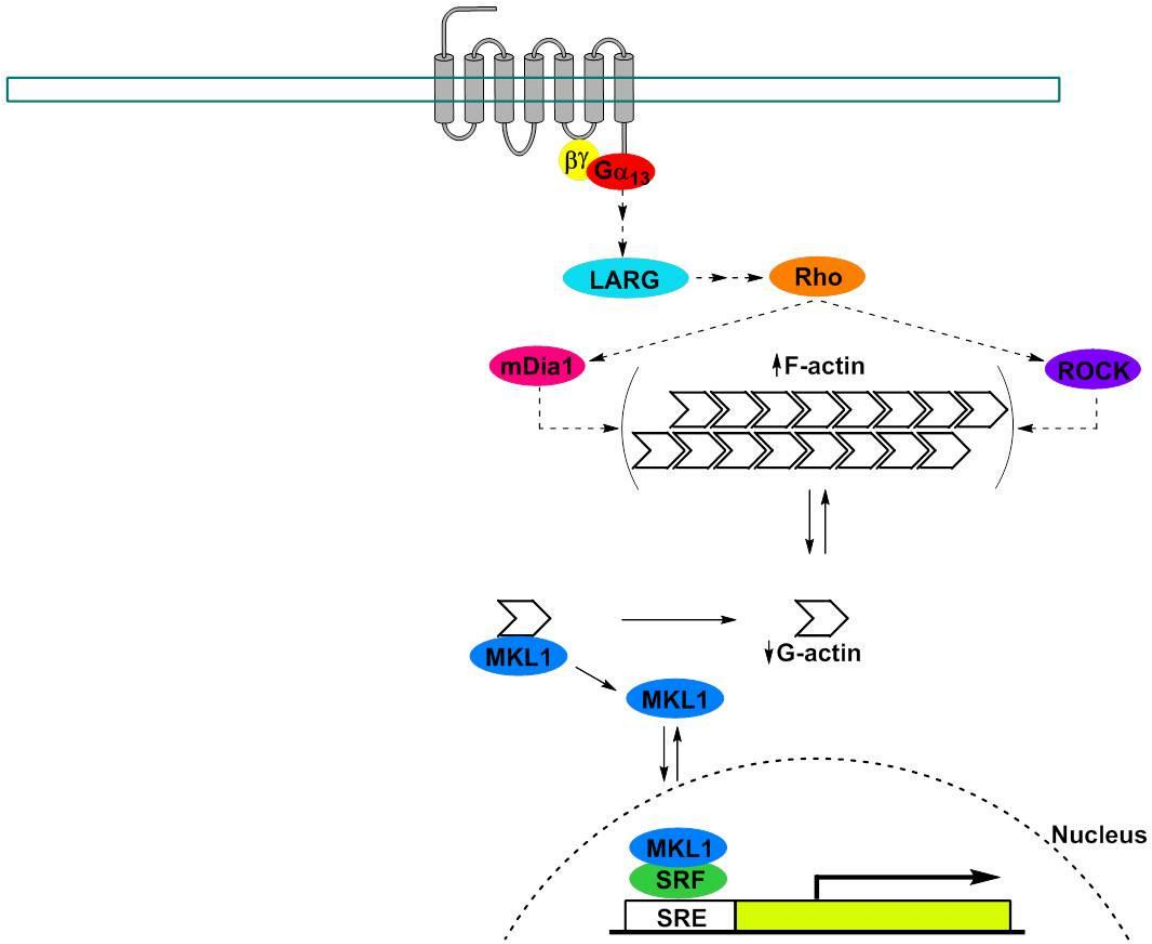

Figure 1.2. RhoA-initiated MKL1/SRF Transcriptional Regulation Pathway. Activation of the GPCR by its respective ligand activates RhoGEFs through the Gα12 family of proteins, which in turn activates Rho signaling. Rho activates Rho kinase (ROCK) and mDia1, which facilitate the polymerization of free monomeric G-actin into polymeric F-actin. This in turn releases transcriptional co-activator megakaryoblastic leukemia 1 (MKL1), which translocates into the nucleus to interact with serum response factor (SRF) to stimulate gene expression.

RhoA Transcriptional Signaling and Cancer

With the significant effects that members of the RhoA family exert on gene expression in addition to dynamic cytoskeletal functions, it is no surprise that they also play significant roles in cancer. No cancer-associated mutations have been observed in RhoA; however, aberrant regulation (generally through up-regulation/overexpression) contributes to cancer progression and metastasis.[41] Two well-characterized members of this family, Cdc42 and Rac, have been implicated in malignant transformation, tumor growth, migration, and invasion of breast[42], gastric[43], and testicular[44] cancers.

Members of the RhoA subgroup, including RhoA, RhoB, and RhoC, play significant roles in multiple cancers. RhoA and RhoC, which are the focus of this dissertation, contribute to the progression of a myriad of cancers. Unlike RhoA/C, RhoB is often down-regulated[41] and has been suggested to be a tumor suppressor in several cancers[45] and its overexpression can inhibit migration, invasion, and metastasis[45, 46]. RhoA and RhoC were once thought of as functionally identical, but evidence has pointed to distinct differences in cellular control[47] and effects on cellular morphology.[48] RhoA over-expression has been observed in a vast majority of cancers[49] and at almost every stage.[41] Contrarily, RhoC over-expression is observed in aggressive and metastatic tumors[49], such as prostate cancer, where it's necessary for invasion[50]; breast cancer, where it's required for metastasis[51]; pancreatic carcinoma cells, where it's needed to promote motility and invasion[47]; and in melanoma, where it's essential for metastasis.[52] It is obvious that RhoA and RhoC, are crucial for cancer progression, and are therefore highly desirable drug targets.

Rho-associated Kinase (ROCK)

Following activation, Rho GTPases have the ability to bind more than 60 proteins.[53] Rho-associated kinase (ROCK) is a well-documented effector of RhoA/C that enhances motility through formation of stress fibers and focal adhesions and stabilizes F-actin via inhibition of LIM-kinases that promote breakdown of actin filaments.[54] Due to ROCK's significant effects on motility and cytoskeletal functions, it has also been implicated in multiple malignancies, including invasion of rat ascites hepatoma (MM1)[55], high tumor grade in renal cell carcinoma[56], high tumor grade in testicular cancer[44], and invasion and metastasis of bladder cancer.[57] Despite their significant effects on the cytoskeleton and thus cancer, only one ROCK inhibitor (Fasudil, Figure 1.3)[58] has been clinically approved. Approval occurred in Japan in 1995; however, it has not been clinically approved for use in the United States.[59]

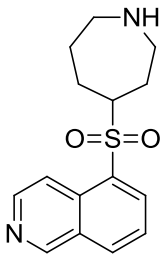

Figure 1.3. Chemical Structure of Fasudil

MKL1/SRF Transcriptional Regulation

While much has been documented regarding RhoGTPases and their effects on the actin cytoskeleton, the regulation of gene transcription via MKL1 and SRF, as well as their roles in cancer, are poorly understood. MKL1 is a co-activator of the transcription factor SRF, which in concert activates the serum response element (SRE) that modulates gene transcription of several genes necessary for cellular growth, migration, and differentiation.[60] Medjkane and colleagues demonstrated that signaling through MKL1/SRF was critical for invasion and metastasis in both breast cancer and melanoma.[61] A recent study by Muehlich, *et al*. found that MKL1/2 is necessary for cell motility upon the loss of tumor suppressor Deleted in Liver Cancer 1 (DLC1).[60]

Targeting the RhoA Transcriptional Signaling Pathway

Due to the lack of specific and direct inhibitors of Rho GTPases and the Rho pathway, the Neubig lab implemented a high-throughput screen to identify novel small molecule inhibitors of the RhoA signaling pathway. As described in Evelyn, *et al.*[62], human embryonic kidney (HEK)293 cells were transiently transfected with Rho-specific serum response element luciferase (SRE.L) and thymidine kinase (TK) *Renilla* luciferase reporter plasmids, and the dual-luciferase assay was used to identify two structurally similar compounds. The more potent compound, **1423** (Figure 1.4), was shown to block RhoA and RhoC-dependent gene transcription with an IC_{50} of ~1 μM (Figure 1.5). Additionally, **1423** was found to inhibit the proliferation of cancer cell lines showing increased RhoA/C expression, as well as inhibiting Matrigel matrix invasion by PC-3 (Table 2.7), a highly invasive human prostate cancer line. A xenograft study was also carried out using **1423** to inhibit the growth and/or metastasis of A375M2 melanoma

cells *in vivo*. While a reduction in tumor size was observed, the toxicity of the compound led to decreased survival in the mice (Wade and Neubig, unpublished).

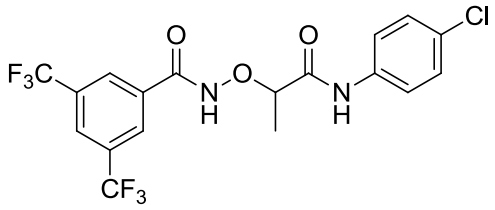

Figure 1.4. High-throughput Lead 1423

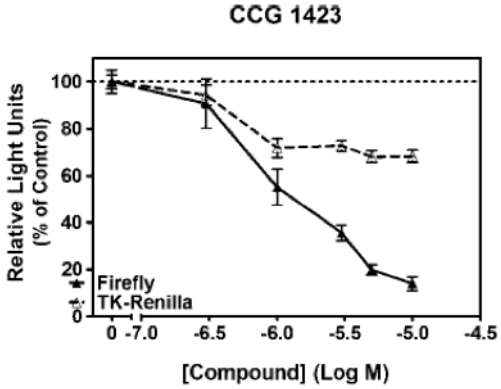

Figure 1.5. Inhibition of SRE-L (Firefly) and TK-*Renilla* Transcription Reporters by 1423

My Work

This leads me to the work presented here, which aims to synthesize and identify novel modulators of the RhoA transcriptional signaling pathway. These small molecules will serve as potential lead compounds for further development into anti-metastatic therapeutics, as well as to further probe the pathway to determine the macromolecular target(s) of our compounds. We undertook four general approaches toward the identification of such modulators that included: (1) traditional medicinal chemistry approaches to lead compound **1423**, including modifications to the linker and aromatic regions; (2) development of 2D and 3D pharmacophore models; (3) an expanded high-throughput screen to identify new leads; and (4) development of affinity reagents to identify the macromolecular target(s) in the signaling pathway. New compounds were evaluated using a cell-based Rho-specific SRE.L-luciferase reporter assay as previously described.[63]

Through modifications of lead **1423**, we were able to develop several analogs with low micromolar potencies and improved selectivity and toxicity profiles. Furthermore, we identified analog **203971**, a modestly active compound (IC_{50} of 6.7 μM, Table 3.2), that has nevertheless shown exciting results in PC-3 prostate cancer cells as well as several melanoma cell lines and has reduced acute toxicity relative to **1423**. Finally, through the use of an affinity reagent containing a benzophenone moiety, we were able to photolabel a 24kD protein of interest for further identification as a potential target within the signaling pathway. Identification of this protein would provide vital information that would allow us to prepare improved cancer therapies targeting the RhoA pathway.

Chapter 2
Linker Modifications

Although **1423** (Figure 1.4) is a potent inhibitor of SRE-Luciferase gene transcription, it exhibits modest acute cellular toxicity toward PC-3 prostate cancer cells at 24 h, as non-specific inhibition of gene expression (Thymidine kinase (TK)-*Renilla*) with a concomitant decrease in WST-1 cell viability were noted (data not shown). Therefore, we set out to improve the potency and/or selectivity of lead **1423** while mitigating its cytotoxicity through modifications of three structural features contained in the "tether" region between the two aromatic rings. First, the N-O bond between the two carboxamides can allow **1423** to non-selectively modify proteins that contain cysteine or to be cleaved by glutathione. Second, the two carboxamides can create a barrier to passive diffusion across the apical and basal membranes into the cell, thereby limiting potency.[64,65] Finally, the flexible acyclic tether region may not be optimal for potency and selectivity.[66] Furthermore, molecular rigidity has been correlated with increased oral availability.[67] Our initial structure-activity relationship (SAR) analysis focused on (1) removal of the N-O bond; (2) bioisosteric replacement of the carboxamides[68]; and (3) conformational restriction[66] of the tether region.

Preliminary Data

Jenny Ryu executed the synthesis of initial analogs exploring the composition and length of the tether region between the two aromatic rings. Scheme 2.1 depicts the synthetic route used and shows a general procedure for a variety of amino acids **1**. Initial acylation using 3,5-bis(trifluoromethyl)benzoyl chloride was performed under basic or anhydrous conditions to afford mono(amides) **2**. The carboxylic acids of **2** were coupled with 4-chloroaniline via *N*-(3-dimethlaminopropyl)-*N′*-ethylcarbodiimide hydrochloride (EDC) and 1-hydroxybenzotriazole (HOBt) mediated amidation to afford bis(amides) **3**.

Scheme 2.1. General Acylation and EDC/HOBt Amidation Conditions

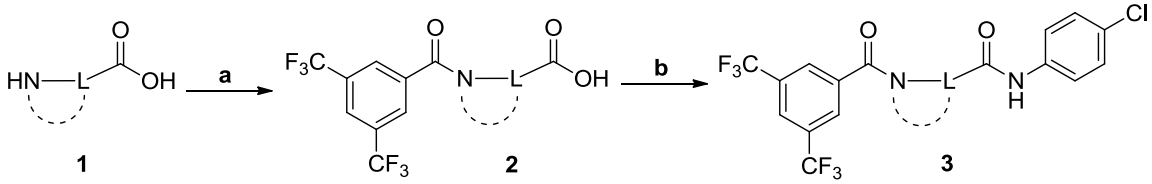

Reagents and conditions: (a) 3,5-bis(CF_3)PhCOCl, aq. NaOH; or 3,5-bis(CF_3)PhCOCl, TEA, DCM; (b) 4-ClPhNH_2, EDC, HOBt, DIPEA, THF

The effects of the synthesized analogs on Rho-mediated gene transcription, non-specific gene expression, and cytotoxicity were determined in transiently transfected PC-3 cells.[63] Data were collected for both potency and maximal efficacy, as it was observed that compounds could maintain equivalent potencies against SRE.L but differ in their maximal responses (efficacies) as shown in subsequent tables. This could be due to several reasons, including differences in maximum cellular permeability, degree of efflux from cells, or different profiles of Rho-pathway target(s) being affected. Because such effects contribute to *in vivo* activity, we considered both potency and efficacy when selecting lead compounds in our SAR analysis. The effects on TK-*Renilla* and WST-1 at 10 and 100 µM concentrations are included to illustrate selectivity and cytotoxicity. Analogs with low potency prevented IC_{50} values from being calculated and are therefore designated as >100 µM.

Table 2.1 summarizes the impact of modifications to the composition and linker length of the tether region between the aromatic rings, as synthesized by Jenny Ryu. For compounds in which IC_{50}s are greater than 100 µM and efficacy and cytotoxicity were calculated, dashes are used. For compounds in which data were not determined, ND is used. Our compounds typically show errors that fall between 1.5- to 2.0-fold the IC_{50}. Removing the methyl group (**100596**) causes only a small decrease in potency and selectivity. Replacing the oxygen with a carbon (**100594**) significantly diminishes cytotoxicity and increases selectivity, but also reduces efficacy and reduces potency 20-fold. Shortening or lengthening the carbon chain of the tether by one or two carbons (**100600** and **100597**, respectively) affects minor changes in activity and selectivity. However, extending to a four-carbon chain (**100686**) abolishes all activity.

Table 2.1. Effects of Tether Composition and Length on Transcription and Cytotoxicity in Transfected PC-3 Cells[a]

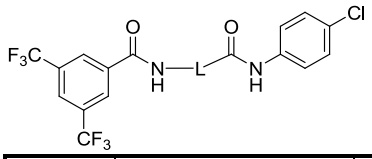

Cmpd No	L	IC_{50} SRE.L (μM)[b]	% inh SRE.L (10, 100 μM)[b]	% inh pRL-TK (10, 100 μM)[c]	% inh WST-1 (10, 100 μM)[d]
1423	-OCH(CH_3)-	1.5	74, ND[e]	48, ND[e]	44, ND[e]
100596	-OCH_2-	4.7	71, 100	53, 89	42, 91
100594	-CH_2CH_2-	38	38, 64	0, 22	0, 10
100600	-CH_2-	33	45, 85	15, 25	0, 30
100597	-$CH_2CH_2CH_2$-	21	37, 79	5, 42	0, 12
100686	-$CH_2CH_2CH_2CH_2$-	>100	0, 12	0, 10	0, 0

[a]For assay descriptions, refer to Ref [63]
[b]Inhibition of Rho-pathway selective serum response element-luciferase reporter
[c]Inhibition of control pRL-thymidine kinase *Renilla* luciferase reporter
[d]Inhibition of mitochondrial metabolism of WST-1
[e]Not determined

Bioisosteric Replacement of the Carboxamides

Due to its moderate decrease in potency and significant reduction in cytotoxicity, compound **100594** was utilized as a template for further exploration of the tether region. Analogs aimed at increasing permeability through the removal of hydrogen bond donors and acceptors using bioisosteric replacement of the carboxamide moieties can be found in Table 2.2. Scheme 2.2-Scheme 2.5 summarize the synthetic routes for bioisosteric replacement analogs.

Synthesis of *N*-methylanilide **101435** and benzylamide **203009** followed similar conditions as depicted in Scheme 2.1 using *N*-methyl-4-chloroaniline and 4-chlorobenzylamine, respectively, in the final amidation step. Preparation of thiazole **102445** and ether **102447** occurred by acylation of commercially available starting amines with 3,5-bis(trifluoromethyl)benzoyl chloride. Condensation of 3-bromopropylamine **4** with excess 4-chloroaniline[69] followed by simple acylation using 3,5-bis(trifluoromethyl)benzoyl chloride provided monoamine **101425** (Scheme 2.2). Construction of regioisomeric amine **102585** took place through acylation of 4-chloroaniline using 3-bromopropionyl chloride **6** to afford **7** which was further utilized in the alkylation of 3,5-bis(trifluoro)benzylamine (Scheme 2.3). Refluxing Borane-THF complex reduced **100594** to provide diamine analog **102532** (Table 2.2).

Scheme 2.2. Synthesis of Monoamine 101425

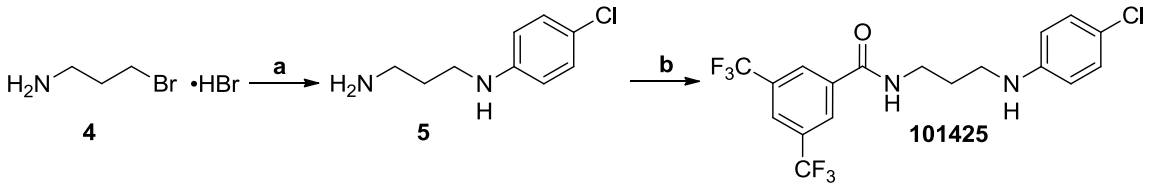

Reagents and conditions: (a) 4-ClPhNH$_2$, PhMe, reflux; (b) 3,5-bis(CF$_3$)PhCOOH, HOBt, EDC, DIPEA, THF

Scheme 2.3. Synthesis of Regioisomeric Monoamine 102585

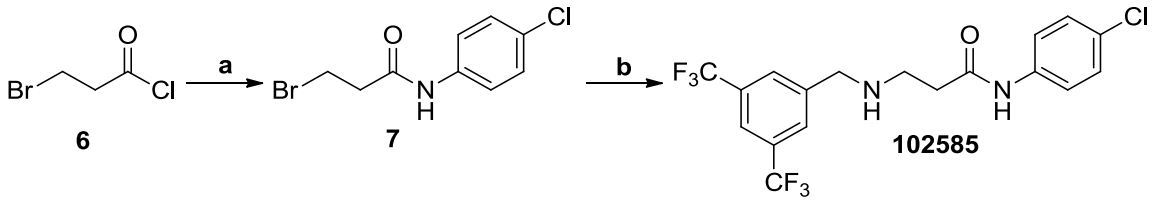

Reagents and conditions: (a) 4-ClPhNH$_2$, MeCN, reflux; (b) 3,5-bis(CF$_3$)PhCH$_2$NH$_2$, MeCN, reflux

Finally, we explored cyclic bioisosteres. Cycloaddition of the nitrile-oxide formed from oxime **9**[70] in combination with *N*-(4-chlorophenyl)but-3-enamide[71] afforded isoxazoline **203003** as shown in Scheme 2.4. We attempted further oxidation to the isoxazole using DDQ; (diacetoxy)iodobenzene[72]; manganese(IV) oxide[73]; nitrile oxide 1,3-dipolar cycloaddition[74]; and bromination/dehydrobromination[75]. However, the isoxazole could not be generated. Diazotization/azidation of 3,5-bis(trifluoromethyl)aniline (**14**) and 4-chloroaniline (**16**) followed by copper-catalyzed Click chemistry[76] with alkynes **11** and **13**, respectively, yielded triazoles **203011** and **203017** (Scheme 2.5).

Scheme 2.4. Synthesis of 203003

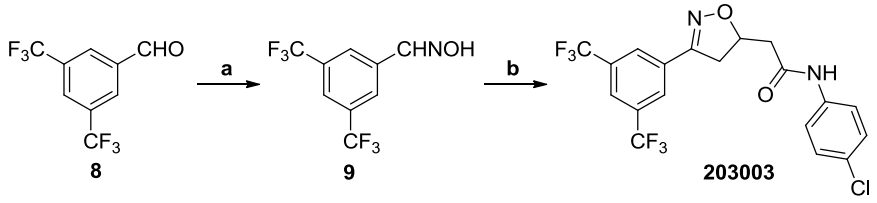

Reagents and conditions: (a) HONH$_2$•HCl, MeOH, reflux; (b) *N*-(4-chlorophenyl)but-3-enamide, NaOCl, DCM, 0°C to RT

Scheme 2.5. Synthesis of Triazoles 203001 and 203017

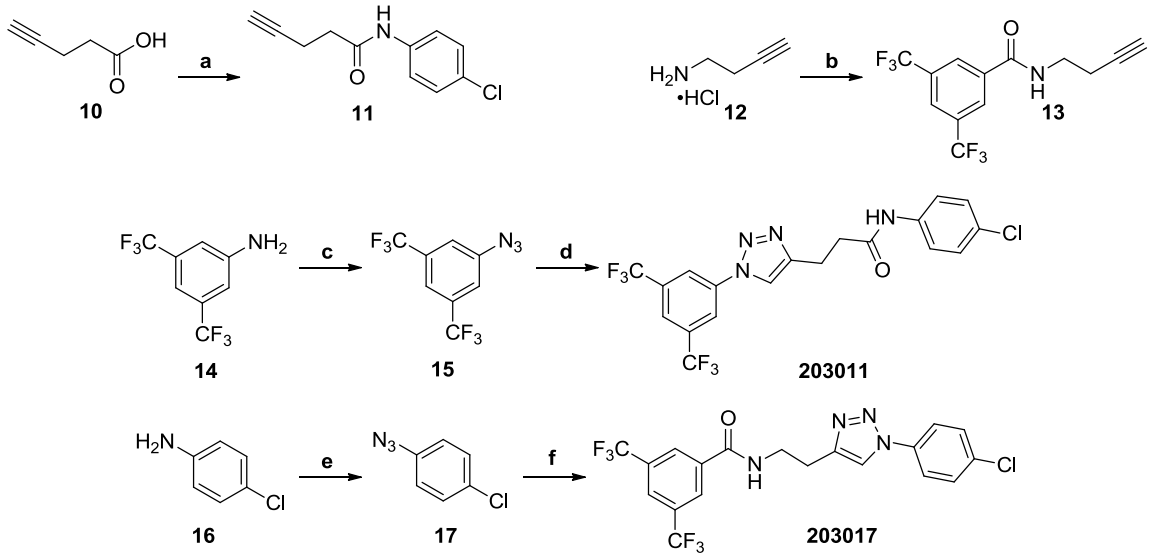

Reagents and conditions: (a) 4-ClPhNH$_2$, HOBt, EDC, DIPEA, THF, RT; (b) 3,5-bis(CF$_3$)COCl, TEA, DCM, RT; (c) i. TFA, -10 °C, NaNO$_2$; ii. NaN$_3$, -10 °C to RT; (d) **11**, CuSO$_4$•5H$_2$O, L-Ascorbic acid, H$_2$O/*t*-BuOH, 1:1, RT; (e) i. 6M HCl, 0 °C, NaNO$_2$; ii. NaN$_3$, 0 °C; (f) **13**, CuSO$_4$•5H$_2$O, L-Ascorbic acid, H$_2$O/*t*-BuOH, 1:1, RT

Table 2.2 summarizes bioisosteric modifications of the secondary amides. The simplest bioisosteric replacement of a secondary amide with a tertiary amide by *N*-methylation of the 4-chloroaniline (**101435**), resulted in a complete loss of activity. Similarly, replacement of one anilide with a benzyl amide (**203009**) was detrimental to activity. Reduction of one or both of the amide moieties significantly increased potency and efficacy against Rho-dependent gene transcription. *Analog **101425** exhibited potency similar to that of aminoxyacetic acid **100596** and maintained the modest selectivity and cytotoxicity of **100594**, which made it the most interesting analog of this series.* While monoamine **102585** and diamine **102532** exhibited increases in potencies, they maintained poor selectivity versus non-specific gene expression and introduced significant and undesirable cytotoxicity. Further exploration of monoamide replacement (**102445**, **102447**, and **203003**), while showing increases in potency in comparison with **100594**, reduced selectivity and/or increased cytotoxicity. Disappointingly, triazoles **203011** and **203017** were completely inactive, which may suggest poor permeability.

Table 2.2. Effects of Amide Bioisosteric Replacement on Transcription and Cytotoxicity in Transfected PC-3 Cells

Cmpd No	Structure	IC_{50} SRE.L (μM)[a]	% inh SRE.L (10, 100 μM)[a]	% inh pRL-TK (10, 100 μM)[a]	% inh WST-1 (10, 100 μM)[a]
100594[b]	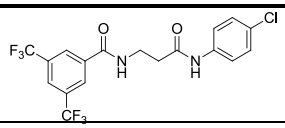	38	38, 64	0, 22	0, 10
101435[c]	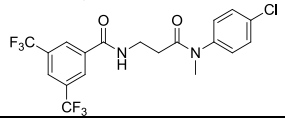	>100	-	-	-
203009	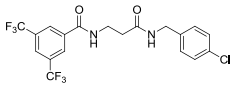	>100	-	-	-
101425	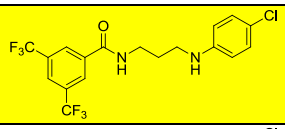	5.1	70, 80	37, 35	0, 11
102585	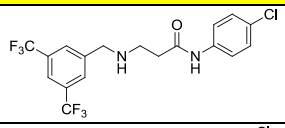	8.1	64, 100	13, 91	0, 92
102532	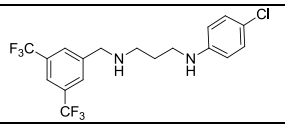	9.1	65, 100	6, 90	0, 89
102445	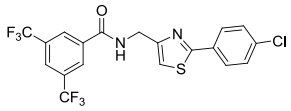	4.1	50, 45	39, 38	0, 0
102447	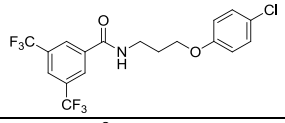	8.9	55, 86	28, 65	0, 38
203003	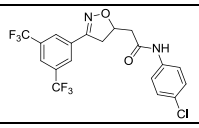	4.2	70, 84	51, 60	0, 38
203011	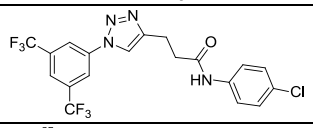	>100	-	-	-
203017	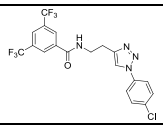	>100	-	-	-

[a]See Table 2.1for assay descriptions
[b]Synthesized by Nicole Harzdorf
[c]Synthesized by Kamali Sripathi

Conformational Restriction

Passive diffusion is one of the main contributions to oral bioavailability. A study by Veber *et al*. demonstrated that the number of rotatable bonds present in a molecule decreases passive diffusion, and therefore limits oral bioavailability.[67] We wanted to incorporate conformational restriction to increase passive permeability and thus oral bioavailability. Furthermore, we wanted to examine its effects on affinity and/or selectivity of restricted analogs. Binding affinity follows the Gibbs energy of binding,

Equation 2.1. Gibbs Energy of Binding

$$K_a = e^{-\Delta G/RT}$$

with ΔG being comprised of both enthalpic and entropic contributions. Variations of these enthalpic and entropic contributions can produce the same ΔG, consequently yielding the same binding affinity. While enthalpic optimization can lead to increased binding affinity and selectivity versus entropic optimization, it is often more difficult to achieve.[77] We chose to investigate conformational restriction as a means to maintain favorable solvation entropy while minimizing conformational degrees of freedom lost and hence conformational entropy loss upon binding. Increasing affinity could also result in an increase in selectivity of our analogs.

Again using **100594** as a template, we explored the multiple ways we could restrain the molecule in 5- or 6-membered rings, several of which can be found in Figure 2.1. The numbers within brackets refer to the atoms of **100594** that have been connected, and the constraining bonds are denoted with a dashed line.

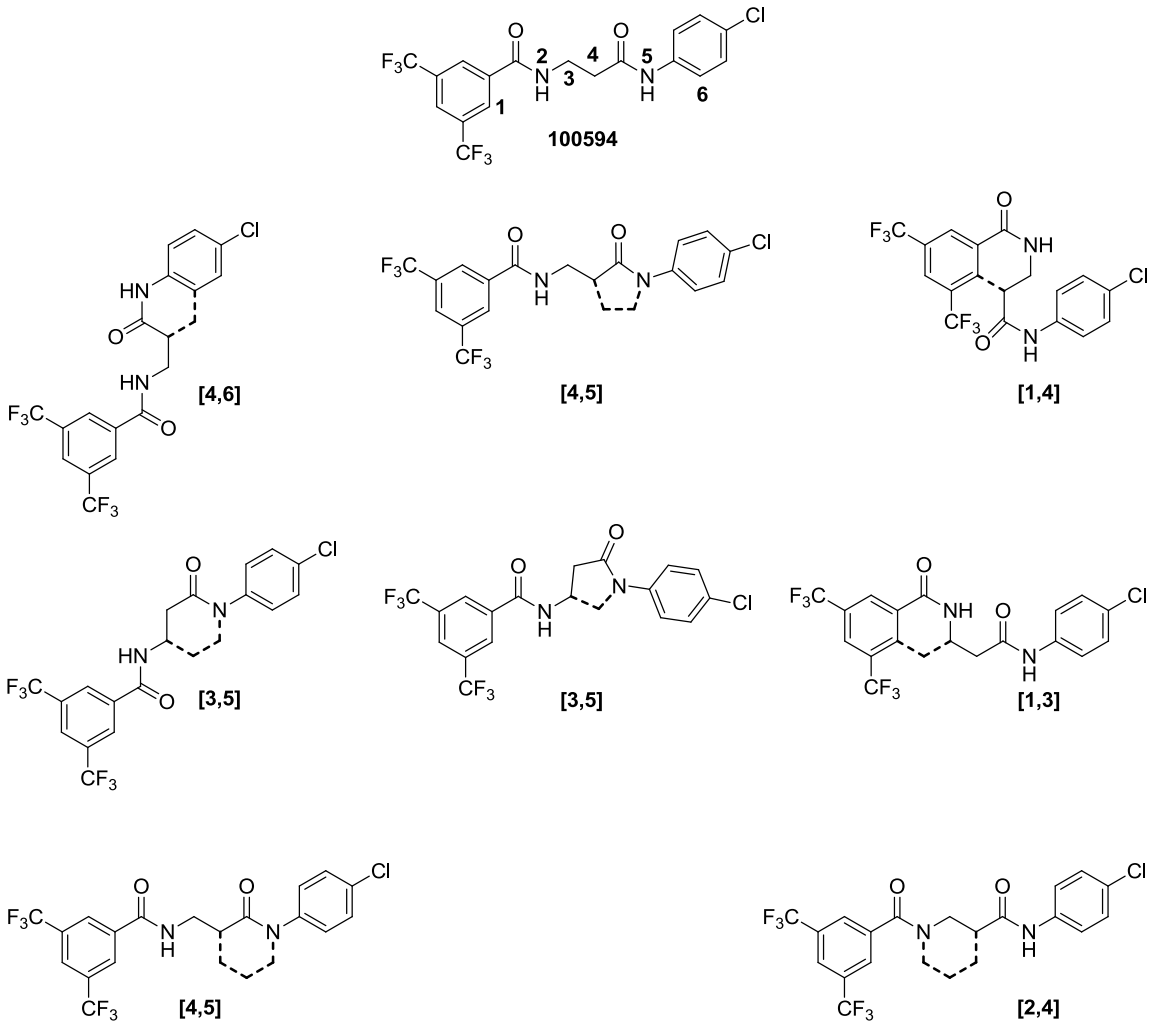

Figure 2.1. Examples of Conformationally Restricted Analogs of 100594

Preliminary Data

Jenny Ryu executed the initial chemistry, using the general synthetic route shown in Scheme 2.1, and the results are shown in Table 2.3. She prepared initial analog **100602**, which constrained **100594** in a 6-membered ring by connecting bonds 2 and 4. The compound exhibits improved potency and efficacy while maintaining similar cytotoxicity to that of **100594**. Compound **100690**, the isonipecotic isomer, shows similar potency and efficacy to nipecotic analog **100602**. However, it introduces moderate cytotoxicity, which is undesirable. Analog **100692** is a highly-constrained 5-membered ring with only one carbon between the two amides. This constraint proved to be detrimental to potency.

Table 2.3. Preliminary Data on Effects of Conformation Restriction on Transcription and Cytotoxicity in Transfected PC-3 Cells

Cmpd No	Structure	IC_{50} SRE.L (μM)[a]	% inh SRE.L (10, 100 μM)[a]	% inh pRL-TK (10, 100 μM)[a]	% inh WST-1 (10, 100 μM)[a]
100594[b]	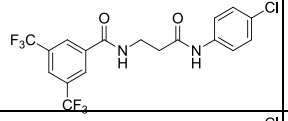	38	38, 64	0, 22	0, 10
100602[c]	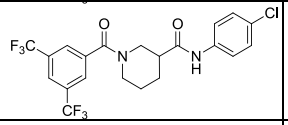	9.8	37, 78	20, 34	0, 14
100690[c]	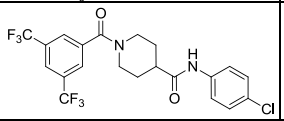	16	17, 87	0, 17	0, 39
100692[c]	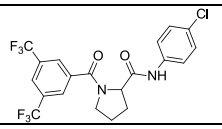	69	23, 83	12, 27	0, 22

[a]See Table 2.1for assay descriptions
[b]Synthesized by Nicole Harzdorf
[c]Synthesized by Jenny Ryu

We synthesized additional analogs to further examine conformational restriction with results shown in Table 2.4. First, we explored the tether region containing a benzene moiety with the 4-chloroanilide in a *para*- position (**101329**) compared to a *meta*- (**101343**) and *ortho*- position (**101433**). Scheme 2.1 depicts the chemistry employed. However, the preparation of **101433** did not yield the desired product directly (Scheme 2.6). Instead, intermediate **20** was isolated and was treated with 4-chloroaniline and DMAP to facilitate ring-opening/coupling to the desired analog.

Scheme 2.6. Synthesis of 101433

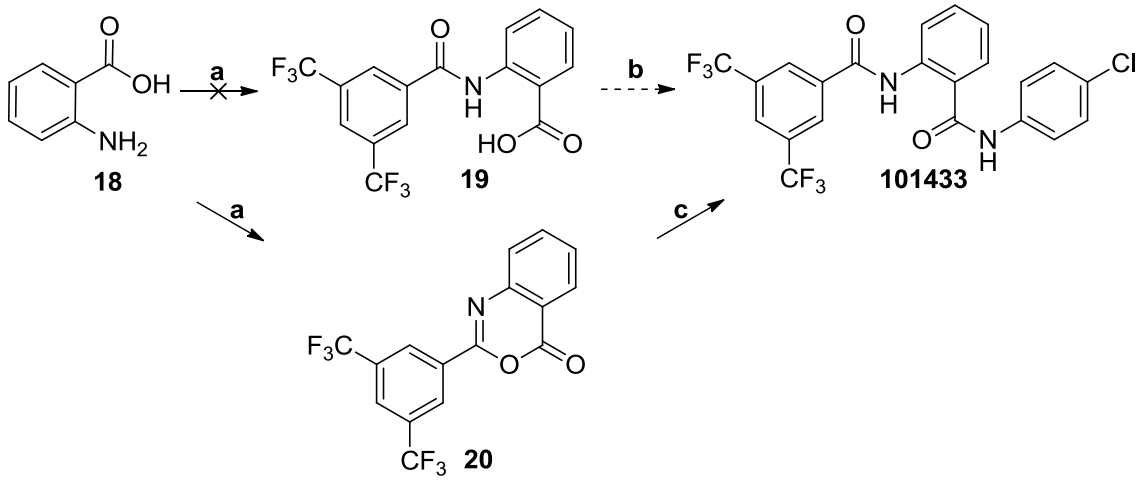

Reagents and conditions: (a) 3,5-bis(CF_3)PhCOCl, TEA, DCM; (b) EDC, HOBt, DIPEA, THF, RT; (c) 4-ClPhNH_2, DMAP, Pyr, 80 °C

We also synthesized compounds **102443**, **102526**, and **203001** (Table 2.4) utilizing the chemistry shown in Scheme 2.1. Assembly of conformationally restricted lactam **203005** required a multi-step synthesis as found in Scheme 2.7. Deprotection of commercially available *N*-(Boc)-4-piperidinone **21** followed by acylation with 3,5-bis(trifluoromethyl)benzoyl chloride afforded benzamide **22**. Generation of the oxime (**23**) followed by Beckmann rearrangement yielded the 7-membered diazepinone **24**.[78] *N*-arylation of the lactam using 4-iodochlorobenzene under Buchwald conditions afforded the ring-expanded final compound.[79,80]

Scheme 2.7. Synthesis of Ring-expanded 203005

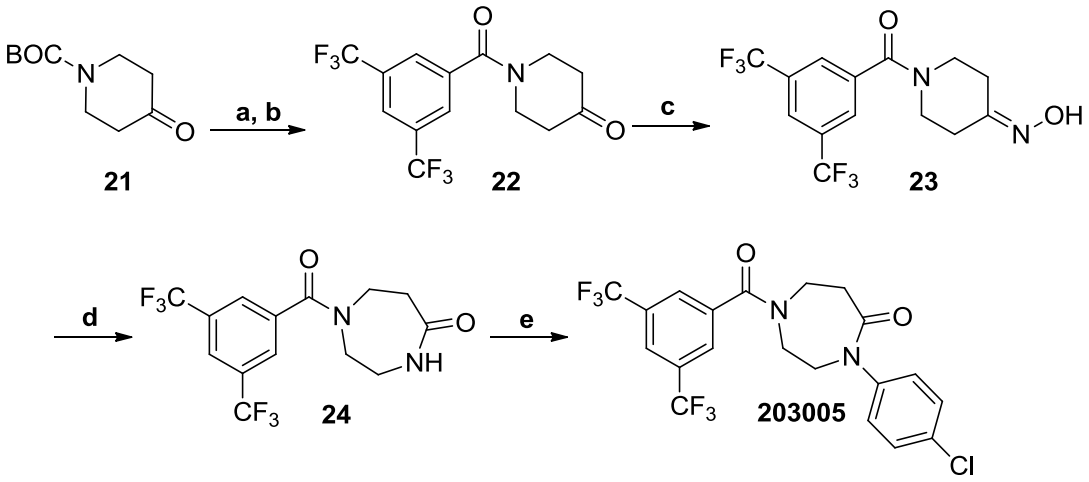

Reagents and conditions: (a) TFA, DCM, 0 °C to RT; (b) 3,5-bis(CF_3)PhCOCl, aq NaOH, RT; (c) NH_2OH•HCl, Pyr, 3Å sieves, RT; (d) Na_2CO_3, *p*-TsCl, Acetone, RT; (e) 4-IPhCl, $MeNHCH_2CH_2NHMe$, CuI, Cs_2CO_3, Dioxane, 100 °C

Table 2.4 summarizes the impact of conformational restriction of the tether region between the two carboxamides of **100594** as a way to improve potency and selectivity. We see an increase in potency upon comparison of cyclic **102443** with corresponding acyclic analog **101435** (Table 2.2) and cyclic compounds **203001** and **203015** compared with **100594**. Unfortunately, the restricted analogs did not offer any increase in selectivity over their acyclic counterparts. Analogs containing an aromatic ring in the linker with substituents in the *para*- and *ortho*- positions (**101329** and **101433**, respectively) were inactive. Interestingly, however, the *meta*- version (**101343**) was significantly more potent and efficacious than **100594**. Unfortunately, its cytotoxicity at 10 μM prevented further testing at higher concentrations.

Table 2.4. Effects of Conformational Restriction on Transcription and Cytotoxicity in Transfected PC-3 Cells

Cmpd No	Structure	IC_{50} SRE.L (μM)[a]	% inh SRE.L (10, 100 μM)[a]	% inh pRL-TK (10, 100 μM)[a]	% inh WST-1 (10, 100 μM)[a]
100594[b]	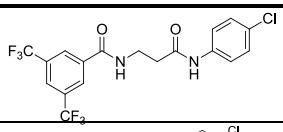	38	38, 64	0, 22	0, 10
101329	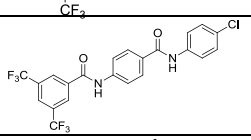	>100	-	-	-
101343	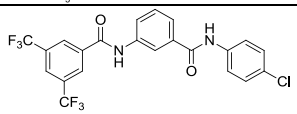	1.7	80, ND[c]	0, ND[c]	38, ND[c]
101433	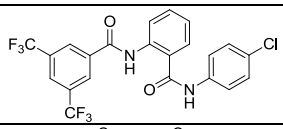	>100	34, ND[c]	0, ND[c]	0, ND[c]
102443	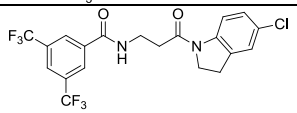	13	15, 40	0, 1	0, 0
102526	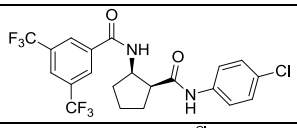	>100	-	-	-
203001	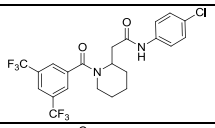	9.5	33, 86	0, 62	0, 14
203005	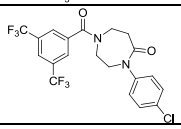	>100	-	-	-
203015	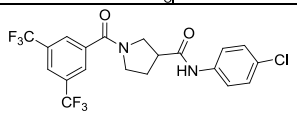	16	30, 100	8, 78	0, 67

[a]See Table 2.1 for assay descriptions
[b]Synthesized by Nicole Harzdorf
[c]Not determined

Stable Cell Line Development

The Neubig lab attempted to establish an optimized HEK293 cell line stably expressing the SRE and *Renilla* Luciferase reporter vectors. This line was intended to decrease labor-intensiveness and reduce cell assay variability. Unfortunately, incorporation of the *Renilla* Luciferase vector could not be achieved. However, several of the previously synthesized compounds were tested in the HEK293 cell line stably expressing SRE.Luc for comparison (Table 2.5). Several newly synthesized compounds were also tested in the stable line assay, as shown in Table 2.6. The IC_{50} values are also shown in the PC-3 prostate cancer cell line for comparison.

Table 2.5. Previously Synthesized Compounds Tested Using HEK293 SRE.L Stable Cell Line

Cmpd No	Structure	IC_{50} SRE.L (μM), PC-3[a]	IC_{50} SRE.L (μM)[a]	% inh SRE.L (10, 100 μM)[a]	% inh WST-1 (10, 100 μM)[a]
1423	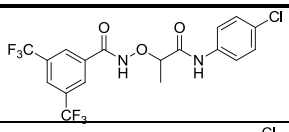	1.5	6.0	66, 98	56, 79
101425	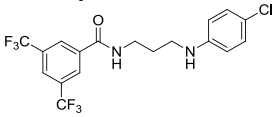	5.1	10	30, 73	22, 38
100692	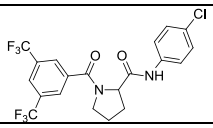	69	32	0, 74	0, 48
100602[b]	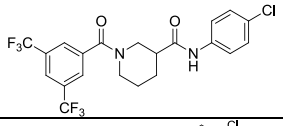	9.8	11	9, 55	5, 34
101329	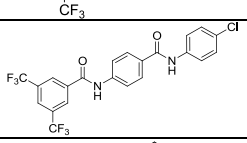	>100	>100	-	-
101343	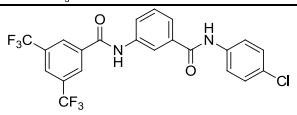	1.7	3.2	66, 84	57, 53
101433	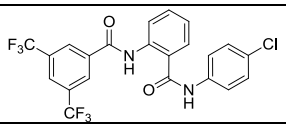	>100	95	0, 42	0, 36
102443	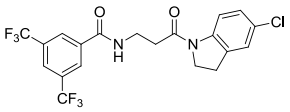	13	19	0, 13	0, 5
102526	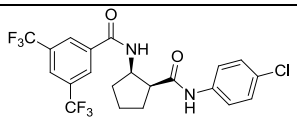	>100	>100	-	-
203001	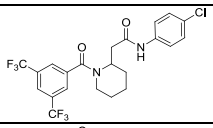	9.5	15	7, 65	0, 41
203005	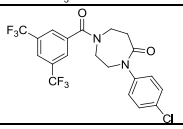	>100	30	0, 23	0, 6
203015	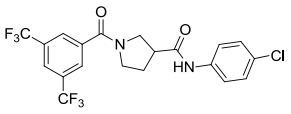	16	19	13, 96	0, 71

[a]See Table 2.1 for assay descriptions
[b]Synthesized by Jenny Ryu

The older analogs proved to have increased cytotoxicity in the HEK cell line when compared to previous testing in the transiently transfected PC-3 cell line. Potencies were similar in comparison, with the exceptions of **100692** and **203005**, which showed increased potency in the HEK line. Finally, efficacies were reduced in a majority of the compounds in the stable transfection. Analog **100602** demonstrated more comparable potency to **1423** in HEK cells than in the PC-3 cells with a modest decrease in efficacy and a significant reduction in cytotoxicity at both concentrations, further indicating its promise for optimization.

Exploration of additional conformationally restricted analogs continued with the synthesis of pyrrolidone analog **203606** and related compounds, shown in Scheme 2.8. Itaconic acid (**25**) was heated with 4-chloroaniline neat to afford intermediate acid **26**, which was treated with diphenylphosphoryl azide (DPPA) to induce Curtius rearrangement to the corresponding isocyanate. The isocyanate was trapped with various substituted alcohols to afford carbamates **203007**, **203065**, and **203604**. In the case of amide **203606**, the isocyanate was trapped with *tert*-butanol to afford Boc-protected amine **27**.[81] The amine was deprotected and acylated to afford the final 5-membered rigid structure **203606**. Preparation of **203846** followed similar conditions using 3,5-difluorobenzoyl chloride to acylate intermediate **28**. Compound **203848** examined the reverse amide of **203606** and was prepared using 3,5-bis(trifluoromethyl)aniline and standard EDC/HOBt amidation of carboxylic acid intermediate **26**.

Scheme 2.8. Synthesis of Cyclic Analog 203606

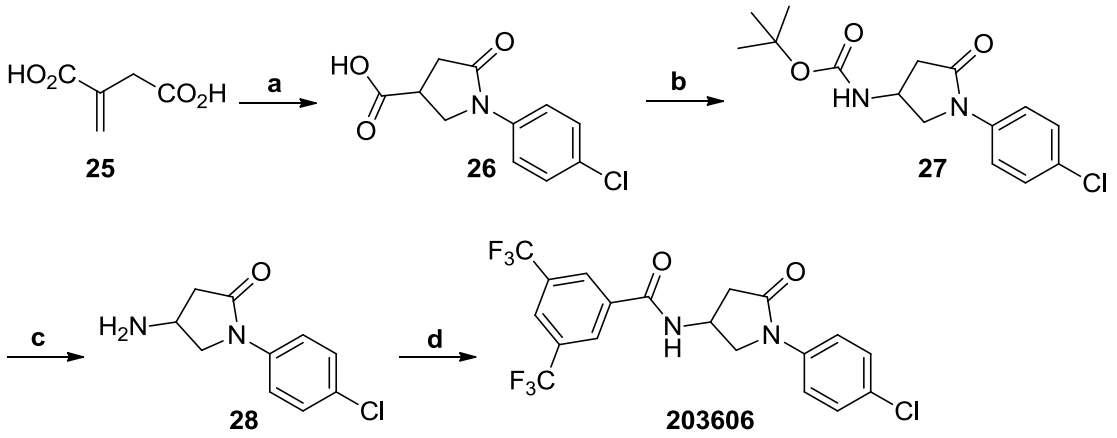

Reagents and conditions: (a) 4-ClPhNH$_2$, neat, 110 °C; (b) DPPA, *t*-BuOH, TEA, PhMe, reflux; (c) TFA, DCM, 0 °C; (d) 3,5-bis(CF$_3$)PhCOCl, TEA, DCM.

Analogs **203845**, **203850**, and **203851** explored additional conformational restriction of **100594** as depicted in Figure 2.1. Scheme 2.9 shows the chemistry used to prepare cyclic analog **203845**. Starting 5-chloro-2-nitrobenzaldehyde (**29**) was converted to the aminopropionic acid **30**[82], which was acylated using 3,5-bis(trifluoromethyl)benzoyl chloride to afford intermediate acid **31**. Reduction of the nitro group to the amine and concomitant cyclization was achieved using iron(II) sulfate heptahydrate[83,84] to afford final compound **203845**.

Scheme 2.9. Preparation of Cyclic Analog 203845

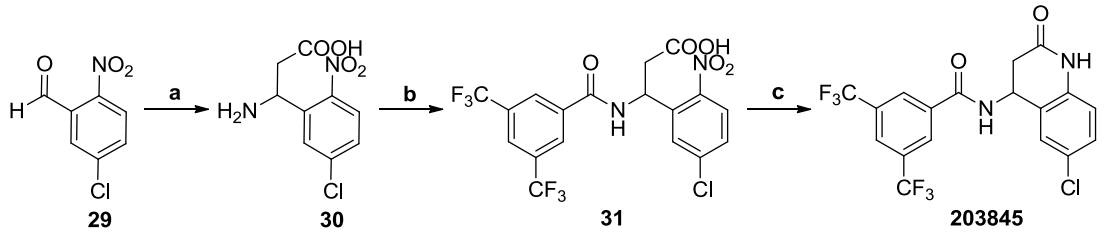

Reagents and conditions: (a) CHCO$_2$H , CH$_2$(COOH)$_2$, NH$_4$HCO$_2$, conc. HCl; (b) 3,5-bis(CF$_3$)PhCOCl; 2M NaOH (aq) (c) FeSO$_4$•7H$_2$O, 10% NH$_4$OH, EtOH, 100 °C

Scheme 2.10 provides the synthesis of analog **203850**. Cyclopropyl cyano ester **32** was heated directly with 4-chloroaniline neat and underwent a ring-opening/recyclization to afford nitrile **33**.[85] Reduction of the nitrile was achieved using Raney Nickel in a Parr reactor[86] to afford intermediate amine **34**, which was then acylated with 3,5-bis(trifluoromethyl)benzoyl chloride to afford **203850**.

Scheme 2.10. Synthesis of Cyclic Analog 203850

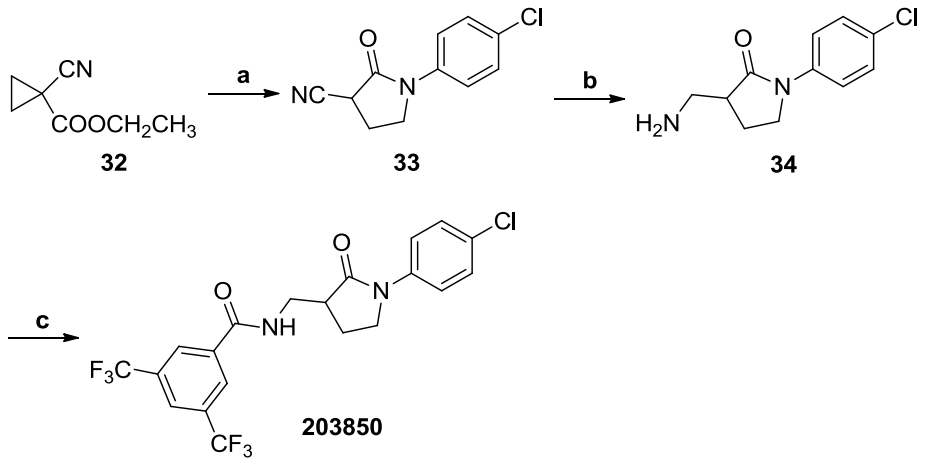

Reagents and conditions: (a) 4-ClPhNH$_2$, neat, 140 °C; (b) Raney Ni, H$_2$, 40 psi, 1M Methanolic ammonia; (c) 3,5-bis(CF$_3$)PhCOCl, TEA, DCM, RT

Compound **203851** was synthesized as shown in Scheme 2.11. 5-Chloroindolin-2-one (**35**) underwent Vilsmeier formylation in DMF. Following completion of the first step, the reaction was cooled and quenched with aqueous ammonia to yield enamine **36**.[87] Acylation of the enamine afforded **203851**. Several attempts to reduce the double bond were undertaken, including hydrogenation with 5% Pd/C in ethanol; reduction using sodium cyanoborohydride[88]; reduction employing triethylsilane and trifluoroacetic acid[89,90]; and atmospheric hydrogenation utilizing 10% Pd/C in ethyl acetate. However, none of the attempts proved successful.

Scheme 2.11. Synthesis of Analog 203851

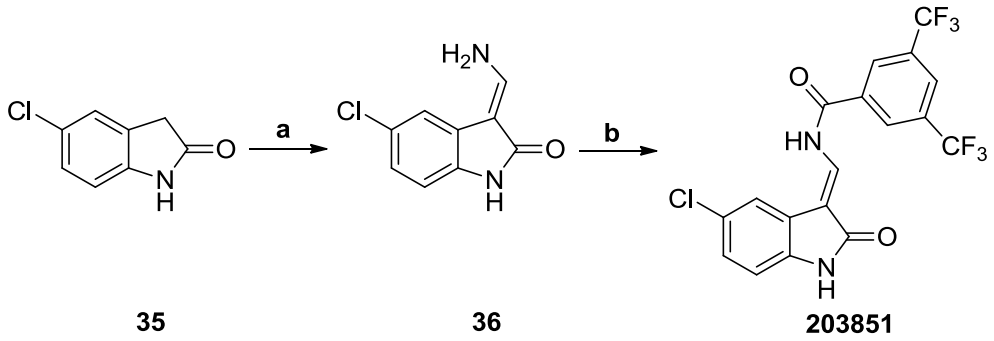

Reagents and conditions: (a) i.) DMF, POCl$_3$, 45 °C; ii.) NH$_3$/NH$_4$OH, 0° C to RT; (b) 3,5-bis(CF$_3$)PhOCl, TEA, DCM

Analogs **203059** and **203063** incorporated a solubilizing pyridine moiety with the nitrogen in the 3- or 2-position, respectively, into the **101425** template. Compound **203061** replaced the bis(trifluoromethyl) moieties with fluorines. The chemistry followed the preparation of **101425** (Scheme 2.2) and proceeded by condensation of 3-bromopropylamine **4** with excess of the desired pyridyl aniline or 4-chloroaniline followed by simple acylation using 3,5-bis(trifluoromethyl)benzoyl chloride or 3,5-difluorobenzoyl chloride.

Analogs **203853** and **203855** explored replacing one of the amides with an amine in the 6- and 5-membered conformationally restricted analogs (Scheme 2.12 and Scheme 2.13, respectively) similar to that of **101425**. Compound **203853** was synthesized by EDC/HOBt mediated amidation of piperidin-3-yl-methanol (**37**) with 3,5-bis(trifluoromethyl)benzoic acid followed by a Parikh-Doering oxidation[91,92] to afford aldehyde **39**. Reductive amination[93] of **39** with 4-chloroaniline afforded the final compound. Compound **203855** (Scheme 2.13) was prepared via arylation[94] of 3-(*tert*-butoxycarbonylamino)pyrrolidine with 1-chloro-4-iodobenzene to afford intermediate **203854**, which was also submitted for testing. Deprotection followed by acylation afforded final compound **203855**. Analog **203847** (Table 2.6) evaluated reduction of both amides of **100602** to the conformationally restricted diamine, which was achieved using LAH reduction.

Scheme 2.12. Synthesis of Monoamine 203853

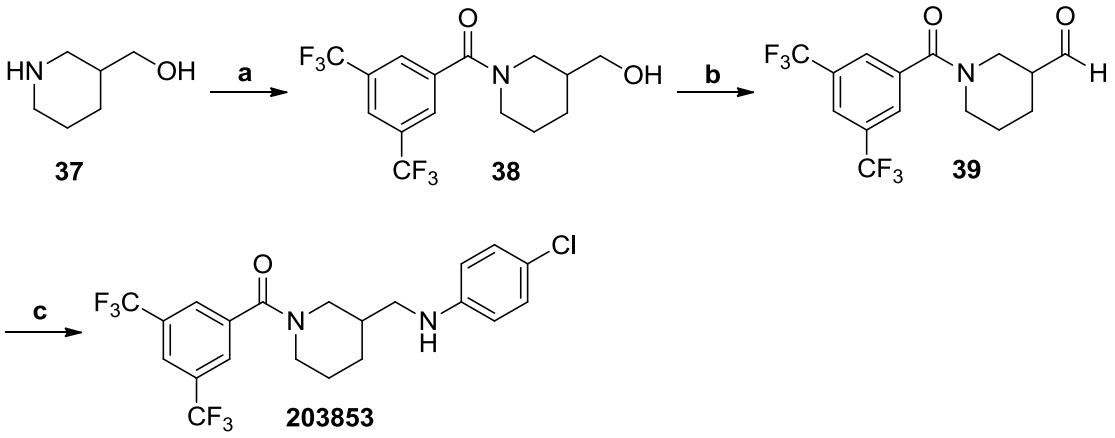

37 **38** **39** **203853**

Reagents and conditions: (a) 3,5-bis(CF_3)$PhCO_2H$, EDC, HOBt, DIPEA, THF, RT; (b) Pyr•SO_3, DMSO, DIPEA, DCM, 0 °C to RT; (c) 4-$ClPhNH_2$, $NaBH(OAc)_3$, DCE, 0 °C to RT

Scheme 2.13. Synthesis of Cyclic Monoamines 203854 and 203855

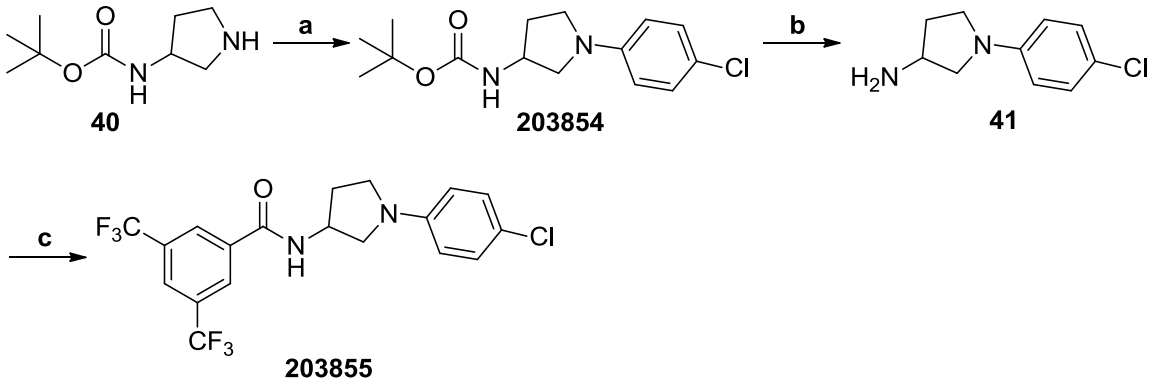

Reagents and conditions: (a) 4-IPhCl, K_2CO_3, DMF, 120 °C; (b) TFA, DCM, 0 °C; (c) 3,5-bis(CF_3)PhCOCl, TEA, DCM

Table 2.6 summarizes the effects of newly synthesized analogs on Rho-mediated gene transcription and cytotoxicity in the HEK293 stably transfected cell line. Examination of the 5-membered conformationally restricted lactams shows that carbamate analogs with no substitution (**203007**) or difluoro substitution (**203604**) on the benzyl are inactive. The same trend is seen with the corresponding amide series. Carbamate **203065** and amide **203606**, both containing bis(trifluoromethyl) substituents, show similar potencies and efficacies. Differences in potencies based on the substitution pattern may indicate that a minimum level of lipophilicity is necessary for activity (see Chapter 3). Analog **203848** reverses the amide bond position of **203606**. While the compound maintains potency and demonstrates excellent efficacy, it is significantly more cytotoxic.

While conformational restriction has shown success, compounds **203845**, **203850**, and **203851** were completely inactive. Upon further exploration of acyclic analogs of **101425**, we find that compounds **203061**, with difluoro-substitution, and **203059**, with a pyridyl nitrogen in the 3-position, show slight decreases in potency with a significant increase in efficacy, perhaps due to better solubility at the higher concentrations. Unfortunately, the compounds also show a significant increase in cytotoxicity. Compound **203063**, with the pyridyl nitrogen in the 2-position, was completely inactive.

Compounds **203853** and **203855** explore monoamines of the 6- and 5-membered conformationally restricted analogs, respectively. Unfortunately, both molecules, in

addition to intermediate **203854,** show complete loss of activity. Conversely, diamine **203847** demonstrates similar activity and cytotoxicity in comparison with **100602** (Table 2.5), but shows higher overall efficacy.

Table 2.6. Newly Synthesized Analogs Tested Using HEK293 SRE.L Stable Cell Line

Cmpd No	Structure	IC_{50} SRE.L (μM)[a]	% inh SRE.L (10, 100 μM)[a]	% inh WST-1 (10, 100 μM)[a]
203007	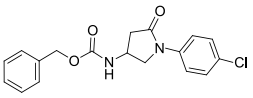	>100	-	-
203065	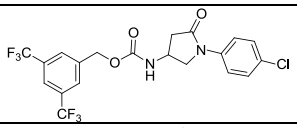	16	16, 62	17, 29
203604	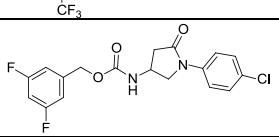	>100	-	-
203606	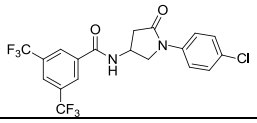	17	17, 54	4, 14
203846	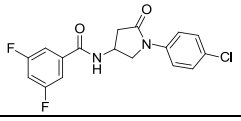	>100	-	-
203848	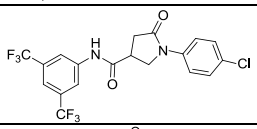	8.6	65, 99	55, 75
203845	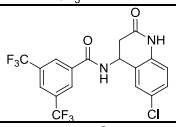	>100	-	-
203850	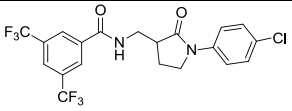	>100	-	-
203851	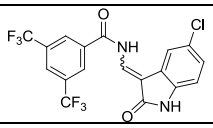	>100	-	-
203061	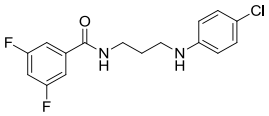	35	0, 96	0, 73
203059	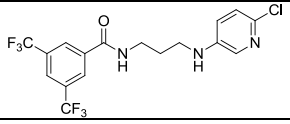	24	0, 95	0, 65

Cmpd No	Structure	IC_{50} SRE.L (μM)[a]	% inh SRE.L (10, 100 μM)[a]	% inh WST-1 (10, 100 μM)[a]
203063	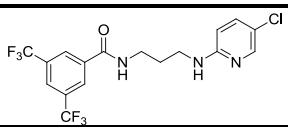	>100	-	-
203853	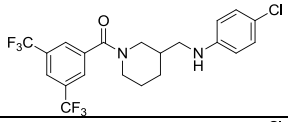	>100	-	-
203847	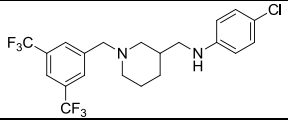	19	1, 70	21, 32
203854	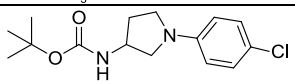	>100	-	-
203855	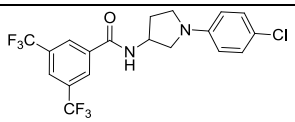	>100	-	-

[a]Refer to Table 2.1 for assay descriptions

The progression of **100594** to **100602** demonstrates that an increase in activity and efficacy with retention of modest selectivity and cytotoxicity is possible by employing conformational restriction. Compound **100602** remained the best performing analog in this series. The more rigid 5-membered analog (**203606**) showed similar potency and efficacy with reduced cytotoxicity. Disappointingly, it demonstrated solubility issues as evidenced by visible precipitation in the cellular assays. The 3,5-bis(trifluoromethyl)benzyl ester **203065** maintains similar activity and potency with modest cytotoxicity and does not appear to precipitate in the assays. Analogs **203606** and **203065** hold potential as new scaffolds for optimization.

PC-3 Prostate Cancer Cell Invasion

In their original publication, the Neubig lab showed that **1423** selectively inhibited spontaneous PC-3 prostate cancer cell invasion through a Matrigel matrix, but had no effect on $G\alpha_i$-dependent SKOV-3 ovarian cancer cell invasion *in vitro*.[62] Consequently, we screened several of the newly synthesized analogs for their ability to inhibit PC-3 prostate cancer cell invasion. We compared the selectivity for invasion versus cytotoxicity (measured using WST-1) with that of **1423**. Table 2.7 presents the results[63] for our selected compounds. In general, we observed a correlation between inhibition of invasion and inhibition of SRE.L in PC-3 cells. Conformationally restricted

analogs **100602**, **100690**, and **100692** demonstrated roughly equivalent efficacies against SRE.L at 10 and 100 µM. Their activities in the Matrigel followed a similar trend. Compound **100602** lacked cytotoxicity at 10 µM and showed 72% inhibition of invasion with modest cytotoxicity at 100 µM. While **1423** maintained 71% invasion at 10 µM, it was significantly cytotoxic. Analog **100602** maintains a more favorable efficacy:toxicity profile at 100 µM when compared with **1423** at just 10 µM. We also found a correlation between selectivity for SRE.L:cytotoxicity and invasion:cytotoxicity in monoamines **101425** and **102585** and diamine **102532**. Although monoamine **101425** shows lower efficacy than **1423** at 10 µM in the invasion assay, it does so without any cytotoxicity. At 100 µM, **101425** exceeds the efficacy of **1423** with half of the cytotoxicity. Analogs **102585** and **101532** demonstrate no cytotoxicity at the lower concentration. However, we see no selectivity in invasion:cytotoxicity at the higher concentration, a trend that is also seen in efficacy versus cytotoxicity in the transfected PC-3 cellular assay (Table 2.2).

Table 2.7. Effects of New Analogs on Cell Invasion and Cytotoxicity

Cmpd No	% inh invasion (10 µM)	% inh WST-1 (10 µM)	% inh invasion (100 µM)	% inh WST-1 (100 µM)
1423	71	54	ND[b]	ND[b]
100594	13	0	62	28
100600	14	0	75	38
100597	6	0	15	1
100686	15	0	25	1
100602	20	0	72	23
100690	14	0	79	36
100692	12	0	78	44
101343	63	31	86	70
101329	2	0	0	1
102443	0	0	0	0
100596	50	14	88	78
101425	54	0	84	27
102585	47	0	96	95
102532	30	0	86	97
102445	18	0	8	0
102447	3	0	26	0
102441	18	0	56	0

[a]Refer to Table 2.1 for assay descriptions
[b]Not determined

Figure 2.2 presents correlation graphs between the average inhibition in the PC-3 Matrigel invasion assay versus the average inhibition of SRE.L expression in transiently transfected PC-3 cells at both 10 and 100 μM concentrations. Data show a positive correlation at both concentrations. However, outliers are present that strongly inhibit SRE.L without significant effects on invasion. The data also suggest that a threshold of approximately 50% of inhibition of SRE.L must be reached before inhibition of invasion is detectable.

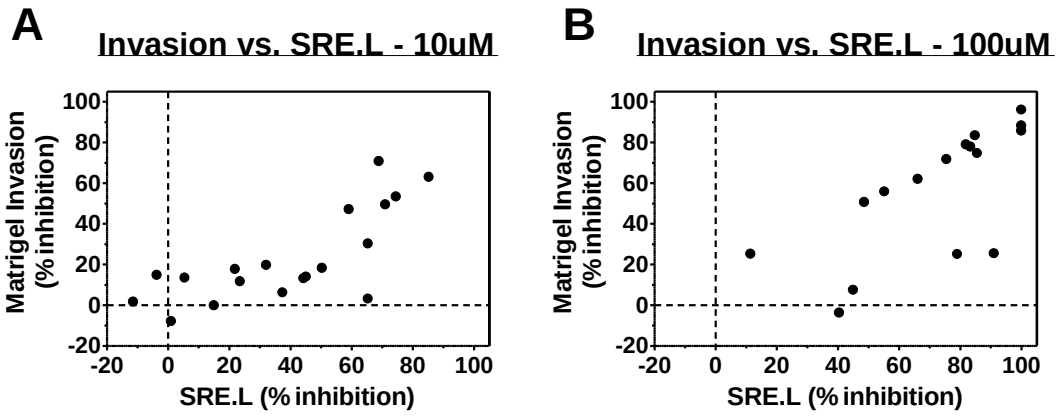

Figure 2.2. Correlation of Matrigel Invasion and SRE.L Expression Inhibition in PC-3 Cells

(A) shows the correlation of % inhibition of Matrigel invasion versus the inhibition of SRE.L at 10 μM (**B)** shows the correlation % inhibition of Matrigel invasion versus the inhibition of SRE.L at 100 μM

In summary, we executed an expanded SAR survey of an inhibitor of Rho-mediated gene transcription (**1423**) aimed at improving potency and/or selectivity while minimizing cytotoxicity. To this end, we employed three strategies: (1) removal of the labile N-O bond; (2) bioisosteric replacement of the secondary carboxamides to improve cell permeability; and (3) conformational restriction to improve activity and/or selectivity. These strategies generated analogs with improved selectivity and cytotoxicity profiles. Unfortunately our best compounds show a 5- to 10-fold reduction in potency. Our most interesting compounds include nipecotic amide **100602**, monoamine **101425**, and 5-membered ring analogs **203606** and the presumably more soluble **203065**. These compounds inhibit SRE.L expression with similar efficacies to **1423** with significant reductions in cytotoxicity. Additionally, for the first time, we have demonstrated a clear

correlation between inhibition of Rho-mediated gene transcription and cell invasion using a Matrigel matrix model of metastasis.

Chapter 3
Aromatic Modifications

Through replacement of the potentially labile N-O bond and conformational restriction of the flexible tether region between the two aromatic rings, we arrived at our lead compound, nipecotic amide **100602**, which offered an improved biological profile over compound **1423**.[63] Although there was a 10-fold decrease in activity, it maintained inhibition of $G\alpha_{12}$QL-stimulated SRE.L-luciferase expression with similar efficacy to **1423**, but with greatly reduced cytotoxicity. Unfortunately, despite the improved biological profile, compound **100602** exhibits poor physicochemical properties, including low solubility and low permeability (Table 3.6).

One of the main issues we've continuously encountered in our SAR campaign is solubility. Lead compound **100602** displays low solubility (Table 3.6), and precipitation is visible in our cellular assays. However, we selected **100602** due to its equivalent efficacy and diminished toxicity to further explore diversity at each of the terminal aromatic rings with the additional goal of improving solubility.

Preliminary Data

Our initial survey of aromatic substitution was conducted on the more potent aminoacetic acid template to magnify the changes in activity, as shown in Table 3.1. Compounds were synthesized using simple acylation of 2-(aminooxy)acetic acid followed by EDC/HOBt mediated amidation (Scheme 2.1). Table 3.1 summarizes the brief preliminary survey of aromatic substitution. Moving the chloro group from the *para*- (**100596**) to the *meta*-position (**101200**) has no effect. Contrarily, completely removing it (**100703**) negatively affects potency as well as efficacy. Removing one of the trifluoromethyl groups (**101202** and **100723**) also negatively affects potency and efficacy, and removing both completely abolishes all activity (**100701**). Swapping the position of the two aromatic rings in **100691** affords a compound with similar potency and overall efficacy with a reduction in cytotoxicity. The results of this brief survey indicate that a

certain level of lipophilicity provided by aromatic substitution is essential for activity, perhaps due to differences in cellular permeability. We utilized **100602** as a template for an expanded analysis of aromatic substituent structure-activity relationships.

Table 3.1. Preliminary Effects of Aromatic Substitution on Transcription and Cytotoxicity in Transfected PC-3 Cells

Cmpd No	Structure	IC_{50} SRE.L (μM)[a]	% inh SRE.L (10, 100 μM)[a]	% inh pRL-TK (10, 100 μM)[a]	% inh WST-1 (10, 100 μM)[a]
100596[b]	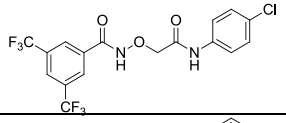	4.7	71, 100	53, 89	42, 91
101200	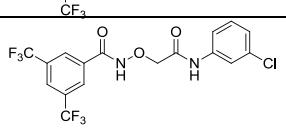	5.9	65, 100	51, 89	49, 97
100703[b]	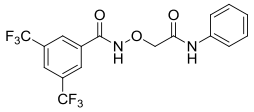	36	13, 65	33, 59	0, 37
101202	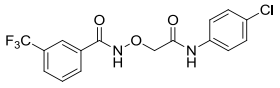	27	25, 86	5, 19	0, 58
100723[b]	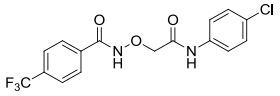	29	26, 91	6, 0	0, 56
100701[b]	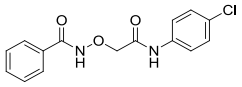	>100	-	-	-
100691[b]	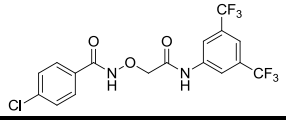	8.6	58, 100	19, 87	0, 39

[a]Refer to Table 2.1for assay descriptions
[b]Synthesized by Jenny Ryu

Library Selection

In order to systematically modify the aromatic substituents, we first explored ring A of compound **100602**, as shown in Figure 3.1. Paul Kirchhoff, a computational chemist in the Hans W. Vahlteich Medicinal Chemistry Core (VMCC) at the University of Michigan, assisted with monomer selection. We utilized the MScreen program of the Center for Chemical Genomics (CCG) at the University of Michigan to screen the Sigma-Aldrich "Selected Structure Sets" for commercially available *meta*-substituted benzoic acids with desirable physicochemical properties. We chose only *meta*-substitutions, as we

expect that they would have greater potential to interact with various areas in the active site than would *ortho*- or *para*- substituents. We utilized Molecular Operating Environment (MOE) software to compute lipophilicity (SLogP) and molecular weight properties based on the parent structure with salt removed. We intended to select diverse carboxylic acids with a calculated SLogP less than that of our 3,5-bis(trifluoromethyl)benzoic acid starting material (2.71) and that would result in a final compound molecular weight of 550 or less. Similarly, we explored ring B, again using MScreen to identify commercially available *meta*-substituted anilines with SLogP less than that of 4-chloroaniline (1.92) and that would result in final compound molecular weights of 550 or less. In choosing only starting acids and anilines with lower SLogP, we hoped to decrease the overall SLogP of our new analogs to enhance solubility.

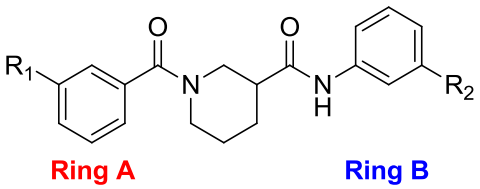

Figure 3.1. Modifications of Aromatic Rings A and B of 100602

The synthetic routes to new analogs of **100602** are presented in Scheme 3.1 and Scheme 3.2. For the acid library (ring A, Scheme 3.1), the starting nipecotic acid **42** was Boc-protected, and the resulting acid (**43**) was coupled to 4-chloroaniline using EDC/DMAP-mediated amidation. Following deprotection, the resulting piperidine was coupled with various commercially available *m*-substituted benzoic acids.[95] The resulting compounds were purified using Amberlyst-15 resin to remove excess aniline, followed by a water wash to remove residual DMF to afford final acid library analogs. This synthesis afforded 20 compounds with yields between 39 and 100% with purities greater than 90%. For the aniline library (ring B, Scheme 3.2) the starting nipecotate **46** was acylated with 3,5-bis(trifluoromethyl)benzoyl chloride followed by saponification to afford the free acid **48**. The acid was then coupled with the commercially available *m*-anilines.[95] Compounds were purified by either aqueous workup or aqueous workup followed by chromatography to afford final aniline library analogs. Synthesized analogs afforded yields between 32 and 100% with purities ranging between 81 to greater than 95%.

Scheme 3.1. Synthesis of Acid Library

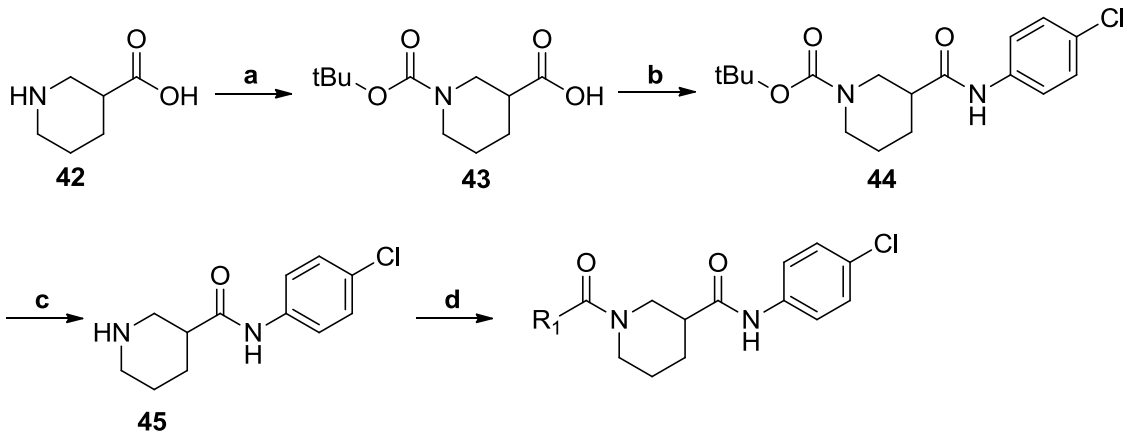

Reagents and conditions: (a) BOC_2O, NaOH, H_2O, Dioxane; (b) 4-ClPhNH$_2$, EDC, DMAP, DCM; (c) TFA, DCM, -10 °C; (d) i. ArCO_2H, EDC, DMAP, DCM/DMF; ii. Amberlyst-15, DCM

Scheme 3.2. Synthesis of Aniline Library

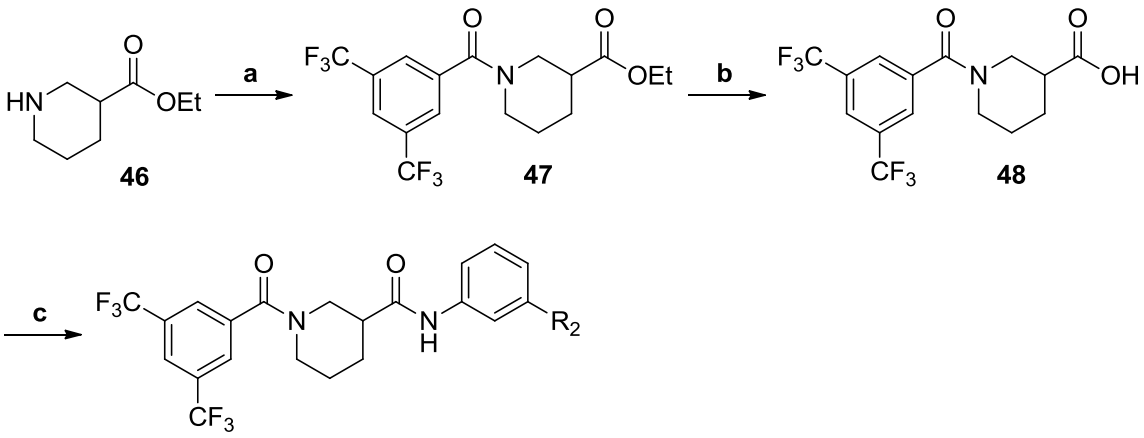

Reagents and conditions: (a) 3,5-bis(CF3)PhCOCl, DIPEA, DCM; (b) LiOH, EtOH; (c) *m*-RPhNH$_2$, EDC, DMAP, DCM

The effects on Rho-mediated gene transcription and cytotoxicity of all newly synthesized analogs were determined in transiently transfected PC-3 cells at an initial concentration of 100 μM. For compounds showing greater than 50% inhibition at 100 μM, a full dose-response curve (DRC) was generated. Table 3.2 summarizes the effects of benzamide analogs of **100602**. Replacement of the bis(trifluromethyl) groups with a substituent in the *meta*-position afforded analogs with little to no cytotoxicity, with the exception of **206115**. A majority of the analogs had lower potency than the lead **100602**.

However, analogs **203971** and **203972** show a slight increase in potency and similar efficacies.

Upon comparing similar analogs, we see that adding a carbon between the amide bond and the aromatic ring (**100602** vs **203960**) has little effect on potency and toxicity. Analog **203973** adds a nitrogen to the furan ring of **203971**, affording a less active oxazole. This substitution increases the topological polar surface area (TPSA) of **203973** to 71Å and decreases the calculated LogP (CLogP) to 3.46 versus a TPSA of 59Å and CLogP of 4.88 exhibited by **203971**, which may account for the reduced activity. A similar trend is observed when examining compounds **203968**, **203979**, and **203963**. Double-bond analog **203968** maintains modest potency (33 μM) and good efficacy (84%) with a TPSA of 49Å and a CLogP of 4.33. Thioether **203963** has the same TPSA and a similar CLogP (4.26) as **203968** and maintains similar potency with a slight decrease in efficacy. However, moving from the thioether to an ether (**203979**) increases TPSA to 59Å and lowers CLogP to 3.82. The analog lost activity with a significant reduction in efficacy. We then explored the relationships between TPSA and activity as well as CLogP and activity for the acid library. We found that TPSA and potency have a weak correlation (Figure 3.2, $r^2 = 0.32$), whereas CLogP has a moderate correlation with potency (Figure 3.3, $r^2 = 0.78$).

*Benzophenone-containing **203972** is one of the most promising analogs in our library. It maintains good activity, confirming that the benzophenone moiety may be suitable for future use as a photoaffinity reagent for determining the molecular target(s) of our compounds.* **203971** shows a two-fold increase in potency and a slight increase in efficacy without cytotoxicity, making it our best compound in the acid-substituted series.

Table 3.2. Effects of Benzamide Substitution on Transcription and Cytotoxicity in Transfected PC-3 Cells

Cmpd No	Structure	IC_{50} SRE.L (μM)[a]	% inh SRE.L (100 μM)[a]	% inh WST-1 (100 μM)[a]
100602[b]	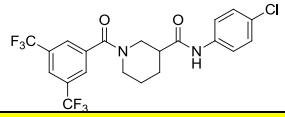	9.8	78	14
203971	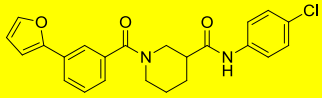	6.4	87	0
203972	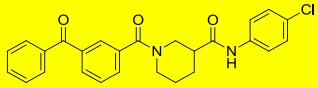	9.9	75	0
203960	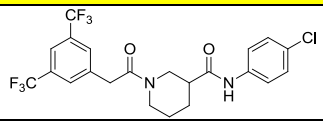	13	69	0
206115	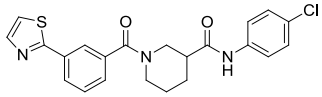	27	92	32
203966	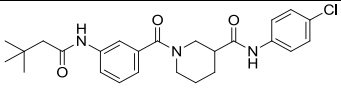	26	69	0
203968	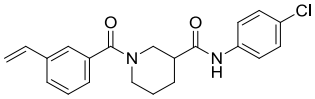	33	84	0
203975	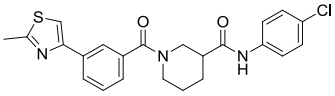	33	81	1
203977	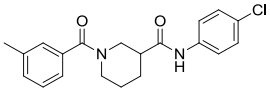	35	63	0
203963	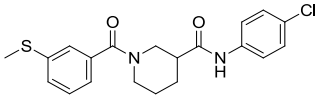	35	76	0
203973	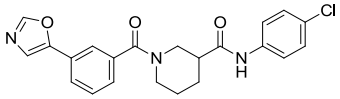	43	72	0
203967	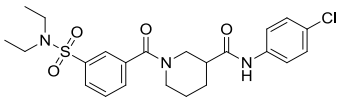	51	69	0
203969	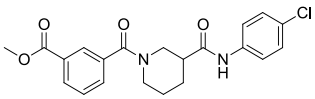	67	64	0

Cmpd No	Structure	IC_{50} SRE.L (μM)[a]	% inh SRE.L (100 μM)[a]	% inh WST-1 (100 μM)[a]
203974	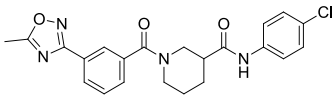	78	59	0
203979	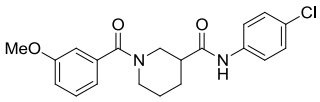	>100[c]	38	0
203962	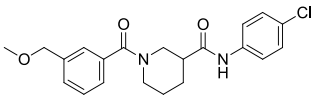	>100[c]	32	0
203965	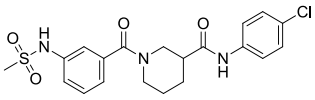	>100[c]	32	3
203961	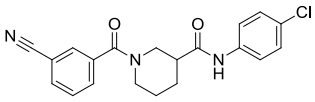	>100[c]	20	0
203970	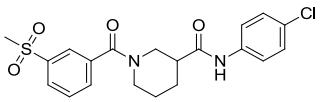	>100[c]	17	2
203978	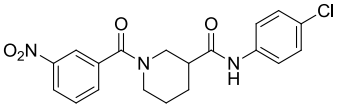	>100[c]	15	0
203964	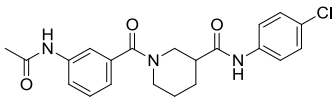	>100[c]	8	4

[a]Refer to Table 2.1for assay descriptions
[b]Synthesized by Jenny Ryu
[c]Full DRC not generated—tested only at 100 μM

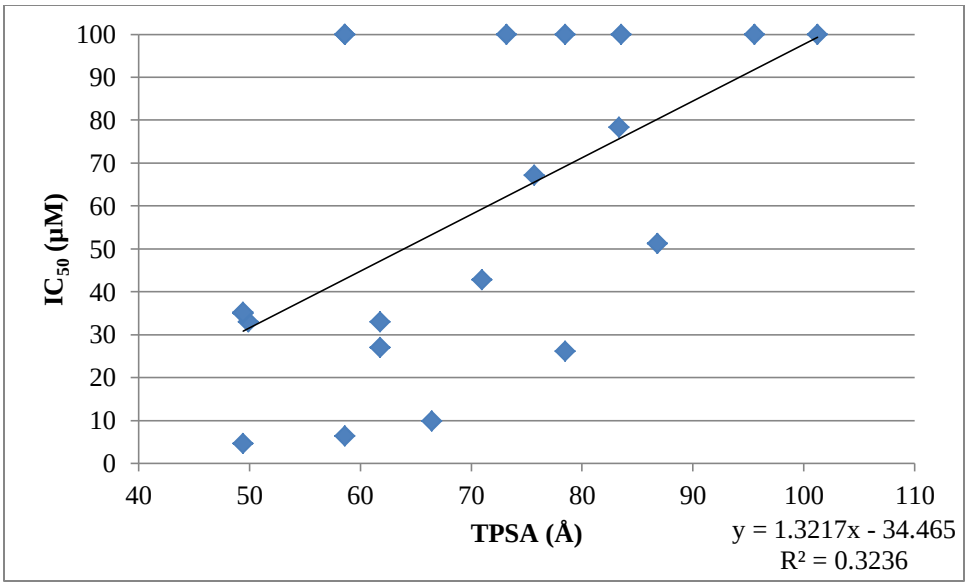

Figure 3.2. Acid Library Topological Polar Surface Area versus Potency

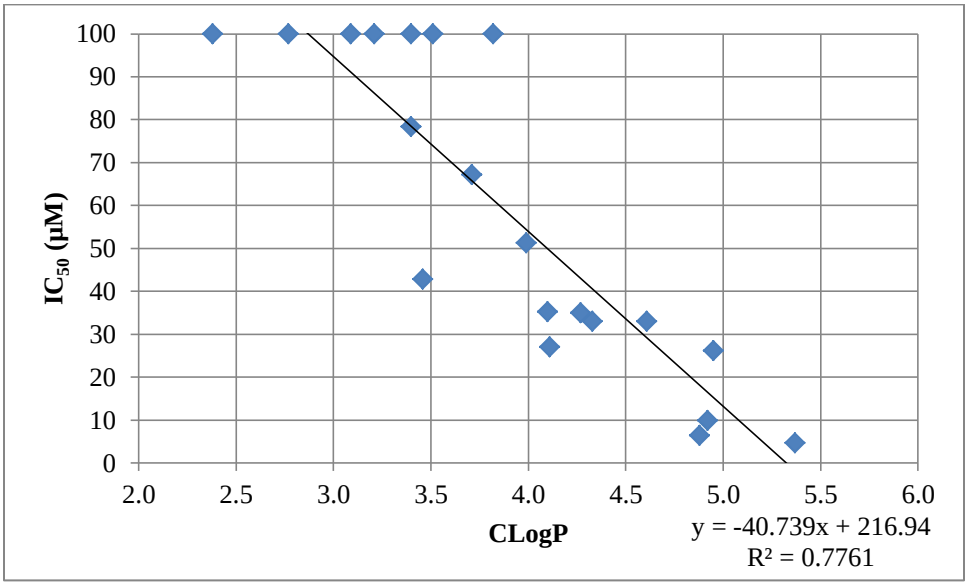

Figure 3.3. Acid Library CLogP versus Potency

The effects of aromatic substitution R_2 on ring B are summarized in Table 3.3. As with the acid-substituted library, most compounds demonstrated low to no cytotoxicity, with the exception of amine **206123**, which had significant cytotoxicity of 51% at 100 µM. Our best analogs **206114** and **206108** show a 10-fold increase in potency with a slight decrease in efficacy. Pyridine **206124** showed a similar increase in potency while maintaining modest efficacy. Analogs **206109**, **206244**, **206102**, **206248**, **206243**, and **206241** all show similar or slight increases in potency.

Although there was very weak to no correlation overall between potency and TPSA as well as potency versus CLogP (Figure 3.4 and Figure 3.5), trends were observed between subsets of similar compounds. Analogs **206105** appends a ketone to **206102**, which increases TPSA, decreases CLogP, and significantly decreases potency. The 5-membered amine **206103** is inactive and highly toxic. The 6-membered morpholine, on the other hand, demonstrates moderate potency and efficacy without toxicity. Analogs **206012**, **206248**, and **206242** show a similar trend as observed in the acid library (Table 3.2) in that the vinyl (**206248**) and ethyl (**206102**), which share similar TPSA and CLogP, also have similar potencies and efficacies. However, the ether analog (**206242**), with increased TPSA and decreased CLogP, maintains less activity. This is also observed between analogs **206114**, **206108**, and **206111**. *Compounds **206114**, **206108**, and **206124** were the most potent analogs in this series and are therefore of greatest interest.*

Although we had intended to select only compounds with limited CLogP to enhance solubility, we mistakenly purchased starting materials that exceeded our target. Therefore, we synthesized analogs with CLogP values as high as 6.68. While this is obviously undesirable, it was actually fortuitous, as the compounds with the highest CLogP (**206114** and **206108**) were our most potent analogs. The added lipophilicity appeared to increase the permeability of the compounds, as demonstrated in our parallel artificial membrane permeability assay (PAMPA), as shown in Table 3.6.

Table 3.3. Effects of Aniline Substitution on Transcription and Cytotoxicity in Transfected PC-3 cells

Cmpd No	Structure	IC_{50} SRE.L (μM)[a]	% inh SRE.L (100 μM)[a]	% inh WST-1 (100 μM)[a]
100602[b]	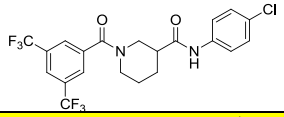	9.8	78	14
206114	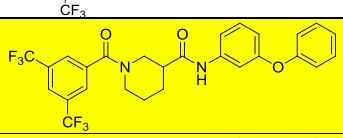	1.5	59	1
206108	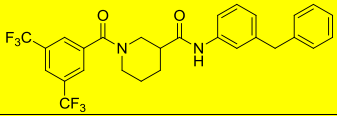	1.6	59	0
206124	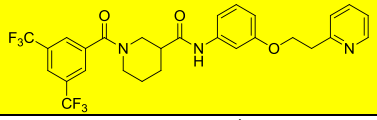	2.3	82	5
206109	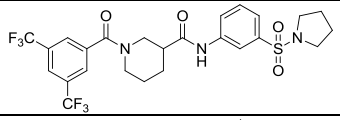	5.6	70	0
206244	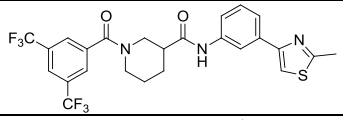	6.1	73	1
206102	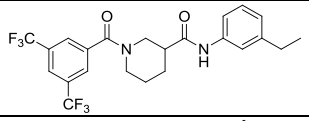	8.1	66	0
206248	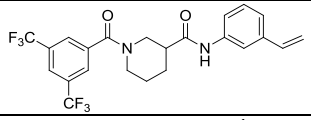	11	53	1
206243	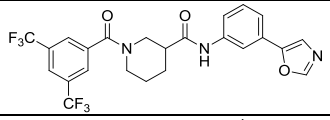	12	87	9
206241	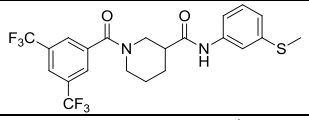	12	60	0
206110	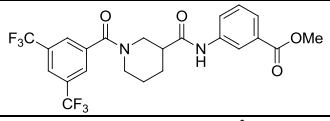	26	63	0
206242	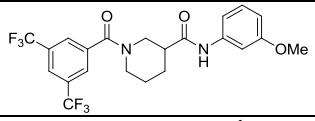	30	51	0
206104	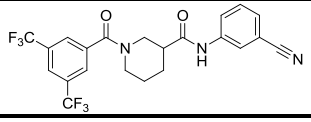	32	77	0

Cmpd No	Structure	IC_{50} SRE.L (μM)[a]	% inh SRE.L (100 μM)[a]	% inh WST-1 (100 μM)[a]
206247	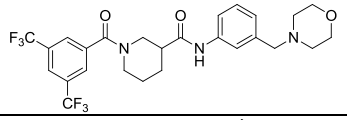	32	73	0
206103	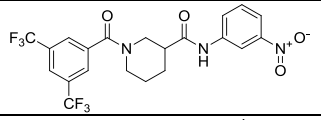	66	65	9
206105	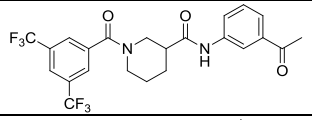	76	73	0
206123	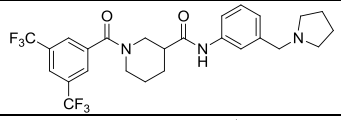	>100[c]	94	51
206112	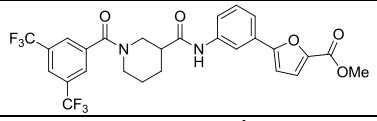	>100[c]	39	0
206240	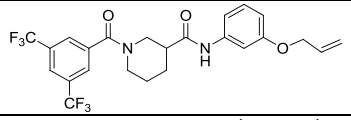	>100[c]	38	0
206111	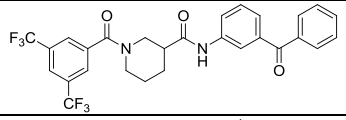	>100[c]	38	0
206245	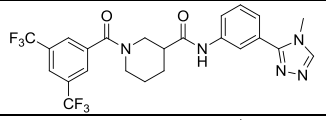	>100[c]	36	0
206113	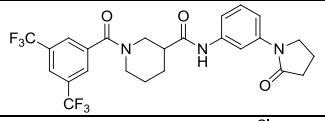	>100[c]	35	0
206125	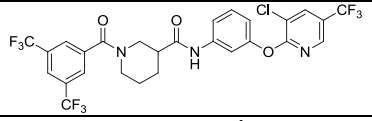	>100[c]	25	0
206107	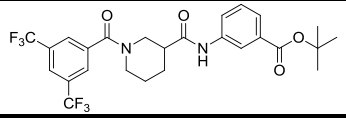	>100[c]	24	0

[a]Refer to Table 2.1 for assay descriptions
[b]Synthesized by Jenny Ryu
[c]Full DRC not generated—tested only at 100 μM

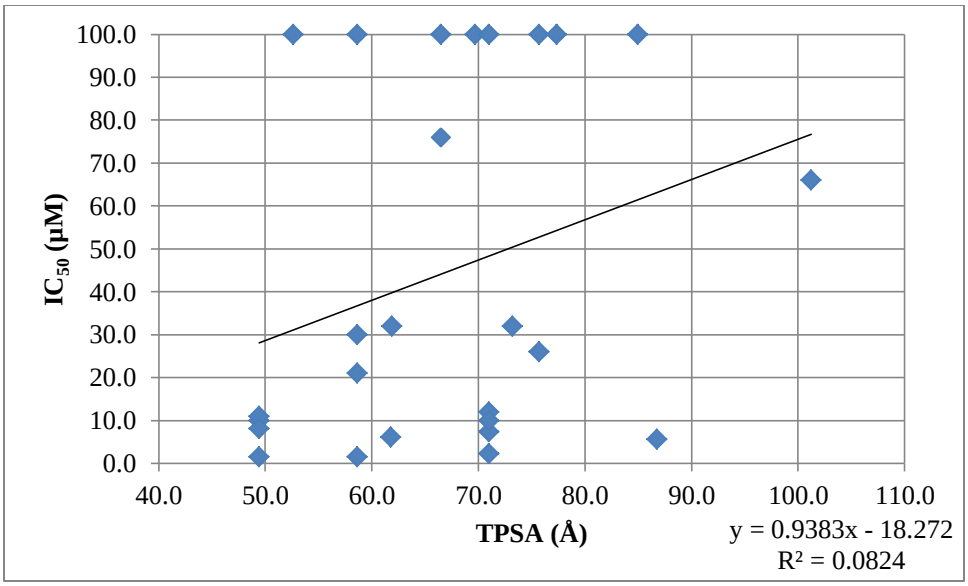

Figure 3.4. Aniline Library Topological Polar Surface Area versus Potency

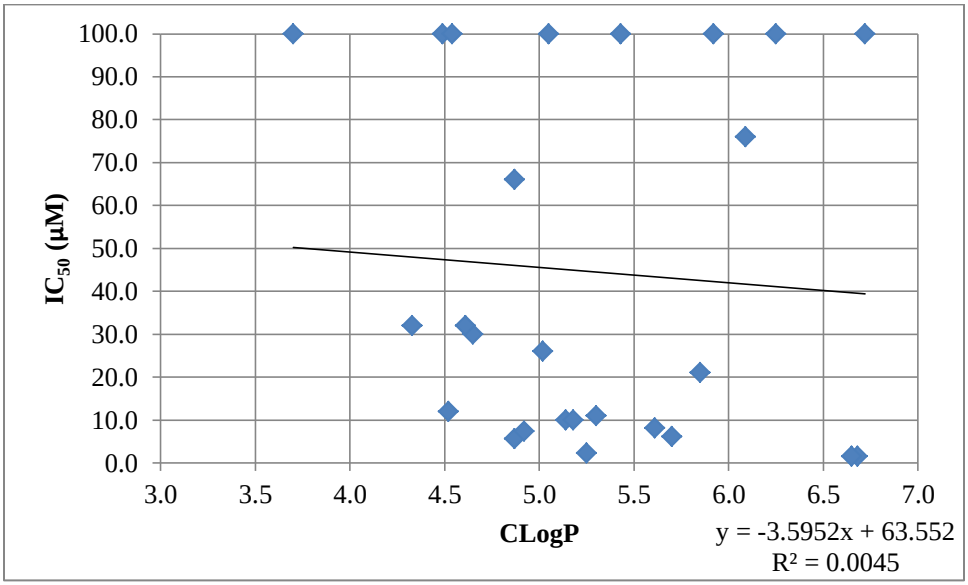

Figure 3.5. Aniline Library Calculated LogP versus Potency

Based on the results from the acid- and aniline-substituted libraries, three series of follow-up analogs were examined, as found in Table 3.4. First, we examined additional substitutions of **100602**. Analog **206455** replaced the furan of **203971** with a thiophene, which slightly increased potency and maintained low cytotoxicity. Analog **206119** moved the furan of **203971** from the *meta*- to the *para*-position, which caused a small loss in potency with introduction of minimal cytotoxicity. Analog **206122** reversed the furan from ring A to ring B, which led to a loss of potency and efficacy. Compounds **208798**

and **206681** shortened the length between the pyridyl ether of **206124** (Table 3.3) by one and two carbons, respectively. Shortening the tether by one carbon reduced potency 3-fold and introduced modest cytotoxicity. Shortening by two carbons reduced potency almost 5-fold with a moderate loss in efficacy without cytotoxicity. Analogs **206101**, **206106**, and **206682** looked at pyridyl moieties with the nitrogen in the 2-, 3-, and 4-positions, respectively, which all showed losses in potency compared with **100602**, with **206106** showing significant cytotoxicity.

Next, we examined "hybrid" analogs of our most promising compounds, which maintained the furan moiety on ring A, as found in **203971** (Table 3.2). Compound **206683** blended analog **203963** (Table 3.2), which offered little increase in activity. Analog **206460** combined **203971** and **206106**, which led to a significant decrease in potency with a moderate increase in cytotoxicity. Compound **206120** hybridized **203606** (Table 2.6) with **203971**, which led to a decrease in potency and efficacy; however, it did not demonstrate cytotoxicity. Compounds **206451** and **206450** combined **203971** with **206114** and **206108**, our most potent analogs of the aniline library (Table 3.3), with IC_{50}s of 1.5 and 1.6 μM, respectively. Disappointingly, these "hybrid" compounds resulted in a complete loss of activity.

Table 3.4. Effects of Additional Substitutions on Transcription and Cytotoxicity in Transfected PC-3 Cells

Cmpd No	Structure	IC_{50} SRE.L (μM)[a]	% inh SRE.L (100 μM)[a]	% inh WST-1 (100 μM)[a]
206455	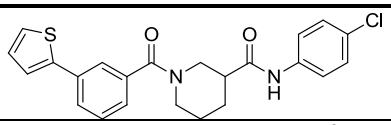	4.7	81	4
206119	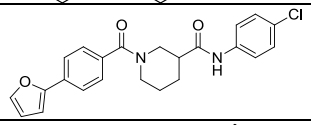	9.2	80	6
206122	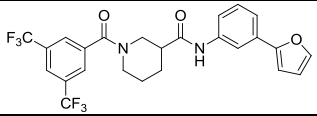	21	63	0
206683	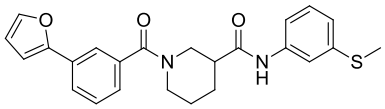	10	63	0
208798	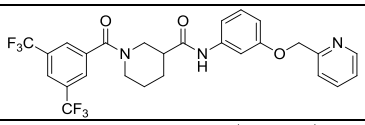	7.4	79	15
206681	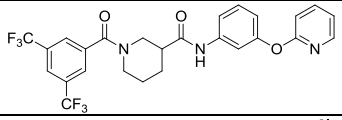	10	60	0
206101	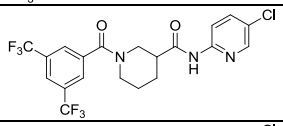	>100	37	0
206106	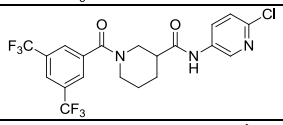	31	88	25
206682	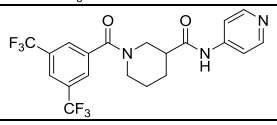	84	54	0
206460	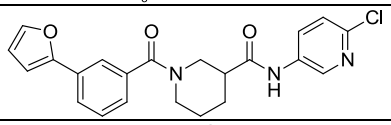	45	88	10
206120	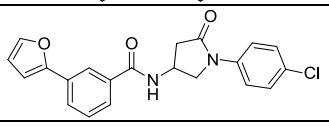	54	49	0
206451	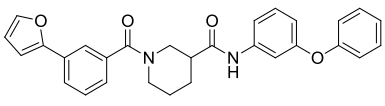	>100	21	0
206450	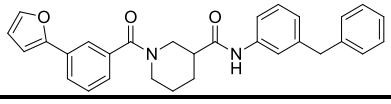	>100	21	0

[a]Refer to Table 2.1 for assay descriptions

Physicochemical Properties

We selected six lead compounds from our completed SAR to examine the effects of structural modification on solubility and permeability. Detailed solubility and permeability assay conditions can be found in the experimentals described in Chapter 6. These six analogs (**100594**, **203971**, **206108**, **206114**, **206455**, and **203606**) were compared to initial hit **1423** and lead **100602** (Table 3.6). Compound **1423** showed moderate solubility (between 18.6 and 11.9 µg/mL). Unfortunately, kinetic solubilities of all the remaining analogs, including **100602,** were binned as low solubility (<10 µg/mL, Table 3.5). We also evaluated the analogs using PAMPA as an estimate of passive permeability (Table 3.5) using the PAMPA Explorer Kit (*p*ION). Only analogs **206108**, **206114**, and **203606** demonstrate moderate permeability in the assay (Table 3.6). The remaining compounds exhibited low permeability. Compounds **206108**, **206114**, and **203606** have calculated partition coefficients (CLogP) of 6.0 or greater (as determined by ChemBioDraw Ultra 12.0), which reflects lipophilicity. It is possible that the increased potency of these lead compounds may be attributed to increased lipophilicity, as higher lipophilicity generally correlates with greater cell permeability. When conducting experiment utilizing a single pH, the PAMPA software utilizes a "two-way flux equation." While retention in the membrane is not considered using the two-way flux equation, the PAMPA analysis software runs a modified version that factors in the amount of sample lost to the membrane. While lipophilicity can correlate with greater cell permeability, compounds with a LogP greater than 5 are more likely to become lodged in the membrane. Several of our compounds returned non-detectable results. It is possible that our standard 4 hour incubation period is not long enough to allow the compounds to move through the multiple bilayered-membrane. Further investigation and optimization of incubation time should be explored.

Table 3.5. Classifications for Solubility and Permeability

BIN	**SOLUBILITY** (µg/mL)[a]	**Log P_{eff}** (cm/s)[b]
LOW	<10	<-5
MODERATE (MOD)	10-60	-5 to -4
HIGH	>60	>-4

[a]Kinetic solubility, ranges found in Ref[96]

[b]Log of effective permeability, ranges found in Ref[97]

Table 3.6. Physicochemical Property Data for Top Analogs

Cmpd No	Structure	Solubility (μg/mL)[a]	CLogP[b]	Log P_{eff} (cm/s)[c]
1423	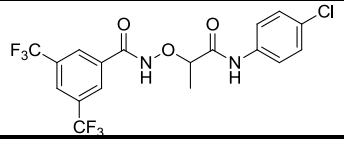	18.6-11.9 (**MOD**)	5.01	-8.8 ± 2.3 (**LOW**)
100594	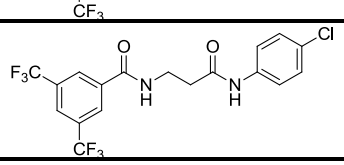	3.45-2.21 (**LOW**)	5.40	-10 ± 0.00 (**LOW**)
100602	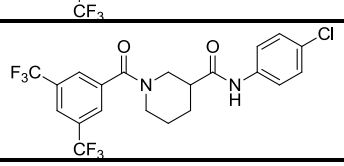	7.99-4.50 (**LOW**)	5.55	-10 ± 0.00 (**LOW**)
203971	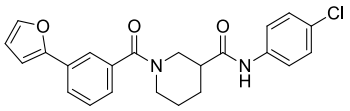	3.09-4.26 (**LOW**)	4.88	-8.3 ± 2.3 (**LOW**)
206455	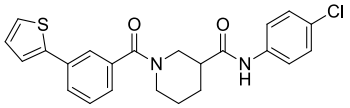	2.41-1.36 (**LOW**)	5.37	-10 ± 0.00 (**LOW**)
206108	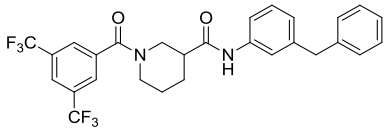	3.85-1.89 (**LOW**)	6.65	-4.7 ± 0.05 (**MOD**)
206114	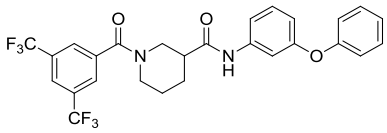	4.30-3.22 (**LOW**)	6.68	-5.1 ± 0.40 (**MOD-LOW**)
203606	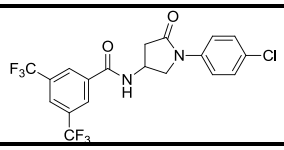	3.21-1.81 (**LOW**)	6.07	-7.6 ± 2.8 (**MOD-LOW**)

[a]Kinetic solubility
[b]Calculated LogP (ChemBioDraw Ultra 12.0)
[c]Log of effective permeability (cm/s) as determined by PAMPA Explorer. Measurements are at minimum N=3.

Chiral Recognition

Chirality is a fundamental component of nature. Proteins are composed of primarily L-amino acids and exhibit specificity for complex molecules. These complex molecules often contain one or more stereocenters.[98,99] In the early 1930s, Easson and Stedman offered the three-point attachment model to describe the stereospecificity of drug receptors for their substrates[100] as depicted in Figure 3.6.[101] The model describes the

sterochemical recognition of enantiomers for a simple molecule containing only one chiral center[98,102] and assumes, although not explicitly stated in the original paper, approach from only one side of the binding site.[103]

The diagrams in Figure 3.6 illustrate the surface of the receptor (IV) and the possible enantiomers (I and II), as well as an achiral molecule (III). The Easson-Stedman model predicts that in order to achieve maximal effect, the enantiomer must interact with the receptor so that A, B, and C of the drug molecule bind to A′, B′, and C′ of the receptor, respectively. Only enantiomer I can do so in this case. As depicted in Figure 3.6, enantiomer II can only form 1 interaction between B and B′. Achiral compound III contains A, B, and C in the proper configuration to bind with the receptor, and should be able to do so with equal activity to I according to the proposed model. The shaded face of achiral molecule III also contains points A, B, and C; however they are not aligned to form three interactions needed for maximal effect.[100]

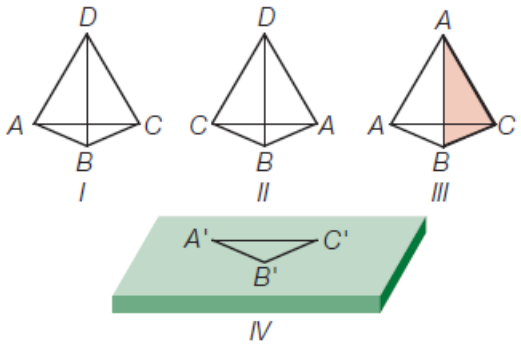

Figure 3.6. Easson-Stedman Three-point Attachment Model. Diagram IV provides a schematic of the receptor, along with depictions of the possible enantiomers I and II, as well as achiral molecule III. The model predicts that to achieve maximal effect, A, B, and C must align with A′, B′, and C′, respectively.

Affinities for each enantiomer can be calculated and compared to yield a 'eudismic ratio' to describe the pharmacological activity between two enantiomers of a drug. The enantiomer exhibiting highest affinity and therefore the highest level of complementarity to the binding site, is known as the 'eutomer.' The lowest affinity enantiomer with the poorest degree of complementarity is known as the 'distomer.'[99,104] Pfeiffer demonstrated that a decrease in the ratio of activity of eutomer:distomer (eudismic ratio) was correlated with a decrease in drug potency and an increase in the total dosage of racemate necessary to elicit a response. In summary, Pfeiffer's Rule states

that in general a greater eudismic ratio is associated with greater potency of drug response at the desired receptor.[105]

Preliminary Data

In order to determine if eudismic ratios were detectable in our series, Jenny Ryu synthesized enantiomers of **100602** using commercially available (*S*)- and (*R*)-nipecotic acid affording analogs **100687** and **100688**, respectively. Unfortunately, these enantiomers showed no apparent stereorecognition by the molecular target.

Table 3.7. Effects of Chirality on Transcription and Cytotoxicity in Transfected PC-3 Cells

Cmpd No	Structure	IC_{50} SRE.L (μM)[a]	% inh SRE.L (100 μM)[a]	% inh WST-1 (100 μM)[a]
100602	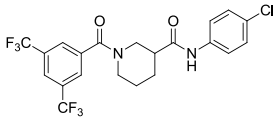	9.8	78	14
100687	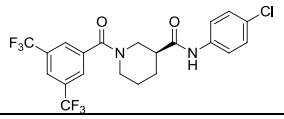	9.8	78	5
100688	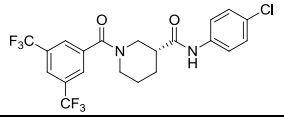	9.7	90	7

[a]Refer to Table 2.1 for assay descriptions

Further Exploration of Stereochemical Recognition

We decided to further explore stereochemical recognition by synthesizing enantiomers of the more rigid five-membered ring analog **203606** (Table 2.6). The enantiomeric synthesis is summarized in Scheme 3.3. Synthesis began with (*R*)-hydroxypyrrolidin-2-one (**49**) which underwent a modified Goldberg reaction[106] to afford amidation product **50** which was then converted to the tosylate (**51**) and displaced by azide to yield sterochemically inverted azide **52**. Conversion to the mesylate followed by azide displacement was also explored. However, elimination products were observed immediately and were the major products found. The tosylate still afforded an approximately 1:1 ratio of eliminated:desired product. However, purification methods effected separation of the two materials. Palladium catalyzed hydrogenation at

atmospheric pressure provided amine **53**. Close monitoring of hydrogenation was necessary, as lengthy hydrogenation reduced the chloro moeity. Acylation of the free amine with 3,5-bis(trifluoromethyl)benzoyl chloride afforded the desired enatiomeric product **206684**. The other enantiomer was prepared analogously.

In order to confirm chiral integrity, we prepared Mosher amides[107] using each enantiomer of amine **53** to prepare analogs **208802** and **208805** (Scheme 3.4). We then examined each by proton and fluorine NMR, which confirmed only one enantiomer was present in each sample.

Scheme 3.3. Enantiomeric Synthesis of Analog 203606

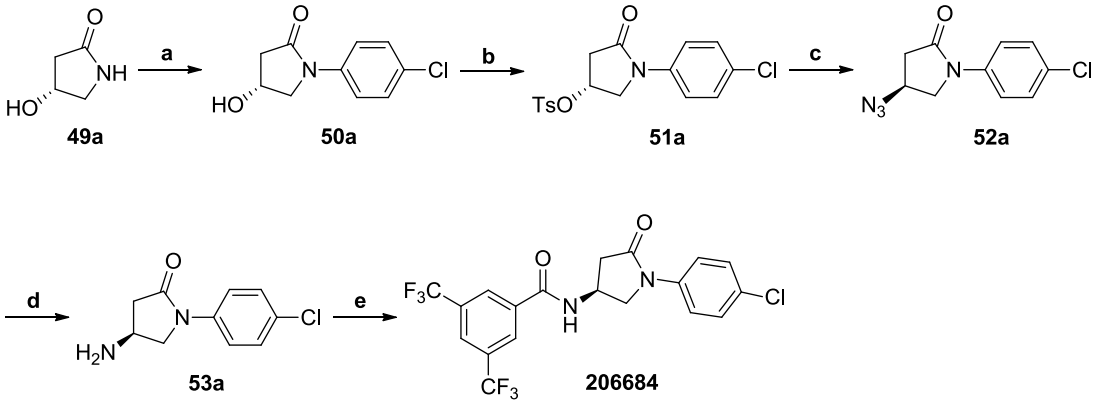

Reagents and conditions: (a) 4-ClPhI, CuI, K_3PO_4, *trans*-1,2-diaminocyclohexane, Dioxane, 110°C; (b) TsCl, Pyr, RT; (c) NaN_3, DMSO, RT; (d) 10% Pd/C, H_2, atm, MeOH, RT; (e) 3,5-bis(CF_3)PhOCl, DIPEA, DCM, RT

Scheme 3.4. Synthesis of Mosher Amides

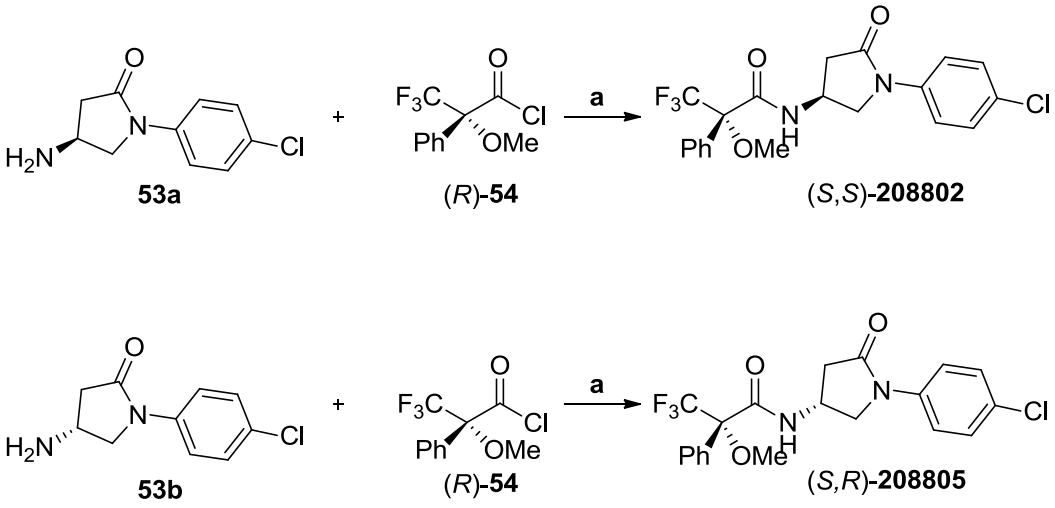

Reagents and conditions: (**a**) DIPEA, DCM, RT

Additionally, we determined the eudismic ratio of enantiomers of **203971**. Compounds **206116** were synthesized using the same chemistry as used in the preparation of the acid libraries (Scheme 3.1) starting with (*R*)- and (*S*)-nipecotic acid, respectively. Furthermore, pharmacophore modeling (Chapter 5) suggested that due to the similarity of the aromatic rings, our compounds have the potential to flip orientation in the binding pocket. Therefore, we investigated the enantiomers of the more unsymmetrical analog **206114**. The synthesis also followed that in Scheme 3.1 using the appropriate enantiomer of the starting acid.

Table 3.8 summarizes the effects of the synthesized enantiomers of **203606**, **203971**, and **206114**. In each of the comparisons, a very small chiral preference was found. For enantiomers of **203606** (**206684** and **206685**) and **203971** (**206116, lots 380445** and **380439**), preference was shown towards the (*S*)-enantiomer. For enantiomers of **206114** (**206686** and **206687**), slight preference was shown for the (*R*)-enantiomer. However, the eudismic ratios were all well below 10, consistent with the relatively low potencies (micromolar) of the racemates, and perhaps indicating that the overall binding affinity is poor or that less than three points of attachment are being made with the receptor.

Table 3.8. Effects of Single Enantiomers on Transcription and Cytotoxicity in Transfected PC-3 Cells

Cmpd No	Structure	IC_{50} SRE.L (μM)[a]	% inh SRE.L (100 μM)[a]	% inh WST-1 (100 μM)[a]
206685	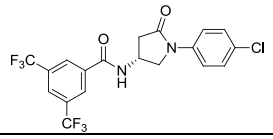	11	66	3
206684	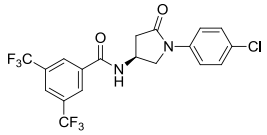	8.2	74	3
206116 Lot 380445	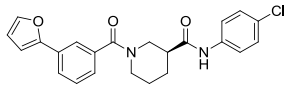	8.2	87	0
206116 Lot 380439	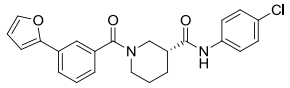	14	83	0
206686	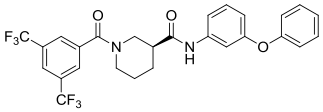	4.0	46	0
206687	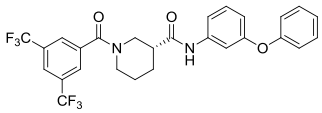	2.9	60	0

[a]Refer to Table 2.1 for assay descriptions

Further Exploration of 203971

Analog **203971**, the best performing analog of the acid library series, showed two-fold activity improvement as well as a slight increase in efficacy with no cytotoxicity in PC-3 prostate cancer cells. We examined the effect of **203971** (Table 3.2) on the migration of PC-3 prostate cancer cells in comparison to less active analog **100594** (Table 2.1), with the results shown in Figure 3.7. Detailed scratch assay conditions can be found in the experimentals described in Chapter 6. Panel A shows the scratch assay at time 0 h and 24 h using DMSO as a control. Compounds **203971** and **100594** were applied at 10 μM concentrations. As illustrated by the graph in panel B, significantly inhibits migration in PC-3 prostate cancer cells following 24 h treatment. We also intend to perform the scratch assay on the remaining compounds found in Table 3.6.

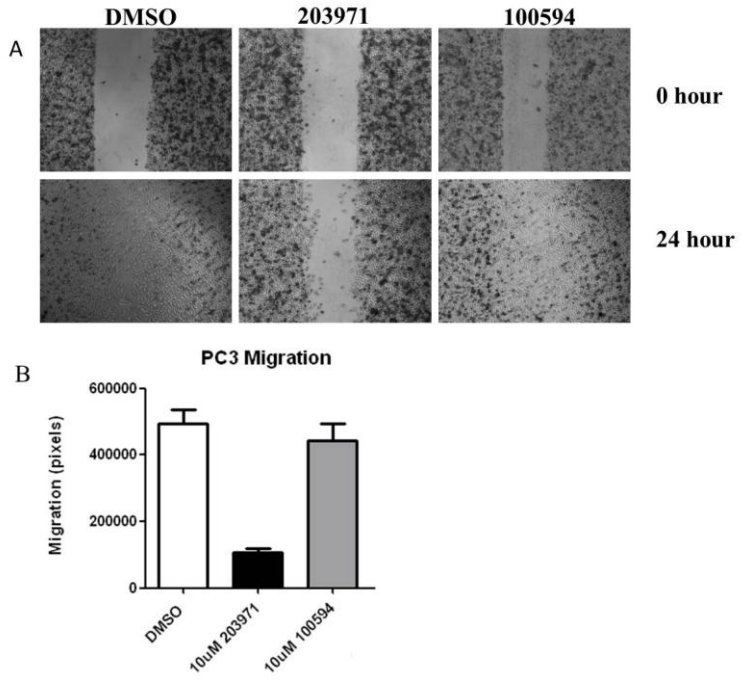

Figure 3.7. Scratch Assay Using PC-3 Prostate Cancer Cells. Panel (**A**) shows cells at time 0 h and the migration of cells following 24 h incubation using DMSO, 10 μM **203971**, and 10 μM **100594**. Panel (**B**) graphically depicts the migration after 24 h, as determined by pixel count.

Upon the initial discovery of **1423**, the Neubig laboratory also observed that it had an effect on the RhoC-overexpressing melanoma cell lines A375M2 and SK-Mel-147.[62] Therefore, we also tested **203971** in the RhoC-SRE.L assay using transiently transfected SK-Mel-147 cells. We observed similar results to the PC-3 cell line, with **203971** displaying an IC_{50} of 5.3 μM and no WST-1 cytotoxicity (data not shown), exhibiting its potential as an inhibitor of metastatic melanoma. The compound has also shown promise in other RhoC-overexpressing cancer targets, which will be disclosed in future publications.

Unfortunately, initial compound **1423** displayed significant *in vitro* and *in vivo* cytotoxicity (Table 2.1) and was therefore too toxic to use in *in vivo* studies. On the other hand, acid library analog **203971** demonstrated single-digit micromolar potency without any cytotoxicity up to 100 μM concentration (Table 3.2). Therefore, we conducted preliminary toxicity studies using the less toxic compound **203971**. A 5-day chronic dosing study was conducted with compound administration at 10, 20, 50, and 100 mg/kg

dissolved in 50 μL of dimethyl sulfoxide (DMSO) per day using 3 mice per dose. Following sacrifice on the 8th day, the mice were weighed and blood samples were collected. Dissection was performed, and the internal organs were weighed and examined for abnormalities. Weight was maintained over the course of the study, with the only abnormality observed being a slight increase in liver weight. All mice survived the 5-day study without any noted abnormal behavior, indicating tolerability. The serum samples were also submitted for determination of drug levels. A single intraperitoneal (IP) dose of 100 mg/kg provided maximum serum levels 3 to 5 times higher than the *in vitro* IC_{50}, indicating its potential use for further *in vivo* studies.

*Future Direction for **203971***

Based on the positive tolerability results, we are currently assessing standard pharmacokinetic parameters as well as the relative bioavailability of **203971**. These results will dictate the feasibility of further *in vivo* exploration such as assessment of treatment regimen as well as the optimal method of administration. Our lab has also recently established an assay to examine metabolic stability. We intend to examine our lead compounds, including **203971**, in our metabolic assay. If further *in vivo* testing is viable, we will move into melanoma xenograft studies.

Future Direction: Third Point of Diversity

Our investigation of the enantiomers of **100602**, **203606**, **203971**, and **206114** resulted in compounds with low micromolar potencies and no apparent stereorecognition by the macromolecular target. The poor potencies and lack of stereo-differentiation may indicate less than three points of attachment are being made with the receptor. Therefore, we intend to pursue installation of a third point of diversity to provide the necessary third interaction. We intend to use conformationally restricted analog **203971** to further probe this third point of diversity.

We envision the synthesis proposed in Scheme 3.5. Our progress to date is summarized here. First, 3,5-pyridinedicarboxylic acid is esterified to provide diester **56**[108] which is then treated with potassium hydroxide to form monoacid **57**.[109] The acid then undergoes Curtius rearrangement to the isocyanate, which is trapped by *t*-butanol to afford Boc-protected intermediate **58**. Ester **58** is saponified to afford free acid **59**[110],

which is then hydrogenated using Rhodium on Alumina to afford a single diastereomer (presumably *cis*-) **60**.[111] Acylation with 3-(furan-2-yl)benzoyl chloride followed by amidation with 4-chloroaniline under standard EDC/HOBt-mediated coupling conditions provides intermediate **62**.

We anticipate that deprotection of the primary amine will provide key common intermediate amine **63**, and that various functional groups can then be added via acylations, sulfonylations, reductive aminations, etc. Because only one diastereomer is afforded using the above hydrogenation conditions (presumably *cis*-), it will be necessary to independently prepare the *trans*-isomer for further exploration.

Scheme 3.5. Proposed Synthesis for Third Point of Diversity Using 100602 Template

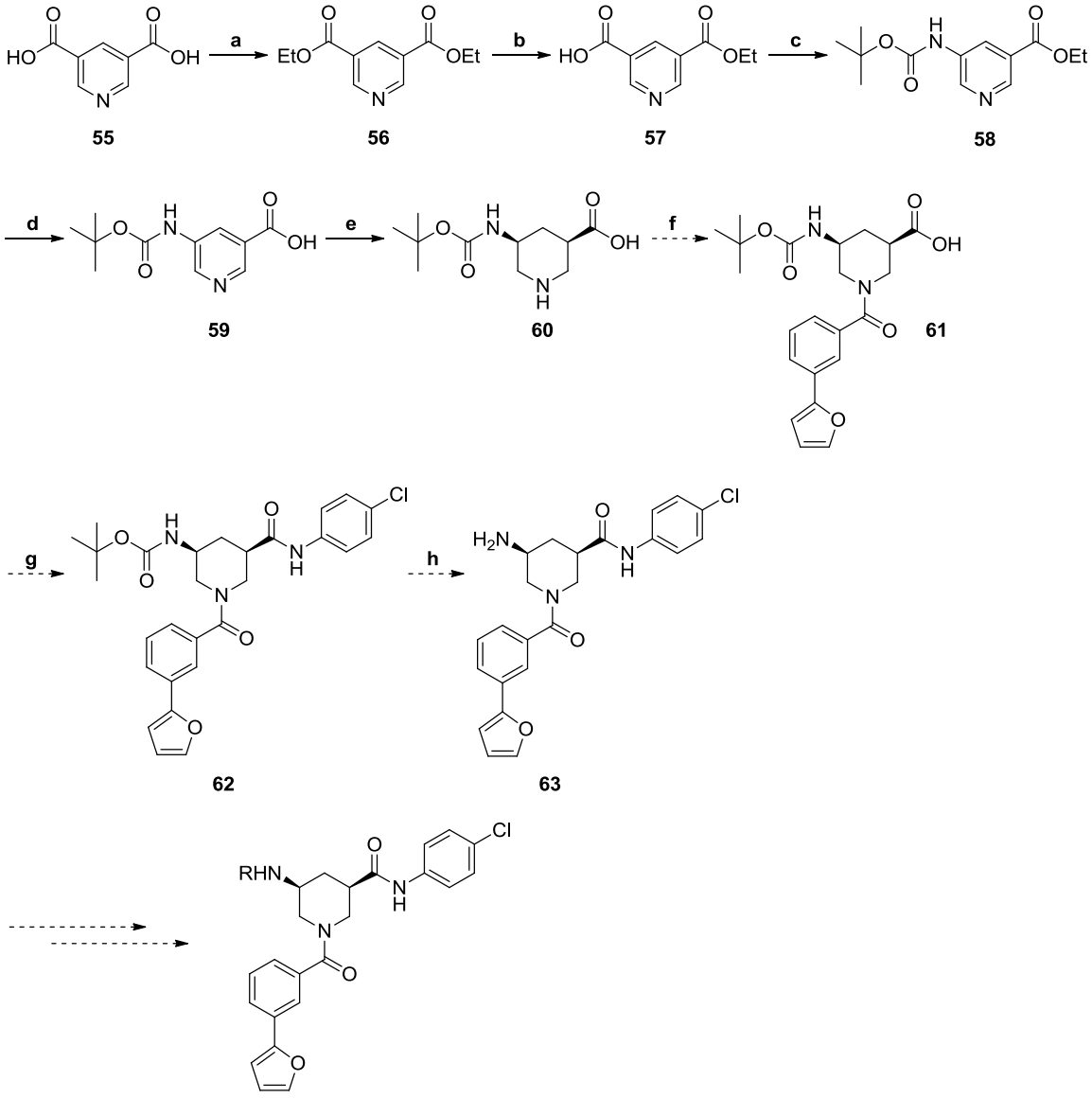

Reagents and conditions: (a) $SOCl_2$, EtOH; (b) KOH, EtOH, $CHCl_3$; (c) DPPA, TEA, *t*-BuOH; (d) NaOH, MeOH, RT; (e) Rh–Al_2O_3, H_2O, NH_4OH, H_2, 40 psi, 72h; (f) *m*-FuranylPhCOCl, TEA, DCM; (g) 4-ClPhNH_2, EDC, HOBt, DIPEA, DCM; (h) TFA, DCM, -10 °C

Chapter 4
Photoaffinity Reagents

In 2007, the Neubig lab identified small molecule **1423** as an inhibitor of RhoA transcriptional signaling in HEK293 cells using a high-throughput screening assay. Mechanistic analysis demonstrated that **1423** acts downstream of RhoA and targets MKL/SRF-dependent transcriptional activation. However, the exact mechanism of action has not yet been deciphered. Their findings suggest that **1423** could affect the functions of MKL1 in various ways, including preventing its release from actin; blocking translocation from the cytoplasm to the nucleus; repressing transcription via increasing sumoylation; disrupting the interaction between MKL1 and its transcoactivator SRF, or inhibiting its coactivator function.[62] Due to the multitude of effectors activated by the RhoA family, determining the exact role of the signaling cascade in cancer is convoluted. However, discovery of **1423** as an inhibitor of Rho-mediated gene transcription and our further optimization into more potent and specific analogs with low cytotoxicity may allow us to probe its mechanism of action and identify its macromolecular target(s).

Identification of the macromolecular target(s) of our small bioactive molecules would allow us to employ rational and structure-based drug design to create more potent and selective therapeutics for the treatment of RhoA-related cancers. There are several methodologies one can use to identify target proteins. Our interests focus on three such strategies that include affinity matrices, biotinylated reagents, and tag-free photoaffinity probes. Each approach has advantages and disadvantages, which will be discussed in subsequent sections. Following the isolation and purification of a target protein, its identity can be determined using immunohistochemical analysis, peptide microsequencing, or modern degradative mass spectrometry.[112] These techniques will not be discussed in detail. However, we plan to employ mass spectrometry for protein identification.

Affinity Matrices

The preparation of affinity matrices is the simplest method for protein identification and is achieved by the attachment of modified lead compounds to a solid support. These supports are usually agarose[113] or sepharose[114] beads that can contain various functional groups for easy ligand attachment. The support is then incubated with cellular lysate to allow protein binding. Following incubation, the resin and bound protein are isolated (simple filtration) and are washed repeatedly using aqueous buffer. The washing steps remove any nonbinding proteins, affording only proteins that are bound to the desired ligand or nonspecifically to the matrix. Binding proteins can then be eluted from the resin through incubation with free ligand or under denaturing conditions.[115] The protein can then be isolated via sodium dodecyl sulfate polyacrylamide gel electrophoresis (SDS-PAGE) and subjected to various techniques for identification.

Solid supports such as agarose and sepharose are designed to prevent nonspecific binding of hydrophobic or charged proteins.[112] However, such nonspecific interactions still occur with the matrix. Therefore control matrices should be used to help determine binding specificity. Construction of a control matrix can be executed using a resin-only control or an inactive compound control. A resin-only control can be prepared by using a resin-appropriate blocking agent to cover any activated sites following ligand loading. This leads to charge minimization, which minimizes nonspecific protein interactions.[112] An inactive compound control provides a better comparison for specificity and should be constructed by immobilizing a compound on the resin that is similar to the active ligand, but is inactive itself. The optimal molecule would be an inactive enantiomer of the lead compound; however, structurally similar compounds can work.[116] The gels are then compared, and proteins appearing in both would be considered nonspecific binders.

Another control experiment to determine specificity of binding is a competition experiment in which excess free ligand is incubated with the lysates and ligand-bound affinity matrix.[117] The excess free ligand binds the target protein, preventing it from interacting with the resin. Therefore, upon comparing gels, certain protein bands would no longer be present, indicating a specific interaction with the small molecule.

There are several limitations to using affinity matrices. One significant limitation is the inability to determine ligand binding ability after it has been attached to the solid-

phase resin. To address this issue, hydrophilic polyethylene glycol (PEG) linkers have been utilized to attach the ligand to the resin.[112, 117] Activity can then be estimated following installation of a model PEG linker to ensure binding potential is not lost. Additionally, the hydrophilicity of the PEG linker minimizes nonspecific binding, and the spacer projects the ligand away from the resin. This spacer distance has been shown to be crucial for reducing steric hindrance as well as providing conformational flexibility for binding.[118]

Another limiting factor for affinity matrices is the affinity of the ligand for its target. It is best to use a potent molecule with presumably high affinity and selectivity for the target.[116,117] High binding affinity is necessary to preserve protein binding interactions during extensive washing steps required for removal of nonbinding proteins.[112] Therefore, this is a major consideration when determining the proper isolation method.

Preliminary Results

Due to our lack of knowledge regarding the cellular target(s) of the **1423** series and their respective binding affinities, we decided to explore all three affinity methods previously mentioned, starting with affinity matrices. As previously discussed, a spacer unit is necessary to minimize the potential interference of the solid support on binding of the ligand. Most importantly, the spacer must be positioned on the small molecule in a manner that would permit retention of reasonable biological activity.[112] Determination of these potential positions can be done in one of two ways. One, SAR data can provide information regarding the areas that are tolerant to modifications. However, this may require a large amount of prior analog synthesis. We employed a second option that utilized active analogs to append functionality that mimics the spacer unit at various locations on the molecule. Compounds that retained a majority of their activity were then to be used as scaffolds for the preparation of affinity reagents.

In preliminary work, Jenny Ryu synthesized a limited number of analogs of **100596** (Table 2.1) to determine what potential linking functionality could be appended to the chloro-substituted aromatic ring without loss of activity. The groups extending from the aromatic ring explored included –NHAc and –COHNEt, –EtSMe, and –$COCH_2OMe$, and –OMe (data not shown). Only the aromatic methoxy group retained

activity. These observations were then incorporated into the design of our affinity reagents.

Affinity Linker SAR

In order to prepare our active affinity reagent, we selected **100602** to perform preliminary SAR exploring methoxy substitution. While **100602** is less potent than **1423**, it is more selective and less cytotoxic. We observed that placing the methoxy group in the *para*-position on the aromatic ring is superior to the *meta*- position in terms of selectivity over nonspecific gene transcription (pRL-TK *Renilla*) inhibition (Table 4.1). Therefore, our active affinity matrix was based on **101331**.

Following identification of the active ligand, we wanted to select a similar "inactive compound" to function as a negative control. While the ideal inactive molecule would be the distomer of an enantiomeric pair, **100602** maintained a low eudismic ratio, showing no stereochemical recognition. Therefore, we opted to investigate a highly similar acyclic compound **100686**, which differs only by one bridging methylene unit and lacks significant biological activity up to 100 μM (Table 4.1, Figure 4.1). Appending a methoxy group in either the *para*- or *meta*-position reintroduces a small amount of activity. However, we opted to base our affinity reagents on **101339**, the least active compound with the methoxy in the *para*-position.

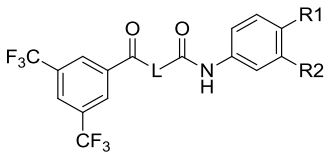

Table 4.1. Affinity Linker SAR

Cmpd No	L	R1	R2	IC_{50} SRE.L (μM)[a]	% inh SRE.L (10, 100 μM)[a]	% inh pRL-TK (10, 100 μM)[a]	% inh WST-1 (10, 100 μM)[a]
100602[b]	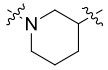	-Cl	-H	9.8	38, 78	20, 34	0, 14
101331	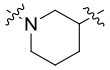	-OMe	-Cl	6	28, 28	4, 6	0, 0
101341	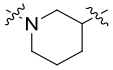	-Cl	-OMe	5	29, 42	15, 15	0, 0
100686[a]	$-NHCH_2CH_2CH_2CH_2-$	-Cl	-H	-	0, 11	0, 14	0, 0
101337	$-NHCH_2CH_2CH_2CH_2-$	-Cl	-OMe	10	18, 46	0, 20	0, 10
101339	$-NHCH_2CH_2CH_2CH_2-$	-OMe	-Cl	20	3, 22	0, 14	0, 0

[a]See Table 2.1 for assay descriptions [b]Synthesized by Jenny Ryu

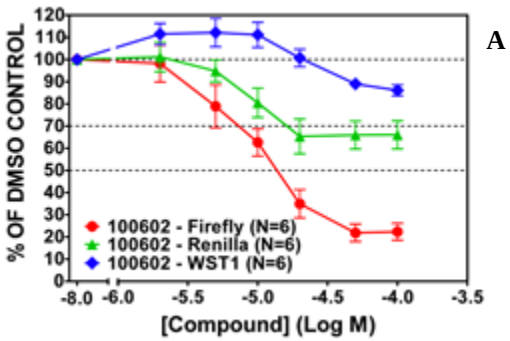

A

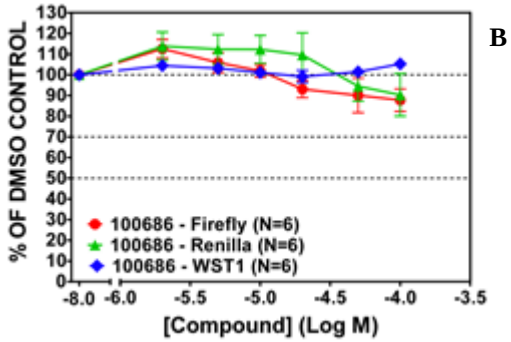

B

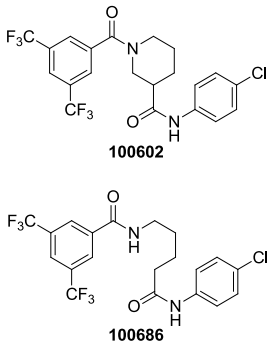

C

Figure 4.1. Active and Inactive CCG-1423 Analogs Selected for Use in Affinity Reagents

(**A**) Active compound **100602** shows good inhibition of SRE.L (Firefly), low cytotoxicity (blue), and modest selectivity of SRE.L versus TK-*Renilla* (green); (**B**) Inactive compound **100686** shows no activity (SRE.L) up to 100 M; (**C**) Structures of active analog (**100602**) and inactive acyclic analog (**100686**)

Initial affinity matrix experiments were carried out by Andrew Haak in the Neubig lab. Agarose beads functionalized with 1,1′-carbonyl diimidazole were coupled through a carbamate bond with active ligand amine **203883** (prepared in Scheme 4.1) to afford the "active" affinity matrix **64** (Figure 4.2). By a precisely analogous route, "inactive" control matrix **65** was prepared starting with 5-aminopentanoic acid instead of nipecotic acid (Scheme 4.1). A third set of blank beads was also used. The remaining active sites on each set of beads were blocked using ethanolamine. Approximately 30 milligrams of total cytosolic and nuclear protein were isolated from roughly 100 million prostate cancer cells. Ten milligrams of protein were incubated with approximately 150 µL of each set of beads. Following incubation, each batch was centrifuged, and the lysate was removed. The beads were then washed with a combination of high and low NaCl buffered solution to removed nonspecific binding. Proteins were then eluted from the solid phase using Laemmli buffer, and samples were run on an SDS page gel. The gel was stained using Coomasie for visualization.

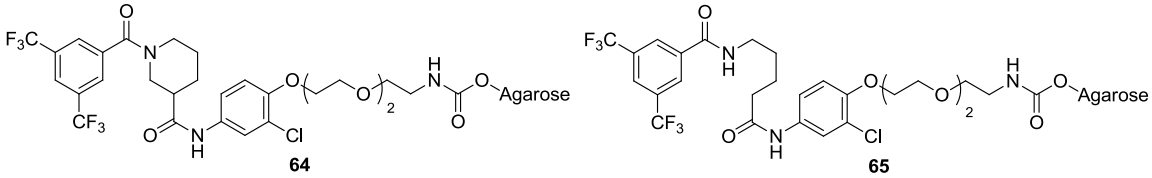

Figure 4.2. Active and Inactive Affinity Matrices Based on 100602 and 100686. Both analogs are linked to agarose beads.

The active ligand sample generated a protein band. Unfortunately, this band was also observed in both the inactive compound as well as the blank control, indicating a nonspecific binding interaction. Due to the modest potency of our compound (9.8 µM, Table 4.1) coupled with the extensive washing steps, we do not believe this is the optimal technique for target identification. Therefore, we made no additional attempts to optimize our affinity matrix experiments.

Biotinylated Reagents

The second technique we were interested in is the use of biotinylated reagents for target identification. Biotinylated reagents offer one major advantage over matrices – they are soluble. Binding of target proteins to a soluble probe may be more facile than binding to a resin-bound probe. Following incubation of reagent with cell lysates, the

probe containing the binding partner(s) can be isolated using a streptavidin resin. Furthermore, incorporation of biotin allows visualization through the use of antibodies against biotin or the use of labeled streptavidin.[112]

Despite significant advantages, there are drawbacks to biotinylated probes. One drawback is that incorporation of biotin likely decreases cell permeability, which prevents their use in whole cells. Furthermore, their incorporation often requires the use of high-boiling solvents due to the poor solubility of biotin in organic solvents. However, this can be overcome by attachment late in probe synthesis.[112]

Based on the previous affinity linker SAR (Table 4.1), we set out to make the biotinylated reagents shown in Figure 4.3. We again incorporated the PEG linker for the same reasons as described above for the affinity matrices and utilized **100602** and **100686** to generate "active" (**203602**) and "inactive" (**203600**) probes, respectively.

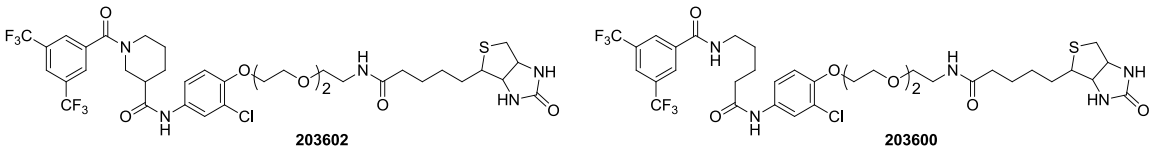

Figure 4.3. Biotinylated Reagents 203602 and 203600

Scheme 4.1 provides the synthesis of active biotinylated reagent **203602**. Synthesis began with nipecotic acid **42**, which was acylated with 3,5-(bistrifluoromethyl)benzoyl chloride to afford acid **48**. Amidation of **48** with **66** was achieved using CDI-mediated coupling[119] to afford amide **67**. The phenol of **67** was alkylated[120] using mesylate **68**[121] to install the hydrophilic linker, yielding **69**. Deprotection followed by biotinylation afforded final affinity reagent **203602**. Inactive probe **203600** was prepared following the same synthetic scheme starting with 5-aminopentanoic acid instead of nipecotic acid.

The final active and inactive probe molecules were submitted to the Neubig lab for testing. However, due to the lack of success with the affinity matrices and our compounds' potentially poor affinity, we decided not to pursue this technique for target identification at this time.

Scheme 4.1. Synthesis of Biotinylated Reagent 203602

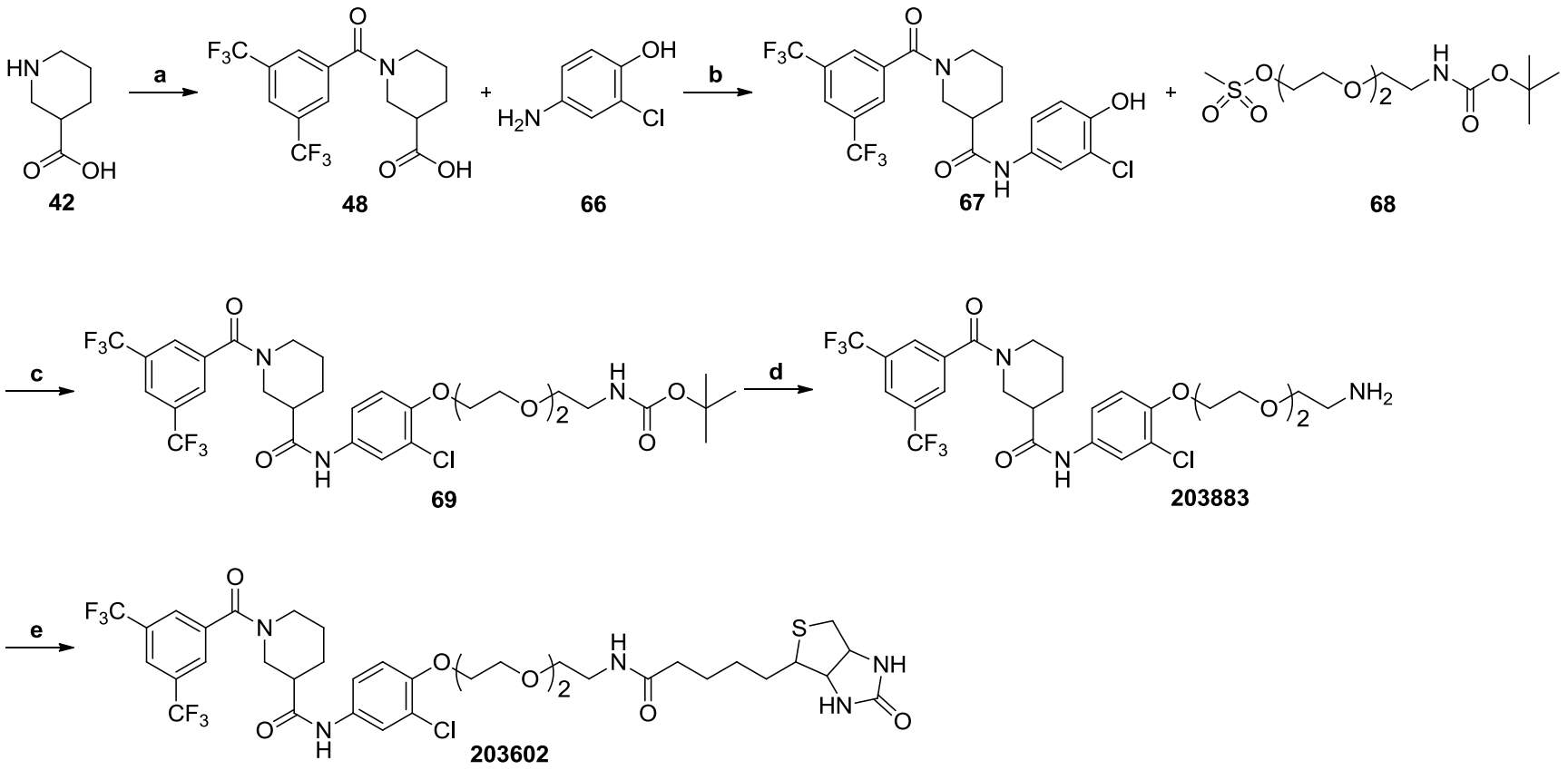

Reagents and conditions: (a) 3,5-bis(CF_3)PhCOCl, 2M NaOH; (b) CDI, THF, RT to 62 °C; (c) Cs_2CO_3, DMF, 75 °C; (d) TFA, DCM, RT; (e) Biotin-OSu, DMF, RT

Tag-free Photoaffinity Probes

As previously mentioned, a high binding affinity of a small molecule ligand for its target is vital to achieving isolation following repeated washing procedures. Because we do not know the affinities of our compounds for their target(s) and because we were unable to successfully isolate specifically bound proteins, we cannot discount loss of binding interaction as being responsible. However, maintenance of such interactions can be permanently achieved through incorporation of cross-linkable functionality into our proposed affinity reagents. Current literature provides multiple examples of successful applications of such reagents incorporating photolabile functionalities such as azides, diazirines, and benzophenones.

Figure 4.4 summarizes how tag-free photoprobes can be utilized in whole cells for target identification. The colors used in the cartoon correlate with the colors used in the molecular structures. First, a photolabile group is appended to a desired active ligand, as depicted in blue. Additionally, a low-molecular weight reactive handle is attached to complete the photoprobe. In this instance, the handle is an acetylene, as shown in purple. After confirming its activity, the photoprobe is incubated with whole cells, allowing the small molecule to interact with its target (light green) under physiological conditions. Following binding, UV irradiation is applied that converts the photolabile group into a highly reactive species that can covalently link the probe to its target. This irreversible modification will allow the application of extensive washings without the fear of losing the interaction between the small molecule and the target protein.[112] The cells are lysed, and the handle can then be used with Click-chemistry to append biotin for streptavidin-mediated isolation or to append a fluorophore for visualization. The desired protein can then be isolated and determined using mass spectroscopy.

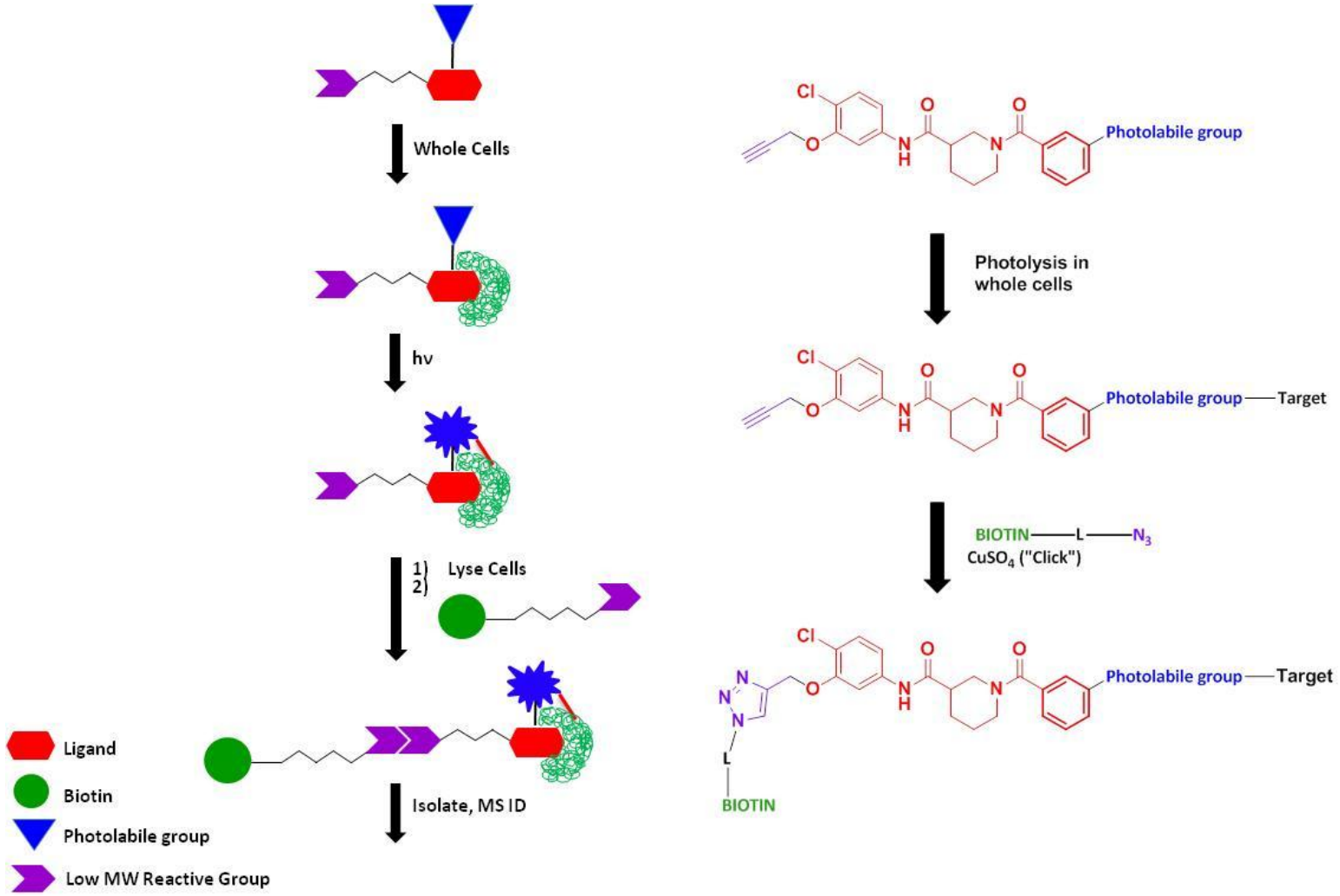

Figure 4.4. Tag-free Photoprobes for Target Identification in Whole Cell

The selection of cross-linking functionality and its distance from the small molecule ligand are also crucial for the outcome of an affinity isolation experiment. Based on their synthetic ease, we initially examined two different photolabile groups, an azide and a benzophenone. As previously described for the other affinity reagents, we prepared the active reagents based on compound **100602** and inactive reagent based on acyclic **100686**. Compound **203972** (Table 3.2), as prepared in the acid library, contains a modification to **100602** that includes a benzophenone moiety. *Analog **203972** was one of the most active analogs in our library, confirming its potential as a photoaffinity reagent.*

Benzophenone Probes

The use of benzophenones for target identification is advantageous for several reasons. One advantage is their superior stability that allows their use under ambient light, unlike aryl azides and diazirines. Furthermore, activation of benzophenones is achieved at around 350 nm. This prevents damage to most proteins, which absorb ultraviolet radiation only at wavelengths less than 300 nm.[122,123] Finally, benzophenones insert into unreactive C-H bonds, both in aqueous media and in the presence of nucleophiles.[122] These properties afford efficient labeling[124] of C-H bonds within 3.1 Å[123] that is site specific.[122]

Figure 4.5 provides the accepted mechanism for benzophenone photochemistry. Upon irradiation with ultraviolet light, the benzophenone containing ligand (**70**) forms a diradical species (**71**) that abstracts a hydrogen from a nearby protein to generate a ketyl radical and a protein radical (**72**). The pair of radicals can then recombine to form a cross-linked C-C bond that irreversibly labels the protein (**73**).[125]

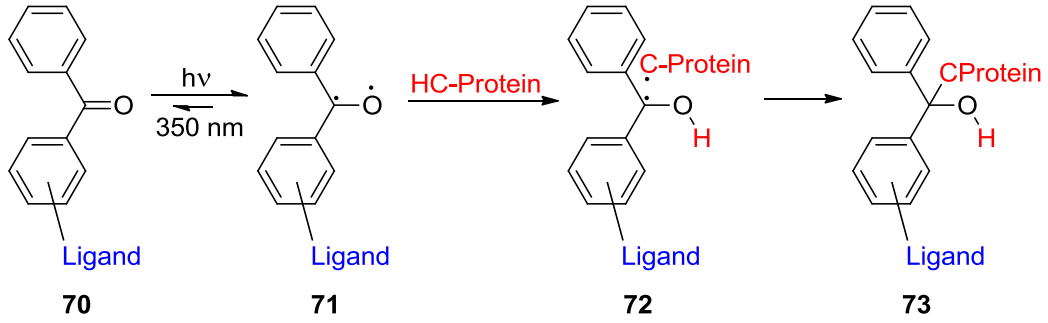

Figure 4.5. Photoaffinity Labeling Steps Using Benzophenone. Probe-containing ligand **70** is photolyzed to form a diradical (**71)** that abstracts a hydrogen from a nearby protein to form a ketyl and a protein radical (**72**). The pair of radicals recombine to form cross-linked protein **73**.

In order to determine potential activity of our desired probes, we synthesized model molecules that installed a methoxy group to function as a propargyloxy mimic. Both the model probes (black) and completed photoaffinity probes (blue) are shown in Table 4.2. We utilized **203972** as a template to explore various aspects of our probes. First, we examined the optimal position of the chloro group on the aromatic ring by preparing *para*- (**206117**) and *meta*-chloro (**206118**) analogs. Second, we positioned the benzophenone on ring B (Figure 3.1) as shown by **206448**. Finally, we examined the linker length between the low molecular weight reactive propargyl group (**206558**) to provide a spacer region for application of Click chemistry following labeling.

Scheme 4.2 provides the synthesis of benzophenone precursor probes **206117** and **206118**, which examine the position of the chloro moiety. Synthesis was carried out starting with Boc-protected nipecotic acid (**43**) and the desired aniline isomer (**74** or **75**), which were subjected to standard amidation conditions to afford amides **76** and **77**, respectively. Deprotection followed by amidation with 3-benzoylbenzoic acid afforded final model analogs **206117** and **206118**, respectively.

Scheme 4.2. Synthesis of Model Benzophenone Probes 206117 and 206118

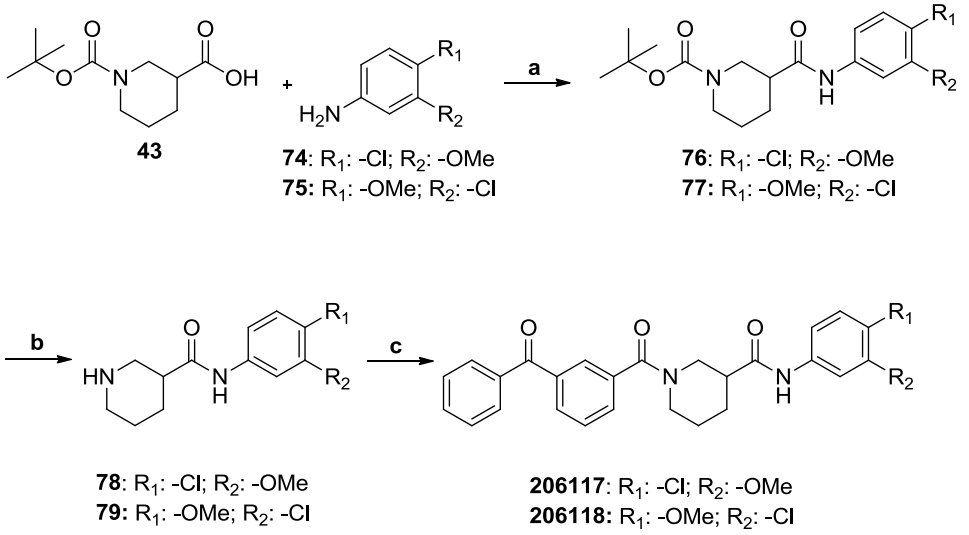

Reagents and conditions: (a) EDC, DMAP, DCM; (b) TFA, DCM, -10 °C; (c) 3-PhCO-PhCO_2H, EDC, DMAP, DCM

Table 4.2 summarizes the data for the benzophenone analogs. Models **206117** and **206118** both retained activity. Model **206117**, with the chloro group in the *para*-position was slightly more potent and efficacious. Therefore we synthesized the benzophenone photoaffinity probe **206454** with the chloro moiety in the *para*-position with the propargyl ether in the *meta*-position as shown in Scheme 4.3. First, 5-amino-2-chlorophenol was Boc-protected to afford intermediate **81**[126], which was then alkylated using propargyl bromide to afford propargyloxy **82**. Following deprotection of **82**, aniline **83** was coupled with Boc-protected nipecotic acid **43** to afford intermediate **84**. Deprotection followed by coupling with 3-benzoylbenzoic acid afforded final probe **206454**.

Scheme 4.3. Synthesis of Benzophenone Photoaffinity Probe 206454

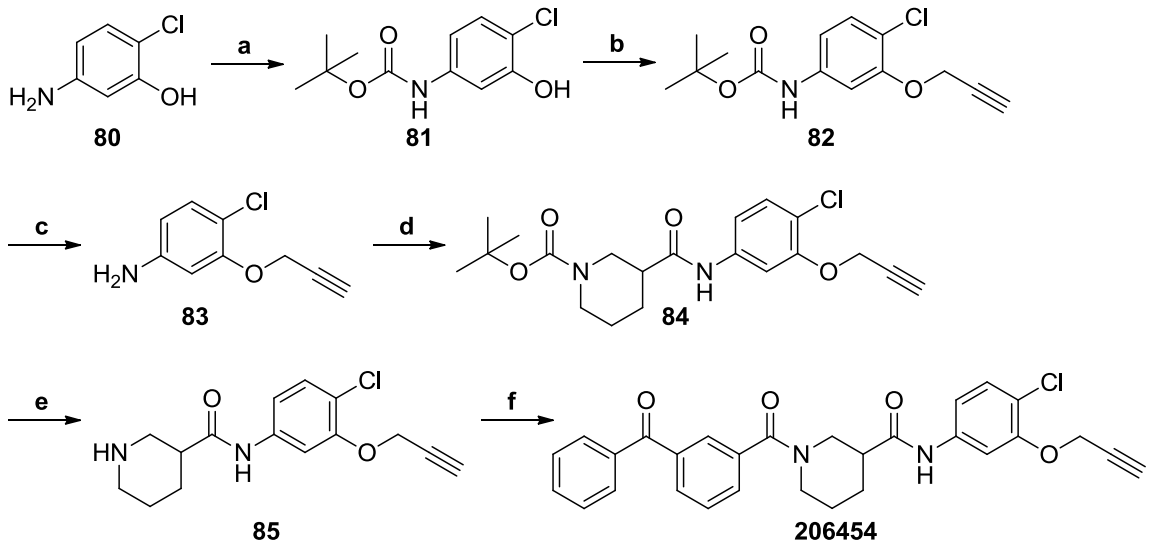

Reagents and conditions: (a) Boc_2O, THF, reflux; (b) $BrCH_2CCH$, K_2CO_3, Dioxane; (c) TFA, DCM, -10 °C; (d) **43**, EDC, DMAP, DCM; (e) TFA, DCM, -10 °C; (f) 3-PhCO-$PhCO_2H$, EDC, DMAP, DCM

Additionally, we synthesized a benzophenone photoaffinity probe with a longer linker unit (**206558**) to minimize steric hindrance if the Click chemistry step does not afford a good yield. The synthesis can be found in Scheme 4.4, which begins with tosylation of 2-(prop-2-yn-1-yloxy)ethanol (**86**), which was received from Bryan Yestrepsky. Alkylation of phenol **81** using **87**, followed by TFA deprotection afforded intermediate aniline **89**, which was then coupled with acid **43**. Boc-deprotection followed by standard EDC/DMAP-mediated coupling conditions with 3-benzoylbenzophenone afforded final compound **206558**. Fortuitously, both affinity reagents **206454** and **206558** were actually more potent than initial benzophenone **203972** and methoxy model analog **206117** (Table 4.2).

Scheme 4.4. Synthesis of Benzophenone Photoaffinity Probe 206558 Containing an Extended Linker Unit

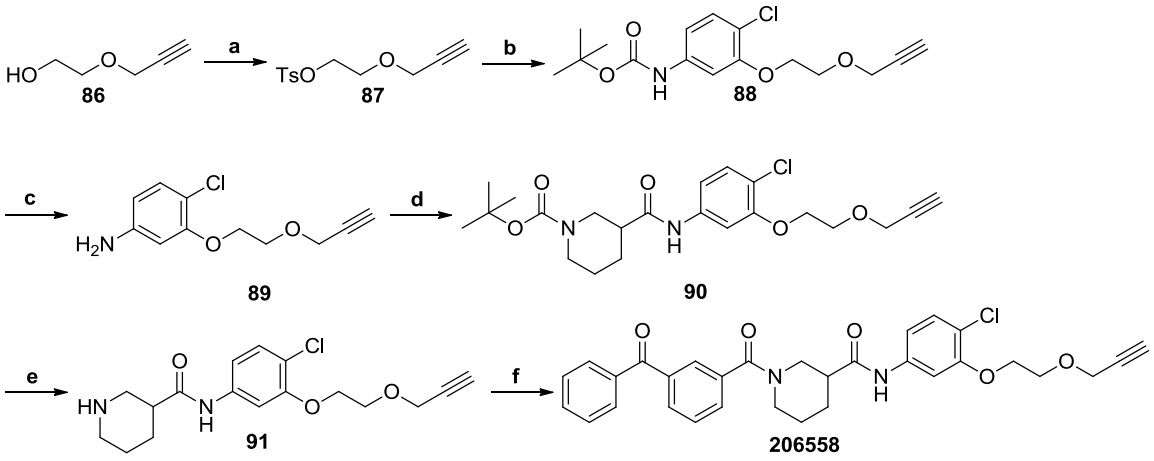

Reagents and conditions: (a) *p*-TsCl, Pyr, 0 to 4 °C; (b) **81**, Cs_2CO_3, DMF, 70 °C; (c) TFA, DCM, -10 °C; (d) **43**, EDC, DMAP, DCM; (e) TFA, DCM, -10 °C; (f) 3-PhCO-$PhCO_2H$, EDC, DMAP, DCM

In the aniline library (Chapter 3), we explored benzophenone placement on ring B (**206111**). Despite its inactivity (Table 3.3, Table 4.2), we synthesized precursor molecule **206448**, which placed a methoxy in the *meta*-position on ring A. The executed route to precursor **206448** is shown in Scheme 4.5. Starting aniline **91** was coupled with acid **43** under standard EDC/DMAP-mediated coupling conditions to afford intermediate **92**. After Deprotection, amine **93** was coupled with 3-methoxy-5-trifluoromethylbenzoic acid (**94**) to afford **206448**. The model analog regained activity, showing an IC50 of 5.3 μM. Therefore, we continued with the synthesis of full photoaffinity reagent (**206559**), which can be found in Scheme 4.6. Starting acid **100** was esterified to produce methyl ester **101**. The phenol was alkylated with propargyl bromide to afford ester **102**, which was then saponified to afford free acid **103**. The acid was then coupled with amine **98** under standard amidation conditions to afford final probe molecule **206559**. As is reflected in Table 4.2, **206559** is also active, allowing the benzophenone placement to be manipulated if additional optimization is necessary.

Scheme 4.5. Synthesis of Ring B Benzophenone Model Analog 206448

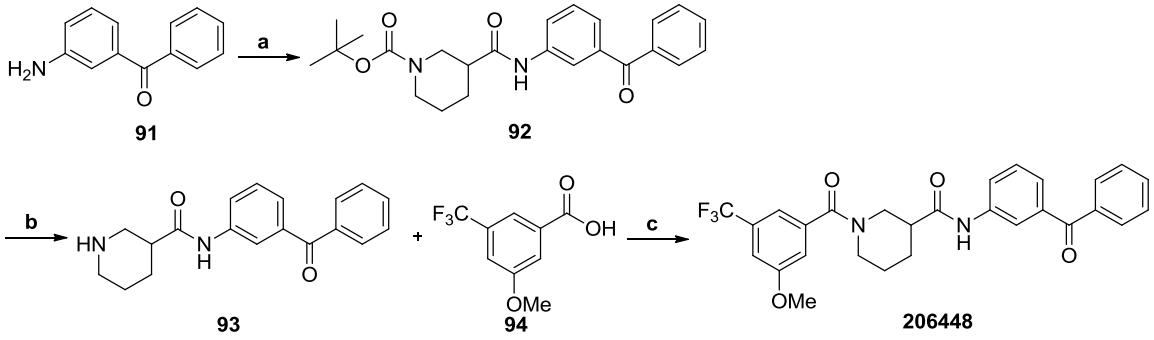

Reagents and conditions: (a) **43**, EDC, DMAP, DCM; (b) TFA, DCM, -10 °C; (c) EDC, DMAP, DCM

Scheme 4.6. Synthesis of Ring B Benzophenone Photoaffinity Reagent 206559

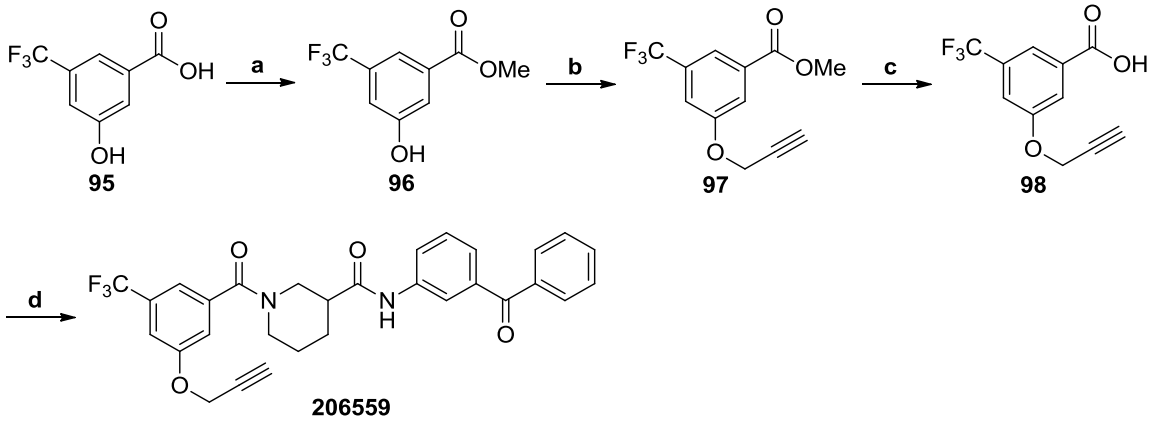

Reagents and conditions: (a) $SOCl_2$, MeOH, 0 °C to RT; (b) $BrCH_2CCH$, Cs_2CO_3, DMF, 70 °C; (c) NaOH, MeOH, H_2O; (d) **93**, EDC, DMAP, DCM

Table 4.2. Effects of Benzophenone Photoaffinity Models and Probes on Transcription and Cytotoxicity in PC-3 Cells

Cmpd No	Structure	IC_{50} SRE.L (μM)[a]	% inh SRE.L (100 μM)[a]	% inh WST-1 (100 μM)[a]
203972	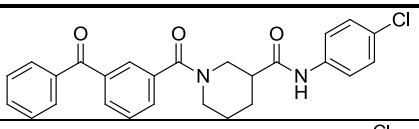	9.9	75	0
206117	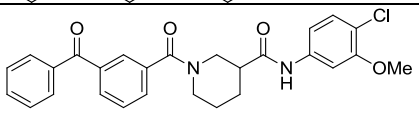	8.3	84	0
206118	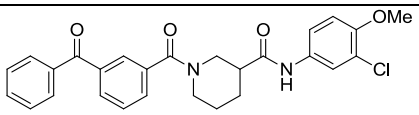	11	64	0
206454	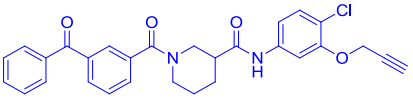	6.6	57	0
206558	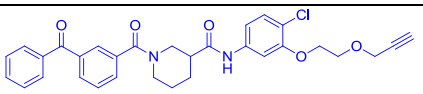	5.0	53	0
206111	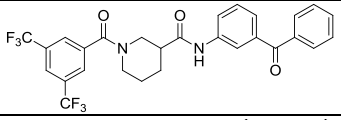	>100	ND	ND
206448	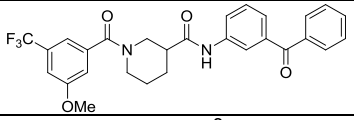	5.3	60	0
206559	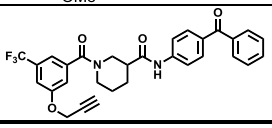	2.7	58	0

[a]Refer to Table 2.1 for assay descriptions. Final probes are colored blue.

Azide Probes

Next we explored probes containing aryl azides. There are several advantages to utilizing azides for labeling. An azide is relatively small and its incorporation provides minimal structural change to the starting compound. Furthermore, azides can afford greater solubility in comparison to other modifications. On the other hand, while many laboratories have exploited aryl azide chemistry, it has been noted that crosslinking efficiency is rather low.[112,124] Complexities and poor efficiency arise from the activation of such azides as depicted in Scheme 4.7.[123,124,127,128] Irradiation at wavelengths shorter than 280 nm produces formation of a singlet nitrene (**100**), which can intersystem cross (ISC) to the triplet ground state (**103**). However, at low temperatures (i.e. 77K), the

energy barrier necessary for this conversion is high and only the singlet is produced.[124] The singlet **100** undergoes rearrangement and ring expansion into ketenimine **101** that can be attacked by a nucleophilic nitrogen or oxygen of a protein to afford an azepine-labeled protein (**102**).[128] An additional complexity of utilizing azides for labeling is that the activation wavelength can cause damage of biological systems, which is undesirable.

Scheme 4.7. Aryl Azide Activation

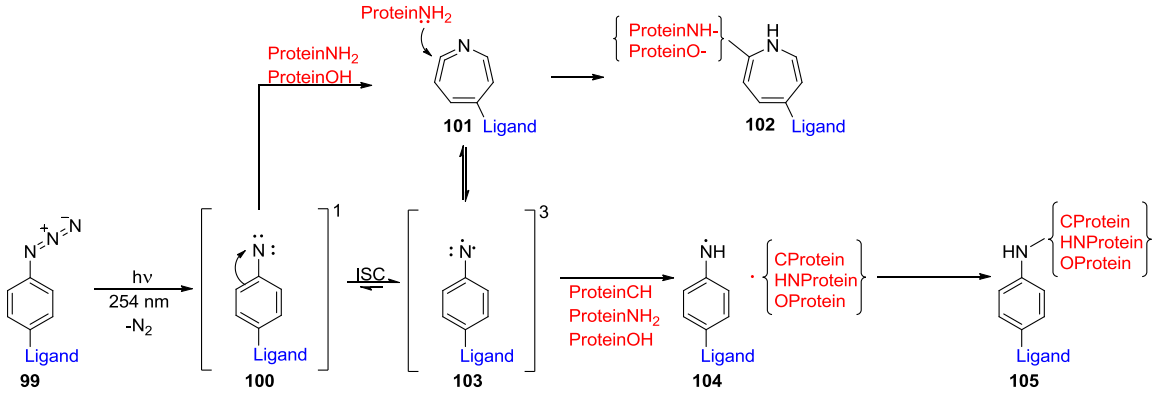

Similar to the preparation of the benzophenone analogs, we synthesized model and photoaffinity reagents using aryl azides, and the results can be found in Table 4.3. One model compound incorporating a methoxy substituent on ring A was prepared (**206449**). Scheme 4.8 provides the chemistry employed. Due to the sensitivity of aryl azides, all chemistry on azide-containing intermediates was executed in the dark. Synthesis began with the acylation of 4-chloro-3-nitroaniline (**106**) to provide intermediate **107**. The nitro group was then reduced using iron and hydrochloric acid to afford aniline **108**. The azido group was introduced by diazotization/azidation of **108**. Deacetylation with potassium hydroxide afforded aniline **110**, which was then coupled with **43** (Scheme 3.1) using standard amidation conditions. Deprotection of **111** followed by coupling with acid **94** afforded **206449**. As shown in Table 4.3, **206449** maintained activity in PC-3 prostate cancer cells. Therefore, the synthesis of aryl azide photoaffinity probe **206569** (Table 4.3) was carried out through coupling azide **112** (Scheme 4.8) with acid **98** (Scheme 4.6) under EDC/DMAP-mediated amidation conditions. Additionally, we investigated installation of the azide in ring A (**206452**). The synthetic route can be found in Scheme 4.9. Introduction of the azide in **114** was accomplished via diazotization/azidation of **113** followed by standard coupling conditions with **85** (Scheme

4.3) to afford final aryl azide photoprobe **206452**. As with aryl azide **206569**, photoaffinity probe **206452** retained activity (Table 4.3). However, it was the least potent of all of the photoaffinity reagents.

Scheme 4.8. Synthesis of Aryl Azide Precursor Analog 206449

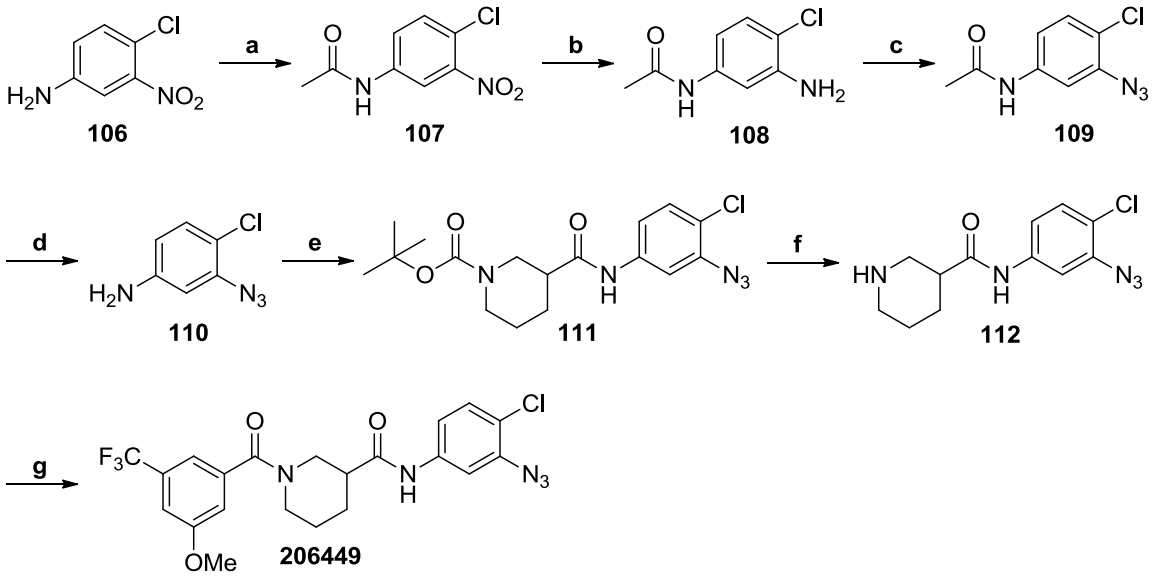

Reagents and conditions: (a) Ac_2O; (b) Fe/HCl, EtOH/H_2O; (c) $NaNO_2$, NaN_3, H_2O/HCl; (d) KOH 30%; (e) **43**, EDC, DMAP, DCM; (f) TFA, DCM, -10 °C; (g) **94**, EDC, DMAP, DCM

Scheme 4.9. Synthesis of Aryl Azide Photoaffinity Probe 206452

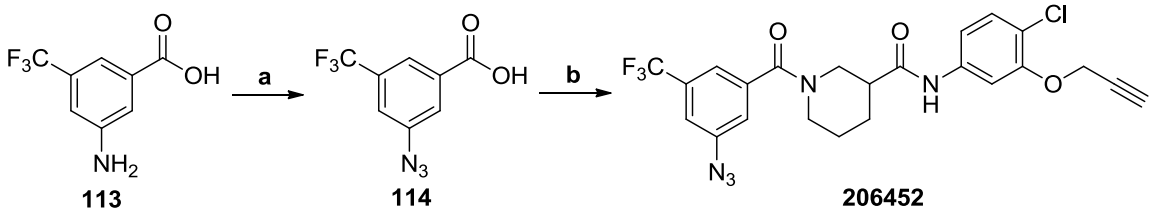

Reagents and conditions: (a) $NaNO_2$, NaN_3, H_2O/HCl, 0 °C; (b) **85**, EDC, DMAP, DCM

Table 4.3. Effects of Aryl Azide Photoaffinity Models and Probes on Transcription and Cytotoxicity in PC-3 Cells

Cmpd No	Structure	IC_{50} SRE.L (μM)[a]	% inh SRE.L (100 μM)[a]	% inh WST-1 (100 μM)[a]
206449	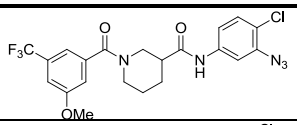	7.0	77	13
206569	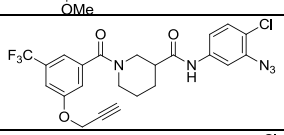	11	75	4
206452	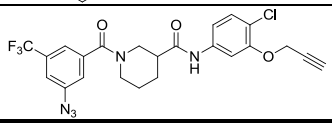	17	54	2

[a]Refer to Table 2.1 for assay descriptions

Preliminary Photoaffinity Labeling Experiments

We selected benzophenone photoaffinity probe **206559** (Table 4.2) to perform preliminary photoaffinity labeling (PAL) experiments based on its potency in PC-3 prostate cancer cells (2.7 μM). Initial PAL experiments were executed in the Neubig lab by Yihan Sun as follows. Parental PC-3 cells were grown to confluence in medium containing 10% fetal bovine serum (FBS) and 1% Penicillin/Streptomyin. The medium was removed, and the cells were washed with phosphate buffered saline (PBS). Cells were then incubated in PBS with 0.3 μM **206559** for 30 minutes. A competition experiment was also performed by incubating cells in PBS with 0.3 μM **206559** and 10 μM **203971** (Table 3.2) for 30 minutes. UV irradiation was applied for 30 minutes at room temperature. Cells were then lifted, and the cell suspension was transferred and centrifuged to recover the cell pellet, which was resuspended in lysis buffer and sonicated. Click chemistry was performed using and Invitrogen™ Click-iT® Reaction Buffer Kit to attach Cy5.5 dye for visualization, as shown in Figure 4.6.

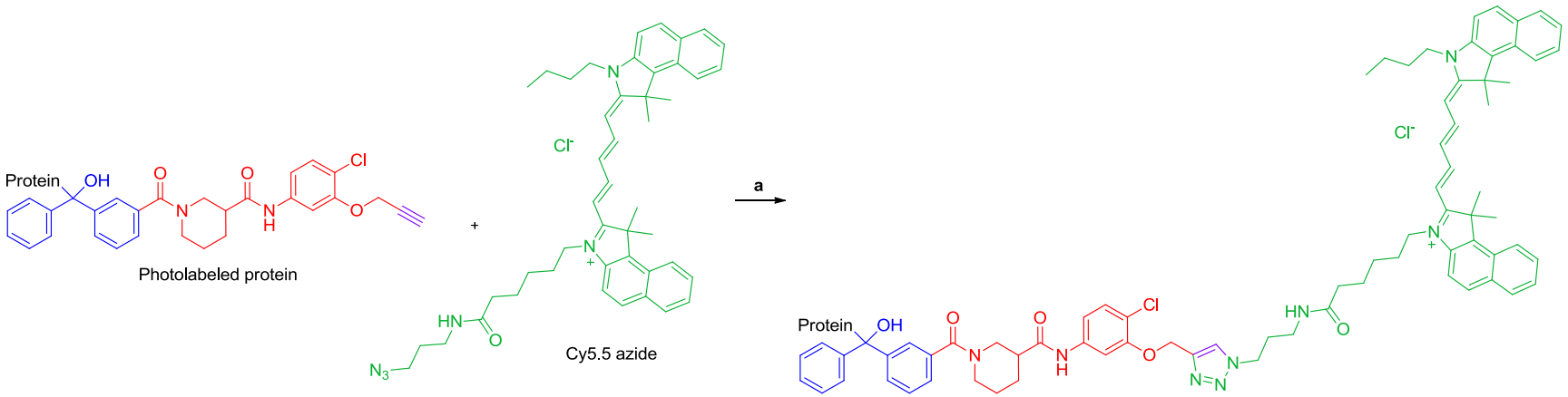

Reagents and conditions: (**a**) Invitrogen Click-iT Protein Reaction Buffer Kit

Figure 4.6. Click Chemistry for Appending Cy5.5 Dye to Photolabeled Protein

Electrophoresis was performed for both the cross-linked probe as well as the competition experiment, using 10 or 20 μg of protein (Figure 4.7). Lane one contains 0.3 μM **206559** with 30 minute UV treatment. Lane two contains the competition experiment using 0.3 μM **206559** with 10 μM **203971** with 30 minute UV treatment. Lane three contains 0.3 μM **206559** without UV treatment.

One band was visualized at approximately 24kD (as indicated by the white box in Figure 4.7) that was present with the UV irradiated photoaffinity probe (lane 1). Upon treatment with 10 μM **203971** (lane 2), the band appears to be competed off, suggesting it is a specific binding interaction. Furthermore, the band is not visible in the non-UV treated lane (lane 3). Based on these results, we investigated making an inactive probe for comparison. The "inactive" probe **208797** was synthesized as found in Scheme 4.10. Unfortunately, appending the propargyl ether restored its activity, making it unsuitable as an inactive nonspecific labeling control.

Scheme 4.10. Synthesis of "Inactive" Probe 208797

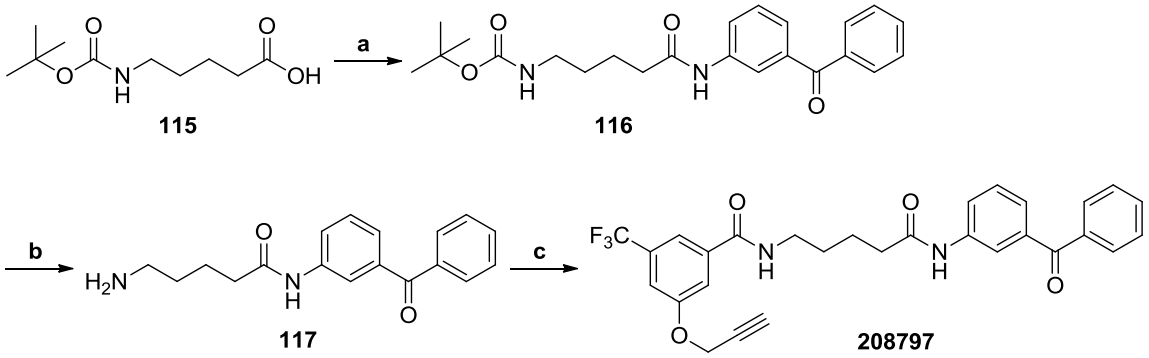

Reagents and conditions: (a) **91**, EDC, DMAP, DCM; (b) TFA, DCM, -10 °C; (c) **98**, EDC, DMAP, DCM

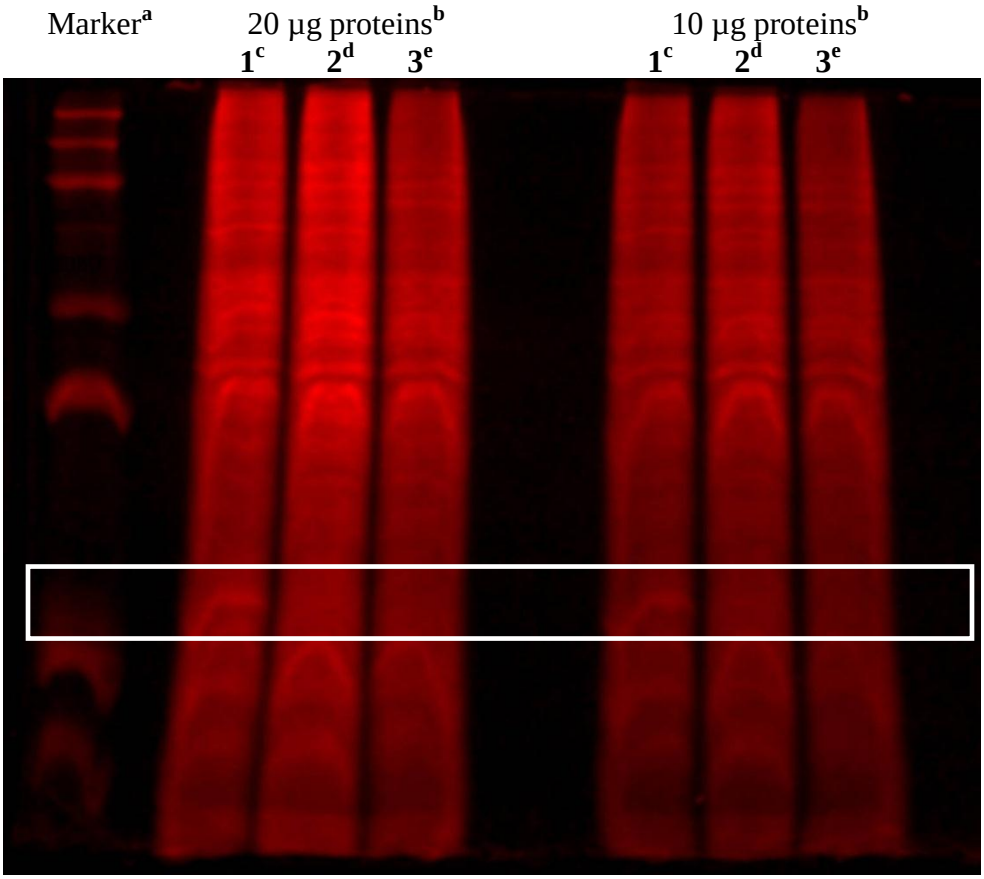

Figure 4.7. SDS-PAGE Gel of Photo Affinity Labeling Experiment

[a]Molecular weight marker
[b]Total amount of protein used in experiment
[c]Lane 1 containing 0.3 µM of **206559** with 30 minute UV treatment
[d]Lane 2 containing competition experiment: 0.3 µM of **206559** and 10 µM **203971** with 30 minute UV treatment
[e]Lane 3 containing 0.3 µM **206559** with no UV treatment

Chemical Validation of Photolabeling Experiment

We attempted to confirm that our probe molecule retains structural integrity during the photolysis process by attempting to capture a generic amino acid. Therefore, we employed **206454** (Scheme 4.11) in capture experiments using *N*-acetyl glycine methyl ester (**118**) to mimic a peptide-bound amino acid residue in the protein. We monitored the progress of the photolysis experiments by HPLC and TLC, allowing them to run up to 12 hours. The small peaks that grew in were examined by LC/MS. However, the molecular weights did not correlate with our desired product (**119**) or any potential side products.

Scheme 4.11. Attempted Chemical Validation of Photolabeling Experiment

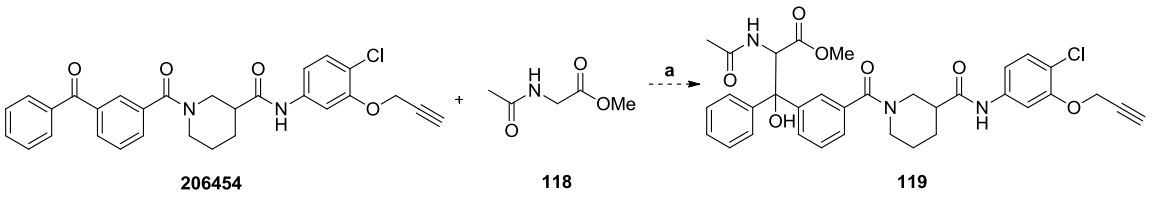

Reagents and conditions: (a) hν (365 nm), MeCN

Future Direction: Photolabeling

Identification of the band discovered in the PAL experiment has not yet occurred, but we are planning to do so in the future. Because our molecules contain an acetylene handle, we can also utilize Click chemistry to append biotin to the cross-linked protein-containing probes to capture with streptavidin. We can then isolate the desired protein(s) for identification and further exploration.

Chapter 5
Expanded Screening Effort

Introduction to Virtual Screening

Virtual screening (VS) methods encompass three-dimensional (3D) methodologies such as high-throughput docking (HTD) and pharmacophore searching (PS), as well as two-dimensional (2D) techniques such as structural similarity searching and quantitative structure-activity relationship (QSAR) models. While such predictive techniques are not 100% accurate, their predictions can provide an "enrichment" in selecting potentially biologically active molecules versus random selection of compounds from a library.[129]

VS techniques can be divided into two main approaches. Structure-based techniques require a 3D structure of the macromolecular target and do not necessarily require known active ligands. Ligand-based techniques require known active ligands but do not necessarily require that the target be known. Furthermore ligand-based techniques may use 2D or 3D methods. Given that the macromolecular target is not known for this project, ligand-based approaches will have to be employed to conduct virtual screening.

Ligand-based 2D methods are often simpler and quicker than 3D methods and can be employed when little structural information or SAR data is available.[130, 131] The basis for such 2D models is that compounds with similar structures often have similar properties and should therefore have similar activities.[132] Therefore, similarity searching at a high level should produce compounds with similar activities. This basic premise is also employed in 2D-QSAR analysis, which utilizes molecular properties to evaluate the biological activity of a compound. These properties are converted to molecular descriptors that are used to predict what analogs are likely to have similar activities based on given properties and their overall contribution to activity.

One 3D ligand-based technique is to generate a pharmacophore model based on ligands which appear to elicit a desired biological response and use that model to search

for other potentially active ligands. A key component of PS is that only a small subset of compounds need be tested to generate a computational pharmacophore model.[133] In the situation where the binding conformations for the active ligands are not known, 3D overlays of the active ligands are generated. A computer program simultaneously minimizes the conformational energies of each of the individual structures while maximizing the overlap between the structures based on features like hydrogen bond donors/acceptors, aromatic rings, hydrophobic groups, etc. Once the overlays are completed, 3D pharmacophore models can then be generated on the features common to the active ligands.[134]

Once a pharmacophore model has been generated, it generally undergoes iterations of validation and refinement. After optimization, it can be employed in virtual screens to survey chemical databases. The model is used to identify ligands that contain similar features in the same spatial alignment to those used to construct the model. This search may retrieve compounds of similar structure to the active ligands, or it may supply novel scaffold structures, known as "scaffold-hopping,"[134, 135] which can expand medicinal chemistry efforts into novel chemical space.

Pharmacophore Model Generation

Because we have not yet identified the macromolecular target(s) of our small molecules, we enlisted the help of Paul Kirchhoff to perform virtual screening of a new 100,000 compound library in the CCG. First, we selected a training set of 11 of our most active conformationally restricted analogs (with the exception of **100601**) in transfected PC-3 prostate cancer cells from a test set of 106 ligands. *We chose a conformationally restricted training set to minimize the number of conformations the ligands could adopt and thus produce less error during minimization.* Ligand overlays were created based on active structures with IC_{50} <15 μM that showed low toxicity of <10% inhibition of WST-1 reduction at 100 μM (Table 5.1). The two most active compounds (**102445** and **203971**) were used to create the initial overlay. MOE defaults for flexible alignment were used with the addition of an aromatic center to the scoring function. After inputting the two structures into MOE, the program simultaneously minimized the conformational energies of each of the individual structures while maximizing the overlap between the structures based on features like hydrogen bond donors/acceptors, aromatic rings, hydrophobic

groups, etc. The resulting coordinates were then frozen, and the next most active structure was added, and the program was re-executed. The process was repeated with each additional structure moving from most potent to least potent, creating the overlay shown in Figure 5.1.

Multiple pharmacophore models were generated from the overlays and tested against the 106 test ligands as part of the pharmacophore validation and refinement. The goal was to find a pharmacophore model which would select the most potent structures while avoiding those which were also toxic. The pharmacophore model chosen is shown in Figure 5.1-Figure 5.4 and was named the "Potent and Low Toxicity (PaLT)" pharmacophore. This model showed some selectivity toward the more potent compounds but failed to discriminate against those that were also toxic.

Table 5.1. Potent and Low Toxicity (PaLT) Analogs in PC-3 Prostate Cancer Cells

Cmpd No	Structure	IC_{50} SRE.L[a] (µM)	% inh WST-1[a] (100 µM)
102445	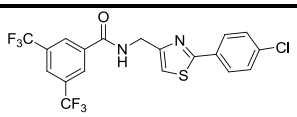	4.1	0
203971	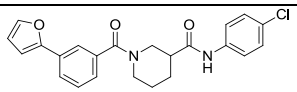	8.2	0
100688	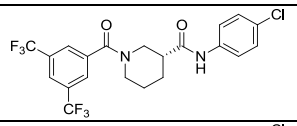	9.7	6.7
100687	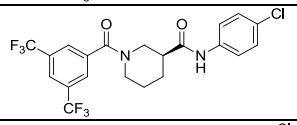	9.8	4.5
203972	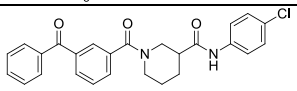	9.9	0
100602	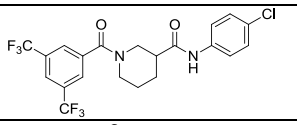	9.9	7.3
102441	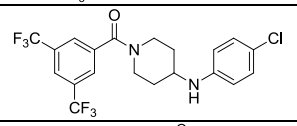	10.8	0
203606	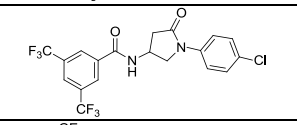	12	0
203960	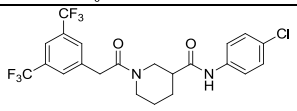	13	0
102443	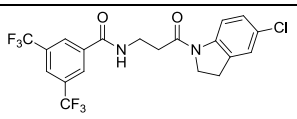	13.2	0
100601	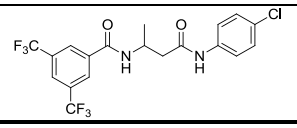	13.8	0

[a]Refer to Table 2.1 for assay descriptions

The model considers the four features shown as essential—the two aromatic rings (F1, F3; green), the hydrophobic/aromatic atom (F4; cyan), and the hydrogen bond acceptor (F2; red) as shown in the structural overlay in Figure 5.1. Figure 5.2 through Figure 5.4 show the distances in Angstroms between each essential feature.

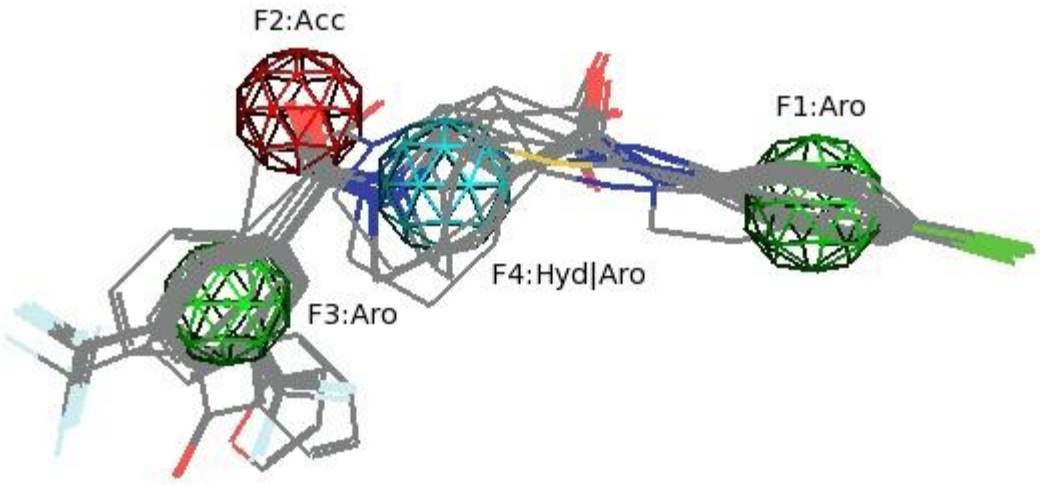

Figure 5.1. Potent and Low Toxicity Pharmacophore Model with Structural Overlay

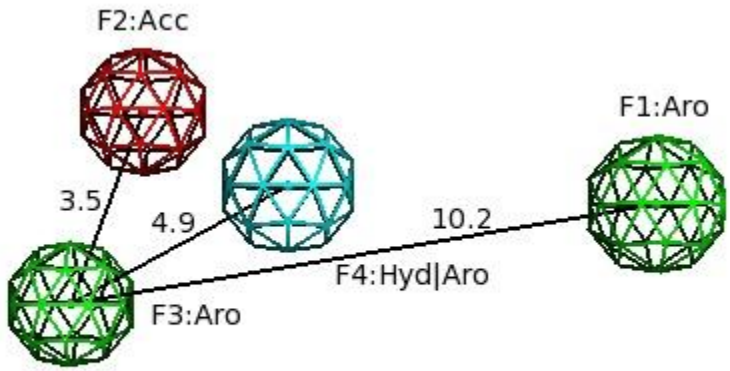

Figure 5.2. Potent and Low Toxicity Pharmacophore Model with Distances from Aromatic Feature 3

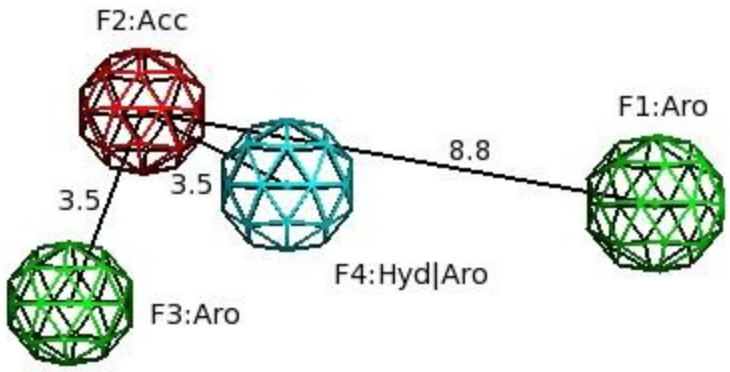

Figure 5.3. Potent and Low Toxicity Pharmacophore Model with Distances from Hydrogen Bond Acceptor Feature 2

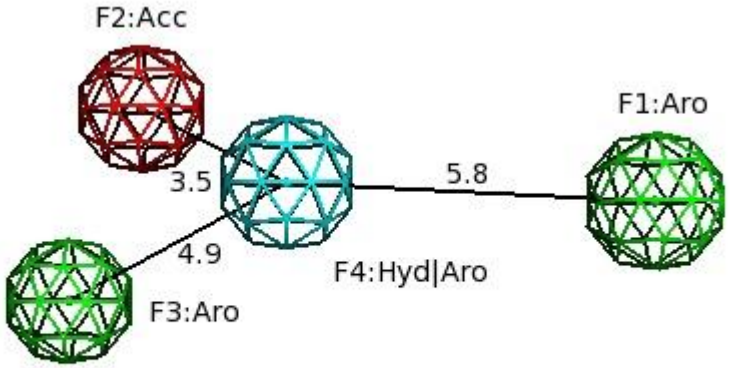

Figure 5.4. Potent and Low Toxicity Pharmacophore Model with Distances from Hydrophobic/Aromatic Feature 4

A second pharmacophore model was constructed using 9 active compounds with IC_{50}<15 μM that showed significant WST-1 toxicity of >60% inhibition at 100 μM (Table 5.2) and was labeled "Potent and Toxic (PaT)." The idea here is that this model could be used to eliminate toxic compounds identified by a virtual screen with the PaLT model. Note that the training set was not restricted to rigid analogs. The PaT model considers five features shown as essential for potent and toxic compounds—two aromatic rings (F2, F3; green), the hydrophobic atoms (F1, F4; black), and the hydrogen bond donor (F5, fuchsia) as shown in the structural overlay in Figure 5.5. The model was constructed analogously to the PaLT pharmacophore. The two most toxic compounds (**101200** and **100691**) were used to create the initial high toxicity model parameters using MOE. The resulting coordinates were then frozen, and the next most toxic structure was added, and the program was re-executed. The iterative process continued moving from most to least toxic, resulting in the PaT pharmacophore shown in Figure 5.5-Figure 5.8.

Table 5.2. Potent and Toxic (PaT) Analogs in PC-3 Prostate Cancer Cells

Cmpd No	Structure	IC_{50} SRE.L[a] (μM)	% inh WST-1[a] (100 μM)
101200	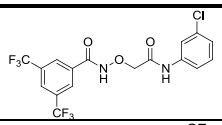	5.9	96.8
100691	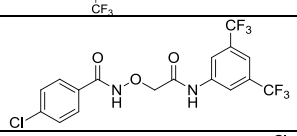	8.6	95.6
100689	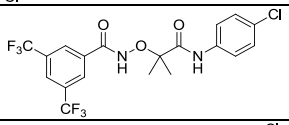	2.4	92.5
102585	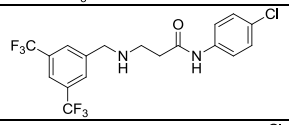	8.1	91.8
100596	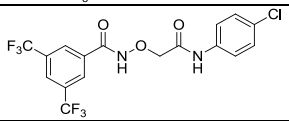	4.7	90.8
102532	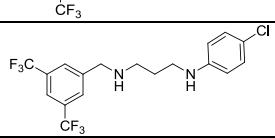	9.1	89.4
100721	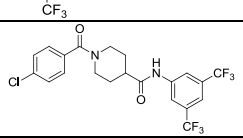	9.9	87.8

Cmpd No	Structure	IC_{50} SRE.L[a] (µM)	% inh WST-1[a] (100 µM)
100745	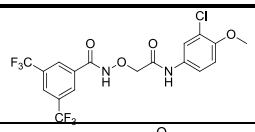	11	78.1
203848*	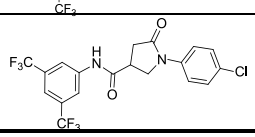	8.6	75.2

[a]Refer to Table 2.1 for assay descriptions
*Tested in HEK293 cell line

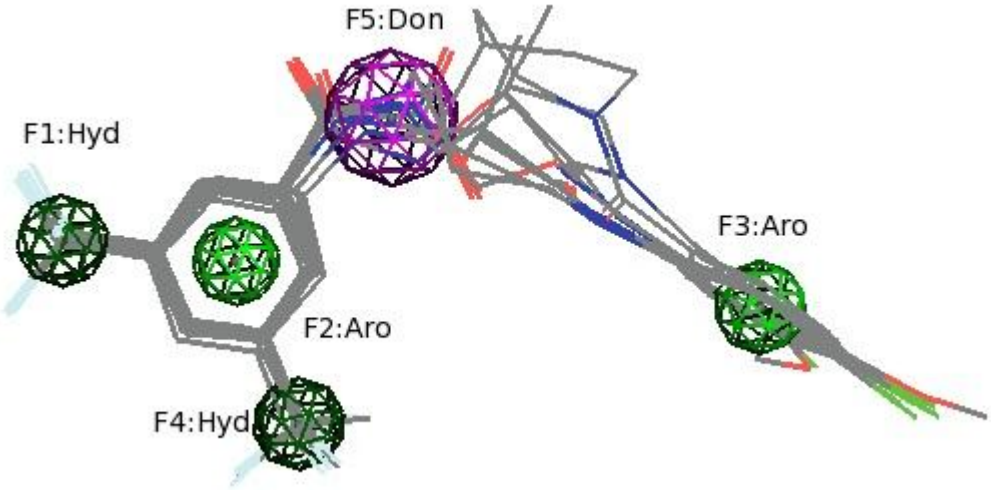

Figure 5.5. Potent and Toxic Pharmacophore Model with Structural Overlay

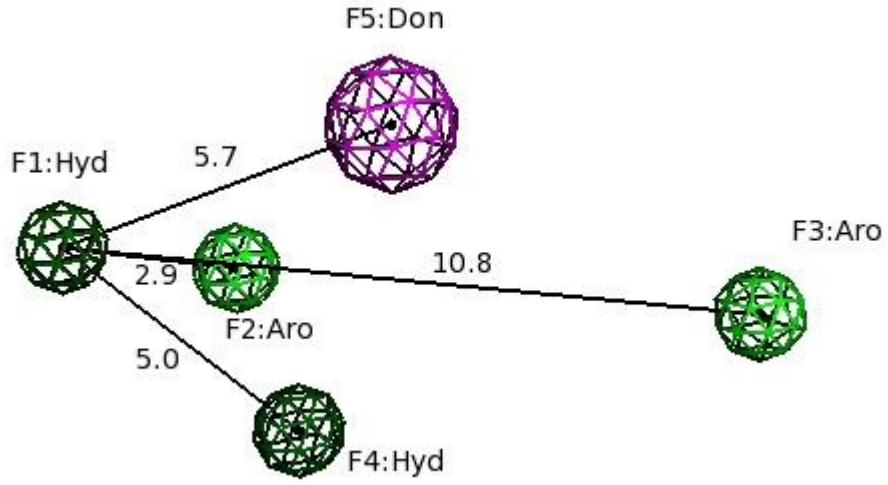

Figure 5.6. Potent and Toxic Pharmacophore Model with Distances from Hydrophobic Feature 1

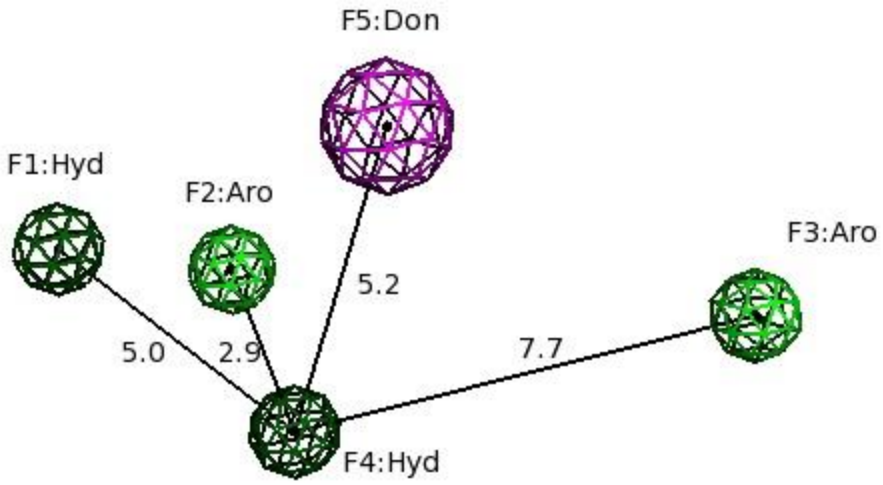

Figure 5.7. Potent and Toxic Pharmacophore Model with Distances from Hydrophobic Feature 4

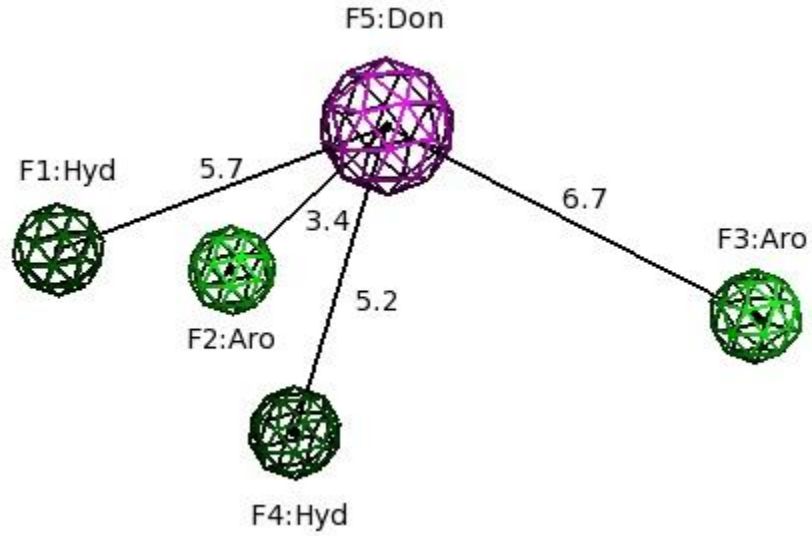

Figure 5.8. Potent and Toxic Pharmacophore Model with Distances from Hydrogen Bond Donor Feature 5

Virtual Screen

We were interested in virtually screening a new 100K library recently added to the CCG-collection. Before performing the screen, we needed to determine whether our models were capable of enriching the hit rate. Therefore, we tested our pharmacophore models retrospectively based on the results from our prior 54K high-throughput screen using five methodologies. Table 5.3 summarizes the results of each model using Güner and Henry's metrics for analyzing pharmacophores.[9] The labels are as follows: hit list (H_t) represents the number of compounds that the model identifies as active, and the hit

list actives (H_a) describes the number of actual actives within the hit list. *D* represents the total number of compounds in the database, in this case 54,161 and *A* is the number of confirmed active compounds in the library, in this case 103 (see Figure 5.9 and discussion).

The calculations found in Table 5.3 are determined as follows[136]: the percent yield of actives (*%Y*) is calculated as:

Equation 5.1. Percent Yield of Actives (*%Y*)

$$\%Y = \frac{H_a}{H_t} \times 100$$

and the percent ratio of actives (*%A*) in the hit list is given by:

Equation 5.2. Percent Ratio of Actives (*%A*)

$$\%\mathrm{A} = \frac{\mathrm{H_a}}{\mathrm{A}} \times 100$$

The enrichment (or enhancement, *E*) is determined by:

Equation 5.3. Enrichment (or Enhancement, *E*)

$$\mathrm{E} = \frac{\frac{\mathrm{H_a}}{\mathrm{H_t}}}{\frac{\mathrm{A}}{\mathrm{D}}} = \frac{\mathrm{H_a\ x\ D}}{\mathrm{H_t\ x\ A}}$$

The overall goodness of hit list (*GH*) is given as:

Equation 5.4. Goodness of Hit List (*GH*)

$$\mathrm{GH} = \left(\frac{(\mathrm{H_a}(3\mathrm{A}+\mathrm{H_t})}{(4\mathrm{H_t A})}\right) \times \left(1 - \frac{\mathrm{H_t}-\mathrm{H_a}}{\mathrm{D}-\mathrm{A}}\right)$$

We examined each of the models for their ability to enrich the hit rate over the actual hit rate of the entire high-throughput screen. The first model employed our potent and low toxicity pharmacophore (Pharma PaLT). The model retrieved 7376 compounds it considered active, however only 20 of those were actually active, affording a poor percent yield of actives. This also afforded a low percent ratio of actives. In the ideal situation, these should be maximized and equal to one another. When they are not, the goodness of hit list suffers. This score ranges from 1 (best) to 0 (worst), and calculates the balance between the maximum yield and maximum percent of actives retrieved.

Secondly, we utilized our potent and toxic pharmacophore (Pharma PaT) to remove any toxic compounds from pharmacophore PaLT (Table 5.3), which afforded a hit list of 7339. However, while this removed 37 compounds, it did not enhance enrichment over the PaLT model, again yielding disappointing results.

Next, we examined 2D calculations, first using a similarity search of greater than 65% similarity to the eleven compounds originally used in our potent and low toxicity model. Although it only retrieved one active compound, the similarity search afforded the best results in terms of enrichment, with 9 times enrichment versus random selection from the library. A QSAR model using the same PaLT compounds was also explored, with an activity cutoff of 10^{-6} M. A second QSAR model removing compounds with toxicity greater than 30% (QSAR PaT (30%)) was also employed. Both yielded slight enrichment of around 3 times over random selection. The 2D methods appeared to actually outperform the 3D methods. This is likely due to our lack of knowledge of the actual binding conformation. We selected our training set from conformationally restricted analogs. The forced rigidity in combination with lacking knowledge regarding the actual binding pose may have further complicated the use of a 3D pharmacophore. Furthermore, the algorithm used for conformational energy minimization may introduce additional error into our 3D model. A study conducted by Venkatraman, *et al*. arrived at a similar conclusion and prefaced that virtual screening results are strongly influenced by the target family, the structure and conformation of the query, and the types of ligand sets used. While 2D models can be more efficient virtual screening methods, they can nevertheless be problematic. The overall 3D shape is critical for binding interactions with the active site, which cannot be predicted using 2D models. Additionally, only 3D models are well-suited for scaffold hopping for exploration of new chemical space.[137]

Disappointingly, our 3D pharmacophore models did not provide any significant enrichment versus random selection. While our 2D similarity search yielded the best results, it did not achieve a high enough level of enrichment to be useful, i.e. it would not be predicted to select a small enough subset of the CCG collection to make screening cost-effective. [136] In all of our pharmacophore models, we achieved a poor GH score, ranging from 0.02 to 0.05. Therefore, we decided not to perform a virtual screen of the new 100K library housed in the CCG.

Table 5.3. Pharmacophore 3D and 2D Analysis

	3D Pharma PaLT[a]	3D Pharma PaT[b]	2D 65%+ Similarity PaLT[c]	2D QSAR PaLT (6)[d]	2D QSAR PaT (30%)[e]
Hit List(H_t)	7376	7339	57	3907	3844
Hit List Actives(H_a)	20	20	1	22	21
% Yield Actives(%Y)	0.27	0.27	1.75	0.56	0.55
% Ratio Actives (%A)	19.42	19.42	0.97	21.36	20.39
Enrichment (E)	1.43	1.43	9.23	2.96	2.87
Goodness of Hit (GH)	0.04	0.04	0.02	0.05	0.05

[a]Application of potent and low toxicity pharmacophore, IC_{50} <15 µM; WST-1 toxicity <10%
[b]Results following subtraction of potent and toxic pharmacophores IC_{50} <15 µM; WST-1 toxicity >60% from potent and low toxicity pharmacophore model
[c]65% Similarity search using potent and low toxicity pharmacophore, IC_{50} <15 µM; WST-1 toxicity <10%
[d]QSAR model using potent and low toxicity pharmacophore, IC_{50} <15 µM; WST-1 toxicity <10% with an activity cutoff of 10^{-6} M.
[e]QSAR model subtracting toxic pharmacophores from potent and low toxicity model with an activity cutoff of 10^{-6} M and WST-1 toxicity >30%.

High-throughput Screen

In 2007, a primary high-throughput screen (HTS) similar to the HTS that discovered lead compound **1423**[62] was conducted on a 54,161 compound screening collection. The collection was tested at 10 µM concentration in an SRE.L assay performed at the CCG at the University of Michigan. Due to testing limitations at the time, the primary screening data were not followed up on as completely as is now possible.

Figure 5.9 provides the HTS triage funnel for the 54K screen in our reevaluation of the 2007 data. The primary assay conducted at 10 µM in HEK293 cells afforded 2547 active compounds, which were triaged to eliminate compounds that were luciferase inhibitors, promiscuous, or contained structural alerts to afford 1500 compounds for confirmation. The primary screen was repeated at 10 µM concentration for the 1500 active compounds, which yielded 170 confirmed actives (11.3% confirmation rate). Dose response confirmation was performed on the 170 confirmed actives (original DMSO stock), which provided 107 titrating compounds (62.9% titration rate). Four compounds were also eliminated at this step, as they were found to be luciferase inhibitors. This provided 103 small molecules for follow up.

Due to budgetary constraints, we purchased 61 commercially available fresh powders from ChemDiv. We selected representative compounds from individual clusters to avoid selecting highly similar compounds, maintaining diversity in our analog set. The 61 fresh powder samples were tested in two assays, each at a single dose of 10 µM and 100 µM concentrations using SRE.L and WST-1 assays in transiently transfected PC-3 prostate cancer cells. This secondary assay was performed by Sue Wade in the Neubig laboratory. Compounds with > 50% SRE.L inhibition and <20% WST-1 inhibition afforded 30 compounds for follow up dose response. Of these 30 compounds, we selected 3 top compounds with nanomolar potencies for further study. The structures and IC_{50}s of the 3 small molecules can be found in Figure 5.10.

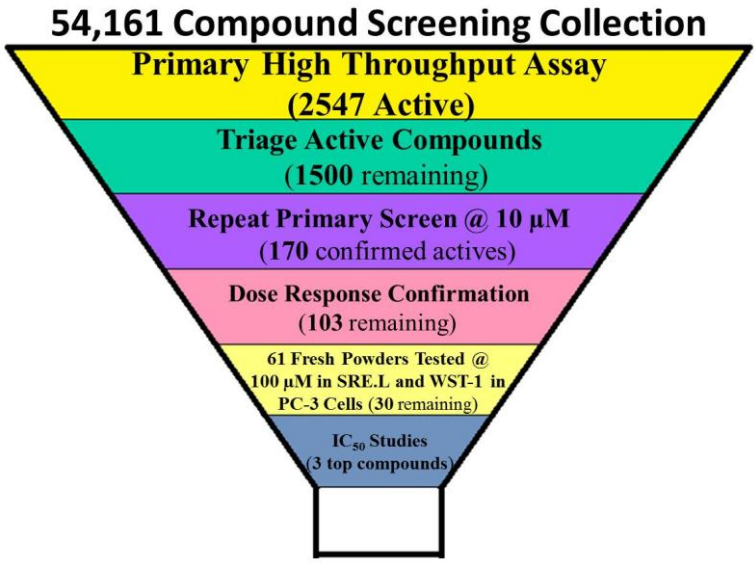

Figure 5.9. High-throughput Screen Triage Funnel

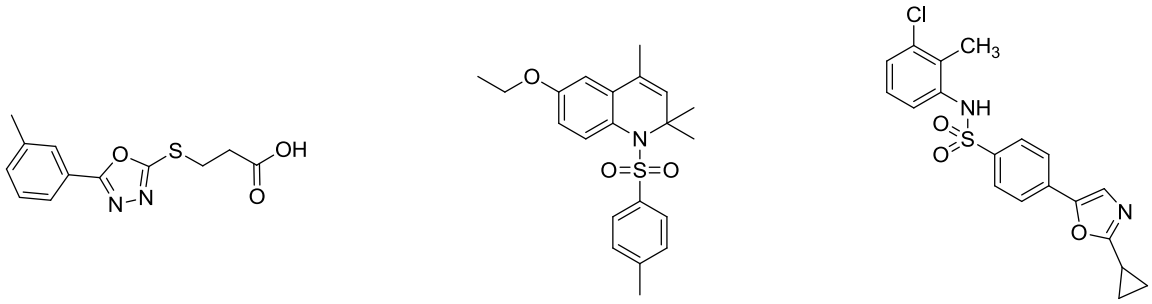

58146 (390 nM) **5677** (260 nM) **86769** (17 nM)

Figure 5.10. Structures of the Top 3 Compounds for Follow Up from High-throughput Screen of 54K Library

We were interested in preliminary elucidation of SAR for the three confirmed actives of greatest interest. The CCG library contained data on compounds that had already been tested in the original HTS SRE.L assay in HEK293 cells at 10 μM with greater than 70% similarity to **58146**. Table 5.4 illustrates the compounds previously tested. Analog **58150** removes the *meta*-methyl and provides 2,4-dichloro groups, which maintains activity. Shortening the tether region 1 carbon, and installing an ester (**96396** and **8610**) significantly reduces activity, with a longer ester length corresponding with even less activity. Much of the remaining analogs tested are completely inactive and are indicative of the narrow SAR of this series.

Table 5.4. Previously Tested Compounds with Greater than 70% Similarity to 58146

Cmpd No	Structure	% inh SRE.L (10 μM)[a]
58146	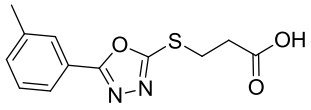	91.2
58150	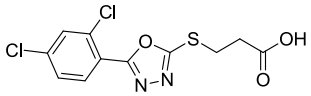	84.2
96396	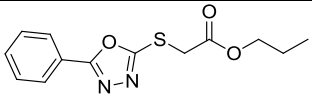	26.2
8610	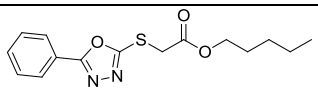	3.8
98080	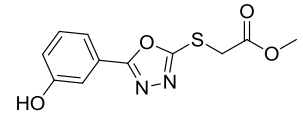	3.4
57251	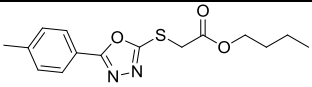	2.4
96527	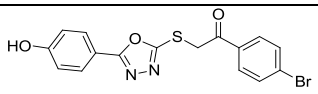	NA[b]
58218	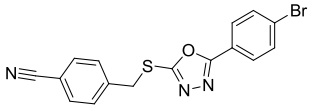	NA[b]

Cmpd No	Structure	% inh SRE.L (10 µM)[a]
58128	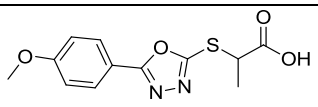	NA[b]
96486	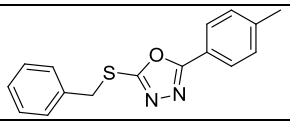	NA[b]
77601	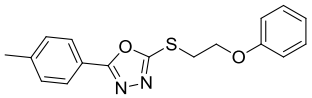	NA[b]
61321	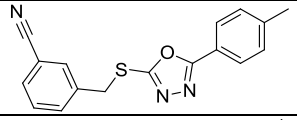	NA[b]
80725	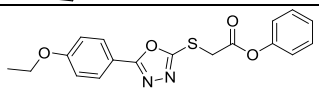	NA[b]
94779	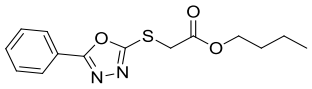	NA[b]
58148	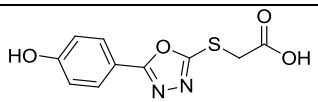	NA[b]
59646	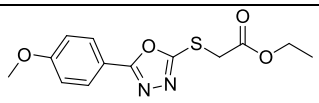	NA[b]
23366	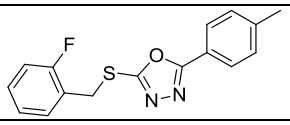	NA[b]
62445	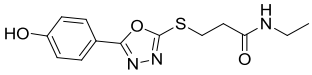	NA[b]
57227	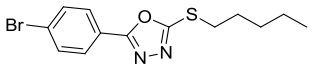	NA[b]
61317	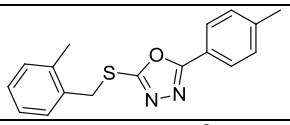	NA[b]
16688	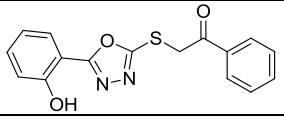	NA[b]
61319	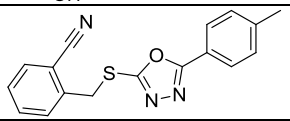	NA[b]

Cmpd No	Structure	% inh SRE.L (10 µM)[a]
58292	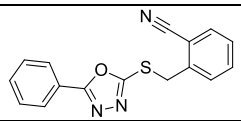	NA[b]
19867	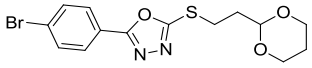	NA[b]
20321	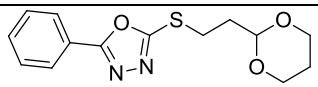	NA[b]
43678	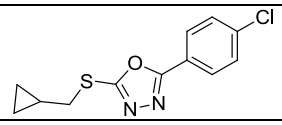	NA[b]
7173	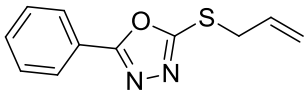	NA[b]

[a]Refer to Table 2.1 for assay descriptions
[b]No activity

The Neubig laboratory obtained samples from the CCG library for a limited number of analogs for each of the three small molecules and performed an SRE.L/Renilla dual-luciferase assay as well as monitored WST-1 cytotoxicity for each in PC-3 prostate cancer cells. These samples were from a new collection that was not included in the original high-throughput screen. Preliminary SAR for **58146** (Table 5.5) shows that replacing the methyl group with an electron withdrawing, lipophilic chlorine (**123851**) significantly reduces potency and decreases selectivity over TK-*Renilla*. Replacement of the 3-methylphenyl with a benzyl moiety (**123857**) somewhat reduces potency and greatly reduces efficacy. Amazingly, shortening the tether region between the thiol and acid moieties by a single carbon (**123860**) abolishes activity. No cytotoxicity was observed in the analogs tested.

Table 5.5. Preliminary SAR for CCG-58146

Cmpd No	Structure	IC_{50} SRE.L[a] (μM)	% inh SRE.L[a] (0.03, 10 μM)	% inh pRL-TK[a] (0.03, 10 μM)	% inh WST-1[a] (0.03, 10 μM)
58146[b]	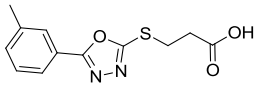	0.20	56, 91	0, 0	0, 0
123851	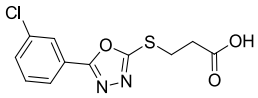	1.3	30, 84	16, 14	0, 0
123857	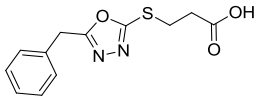	0.58	6, 30	0, 0	0, 0
123860	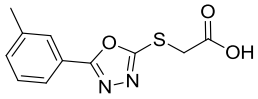	NC[c]	20, 30	6, 4	0, 0

[a]Refer to Table 2.1 for assay descriptions.
[b]N = 2
[c]Could not be calculated

Table 5.6 compares a single analog (**112019**) with compound **5677**. Replacement of the methyl group with the chloro group reduces potency slightly, increases efficacy, and has little effect on selectivity at 10 μM. Neither compound shows any cytotoxicity.

Table 5.6. Comparison of 58146 and Analog 112019

Cmpd No	Structure	IC_{50} SRE.L[a] (μM)	% inh SRE.L[a] (0.03, 10 μM)	% inh pRL-TK[a] (0.03, 10 μM)	% inh WST-1[a] (0.03, 10 μM)
5677[b]	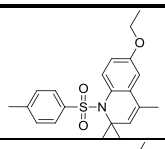	0.12	40, 55	11, 45	0, 0
112019	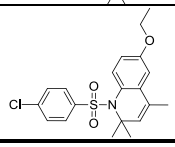	0.30	40, 68	0, 49	0, 0

[a]Refer to Table 2.1 for assay descriptions
[b]N = 1

Preliminary SAR for remaining compound **86769** can be found in Table 5.7. Removal of the methyl group (**186414**) significantly reduces activity and selectivity. Removal of the chloro group (**186447**) significantly reduces potency, but improves selectivity versus TK-*Renilla*. Moving the sulfonamide from the *para*-position to the *meta*-position and adding a methyl substituent to the center aromatic ring (**186528**) is

detrimental to potency and efficacy. As with the other scaffolds, none of the analogs in this series demonstrates cytotoxicity.

Table 5.7. Preliminary SAR for CCG-86769

Cmpd No	Structure	IC_{50} SRE.L (μM)[a]	% inh SRE.L (0.03, 10 μM)[a]	% inh pRL-TK (0.03, 10 μM)[a]	% inh WST-1 (0.03, 10 μM)[a]
86769[b]	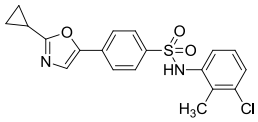	0.10	40, 62	20, 87	0, 0
186414	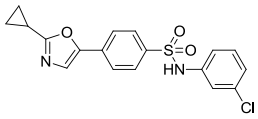	2.4	33, 69	16, 97	0, 0
186447	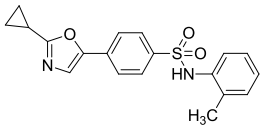	3.1	37, 60	0, 50	0, 0
186528	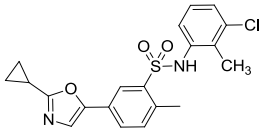	14	15, 50	39, 88	0, 0

[a]Refer to Table 2.1 for assay descriptions
[b]N = 1

Future Direction

The observed SAR for **58146** indicates that modifications can be made to this highly potent structure with retention of activity, but that the SAR is narrow, which can be indicative of a well-defined binding site. As a low molecular weight molecule, it is ideal for further derivatization. The Neubig lab is currently performing functional assays to ensure that the compound is inhibiting Rho-mediated gene transcription and is not a luciferase inhibitor. Our triage should have eliminated this possibility; however before purchasing additional analogs or executing extensive synthesis, we would like to confirm the basis of its activity.

Chapter 6
Conclusions

Despite the well-documented role for the RhoA transcriptional signaling pathway in the progression and metastasis of multiple cancers, there are few chemical inhibitors of the pathway. Much of the effort has focused on modifications of RhoGTPases as well as on the downstream effectors of Rho GTPases, such as ROCK. Targeting ROCK, while showing great promise, fails to target the RhoA pathway in its entirity, as the effector acts through only one portion of the pathway (Figure 1.2).

Previous work by Chris Evelyn indicates that compound **1423** inhibits downstream of RhoA, but distinct from the interaction of the serum response factor (SRF) with the serum response element (SRE). Results suggest that the compound interferes with SRF/MKL1-dependent transcriptional activation; however, the exact mechanism could not be elucidated. Evidence suggests that effects on MKL1/SRF function, such as affecting nuclear translocation/efflux, recruitment, posttranslational modification, or the interaction of MKL with SRF or the transcritptional machinery are likely.[62]

To our knowledge, **1423** and its analogs are uniquely targeting the RhoA transcriptional signaling pathway by acting on an aspect of MKL1-related function. Furthermore, **1423** and its analogs are the only known compounds specifically targeting the RhoA pathway in this manner. A recent paper has further demonstrated the ability of **1423** to prevent nuclear accumulation of MKL1, and therefore block the stimulation of SRF-dependent transcription. The Patti lab has recently demonstrated that patients with type 2 diabetes (T2D) as well as insulin-resistant subjects with normal insulin levels and a family history (FH^+) of T2D maintain increased expression levels of MKL1 and SRF target genes. Furthermore, upregulation of STriated muscle Activator of Rho Signaling (STARS), which activates SRF, was also discovered in these subjects. Upregulation of STARS correlates with insulin resistance, which is often associated with T2D.

Pharmacological inhibition of MKL1-dependent SRF transcriptional activation using **1423** led to increased glucose uptake and glucose tolerance in mice. Specifically targeting MKL1-dependent SRF activation may provide an additional therapeutic avenue for type 2 diabetes.[138]

There are three significant goals for moving this project forward. The first goal is to identify the protein band discovered using our photoaffinity labeling experiment. Identification of the band could provide a novel target(s) which could lead to identification of the mechanism of action. Due to the modest potency of our probes and the possibility that the target is in low abundance, we will also explore using Stable Isotope Labeling by Amino Acids (SILAC)[139] as a more global and sensitive method for detecting the binding target for our compounds. Discovery of the target and/or mechanism of action could allow us to pursue more rational, structure-based drug design.

Second, we would like to identify and optimize a new scaffold. Synthesis of the libraries exploring aromatic modifications provided little improvement in the potency of our analogs. Although analog **203971** demonstrated a modest IC_{50} of 6.4 μM, it has shown significant anti-migratory properties in PC-3 prostate cancer cells. Recent evidence has shown that efficacy may be more important than potency in determining the effects on migration (Haak, Neubig, unpublished). However, after synthesizing our small libraries, we feel we have exhausted potential SAR using the current scaffold. We hope that one of our newly identified compounds from the recent HTS follow up will provide a novel more potent leadfor optimization.

Finally, we are interested in continued testing of **203971**. We are interested in determining the pharmacokinetic parameters as well as the relative bioavailability to determine the feasibility of further *in vivo* exploration. If further *in vivo* testing appears viable, we will explore the metabolic stability of the analog, as well as move into melanoma xenograft studies.

Chapter 7
Experimentals

All starting materials were obtained from commercial suppliers and were used without purification. All reactions involving air- or moisture-sensitive compounds were performed under an N_2 atmosphere. NMR spectra were recorded on a Bruker instrument at 500 MHz, Bruker instrument at 300 MHz, or a Varian instrument at 400 MHz for ^{1}H. Chemical shift values are recorded in δ units (ppm). Mass spectra were recorded on a Waters Corporation LCT Time-of-Flight mass spectrometer or on an Agilent Technologies LC/MS system using a 1200 Series LC and 6130 Quadrupole LC/MS (Agilent Technologies, Santa Clara, CA, USA) in positive mode with 5–10 μL injection volume and a linear gradient of 10% Solvent D (0.02% TFA and 0.1% acetic acid in acetonitrile) in Solvent C (0.02% TFA and 0.1% acetic acid in water) to 90% Solvent D in Solvent C over 6 min with a hold at 90% for 7 min, as indicated. HPLC retention times were recorded using an Agilent 1100 Series employing an Agilent ZORBAX Eclipse Plus C18 column (4.6 x 75 mm, 3.5 μm). Retention times were collected using Gradient A (10-90% Acetonitrile/Water over 13 minutes) or Gradient B (50-90% Acetonitrile/Water over 13 minutes) as indicated.

General Procedure for Acylation of Amine (Procedure A). Amine (1.42 mmol) was dissolved in 2M NaOH (2.36 mL) and was treated with desired acyl chloride (1.18 mmol). The reaction was allowed to stir overnight at room temperature. The resulting solution was washed with DCM (15 mL), and the aqueous layer was acidified to pH 2 using 2M HCl. The aqueous layer was extracted with EtOAc (2 x 20 mL). The combined extracts were washed with brine (20 mL), dried ($MgSO_4$), and concentrated to afford title compounds that were used without further purification unless indicated.

General Procedure for Acylation of Amine (Procedure B). Dichloromethane (11.2 mL) was added to a flask containing desired amine (1.18 mmol) and was treated with desired acyl chloride (1.18 mmol) and TEA (1.18 mmol). The mixture was allowed to stir at room temperature overnight. The mixture was concentrated and then partitioned between 2M HCl (10 mL) and EtOAc (10 mL). The aqueous layer was extracted a second time with EtOAc (10 mL). The organics were combined, washed with brine (20 mL), dried ($MgSO_4$), and concentrated to afford title compounds that were used without further purification unless indicated.

General Procedure for Amide Coupling (Procedure C). Anhydrous THF (0.3 M) was added to a flask containing starting acid (1.18 mmol), and was treated with corresponding amine (1.18 mmol), followed by HOBt (1.42 mmol), EDC (1.42 mmol), and DIPEA (1.42 mmol). The solution was allowed to stir overnight at room temperature and was then diluted with EtOAc (15 mL) and was washed with saturated $NaHCO_3$ (20 mL), followed by 1M HCl (20 mL) and then brine (20 mL). The organics were dried ($MgSO_4$) and concentrated to afford crude product.

General Procedure for Amide Coupling (Procedure D). Anhydrous DCM (1.0 mL) was added to flask containing aniline (0.10 mmol) and was treated with EDC (0.15 mmol) followed by DMAP (0.15 mmol), and corresponding acid (0.11 mmol). The solution was allowed to stir overnight at room temperature and was then diluted with DCM (4 mL) and was washed with 1M HCl (2.5 mL), followed by saturated $NaHCO_3$ (2.5 mL). The organics were dried ($MgSO_4$) and concentrated to afford crude product.

Chapter 2

3-(3,5-bis(trifluoromethyl)benzamido)propanoic acid (2a). Prepared according to Procedure A to afford 0.384 g (1.17 mmol, 99% yield) of title compound as a white crystalline solid. TOF MS-ESI *m/z* $[M-H]^-$ 328.1. ^1H NMR (500 MHz, DMSO-d_6): δ 12.30 (bs, 1H), 9.09-9.05 (m, 1H), 8.49 (s, 2H), 8.32 (s, 1H), 3.53-3.45 (m, 2H), 2.58-2.53 (m, 2H).

***N*-(3-((4-chlorobenzyl)amino)-3-oxopropyl)-3,5-bis(trifluoromethyl)benzamide (203009).** Compound was prepared using **2a** (0.104 g, 0.316 mmol) and 4-Chlorobenzylamine (0.049, 0.348 mmol) according to Procedure C. Crude material was purified using column chromatography (80-90% EtOAc/Hex) to afford 0.084 g (0.186 mmol, 59% yield) of title compound as a white solid. TLC R_f: (80% EtOAc/Hex): 0.24. TOF MS-ESI *m/z* $[M+H]^+$ 453.0; [M+Na] 474.9. HPLC (gradient A): ret time = 7.25 min; purity = 99%. ^{1}H NMR (500 MHz, DMSO) δ 9.12 (t, *J* = 5.6 Hz, 1H), 8.49 (s, 2H), 8.33 (s, 1H), 7.26-7.20 (m, 4H), 4.25 (d, *J* = 5.9 Hz, 2H), 3.54 (q, *J* = 6.5 Hz, 2H), 2.52-2.46 (m, 2H).

***N*-((2-(4-chlorophenyl)thiazol-4-yl)methyl)-3,5-bis(trifluoromethyl)benzamide (102445).** Prepared according to Procedure B using [2-(4-Chlorophenyl)-1,3-thizol-4-yl)]methanamine hydrochloride and 2 eq of TEA. Reaction was re-dissolved in EtOAc (10 mL) and washed with saturated $NaHCO_3$ (10 mL) followed by brine (10 mL). Organic layer was dried ($MgSO_4$) and concentrated to afford 0.153 g (0.329 mmol, 89% yield) of title compound as a yellow solid. TOF MS-ESI *m/z* $[M+H]^+$ 464.9; [M+Na] 486.9. HPLC (gradient A): ret time = 8.69 min; purity = 99%. ^{1}H NMR (500 MHz, DMSO-d_6): δ 9.64 (t, *J* = 5.6 Hz, 1H), 8.58 (s, 2H), 8.35 (s, 1H), 7.95 (d, *J* = 8.4 Hz, 2H), 7.64 (s, 1H), 7.57 (d, *J* = 8.4 Hz, 2H), 4.68 (d, *J* = 5.6 Hz, 2H).

***N*-(3-(4-chlorophenoxy)propyl)-3,5-bis(trifluoromethyl)benzamide (102447).** Prepared according to Procedure B using 3-(4-chlorophenoxy)propan-1-amine hydrochloride and 2 eq of TEA to afford 0.471 g (1.11 mmol, 94% yield) of title compound as a yellow solid. TOF MS-ESI *m/z* $[M+H]^+$ 426.0; [M+Na] 448.0. HPLC (gradient A): ret time = 8.51 min; purity = 99%. ^{1}H NMR (500 MHz, DMSO-d_6): δ 9.05 (t, *J* = 5.5 Hz, 1H), 8.49 (s, 2H), 8.32 (s, 1H), 7.32 (d, *J* = 8.8 Hz, 2H), 6.96 (d, *J* = 8.8 Hz, 2H), 4.07-4.03 (m, 2H), 3.48 (dd, *J* = 12.6 Hz, 6.5 Hz, 2H), 2.01 (p, *J* = 6.4 Hz, 2H).

***N*^{1}-(4-chlorophenyl)propane-1,3-diamine (5).**[69] A solution of 4-Chloroaniline (0.536 g, 4.20 mmol) in toluene (4.2 mL) was treated with 3-Bromopropylamine hydrobromide (**4**) (0.306 g, 1.40 mmol) and was heated at reflux for 30 minutes. After cooling, precipitate

was collected and treated with aqueous 2M NaOH (5 mL), and the aqueous layer was extracted with DCM (2 x 20 mL). Combined extracts were washed with water (5 mL), dried ($MgSO_4$), and concentrated to afford a light brown oil. Crude material was purified by flash chromatography (0-10% Methanolic ammonia/DCM) to afford 0.099 g (0.536 mmol, 38% yield) of title compound as a yellow oil. TLC R_f (10% Methanolic ammonia/DCM): 0.39. ^{1}H NMR (500 MHz, DMSO-d_6): 7.14-7.10 (m, 2H), 6.56-6.52 (m, 2H), 3.19 (t, J = 6.8 Hz, 2H), 2.87 (t, J = 6.7 Hz, 2H), 1.78 (p, J = 6.7 Hz, 2H), 1.50 (bs, 2H).

***N*-(3-((4-chlorophenyl)amino)propyl)-3,5-bis(trifluoromethyl)benzamide (101425)**. Prepared using **5** according to Procedure C. Crude material was purified by flash chromatography (33% EtOAc/Hex) to afford 0.073 g (0.172 mmol, 45% yield) of title compound as a light brown solid. TLC R_f (33% EtOAc/Hex): 0.38. TOF MS-ESI *m/z* $[M+H]^+$ 425.1; [M+Na] 447.1. HPLC (gradient A): ret time = 7.60 min; purity = 99%. ^{1}H NMR (500 MHz, $CDCl_3$): δ 8.03 (s, 1H), 7.21-7.11 (m, 2H), 6.74-6.66 (m, 1H), 6.64-6.56 (m, 2H), 3.67 (q, J = 6.4 Hz, 2H), 3.29 (t, J = 6.3 Hz, 2H), 1.98 (p, J = 6.3 Hz, 2H).

***N*-(3-((4-chlorophenyl)amino)propyl)-3,5-bis(trifluoromethyl)benzamide hydrochloride (101425 B2).** Compound **5** (0.104 g, 0.245 mmol) was dissolved in a 1.05 M methanolic HCl solution (2 mL), and the reaction was allowed to stir at room temperature for 4 hours. The solvent was removed *in vacuo* and the resulting solid was sonicated in ether and dried *in vacuo* to afford 0.111 g (0.241 mmol, 98% yield) of title compound as a white solid. Elemental Analysis: C = 46.62%, H = 3.24%, N = 5.94%, consistent with desired HCl salt. HPLC (gradient A): ret time = 7.61 min; purity = 97%. TOF MS-ESI *m/z* $[M+H]^+$ 424.9. ^{1}H NMR (500 MHz, $CDCl_3$): δ 11.35 (s, 2H), 8.61 (s, 1H), 8.49 (s, 2H), 8.01 (s, 1H), 7.57 (d, J = 8.0 Hz, 2H), 7.39 (d, J = 7.8 Hz, 2H), 3.67 (s, 2H), 3.40 (s, 2H), 2.29 (s, 2H).

***N*^{1}-(3,5-bis(trifluoromethyl)benzyl)-*N*^{3}-(4-chlorophenyl)propane-1,3-diamine (102532).** Compound **100594** (0.050 g, 0.114 mmol) was dissolved in anhydrous THF (5.0 mL), cooled to 0 °C, and treated with Borane-THF complex (0.400 mL, 4.08 mmol).

Reaction was then refluxed for 14 h and was then cooled to room temperature and quenched by the addition of 1N HCl (15 mL). The mixture was refluxed for 1 h and was cooled to 0 °C. The pH was adjusted to 10 using 2M NaOH and was extracted with EtOAc (3 x 25 mL). The combined organics were washed with brine (25 mL), dried ($MgSO_4$), and concentrated. Crude material was purified using flash chromatography (1-5% Methanolic ammonia/DCM) to afford 0.027 g (0.066 mmol, 58% yield) of title. TLC R_f (1% Methanolic ammonia/DCM): 0.11. TOF MS-ESI *m/z* $[M+H]^+$ 410.9. HPLC (gradient A): ret time = 6.32 min; purity = 96%. ^{1}H NMR (500 MHz, $CDCl_3$): δ 7.81 (s, 2H), 7.78 (s, 1H), 7.17-7.05 (m, 2H), 6.57-6.45 (m, 2H), 3.92 (s, 2H), 3.20 (t, *J* = 6.6 Hz, 2H), 2.79 (t, *J* = 6.5 Hz, 2H), 1.83 (p, *J* = 6.5 Hz, 2H).

3-bromo-*N*-(4-chlorophenyl)propanamide (7).[140] 4-Chloroaniline (0.151 g, 1.18 mmol) was dissolved in hot acetonitrile (5.60 mL). The solution was treated with 3-bromopropionyl chloride (0.183 mL, 1.82 mmol) in acetonitrile (1.0 mL) over several minutes. The reaction was heated at reflux for 3h. The reaction was cooled, concentrated, and re-dissolved in EtOAc (20 mL). The organic layer was washed with saturated $NaHCO_3$ (20 mL) followed by 1N HCl (20 mL) and then brine (20 mL). It was then dried ($MgSO_4$) and concentrated to afford 0.291 g (1.11 mmol, 94% yield) of title compound as a white solid. ^{1}H NMR (500 MHz, DMSO-d_6): δ 10.20 (s, 1H), 7.63 (d, *J* = 8.9 Hz, 2H), 7.37 (d, *J* = 8.9 Hz, 2H), 3.73 (t, *J* = 6.4 Hz, 2H), 2.95 (t, *J* = 6.4 Hz, 2H).

3-((3,5-bis(trifluoromethyl)benzyl)amino)-*N*-(4-chlorophenyl)propanamide (102585).[140] Compound **7** was dissolved in acetonitrile (0.65 mL) and was treated with 3,5-bis(trifluoromethyl)benzyl amine (0.171 g, 0.704 mmol). The solution was heated at reflux for 6 hour and 40 minutes. Upon cooling, the solution was diluted with water (5 mL), and the pH was adjusted to 10. The solution was extracted with DCM (3 x 10 mL), and the combined extracts were washed with saturated $NaHCO_3$ (10 mL) followed by brine (10 mL). Organics were dried ($MgSO_4$) and concentrated to afford 0.084 g (0.198 mmol, 104% yield). TOF MS-ESI *m/z* $[M+H]^+$ 424.9; [M+Na] 446.9. HPLC (gradient A): ret time = 6.18 min; purity = 95%. ^{1}H NMR (500 MHz, DMSO-d_6): δ 9.56 (s, 1H),

7.78 (s, 3H), 7.44 (d, *J* = 8.7 Hz, 2H), 7.27 (d, *J* = 8.7 Hz, 2H), 3.96 (s, 2H), 3.11-2.94 (m, 2H), 2.62-2.48 (m, 2H).

3,5-bis(trifluoromethyl)benzaldehyde oxime (9).[70] Hydroxylamine hydrochloride (0.073 g, 1.05 mmol) was dissolved in Methanol (1.0 mL) and was treated with 3,5-Bis(trifluoromethyl)benzaldehyde (0.165 ml, 1.00 mmol) added dropwise. The reaction mixture was refluxed for 5 hours, was allowed to cool to room temperature, and was poured into ice water. Formed precipitate was filtered and washed with water. The solid was then dried *in vacuo* to afford 0.176 g (0.684 mmol, 68% yield) of title compound as a white solid. Compound was used without further purification. ^{1}H NMR (500 MHz, DMSO-d_6): δ 11.85 (s, 1H), 8.38 (s, 1H), 8.25 (s, 2H), 8.12 (s, 1H).

***N*-(4-chlorophenyl)but-3-enamide**.[71] But-3-enoic acid (0.170 ml, 2.00 mmol) was dissolved in dichloromethane (3.20 mL) and placed under N_2. DMAP (0.008 g, 0.065 mmol) and 4-chloroaniline (0.510 g, 4.00 mmol) were added, and the mixture was cooled to 0-5 °C. EDC (0.383 g, 2.00 mmol) was added and the solution was stirred for 10 minutes. The solution then stirred at RT for an additional 6 hours. After stirring, DCM (10 mL) was added. Organics were washed with 10% HCl (10 mL) followed by saturated $NaHCO_3$ (10 mL). Reaction was concentrated to yield 0.343 g (1.75 mmol, 88% yield) of title compound as an off-white solid. ^{1}H NMR (500 MHz, DMSO-d_6): δ 10.11 (s, 1H), 7.65-7.60 (m, 2H), 7.39-7.30 (m, 2H), 6.03-5.88 (m, 1H), 5.22-5.11 (m, 2H), 3.13 (dd, *J* = 6.9 Hz, 0.9 Hz, 2H).

2-(3-(3,5-bis(trifluoromethyl)phenyl)-4,5-dihydroisoxazol-5-yl)-*N*-(4-chlorophenyl)acetamide (203003).[74] Compound **9** (0.075 g, 0.292 mmol) was added to a stirring solution of *N*-(4-chlorophenyl)but-3-enamide (0.039 g, 0.200 mmol) in DCM (2.1 ml), and the reaction was cooled to 0 °C. Sodium hypochlorite (1.134 g, 0.800 mmol) was added dropwise over 20 minutes and the resulting mixture was stirred and allowed to warm to ambient temperature. The solution continued to stir overnight. Water (5 mL) was added to the solution, and the product was extracted using DCM (3 x 5 mL). Combined organics were dried ($MgSO_4$) and concentrated to afford 0.094 g (0.209 mmol, 104%

yield) of title compound as an off-white solid. No further purification was performed. TOF MS-ESI *m/z* $[M+H]^+$ 451.0; [M+Na] 473.0. HPLC (gradient B): ret time = 6.37 min; purity = 82%. ^{1}H NMR (500 MHz, DMSO-d_6): δ 10.22 (s, 1H), 8.28 (s, 2H), 8.24 (s, 1H), 7.63 (d, *J* = 8.7 Hz, 2H), 7.37 (d, *J* = 8.7 Hz, 2H), 5.25-5.17 (m, 1H), 3.77-3.68 (m, 1H), 3.46-3.39 (m, 1H), 2.85-2.69 (m, 2H).

1-azido-3,5-bis(trifluoromethyl)benzene (15).[141]

***N*-(4-chlorophenyl)pent-4-ynamide (11).** Compound was prepared according to Procedure C using 1.1 eq of 4-Chloroaniline to afford 0.129 g (0.621 mmol, 83% yield) of title compound as a tan solid. TOF MS-ESI *m/z* [M+Na] 230.0. ^{1}H NMR (500 MHz, $CDCl_3$): δ 7.47 (d, *J* = 8.8 Hz, 2H), 7.42 (s, 1H), 7.28 (d, *J* = 8.8 Hz, 2H), 2.68-2.55 (m, 4H), 2.08-2.06 (m, 1H).

3-(1-(3,5-bis(trifluoromethyl)phenyl)-1*H*-1,2,3-triazol-4-yl)-*N*-(4-chlorophenyl)propanamide (203011).[76] Compound **15** (0.050 g, 0.196 mmol) and compound **11** (0.041 g, 0.197 mmol) were suspended in a 1:1 mixture of t-Butanol (0.392 mL) and Water (0.392 mL). L-Ascorbic acid (0.020 ml, 0.020 mmol) was added, followed by copper(II) sulfate pentahydrate (6.53 µl, 1.96 µmol). The heterogeneous mixture was stirred vigorously overnight and was then diluted with water (2 mL), cooled in ice, and the brown solid was collected by filtration. The precipitate was washed with cold water (2 x 10 mL) and was dried *in vacuo*. Crude material was purified using column chromatography (35-50% EtOAc/Hex) to afford 0.017 g (0.037 mmol, 19% yield) of title compound as a colorless oil. TLC R_f: (50% EtOAc/Hex): 0.30. TOF MS-ESI *m/z* $[M+H]^+$ 463.0; [M+Na] 484.9. ^{1}H NMR (500 MHz, $CDCl_3$): δ 8.21 (s, 2H), 7.99 (s, 1H), 7.93 (bs, 1H), 7.65 (bs, 1H), 7.45 (d, *J* = 8.8 Hz, 2H), 7.29-7.25 (m, 2H), 3.32-3.19 (m, 2H), 2.99-2.86 (m, 2H).

***N*-(but-3-yn-1-yl)-3,5-bis(trifluoromethyl)benzamide (13).** 3-Butyn-1-amine hydrochloride (**12**) (0.053 g, 0.500 mmol) was suspended in DCM (5.0 mL) and was treated with 3,5-bis(trifluoromethyl)benzoyl chloride (0.099 ml, 0.550 mmol), followed

by triethylamine (0.150 ml, 1.07 mmol). The reaction was stirred vigorously overnight at room temperature. The yellow solution was concentrated *in vacuo* to afford 0.150 g (0.485 mmol, 97% yield) of title compound as a yellow oil. The compound was used without further purification. TOF MS-ESI *m/z* $[M+H]^+$ 463.0; [M+Na] 484.9. ^{1}H NMR (500 MHz, $CDCl_3$): δ 8.23 (s, 2H), 8.02 (s, 1H), 6.67 (s, 1H), 3.70-3.63 (m, 2H), 2.62-2.54 (m, 2H), 2.11-2.07 (m, 1H).

1-azido-4-chlorobenzene (17).[142]

***N*-(2-(1-(4-chlorophenyl)-1*H*-1,2,3-triazol-4-yl)ethyl)-3,5-bis(trifluoromethyl)benzamide (203017).**[76] Compound **17** (0.023 g, 0.150 mmol) and compound **13** (0.046 g, 0.150 mmol) were suspended in a 1:1 mixture of t-Butanol (0.300 mL) and Water (0.300 mL). L-Ascorbic acid (0.015 ml, 0.015 mmol) was added, followed by Copper(II) sulfate pentahydrate (0.010 mL, 0.003 mmol). The heterogeneous mixture was stirred vigorously for 48 h and was then diluted with water (2 mL), cooled in ice, and the brown solid was collected by filtration. The precipitate was washed with cold water (2 x 10 mL) and was dissolved in EtOAc. The filtrate was extracted with EtOAc (2 x 2 mL) and the organics were combined with the dissolved precipitate. Combined organics were washed with brine (5 mL), dried ($MgSO_4$) and concentrated *in vacuo*. Crude material was purified using a Biotage (30-60% EtOAc/Hex) to afford 0.006 g (0.037 mmol, 28% yield) of title compound as an off-white solid. TLC R_f (50% EtOAc/Hex): 0.34. TOF MS-ESI *m/z* $[M+H]^+$ 463.0; [M+Na] 485.0. HPLC (gradient A): ret time = 7.83 min; purity = 99%. ^{1}H NMR (500 MHz, $CDCl_3$): δ 8.29 (s, 2H), 8.00 (s, 1H), 7.84 (s, 1H), 7.70-7.61 (m, 2H), 7.55 (s, 1H), 7.59-7.44 (m, 3H), 3.96-3.91 (m, 2H), 3.17-3.12 (m, 2H).

4-(3,5-bis(trifluoromethyl)benzamido)benzoic acid (2b). Prepared according to Procedure B to afford 0.432 g (1.15 mmol, 98% yield) of title compound as a white solid. TOF MS-ESI *m/z* $[M-H]^-$ 375.9. ^{1}H NMR (500 MHz, DMSO-d_6): δ 12.81 (s, 1H), 10.91 (s, 1H), 8.64 (d, *J* = 12.2 Hz, 2H), 8.65-8.40 (m, 1H), 8.00-7.90 (m, 4H).

***N*-(4-((4-chlorophenyl)carbamoyl)phenyl)-3,5-bis(trifluoromethyl)benzamide (101329).** Prepared using **2b** according to Procedure C. Crude material was triturated with EtOAc to afford 0.201 g (0.413 mmol, 36% yield) of title compound as a light yellow solid. TLC R_f (50% EtOAc/Hex): 0.62. TOF MS-ESI *m/z* $[M+H]^+$ 487.0; [M+Na] 509.0. HPLC (gradient A): ret time = 8.46 min; purity = >95%. ^{1}H NMR (500 MHz, DMSO) δ 10.93 (s, 1H), 10.35 (s, 1H), 8.65 (s, 2H), 8.42 (s, 1H), 8.11-8.01 (m, 2H), 8.01-7.91 (m, 2H), 7.90-7.81 (m, 2H), 7.51-7.37 (m, 2H).

3-(3,5-bis(trifluoromethyl)benzamido)benzoic acid (2c). Prepared according to Procedure B to afford 0.429 g (1.14 mmol, 96% yield) of title compound as a white solid. TOF MS-ESI *m/z* $[M-H]^-$ 375.9. ^{1}H NMR (500 MHz, DMSO-d_6): δ 13.18 (bs, 1H), 10.81 (s, 1H), 8.66 (s, 2H), 8.39-8.38 (m, 2H), 8.08 (d, *J* = 7.5 Hz, 1H), 7.73 (d, *J* = 7.6 Hz, 1H), 7.55-7.45 (m, 1H).

***N*-(3-((4-chlorophenyl)carbamoyl)phenyl)-3,5-bis(trifluoromethyl)benzamide (101343).** Prepared using **2c** according to Procedure C. Crude material was purified using Combiflash (33-66% EtOAc/Hex) to afford 0.222 g (0.437 mmol, 38% yield) of title compound as a brown solid. TLC R_f (50% EtOAc/Hex): 0.66. TOF MS-ESI *m/z* $[M+H]^+$ 487.0; [M+Na] 509.0. HPLC (gradient A): ret time = 8.44 min; purity = >95%. ^{1}H NMR (500 MHz, DMSO-d_6): δ 10.86 (s, 1H), 10.46 (s, 1H), 8.67 (s, 2H), 8.41 (s, 1H), 8.28 (s, 1H), 8.11 (d, *J* = 8.1 Hz, 1H), 7.84 (d, *J* = 8.8 Hz, 2H), 7.77 (d, *J* = 7.7 Hz, 1H), 7.59 (t, *J* = 7.9 Hz, 1H), 7.44 (d, *J* = 8.8 Hz, 2H).

2-(3,5-bis(trifluoromethyl)phenyl)-4*H*-benzo[d][1,3]oxazin-4-one (20). Prepared according to Procedure C. Desired product was actually *N*-(2-((4-chlorophenyl)carbamoyl)phenyl)-3,5-bis(trifluoromethyl)benzamide. Crude material was triturated with DCM to afford 0.103 g of title compound as a white solid. ^{1}H NMR (500 MHz, DMSO-d_6): δ 8.78 (s, 2H), 8.31-8.28 (m, 1H), 8.08 (s, 1H), 7.93-7.89 (m, 1H), 7.79-7.77 (m, 1H), 7.64-7.60 (m, 1H).

***N*-(2-((4-chlorophenyl)carbamoyl)phenyl)-3,5-bis(trifluoromethyl)benzamide (101433).**[143] Compound **20** (0.050 g, 0.139 mmol) and 4-Chloroaniline (0.035 g, 0.278 mmol) were added to a tube and were treated with DMAP (0.017 g, 0.139 mmol) dissolved in Pyridine (1.0 mL) and stirring began. Additional Pyridine (1.0 mL) was added, and solution was heated to 80 °C for 34 h. Solution was then acidified to pH ~2 using conc. HCl. Resulting white solid was filtered and then washed with water. Crude material was purified using flash chromatography (33% EtOAc/Hex) to afford 0.036 g (0.074 mmol, 53% yield) of title compound as a white solid. TOF MS-ESI *m/z* [M+Na] 509.0. HPLC (gradient A): ret time = 9.35 min; purity = >95%. ^{1}H NMR (500 MHz, DMSO-d_6): δ 11.27 (s, 1H), 10.59 (s, 1H), 8.49 (s, 2H), 8.40 (s, 1H), 7.96 (d, *J* = 7.9 Hz, 1H), 7.81 (d, *J* = 7.5 Hz, 1H), 7.74 (d, *J* = 8.8 Hz, 2H), 7.65-7.61 (m, 1H), 7.42-7.36 (m, 3H).

***N*-(3-(5-chloroindolin-1-yl)-3-oxopropyl)-3,5-bis(trifluoromethyl)benzamide (102443).** Prepared using **2a** according to Procedure C. Crude material was triturated with EtOAc to afford 0.034 g (0.073 mmol, 7% yield) of title compound as a white solid. TOF MS-ESI *m/z* $[M+H]^+$ 465.0; [M+Na] 487.0. HPLC (gradient A): ret time = 8.10 min; purity = 99%. ^{1}H NMR (500 MHz, DMSO-d_6) δ 9.10 (d, *J* = 5.0 Hz, 1H), 8.51 (s, 2H), 8.32 (s, 1H), 8.07 (d, *J* = 8.6 Hz, 1H), 7.30 (s, 1H), 7.23-7.17 (m, 1H), 4.12 (t, *J* = 8.5 Hz, 2H), 3.61 (dd, *J* = 12.4 Hz, 6.5 Hz, 2H), 3.15 (t, *J* = 8.5 Hz, 2H), 2.80 (t, *J* = 6.9 Hz, 2H).

(1*S*,2*R*)-2-(3,5-bis(trifluoromethyl)benzamido)cyclopentanecarboxylic acid (2d). Prepared according to Procedure A to afford 0.196 g (0.531 mmol, 93% yield) of title compound as a white solid. ^{1}H NMR (500 MHz, DMSO-d_6): δ 12.04 (s, 1H), 8.81 (d, *J* = 7.9 Hz, 1H), 8.44 (s, 2H), 8.31 (s, 1H), 4.65-4.52 (m, 1H), 3.02-2.95 (m, 1H), 2.09-1.74 (m, 5H), 1.62-1.46 (m, 1H).

N-((1*R*,2*S*)-2-((4-chlorophenyl)carbamoyl)cyclopentyl)-3,5-bis(trifluoromethyl)benzamide (102526). Prepared using **2d** according to Procedure C. Crude material was triturated with DCM to afford 0.085 g (0.178 mmol; 35% yield) of

title compound as a white solid. MS-ESI *m/z* [M+Na] 500.0. HPLC (gradient A): ret time = 8.16 min; purity = 99%. ^{1}H NMR (500 MHz, DMSO-d_6): δ 9.96 (s, 1H), 8.83 (d, *J* = 8.2 Hz, 1H), 8.21 (s, 1H), 8.21 (s, 1H), 8.19 (s, 2H), 7.50-7.47 (m, 2H), 7.21-7.17 (m, 2H), 4.76-4.64 (m, 1H), 3.15 (q, *J* = 7.8 Hz, 1H), 2.12-1.78 (m, 5H), 1.59-1.49 (m, 1H).

2-(1-(3,5-bis(trifluoromethyl)benzoyl)piperidin-2-yl)acetic acid (2e). 2-(piperidin-2-yl)acetic acid hydrochloride (0.259 g, 1.44 mmol) was added to a flask, followed by 2M NaOH (2.4 ml) and dichloromethane (2.4 ml). The reaction mixture was stirred vigorously, and 3,5-bis(trifluoromethyl)benzoyl chloride (0.216 ml, 1.20 mmol) was added via syringe. The reaction mixture was stirred vigorously overnight. After stirring overnight the DCM layer was removed and aqueous layer was acidified to ~pH 2 and was extracted using EtOAc (2 x 20 mL). The combined organics were washed with brine (20 mL), dried ($MgSO_4$), and were concentrated. Crude material was purified by flash chromatography (4:6:0.5 EtOAc/Hex/AcOH) to afford 0.091 g (0.237 mmol, 20% yield) of title compound as a yellow oil. TLC R_f (4:6:1 EtOAc/Hex/AcOH): 0.30. ^{1}H NMR (500 MHz, $CDCl_3$): δ 11.61 (s, 1H), 7.92 (s, 1H), 7.85 (s, 2H), 5.42-2.48 (m, 5H), 1.91-1.40 (m, 6H).

2-(1-(3,5-bis(trifluoromethyl)benzoyl)piperidin-2-yl)-*N*-(4-chlorophenyl)acetamide (203001). Prepared using **2e** according to Procedure C. Reaction molarity was 0.24 M, and reaction was diluted with EtOAc (10 mL), and washing steps utilized 15 mL each. Crude material was purified using flash chromatography (1-1.5% Methanolic ammonia/DCM) to afford 0.030 g (0.059 mmol, 25% yield) of title compound as a yellow oil. TLC R_f (1.5% Methanolic ammonia/DCM): 0.21. HPLC (gradient A): ret time = 8.11 min; purity = 99%. TOF MS-ESI *m/z* [M+Na] 514.9. ^{1}H NMR (500 MHz, $CDCl_3$): δ 8.88 (s, 1H), 7.93 (s, 1H), 7.78 (s, 2H), 7.51 (d, *J* = 7.8 Hz, 2H), 7.23 (d, *J* = 8.6 Hz, 2H), 3.48-3.40 (m, 1H), 3.33-3.22 (m, 1H), 3.06-2.94 (m, 1H), 2.80-2.63 (m, 1H), 1.94-1.44 (m, 6H).

Piperidin-4-one, TFA salt (21a). *tert*-Butyl 4-oxopiperidine-1-carboxylate (0.448 g, 2.25 mmol) was dissolved in DCM (17.4 mL), cooled to 0 °C, and treated with TFA (8.6

mL, 112 mmol). Reaction was allowed to stir overnight and was concentrated to afford 0.602 g (2.82 mmol, 126% yield) of title compound as a yellow oil. ^{1}H NMR (500 MHz, DMSO-d_6): δ 9.12 (bs, 2H), 3.44 (s, 4H), 2.60-2.53 (m, 4H).

1-(3,5-bis(trifluoromethyl)benzoyl)piperidin-4-one (22). Compound **21a** (0.233 g, 1.10 mmol) was dissolved in DCM (2.2 mL) and was treated with 3,5-bis(trifluoromethyl)benzoyl chloride (0.242 mL, 1.33 mmol) and TEA (0.460 mL, 3.30 mmol). The reaction was stirred overnight at room temperature. Mixture was then diluted with DCM (2.0 mL) and was washed with saturated $NaHCO_3$ (20 mL) followed by aqueous 1N HCl (20 mL) and then brine (20 mL). Organic layer was dried ($MgSO_4$) and concentrated. Crude material was purified by flash chromatography (50% EtOAc/Hex) to afford 0.109 g (0.321 mmol, 29% yield) of title compound as a yellow oil. TLC R_f (50% EtOAc/Hex): 0.36. ^{1}H NMR (500 MHz, DMSO-d_6): δ 7.99 (s, 1H), 7.69 (s, 2H), 4.13-3.65 (m, 4H), 2.75-2.40 (m, 4H).

(3,5-bis(trifluoromethyl)phenyl)(4-(hydroxyimino)piperidin-1-yl)methanone (23).[78] To a solution of **22** (0.345 g, 1.02 mmol) in pyridine (2.8 mL) was added molecular sieves (3Å, 8-12 mesh, 0.34 g), and the mixture was stirred at room temperature for 10 minutes, followed by the addition of hydroxylamine hydrochloride (0.177 g, 2.55 mmol). The reaction was allowed to stir overnight at room temperature. Reaction mixture was filtered through celite and was rinsed with additional pyridine. The filtrate was diluted with water (10 mL) and was extracted with EtOAc (30 mL). Organic layer was dried ($MgSO_4$) and concentrated to afford 0.190 g (0.536 mmol, 53% yield) of title compound as a white solid. ^{1}H NMR (500 MHz, $CDCl_3$): δ 7.97 (s, 1H), 7.91 (s, 2H), 3.89 (bs, 2H), 3.53 (bs, 2H), 2.81 (bs, 1H), 2.66 (bs, 1H), 2.56 (bs, 1H), 2.38 (bs, 1H).

1-(3,5-bis(trifluoromethyl)benzoyl)-1,4-diazepan-5-one (24). Compound **23** (0.190 g, 0.536 mmol) was suspended in acetone (2.3 ml) and was treated with sodium carbonate (0.171 g, 1.61 mmol) in water (0.531 ml), and the mixture was stirred for 10 minutes. A solution of *p*-toluenesulfonyl chloride (0.153 g, 0.805 mmol) in acetone (0.574 ml) was added slowly while stirring. The mixture stirred for 3 hours. The acetone was then

removed from the mixture, and additional water (10 mL) was added. The aqueous mixture was extracted with dichloromethane (3 x 20 mL). Combined organics were dried ($MgSO_4$) and concentrated. Crude material was purified by flash chromatography (5% Methanolic ammonia/DCM) to afford 0.116 g (0.327 mmol, 61% yield) of title compound as a pale yellow solid. TLC R_f: (5% Methanolic ammonia/DCM): 0.21. TOF MS-ESI *m/z* $[M+H]^+$ 355.0; [M+Na] 377.0. ^1H NMR (500 MHz, $CDCl_3$) δ 7.98 (s, 1H), 7.87 (s, 2H), 6.25 (s, 1H), 4.10-3.20 (m, 6H), 2.86-2.54 (m, 2H).

1-(3,5-bis(trifluoromethyl)benzoyl)-4-(4-chlorophenyl)-1,4-diazepan-5-one (203005).[80, 144] 1-chloro-4-iodobenzene (0.239 g, 1.00 mmol) was dissolved in dioxane (1.0 mL) and was treated with **24** (0.027 g, 0.076 mmol), Copper(I) iodide (3.0 mg, 0.016 mmol), cesium carbonate (0.048 g, 0.147 mmol), and *N*,*N*-dimethylethylenediamine (1.7 µl, 0.016 mmol). The tube was evacuated and backfilled with nitrogen two times. The reaction was then heated to 100 °C and capped. The reaction was allowed to stir at 100 °C for 24 hours. The mixture was allowed to cool to room temperature and was filtered through a 2 x 0.5 cm pad of silica gel eluting with 10 mL of ethyl acetate. The EtOAc was evaporated. Crude material was purified using column chromatography (50-66% EtOAc/Hex) to afford 0.017 g (0.037 mmol, 48% yield) of title compound as a colorless oil. TLC R_f: (66% EtOAc/Hex): 0.29. TOF MS-ESI *m/z* $[M+H]^+$ 465.0; [M+Na] 487.0. HPLC (gradient A): ret time = 7.40 min; purity = 99%. ^1H NMR (500 MHz, $CDCl_3$): δ 7.99 (s, 1H), 7.90 (s, 2H), 7.37 (d, *J* = 6.2 Hz, 2H), 7.15 (bs, 2H), 4.20-3.55 (m, 6H), 3.06-2.78 (m, 2H).

***tert*-butyl 3-((4-chlorophenyl)carbamoyl)pyrrolidine-1-carboxylate.** Prepared using *N*-Boc-*β*-proline (0.108 g, 0.500 mmol) and 4-chloroaniline (0.070 g, 0.550 mmol) according to Procedure C to afford 0.129 g (0.397 mmol, 79% yield) of title compound as an amber oil. Crude material was used without any further purification. TOF MS-ESI *m/z* [M+Na] 347.1. ^1H NMR (500 MHz, $CDCl_3$): δ 7.49 (d, *J* = 8.8 Hz, 2H), 7.28 (d, *J* = 8.7 Hz, 2H), 3.78-3.49 (m, 3H), 3.45-3.33 (m, 1H), 3.00 (s, 1H), 2.36-2.11 (m, 2H), 1.49 (s, 9H).

***N*-(4-chlorophenyl)pyrrolidine-3-carboxamide.** *tert*-butyl 3-((4-chlorophenyl)carbamoyl)pyrrolidine-1-carboxylate (0.129 g, 0.397 mmol) was dissolved in dichloromethane (3.45 ml). The solution was then cooled to 0 °C, and trifluoroacetic acid (1.04 ml, 13.50 mmol) was added dropwise. The solution stirred at room temperature for 2 hours and then the solvent was removed *in vacuo* to afford 0.050 g (0.223 mmol, 56% yield) of title compound as a sticky brown oil. ^{1}H NMR (500 MHz, $CDCl_3$): δ 9.37 (s, 1H), 8.53 (s, 1H), 7.84 (s, 1H), 7.45-7.40 (m, 2H), 7.35-7.28 (m, 2H), 3.75-3.63 (m, 2H), 3.60-3.45 (m, 3H), 2.55-2.42 (m, 1H), 2.40-2.30 (m, 1H).

1-(3,5-bis(trifluoromethyl)benzoyl)-*N*-(4-chlorophenyl)pyrrolidine-3-carboxamide (203015). Compound was prepared using *N*-(4-chlorophenyl)pyrrolidine-3-carboxamide (0.050 g, 0.148 mmol), 3,5-bis(trifluoromethyl)benzoyl chloride (0.029 mL, 0.162 mmol), and triethylamine (0.046 mL, 0.325 mmol) according to Procedure B. Crude material was purified using a Biotage (45% EtOAc/Hex) to afford 0.018 g (0.039 mmol, 26% yield) of title compound as a clear oil. TOF MS-ESI *m/z* $[M+H]^+$ 465.0; [M+Na] 486.9. HPLC (gradient A): ret time = 7.69 min; purity = 99%. ^{1}H NMR (500 MHz, $CDCl_3$): δ 8.27-8.08 (m, 1H), 8.03-7.98 (m, 2H), 7.97-7.93 (m, 1H), 7.48 (d, *J* = 8.6, 1H), 7.43 (d, *J* = 8.6, 1H), 7.30-7.20 (m, 2H), 4.03-3.45 (m, 4H), 3.23-3.04 (m, 1H), 2.41-2.28 (m, 1H), 2.26-2.15 (m, 1H).

1-(4-chlorophenyl)-5-oxopyrrolidine-3-carboxylic acid (26). A neat mixture of 4-chloroaniline (0.511 g, 4.01 mmol) and itaconic acid (0.521 g, 4.00 mmol) was heated at 110 °C for 2 h. Crude material was re-crystallized from water/ethanol to yield 0.353 g (1.47 mmol, 37% yield) of title compound as a tan solid. TOF MS-ESI *m/z* $[M-H]^-$ 238.0. ^{1}H NMR (500 MHz, DMSO-d_6): δ 12.83 (s, 1H), 7.69 (d, *J* = 9.0 Hz, 2H), 7.43 (d, *J* = 9.0 Hz, 2H), 4.06-3.94 (m, 2H), 2.79-2.68 (m, 2H).

***tert*-butyl (1-(4-chlorophenyl)-5-oxopyrrolidin-3-yl)carbamate (27).**[81] Compound **26** (0.076 g, 0.317 mmol) was suspended in toluene (5.29 mL) and to the mixture were added *t*-butanol (0.090 mL, 0.951 mmol), triethylamine (0.067 mL, 0.476 mmol), and DPPA (0.082 mL, 0.381 mmol). The mixture was refluxed overnight, cooled, and

concentrated *in vacuo*. Crude material was purified using a CombiFlash system (30% EtOAc/Hex) to afford 0.038 g (0.122 mmol, 39% yield) of title compound as a white solid. TLC R_f (50% EtOAc/Hex): 0.31. ^{1}H NMR (500 MHz, DMSO-d_6): δ 7.72-7.63 (m, 2H), 7.50-7.36 (m, 3H), 4.20 (s, 1H), 4.06 (dd, *J* = 10.0, 7.0 Hz, 1H), 3.59 (dd, *J* = 10.1, 3.8 Hz, 1H), 2.83 (dd, *J* = 17.1, 8.2 Hz, 1H), 2.42 (dd, *J* = 17.1, 4.6 Hz, 1H), 1.39 (s, 9H).

4-amino-1-(4-chlorophenyl)pyrrolidin-2-one (28). Compound **27** (0.038 g, 0.122 mmol) was dissolved in DCM (0.815 mL) and was cooled to 0 °C. TFA (0.408 mL) was slowly added to the stirring solution, and the reaction continued stirring at 0 °C for 1 hr 45 min. The solution was slowly added to 10 mL of cooled 1M NaOH. The mixture was then extracted with DCM (2 x 5 mL) and was concentrated *in vacuo* to afford 0.023 g (0.071 mmol, 58% yield) of title compound. Compound was used without further purification. ^{1}H NMR (500 MHz, $CDCl_3$): δ 7.58-7.53 (m, 2H), 7.34-7.29 (m, 2H), 4.01 (dd, *J* = 9.6, 6.6 Hz, 1H), 3.86-3.79 (m, 1H), 3.50 (dd, *J* = 9.8, 4.0 Hz, 1H), 2.88 (dd, *J* = 17.1, 7.3 Hz, 1H), 2.38 (dd, *J* = 17.0, 4.8 Hz, 1H), 1.49 (s, 2H).

***N*-(1-(4-chlorophenyl)-5-oxopyrrolidin-3-yl)-3,5-bis(trifluoromethyl)benzamide (203606).** Compound **28** (0.023 g, 0.109 mmol) was dissolved in DCM (0.218 mL). To the stirring solution was added 3,5-bis(trifluoromethyl)benzoyl chloride (0.022 mL, 0.120 mmol) followed by Triethylamine (0.031 mL, 0.218 mmol). The reaction mixture was stirred at room temperature overnight. The mixture was diluted with 10 mL of DCM and was washed with 1M aq HCl (5 mL) followed by a wash with sat. aq. $NaHCO_3$ (5 mL) and brine (5 mL), and was dried ($MgSO_4$) and concentrated *in vacuo*. Crude material was triturated with DCM to afford 0.021 g (0.047 mmol, 43% yield) of title compound as a white solid. TOF MS-ESI *m/z* $[M+H]^+$ 451.0; [M+Na] 473.0. HPLC (50-90% Acetonitrile/Water over 6 minutes): ret time = 4.20 min; purity = >90%. ^{1}H NMR (500 MHz, DMSO-d_6): δ 9.37 (d, *J* = 6.7 Hz, 1H), 8.52 (s, 2H), 8.34 (s, 1H), 7.81-7.71 (m, 2H), 7.51-7.41 (m, 2H), 4.76-4.68 (m, 1H), 4.26 (dd, *J* = 10.4, 6.9 Hz, 1H), 3.83 (dd, *J* = 10.4, 2.9 Hz, 1H), 3.06 (dd, *J* = 17.4, 8.5 Hz, 1H), 2.64 (dd, *J* = 17.5, 3.3 Hz, 1H).

***N*-(1-(4-chlorophenyl)-5-oxopyrrolidin-3-yl)-3,5-difluorobenzamide (203846).** 3,5-difluorobenzoic acid (0.014 g, 0.085 mmol) was dissolved in DCM (0.4 mL). DMAP (0.217 mg, 1.780 µmol) was added, followed by **28** (0.015 g, 0.071 mmol), and then EDC (0.014 g, 0.071 mmol). The solution was stirred at room temperature overnight. DCM (2 mL) was then added. The solution was washed with 1N HCl (2 mL) followed by saturated $NaHCO_3$ (2 mL). The solvent was concentrated *in vacuo*. Crude material was purified by column chromatography (50-60% EtOAc/Hex) to afford 0.012 g (0.034 mmol, 48% yield) of title compound as a white solid. TLC R_f (50% EtOAc/Hex): 0.26. TOF MS-ESI *m/z* $[M-H]^-$ 349.0. ^1H NMR (500 MHz, DMSO) δ 9.08 (d, *J* = 6.6 Hz, 1H), 7.76-7.69 (m, 2H), 7.63-7.58 (m, 2H), 7.49 (tt, *J* = 9.3, 2.4 Hz, 1H), 7.46-7.40 (m, 2H), 4.70-4.61 (m, 1H), 4.25-4.20 (m, 1H), 3.76 (dd, *J* = 10.4, 3.0 Hz, 1H), 3.01 (dd, *J* = 17.3, 8.4 Hz, 1H), 2.59 (dd, *J* = 17.4, 3.5 Hz, 1H).

***N*-(3,5-bis(trifluoromethyl)phenyl)-1-(4-chlorophenyl)-5-oxopyrrolidine-3-carboxamide (203848).**[145] To a stirring solution of **26** (0.050 g, 0.209 mmol) and 3,5-bis(trifluoromethyl)aniline (0.039 ml, 0.250 mmol) in DMF (0.417 ml) was added EDC (0.048 g, 0.250 mmol). The reaction was stirred overnight at room temperature. After stirring overnight, the DMF was removed *in vacuo*. Water was then added (10 mL), and the aqueous layer was extracted with EtOAc (3 x 10 mL), and the combined organic layers were washed with brine (10 mL), dried ($MgSO_4$), and concentrated *in vacuo.* Crude material was triturated with DCM to afford 0.045 g (0.100 mmol, 48% yield) of title compound as a white crystalline solid. TOF MS-ESI *m/z* $[M-H]^-$ 449.0. ^1H NMR (500 MHz, DMSO-d_6) δ 10.87 (s, 1H), 8.28 (s, 2H), 7.80 (m, 1H), 7.72 (d, *J* = 8.7 Hz, 2H), 7.45 (dd, *J* = 8.8, 1.8 Hz, 2H), 4.16-4.02 (m, 2H), 3.53-3.45 (m, 1H), 2.94-2.76 (m, 2H).

Benzyl (1-(4-chlorophenyl)-5-oxopyrrolidin-3-yl)carbamate (203007).[81] Compound **26** was suspended in toluene (17.0 mL) and was treated with benzyl alcohol (0.312 mL, 3.00 mmol), TEA (0.259 mL, 1.86 mmol), and DPPA (0.209 mL, 0.967 mmol). Reaction was refluxed for 6 h, and the solution was concentrated. Crude material was purified by flash chromatography (33-60% EtOAc/Hex) to afford 0.232 g (0.673 mmol, 67% yield)

to afford title compound as a white solid. TLC R_f (50% EtOAc/Hex): 0.21. ^{1}H NMR (500 MHz, DMSO-d_6): δ 7.88 (d, *J* = 6.4 Hz, 1H), 7.68 (d, *J* = 8.9 Hz, 2H), 7.46-7.03 (m, 7H), 5.04 (s, 2H), 4.30-4.23 (m, 1H), 4.13-4.05 (m, 1H), 3.64 (dd, *J* = 10.1 Hz, 3.6 Hz, 1H), 2.88 (dd, *J* = 17.2 Hz, 8.2 Hz, 1H), 2.44 (dd, *J* = 17.1 Hz, 4.4 Hz, 2H).

3,5-difluorobenzyl (1-(4-chlorophenyl)-5-oxopyrrolidin-3-yl)carbamate (203604).[81] Compound **26** (0.030 g, 0.125 mmol) was suspended in toluene (2.09 mL) and to the mixture were added 3,5-difluorobenzyl alcohol (0.043 mL, 0.376 mmol), triethylamine (0.026 ml, 0.188 mmol), and DPPA (0.032 mL, 0.150 mmol). Reaction mixture was refluxed for 6 hours. The reaction was cooled to room temperature and concentrated *in vacuo*. Crude material was purified using a CombiFlash system (18-45% EtOAc/Hex) to afford 0.039 g (0.102 mmol, 82% yield) of title compound as a clear oil. TLC R_f (50% EtOAc/Hex): 0.19. ^{1}H NMR (500 MHz, $CDCl_3$): δ 7.55-7.43 (m, 2H), 7.32-7.20 (m, 2H), 6.90-6.80 (m, 2H), 6.78-6.68 (m, 1H), 5.77-5.62 (m, 1H), 5.12-5.00 (m, 2H), 4.53-4.35 (m, 1H), 4.15-4.00 (m, 1H), 3.79-3.59 (m, 1H), 2.96 (dd, *J* = 17.5, 8.3 Hz, 1H), 2.51 (dd, *J* = 17.5, 4.3 Hz, 1H).

3,5-bis(trifluoromethyl)benzyl (1-(4-chlorophenyl)-5-oxopyrrolidin-3-yl)carbamate (203065).[81] Compound **26** (0.050 g, 0.209 mmol) was suspended in toluene (3.5 ml) and to the mixture were added 3,5-bis(trifluoromethyl)benzyl alcohol (0.154 g, 0.631 mmol), triethylamine (0.044 ml, 0.313 mmol), and DPPA (0.054 ml, 0.250 mmol). Mixture was refluxed for 6 hours. The reaction was cooled to room temperature and concentrated *in vacuo*. Crude material was purified using CombiFlash system (25-40% EtOAc/Hex) followed by trituration with $CHCl_3$ to afford 0.049 g (0.102 mmol, 49% yield) of title compound as an off-white solid. TLC R_f (50% EtOAc/Hex): 0.43. HPLC (gradient A): ret time = 7.98 min; purity = 99%. TOF MS-ESI *m/z* $[M+H]^+$ 480.9; [M+Na] 502.9. ^{1}H NMR (500 MHz, $CDCl_3$): δ 7.82 (m, 3H), 7.50 (d, *J* = 6.2 Hz, 2H), 7.35-7.10 (m, 3H), 5.64 (s, 1H), 5.21 (s, 2H), 4.48 (s, 1H), 4.18-4.08 (m, 1H), 3.75 (d, *J* = 8.8 Hz, 1H), 3.03-2.93 (m, 1H), 2.58-2.46 (m, 1H).

3-amino-3-(5-chloro-2-nitrophenyl)propanoic acid (30).[82] A mixture of 5-chloro-2-nitrobenzaldehyde (**29**) (0.200 g, 1.078 mmol), formic acid (0.165 ml, 4.31 mmol), and malonic acid (0.146 g, 1.401 mmol) was heated to 45 °C with stirring and was then treated with ammonium formate (0.170 g, 2.69 mmol). The temperature was increased to 70 °C and held for one hour. The temperature was then increased to 95 °C. After 4 hours, concentrated HCl (0.400 mL) was added and heating continued for 1 hour. The mixture was then cooled and diluted with water (1 mL), followed by extraction with methyl isobutyl ketone (3 x 2 mL). The aqueous layer was separated and its pH was adjusted to approximately 4 by addition of 50% KOH solution. The precipitate was collected and dried *in vacuo* to afford 0.098 g (0.401 mmol, 37% yield) of title compound as a yellow solid. No further purification was performed. ^{1}H NMR (500 MHz, DMSO-d_6): δ 7.97 (d, J = 2.4 Hz, 1H), 7.93 (d, J = 8.7 Hz, 1H), 7.58 (dd, J = 8.7, 2.3 Hz, 1H), 6.27 (bs, 2H), 4.61 (dd, J = 8.8, 5.0 Hz, 1H), 2.64-2.56 (m, 1H).

3-(3,5-bis(trifluoromethyl)benzamido)-3-(5-chloro-2-nitrophenyl)propanoic acid (31). Compound **30** (0.041 g, 0.168 mmol) was dissolved in 2M NaOH (0.335 ml) and then treated with 3,5-bis(trifluoromethyl)benzoyl chloride (0.033 ml, 0.184 mmol). The mixture was stirred overnight at room temperature under nitrogen. The basic mixture was acidified to pH ~2 using 2M HCl. The acidic mixture was then filtered, and the resulting solid was rinsed with water. The solid was dried *in vacuo* to afford 0.050 g (0.103 mmol, 62% yield) of title compound as a fluffy white solid. No further purification was performed. ^{1}H NMR (500 MHz, DMSO-d_6) δ 12.62 (s, 1H), 9.55 (d, J = 6.8 Hz, 1H), 8.49-8.42 (m, 4H), 8.37 (s, 1H), 8.05-8.01 (m, 1H), 7.85-7.83 (m, 1H), 7.66-7.62 (m, 1H), 5.84-5.77 (m, 1H), 3.04-2.96 (m, 1H), 2.93-2.87 (m, 1H).

***N*-(6-chloro-2-oxo-1,2,3,4-tetrahydroquinolin-4-yl)-3,5-bis(trifluoromethyl)benzamide (203845).**[83, 84] Compound **31** (0.021 g, 0.043 mmol) was heated with iron(II) sulfate heptahydrate (0.120 g, 0.433 mmol) at 100 °C for 1 hour in 10% NH_4OH (0.722 ml) and Ethanol (0.722 ml). The reaction was cooled and additional ethanol was added. The mixture was filtered, then extracted using ethyl acetate (3 x 5 mL). The organic layer was dried ($MgSO_4$) and concentrated to yield 0.022 g of an off-

white residue. The residue was then triturated with chloroform to afford 0.007 g (0.016 mmol, 37% yield) of title compound as a white solid. TOF MS-ESI *m/z* $[M-H]^-$ 435.0. ^1H NMR (500 MHz, DMSO-d_6) δ 10.45 (s, 1H), 9.42 (d, *J* = 7.4 Hz, 1H), 8.55 (s, 2H), 8.35 (s, 1H), 7.37-7.31 (m, 2H), 6.96 (d, *J* = 8.4 Hz, 1H), 5.39 (q, *J* = 7.2 Hz, 1H), 2.88-2.68 (m, 2H).

1-(4-chlorophenyl)-2-oxopyrrolidine-3-carbonitrile (33).[85] A mixture of ethyl 1-cyanocyclopropanecarboxylate (**32**) (0.186 ml, 1.437 mmol) and 4-chloroaniline (0.183 g, 1.437 mmol) was heated at 140 °C overnight. The mixture was cooled and the crude material was purified using a CombiFlash system (25-50% EtOAc/Hex) to afford 0.034 g of title compound as a brown solid. A second purification was performed using a CombiFlash system (15% EtOAc/Hex) to afford an additional 0.043 g of title compound as a brown solid, totaling 0.077 g (0.349 mmol, 24% yield). TLC R_f (50% EtOAc/Hex): 0.38. ^1H NMR (500 MHz, $CDCl_3$): δ 7.58-7.49 (m, 2H), 7.40-7.32 (m, 2H), 3.98-3.85 (m, 2H), 3.80-3.73 (m, 1H), 2.71-2.60 (m, 1H), 2.57-2.45 (m, 1H).

3-(aminomethyl)-1-(4-chlorophenyl)pyrrolidin-2-one (34).[86] Compound **33** (0.038 g, 0.172 mmol) was dissolved in 1M methanolic ammonia (3.5 ml), and to the solution was added a spatula tip of Raney nickel catalyst. The mixture was placed on a Parr shaker at ~34 psi at room temperature for 2 hours. The mixture was filtered through a plug of celite topped with $MgSO_4$. The celite was rinsed repeatedly with MeOH, and the filtrate was concentrated *in vacuo.* The compound was then triturated and filtered to afford 0.025 g (0.111 mmol, 65% yield) of brown solid.

***N*-((1-(4-chlorophenyl)-2-oxopyrrolidin-3-yl)methyl)-3,5-bis(trifluoromethyl)benzamide (203850).** Prepared according to Procedure B using **34** (0.015 g, 0.067 mmol), 3,5-bis(trifluoromethyl)benzoyl chloride (0.014 ml, 0.080 mmol), and TEA (0.011 ml, 0.080 mmol). Crude material was purified by column chromatography (20-50% EtOAc/Hex) to afford 0.010 g (0.020 mmol, 30% yield) of title compound as a crystalline white solid. TLC R_f (50% EtOAc/Hex): 0.33. TOF MS-ESI *m/z* $[M-H]^-$ 463.0. HPLC (gradient A): ret time = 8.07 min; purity = 99%. ^1H NMR (500

MHz, $CDCl_3$) δ 8.29 (s, 2H), 8.01 (s, 1H), 7.96-7.91 (m, 1H), 7.62-7.49 (m, 2H), 7.42-7.30 (m, 2H), 4.20-4.09 (m, 1H), 3.92-3.76 (m, 2H), 3.54-3.47 (m, 1H), 3.00-2.92 (m, 1H), 2.50-2.38 (m, 1H), 2.03-1.93 (m, 1H).

3-(aminomethylene)-5-chloroindolin-2-one (36).[87] DMF (0.878 ml, 11.34 mmol) and phosphorus oxychloride (0.061 ml, 0.649 mmol) were heated up to 45 °C using an oil bath. 5-Chlorooxindole (0.100 g, 0.597 mmol) was added to the mixture, and the temperature was held at 45 °C for 1 hr. The reaction was then cooled to 0 °C, and to the cooled mixture was added ammonium hydroxide (17.55 ml, 496 mmol). The mixture was warmed to room temperature and allowed to stir for 30 minutes. Reaction mixture was then extracted with EtOAc (3 x 20 mL), dried ($MgSO_4$), and concentrated *in vacuo*. Crude oil was triturated with DCM to afford 0.020 g (0.100 mmol, 17% yield) of a greenish solid. Filtrate was concentrated and triturated a second time with DCM to yield 0.030 g (0.154 mmol, 26% yield) of a mustard yellow solid. Filtrate was concentrated and triturated a third time with dichloromethane to yield 0.009 g (0.046 mmol, 8% yield) of title compound as a mustard yellow solid. NMR showed a mixture of isomers in batch 1 of solid. Batch 2 appeared to only the *E*-isomer, as found by NOE. **Batch 1**: ^{1}H NMR (500 MHz, DMSO-d_6): δ 10.25 (Isomer 2, s, 1H), 10.04 (Isomer 1, s, 1H), 8.37 (Isomer 2, dd, *J* = 15.1, 4.1 Hz, 1H), 8.22-8.13 (Isomer 2, m, 2H), 7.94 (Isomer 2, dd, *J* = 15.0, 7.6 Hz, 1H), 7.86 (Isomer 1, s, 1H), 7.74 (Isomer 1, d, *J* = 2.0 Hz, 1H), 7.59-7.49 (Isomer 1, m, 1H), 7.44 (Isomer 2, d, *J* = 2.1 Hz, 1H), 7.42-7.34 (Isomer 1, m, 1H), 6.94 (Isomer 1, dd, *J* = 8.2, 2.0 Hz, 1H), 6.89 (Isomer 2, dd, *J* = 8.1, 2.1 Hz, 1H), 6.74 (Isomers 1 and 2, dd, *J* = 11.4, 8.2 Hz, 2H). **Batch 2:** ^{1}H NMR (500 MHz, DMSO-d_6): δ 10.25 (s, 1H), 8.45-8.30 (m, 2H), 8.24-8.11 (m, 2H), 7.94 (dd, *J* = 15.1, 7.6 Hz, 1H), 7.44 (d, *J* = 2.2 Hz, 1H), 6.89 (dd, *J* = 8.2, 2.1 Hz, 1H), 6.75 (d, *J* = 8.2 Hz, 1H).

***N*-((5-chloro-2-oxoindolin-3-ylidene)methyl)-3,5-bis(trifluoromethyl)benzamide (203851).** Compound **36 batch 2** (.010 g, 0.051 mmol) was suspended in DCM (0.150 mL), and to the stirring mixture was added 3,5-bis(trifluoromethyl)benzoyl chloride (10.18 µl, 0.057 mmol) followed by TEA (0.010 mL, 0.071 mmol). The reaction mixture was allowed to stir at room temperature overnight. The mixture was concentrated *in*

vacuo and was redissolved in EtOAc (10 mL). The organic layer was washed with $NaHCO_3$ (5 mL) followed by 1M HCl (5 mL) and then brine (5 mL). The organic layer was then dried ($MgSO_4$) and concentrated *in vacuo*. The solid was triturated with hexanes to yield solid, which was dried and triturated with DCM to afford 0.009 g (0.020 mmol, 39% yield) of title compound. TOF MS-ESI *m/z* $[M-H]^-$ 433.0. ^1H NMR (500 MHz, DMSO-d_6): δ 12.33 (d, *J* = 10.5 Hz, 1H), 11.02 (s, 1H), 8.69 (d, *J* = 10.4 Hz, 1H), 8.53 (s, 1H), 8.49 (s, 2H), 7.98 (d, *J* = 2.3 Hz, 1H), 7.21 (dd, *J* = 8.1, 2.2 Hz, 1H), 6.92 (d, *J* = 8.4 Hz, 1H).

***N*^{1}-(6-chloropyridin-3-yl)propane-1,3-diamine.** 2-Chloro-5-aminopyridine (0.088 g, 0.685 mmol) was dissolved in Toluene (0.700 mL) and treated with 3-Bromopropylamine hydrobromide (**4**) (0.050 g, 0.228 mmol). Mixture was heated at reflux for 40 minutes. After cooling, precipitate was collected and treated with aqueous 15% aq NaOH (1 mL), and the aqueous layer was extracted with DCM (3 x 2 mL). Combined extracts were washed with water (2 mL), dried ($MgSO_4$), and concentrated to afford a purple oil. Crude material was purified by flash chromatography (10-14% Methanolic ammonia/DCM) to afford 0.013 g (0.070 mmol, 31% yield) of title compound as a yellow oil. TLC R_f (10% Methanolic ammonia/DCM): 0.20. ^1H NMR (500 MHz, $CDCl_3$): δ 7.75 (d, *J* = 3.0 Hz, 1H), 7.08 (d, *J* = 8.6 Hz, 1H), 6.86 (dd, *J* = 8.6 Hz, 3.1 Hz, 1H), 4.51 (bs, 1H), 3.20 (t, *J* = 6.6 Hz, 2H), 2.88 (t, *J* = 6.5 Hz, 2H), 1.77 (p, *J* = 6.5 Hz, 2H), 1.35 (bs, 2H).

***N*-(3-((6-chloropyridin-3-yl)amino)propyl)-3,5-bis(trifluoromethyl)benzamide (203059).** Compound was prepared using *N*^{1}-(6-chloropyridin-3-yl)propane-1,3-diamine (0.013 g, 0.070 mmol) and 3,5-bis(trifluoromethyl)benzoic acid (0.020 g, 0.077 mmol) according to Procedure C. Crude material was purified using column chromatography (30-50% EtOAc/Hex) to afford 0.018 g (0.042 mmol, 60% yield) of title compound as a yellow solid. TLC R_f (50% EtOAc/Hex): 0.37. HPLC (gradient A): ret time = 7.42 min; purity = 99%. TOF MS-ESI *m/z* $[M+H]^+$ 425.9; [M+Na] 447.9. ^1H NMR (500 MHz, $CDCl_3$) δ: 7.75 (d, *J* = 3.0 Hz, 1H), 7.08 (d, *J* = 8.6 Hz, 1H), 6.86 (dd, *J* = 8.6, 3.1 Hz,

1H), 3.20 (t, *J* = 6.6 Hz, 2H), 2.88 (t, *J* = 6.5 Hz, 2H), 1.77 (p, *J* = 6.5 Hz, 2H), 1.35 (s, 2H).

N^1-(5-chloropyridin-2-yl)propane-1,3-diamine.[146]

***N*-(3-((5-chloropyridin-2-yl)amino)propyl)-3,5-bis(trifluoromethyl)benzamide (203063).** Compound was prepared using N^1-(5-chloropyridin-2-yl)propane-1,3-diamine (0.025 g, 0.135 mmol) and 3,5-bis(trifluoromethyl)benzoic acid (0.038 g, 0.148 mmol) according to Procedure C. Crude material was purified by column chromatography (50% EtOAc/Hex) to afford 0.033 g (0.078 mmol, 58% yield) of title compound. TLC R_f (50% EtOAc/Hex): 0.38. TOF MS-ESI *m/z* $[M+H]^+$ 425.9; [M+Na] 447.9. ^{1}H NMR (500 MHz, $CDCl_3$): δ 8.36 (s, 2H), 8.24 (t, *J* = 6.5 Hz, 1H), 8.04 (s, 1H), 7.96 (d, *J* = 2.5 Hz, 1H), 7.40-7.34 (m, 1H), 6.42 (d, *J* = 8.8 Hz, 1H), 4.82 (t, *J* = 6.9 Hz, 1H), 3.60-3.55 (m, 4H), 1.92-1.80 (m, 2H).

***N*-(3-((4-chlorophenyl)amino)propyl)-3,5-difluorobenzamide (203061).**[69] Compound was prepared according to Procedure C, with slight modification. 3,5-difluorobenzoic acid (0.047 g, 0.298 mmol) was dissolved in THF and was treated with HOBt and EDC, and was allowed to stir for 20 minutes. DIPEA was added and stirring continued for 10 minutes. Compound **5** (0.050 g, 0.271 mmol) was then added. Crude material was purified using column chromatography (25-36% EtOAc/Hex) to afford 0.032 g (0.099 mmol, 36% yield) of title compound as an off-white solid. HPLC (gradient A): ret time = 6.50 min; purity = 97%. TOF MS-ESI *m/z* $[M+H]^+$ 325.0. ^{1}H NMR (500 MHz, $CDCl_3$): δ 7.24 (d, *J* = 5.0 Hz, 2H), 7.18-7.04 (m, 2H), 7.00-6.89 (m, 1H), 6.81-6.69 (m, 1H), 6.61-6.48 (m, 2H), 4.05 (bs, 1H), 3.55 (q, *J* = 6.4 Hz, 2H), 3.20 (t, *J* = 6.4 Hz, 2H), 1.89 (p, *J* = 6.5 Hz, 2H).

(3,5-bis(trifluoromethyl)phenyl)(3-(hydroxymethyl)piperidin-1-yl)methanone (38). Prepared using 1.05 eq (1.05 mmol) 3,5-bis(trifluoromethyl)benzoic acid according to Procedure C. Crude material was purified by flash chromatography (40-50% EtOAc/Hex) to afford 0.272 g (0.766 mmol, 77% yield) of title compound as a crystalline, off-white

solid. TLC R_f (50% EtOAc/Hex): 0.18. ^{1}H NMR (500 MHz, $CDCl_3$): δ 7.93 (s, 1H), 7.87 (s, 2H), 4.50-4.15 (m, 1H), 3.76-3.36 (m, 3H), 3.34-3.17 (m, 1H), 3.00 (dt, *J* = 38.8, 10.3 Hz, 1H), 2.14-1.63 (m, 4H), 1.55-1.29 (m, 2H).

1-(3,5-bis(trifluoromethyl)benzoyl)piperidine-3-carbaldehyde (39).[91, 92] To a stirring solution of **38** (0.051 g, 0.144 mmol) and DIPEA (0.163 ml, 0.933 mmol) in DCM (0.167 ml) at 0 °C was added sulfur trioxide pyridine complex (0.075 g, 0.474 mmol) in anhydrous DMSO (0.571 mL). The reaction was stirred at 0 °C for 20 minutes and was then warmed to room temperature. Reaction was stirred for 2.5 hours and was quenched with water (3 mL). The aqueous layer was extracted with DCM (3 x 3 mL). Combined organics were washed with 1N HCl (3 mL) followed by brine (3 mL). Organics were then dried ($MgSO_4$) and concentrated *in vacuo*. Crude material was purified using a CombiFlash system (60% EtOAc/Hex) to afford 0.040 g (0.113 mmol, 79% yield) of title compound as an off-white solid. TLC R_f (60% EtOAc/Hex): 0.25. ^{1}H NMR (500 MHz, $CDCl_3$): 1.3:1.0 mixture of rotamers, δ 9.79 (rotamer 1, s), 9.60 (rotamer 2, s, 1H), 7.97-7.80 (m, 3H), 4.49-3.04 (m, 4H), 2.80-2.40 (m, 1H), 2.22-1.45 (m, 4H).

(3,5-bis(trifluoromethyl)phenyl)(3-(((4-chlorophenyl)amino)methyl)piperidin-1-yl)methanone (203853).[93] 4-Chloroaniline (0.004 g, 0.031 mmol) and **39** (0.017 g, 0.047 mmol) in DCE (0.105 ml) was cooled to 0 °C and was treated with sodium triacetoxyborohydride (0.013 g, 0.063 mmol). The reaction was stirred overnight at room temperature. The mixture was diluted with EtOAc (2 mL) and was quenched with DI water (1 mL). Additional EtOAc (2 mL) was added, and the pH of the aqueous layer was adjusted to 10 using saturated $NaHCO_3$ and 2M NaOH. The organic layer was removed, dried ($MgSO_4$), and concentrated *in vacuo*. Crude material was purified by column chromatography (15-30% EtOAc/Hex) to afford 0.012 g (0.026 mmol, 82% yield) of title compound as a clear oil. TLC R_f (30% EtOAc/Hex): 0.29. TOF MS-ESI *m/z* $[M+H]^+$ 465.1; [M+Na] 487.1. HPLC (gradient A): ret time = 8.39 min; purity = 99%. ^{1}H NMR (500 MHz, $CDCl_3$): δ 7.93 (s, 1H), 7.84 (d, *J* = 9.4 Hz, 2H), 7.20-7.00 (m, 2H), 6.56 (d, *J* = 8.4 Hz, 1H), 6.38 (s, 1H), 4.58-4.38 (m, 1H), 4.04-3.35 (m, 2H), 3.26-2.78 (m, 4H),

2.05-1.95 (m, 1H), 1.94-1.78 (m, 1H), 1.77-1.67 (m, 1H), 1.56-1.44 (m, 1H), 1.38 (h, *J* = 7.8, 6.8 Hz, 1H).

***tert*-butyl (1-(4-chlorophenyl)pyrrolidin-3-yl)carbamate (203854).**[94] A solution of racemic BINAP (4.61 mg, 0.016 mmol) and tris(dibenzylideneacetone)dipalladium(0) (7.37 mg, 8.05 µmol) in toluene (4.0 mL) was stirred under nitrogen at 90 °C for 10 minutes and was cooled to 40 °C. 3-(*tert*-Butoxycarbonylamino)-pyrrolidine (0.075 g, 0.403 mmol), 1-chloro-4-iodobenzene (0.106 g, 0.443 mmol), and sodium *tert*-butoxide (0.062 g, 0.644 mmol) were added, and the mixture was stirred at 40 °C under nitrogen for 18 h. The reaction was then heated to 85 °C for five hours. The reaction mixture was cooled to room temperature, diluted with EtOAc (7 mL), and was filtered through a plug of celite. The filtrate was then concentrated *in vacuo*. Crude material was purified using a CombiFlash system (10% EtOAc/Hex) to afford 0.007 g (0.024 mmol, 6% yield) of title compound as an amber oil. TLC R_f (10% EtOAc/Hex): 0.15. ^{1}H NMR (500 MHz, $CDCl_3$) δ 7.20-7.12 (m, 1H), 6.51-6.40 (m, 2H), 4.71 (s, 1H), 4.36 (s, 1H), 3.53 (dd, *J* = 9.6, 5.9 Hz, 1H), 3.42-3.36 (m, 1H), 3.29 (td, *J* = 8.8, 5.3 Hz, 1H), 3.18-3.07 (m, 2H), 2.28 (dq, *J* = 13.8, 7.0 Hz, 1H), 1.98-1.91 (1, 2H), 1.45 (s, 9H).

1-(4-chlorophenyl)pyrrolidin-3-amine (41). Compound **203854** (0.021 g, 0.071 mmol) was dissolved in DCM (0.472 ml) and was cooled 0 °C. TFA (0.236 ml) was slowly added and the solution continued to stir at 0 °C. After 45 minutes, crude material was added to cooled 2M NaOH (5 mL). The mixture was then extracted with DCM (4 x 5 mL). The combined organic layers were dried ($MgSO_4$) and concentrated *in vacuo* to afford 0.012 g (0.061 mmol, 86% yield) of title compound as a yellow solid. No further purification was performed. ^{1}H NMR (500 MHz, $CDCl_3$): δ 7.18-7.12 (m, 2H), 6.47-6.41 (m, 2H), 3.71 (p, *J* = 5.8 Hz, 1H), 3.51-3.39 (m, 2H), 3.33-3.23 (m, 2H), 2.98 (dd, *J* = 9.3, 4.7 Hz, 1H), 2.27-2.18 (m, 1H), 1.85-1.76 (m, 1H).

***N*-(1-(4-chlorophenyl)pyrrolidin-3-yl)-3,5-bis(trifluoromethyl)benzamide (203855).** Compound **41** (0.012 g, 0.061 mmol) was dissolved in DCM (0.610 mL), and to the stirring solution was added 3,5-bis(trifluoromethyl)benzoyl chloride (0.012 ml, 0.067

mmol) followed by TEA (0.026 ml, 0.183 mmol. The reaction was stirred under nitrogen at room temperature overnight. The reaction mixture was concentrated *in vacuo*, and the solid was partitioned between saturated aqueous $NaHCO_3$ (5 mL) and EtOAc (10 mL). The aqueous layer was extracted a second time with EtOAc (10 mL), and the combined organics were washed with brine (10 mL), dried ($MgSO_4$), and concentrated *in vacuo*. Solid was triturated with DCM to afford 0.005 g (0.011 mmol, 18% yield) of title compound as a white solid. TOF MS-ESI *m/z* $[M-H]^-$ 435.0. ^1H NMR (500 MHz, DMSO-d_6): δ 9.12 (d, *J* = 6.7 Hz, 1H), 8.52 (s, 2H), 8.33 (s, 1H), 7.23-7.17 (m, 2H), 6.60-6.54 (m, 2H), 4.71-4.62 (m, 1H), 3.63-3.56 (m, 1H), 3.47-3.23 (m, 1H), 3.29-3.23 (m, 1H), 2.34-2.27 (m, 1H), 2.16-2.06 (m, 1H).

***N*-((1-(3,5-bis(trifluoromethyl)benzyl)piperidin-3-yl)methyl)-4-chloroaniline (203847).** To a stirring solution of **JR-1-012** (0.050 g, 0.104 mmol) in anhydrous tetrahydrofuran (2.1 ml) was added LAH (0.313 ml, 0.313 mmol), and the reaction was stirred at 75 °C overnight. The reaction mixture was cooled to 0 °C and water (0.285 mL) was added dropwise, followed by a 15% aqueous NaOH solution (0.285 mL), followed by water (0.855 mL). The mixture was then filtered and washed with additional THF. The solution was then concentrated *in vacuo*. Crude material was purified by column chromatography (15-25% EtOAc/Hex) to afford 0.014 g (0.031 mmol, 30% yield) of title compound as a yellow oil. TLC R_f (50% EtOAc/Hex): 0.71. TOF MS-ESI *m/z* $[M-H]^-$ 449.0. ^1H NMR (500 MHz, $CDCl_3$) δ 7.81-7.75 (m, 3H), 7.12-7.06 (m, 2H), 6.52-6.45 (m, 2H), 3.76-3.49 (m, 3H), 3.01 (s, 2H), 2.82 (d, *J* = 6.3 Hz, 1H), 2.72-2.62 (m, 1H), 2.13-2.05 (m, 1H), 1.99-1.88 (m, 2H), 1.87-1.77 (m, 1H), 1.76-1.66 (m, 1H), 1.63-1.59 (m, 1H), 1.17-1.03 (m, 1H).

Chapter 3

Kinetic solubility assay. Working compound solutions were prepared by dissolving compound in DMSO to afford 25 mM solutions. Solubility testing was conducted at room temperature in a 96-well NUNC-F plate using pH 7.4 PBS buffer. PBS buffer (199 µL) was added to wells A1-A5; B1-12; C1-12; and D1-12. DMSO (1 µL) was added to wells A1-A5 to serve as blanks. DMSO (50 µL) was added to wells E2-12; F2-12; and G2-12,

and 100 μL of working test compound solution was added to E1; F1; and G1. A series of 2-fold dilutions was prepared using the working stock solutions in E, F, and G1, respectively. Following dilution, 1 μL aliquots were transferred from dilution wells to corresponding test wells (E1 to B1, F1 to C1, G1 to D1, etc.) The 96-well plate was then loaded into the UV/Vis plate reader and was shaken for 5 cycles. Using SoftMax software, wells A1-A5 were labeled as "blank," and each replicate was given its own respective label. Each replicate was plotted logarithmically using concentration versus absorbance value. Data from each replicate was combined, averaged, and graphed logarithmically. The point at which the absorbance begins to increase was identified, and the point of inflection between no absorbance and the point where it begins to rise was considered to be the solubility of the compound.

Parallel Artificial Membrane Permeability Assay. The PAMPA assay was conducted using the PAMPA Explorer kit from *p*ION at a single pH of 7.4. Due to low compound solubility, the system solution was prepared by adding System Solution concentrate (6.75 mL), followed by Milli-Q water (75 mL), acetonitrile (50 mL), and additional Milli-Q water (118.75 mL) while stirring. The pH of the solution was adjusted to 7.4 using freshly prepared 0.5 M NaOH (aq).

A blank plate was prepared by transferring 150 μL of the pH adjusted system solution to a UV plate. The blank was read using *p*ION software to ensure no microbial growth was present. A deep well plate containing the working solutions was prepared by transferring 5 μL of a 10 mM stock solution of desired compound to a corresponding well. This was done in quadruplicate for each compound. Each well was then diluted with 1000 μL of pH adjusted system solution. A reference plate was then prepared by transferring 150 μL of the working solutions from the deep well plate into a UV plate. The plate was then read as the "reference plate" using *p*ION software.

The PAMPA sandwich plate was then prepared using a donor plate and an acceptor plate. The donor plate was prepared by transferring 200 μL of working solutions from the deep well plate to the donor plate. The acceptor plate containing the membrane was inverted and 5 μL of lipid was dispensed on each membrane. The acceptor plate was then inverted and 200 μL of system solution was added to each well. The acceptor plate

was added to the top of the donor plate, establishing the sandwich plate, which was incubated for 4 hours.

Following incubation, the sandwich was separated, and 150 μL from the acceptor wells were transferred to a UV plate and was read as "acceptor plate" using *p*ION software. The same was performed for the donor plate, which was read as "donor plate" using *p*ION software. The *p*ION software then computed permeability, providing a bin of low, medium, or high permeability based on the *p*ION standard ranking system.

Scratch Assay. PC-3 prostate cancer cells in 10% FBS DMEM media were plated into a 12-well plate (~400,000 cells per well) and were incubated for at 37 °C for 24 hours to form a confluent monolayer. A vertical scratch was made across the monolayer using a 200 μLpipette tip. The 10% FBS DMEM buffer was removed and replaced with 0.5% FBS DMEM buffer, and an initial image was captured. Compound or control DMSO was then added to each well, affording a final 0.1% DMSO concentration. The cells were then incubated at 37 °C for 24 hours, and a final image was capture. The scratch area was then analyzed using ImageJ software.

2-((3,5-bis(trifluoromethyl)benzamido)oxy)acetic acid (2f). Prepared according to Procedure A to afford 0.371 g (1.12 mmol, 95% yield) of title compound as a white solid. TOF MS-ESI *m/z* $[M+H]^+$ 332.1. ^{1}H NMR (500 MHz, DMSO-d_6): δ 8.39 (s, 2H), 8.33 (s, 1H), 4.55 (s, 2H).

***N*-(2-((3-chlorophenyl)amino)-2-oxoethoxy)-3,5-bis(trifluoromethyl)benzamide (101200).** Prepared using **2f** according to Procedure C. Crude material was purified by flash chromatography (20-30% EtOAc/hexanes) to afford 0.027 g (0.061 mmol, 5% yield) of title compound. Waters TOF MS-ESI *m/z* $[M+H]^+$ 441.1; [M+Na] 463.0. HPLC (gradient A): ret time = 8.10 min; purity = 99%. ^{1}H NMR (500 MHz, DMSO-d_6): δ 12.70 (bs, 1H), 10.61 (s, 1H), 8.42 (s, 1H), 8.34 (s, 1H), 7.86 (s, 1H), 7.52 (d, J = 10 Hz, 1H), 7.38 (t, J = 10 Hz, 1H), 7.17 (d, J = 10 Hz, 1H), 4.68 (s, 2H).

2-((3-(trifluoromethyl)benzamido)oxy)acetic acid (2g). Prepared according to Procedure A to afford 0.228 g (0.866 mmol, 73% yield) of title compound as a white solid. TOF MS-ESI *m/z* $[M+H]^+$ 263.0; [M+Na] 287.0. ^{1}H NMR (500 MHz, DMSO-d_6): δ 8.25-7.65 (m, 5H), 4.25 (s, 2H).

***N*-(2-((4-chlorophenyl)amino)-2-oxoethoxy)-3,5-bis(trifluoromethyl)benzamide (101202).** Prepared using **2g** according to Procedure C. Crude material was purified by flash chromatography (50-65% EtOAc/Hex) to afford 0.102 g (0.027 mmol, 32% yield) of title compound as a yellow solid. TLC R_f (50% EtOAc/Hex): 0.11. Waters TOF MS-ESI *m/z* $[M+H]^+$ 373.1; [M+Na] 395.0.

1-(*tert*-butoxycarbonyl)piperidine-3-carboxylic acid (43). Nipecotic acid (**42**) (0.200 g, 1.549 mmol), and sodium hydroxide (1.703 ml, 1.703 mmol) were stirred in a solution of dioxane (3.40 mL) and water (1.70 mL). The solution was cooled to 0 °C and di-*tert*-butyl dicarbonate (0.395 ml, 1.703 mmol) was added. The reaction mixture was then warmed to room temperature and was stirred overnight. The solution was concentrated *in vacuo* to approximately 2 mL and was cooled in an ice bath, covered with ~3 mL of ethyl acetate, and acidified with a dilute solution of $KHSO_4$ (10% solution) to pH~2. The aqueous phase was extracted with EtOAc (4 x 15 mL). The organics were combined, washed with brine (20 mL), dried ($MgSO_4$), filtered, and concentrated to afford 0.349 g (1.52 mmol, 96% yield) of title compound as a white solid. No further purification was performed. %. ^{1}H NMR (500 MHz, DMSO-d_6): δ 12.38 (s, 1H), 4.03-3.76 (m, 1H), 3.75-3.60 (bs, 1H), 2.87-2.78 (m, 1H), 2.35-2.25 (m, 1H), 1.95-1.85 (m, 1H), 1.66-1.57 (m, 1H), 1.56-1.46 (m, 1), 1.42-1.28 (m, 11H).

***tert*-butyl 3-((4-chlorophenyl)carbamoyl)piperidine-1-carboxylate (44).** 4-Chloroaniline (0.179 g, 1.407 mmol) was dissolved in dichloromethane (9.4 mL), and to the stirring solution was added EDC (0.270 g, 1.407 mmol) followed by DMAP (0.172 g, 1.407 mmol) and **43** (0.215, 0.938 mmol). The mixture was stirred at room temperature under nitrogen overnight. The dichloromethane layer was removed *in vacuo* and the residue was partitioned between water (25 mL) and ethyl acetate (25 mL). The aqueous

layer was extracted with ethyl acetate (3 x 10 mL). Combined organics were washed with 1N HCl (25 mL) followed by saturated $NaHCO_3$ (25 mL), and brine (25 mL). The organics were dried ($MgSO_4$), filtered, and concentrated *in vacuo* to yield 0.440 g of an amber oil. Oil was partitioned between 1N HCl (20 mL) and ethyl acetate (20 mL). The aqueous layer was extracted with additional ethyl acetate (3 x 10 mL). The organic layers were combined, washed with brine (25 mL), dried ($MgSO_4$), filtered, and concentrated to afford 0.315 g (0.930 mmol, 99% yield) of title compound an amber oil. No further purification was performed. %. ^{1}H NMR (500 MHz, DMSO-d_6): δ 10.15 (s, 1H), 7.66-7.60 (m, 2H), 7.38-7.32 (m, 2H), 3.95-3.80 (m, 2H), 2.84-2.70 (m, 1H), 2.49-2.40 (m, 1H), 1.97-1.90 (m, 1H), 1.75-1.56 (m, 2H), 1.47-1.30 (m, 11H).

***N*-(4-chlorophenyl)piperidine-3-carboxamide (45).** Compound **44** (1.28 g, 3.78 mmol) was dissolved in dichloromethane (25 mL), and the solution was cooled to approximately -10 °C. To the cooled stirring solution was added TFA (12.5 mL). The reaction mixture continued stirring at -10 °C for 1.5 h and then was poured into 100 mL of cooled 2M NaOH. The cooled basic solution was extracted with dichloromethane (3 x 30 mL), and the combined organics were dried ($MgSO_4$), filtered, and concentrated to afford 0.754 g (3.15 mmol, 84% yield) of title compound as a tan solid. No further purification was performed. %. ^{1}H NMR (500 MHz, $CDCl_3$): δ 10.75 (s, 1H), 7.57-7.51 (m, 2H), 7.27-7.24 (m, 2H), 3.33-3.23)m, 1H), 3.15-3.05 (m, 1H), 2.93 (dd, *J* = 5, 10 Hz, 1H), 2.80-2.70 (m, 1H), 2.60-2.53 (m, 1H), 2.10-2.03 (m, 1H), 2.00-1.91 (m, 2H), 1.83-1.70 (m, 2H), 1.63-1.53 (m, 1H).

Ethyl 1-(3,5-bis(trifluoromethyl)benzoyl)piperidine-3-carboxylate (47). Ethyl piperidine-3-carboxylate (**42**) (0.466 ml, 3.00 mmol) was dissolved in dichloromethane (12.0 mL) and to the stirring solution was added triethylamine (0.502 ml, 3.60 mmol) followed by 3,5-bis(trifluoromethyl)benzoyl chloride (0.595 ml, 3.30 mmol). The reaction mixture was stirred overnight at room temperature under nitrogen. The reaction was diluted with 50 mL of dichloromethane and was washed with $NaHCO_3$ (2 x 30 mL) followed by 1M aq HCl (30 mL) and then brine (30 mL). Combined organics were then

dried ($MgSO_4$) and concentrated *in vacuo* to afford 1.44 g of a yellow oil. Crude material was purified by to afford 0.990 g (2.49 mmol, 83% yield) of title compound as a clear oil. ^{1}H NMR (400 MHz, DMSO-d_6): δ 8.22 (s, 1H), 8.18-8.07 (m, 2H), 4.50-3.45 (m, 4H), 3.4-3.23 (under water peak, 1H), 3.18-3.00 (m, 1H), 2.78-2.63 (m, 1H), 2.15-1.87 (m, 1H), 1.85-1.40 (m, 3H), 1.28-1.00 (m, 3H).

1-(3,5-bis(trifluoromethyl)benzoyl)piperidine-3-carboxylic acid (48). Prepared according to Procedure A to afford 0.310 g (0.840 mmol, 70% yield) of title compound as a white solid **OR 47** was dissolved in tetrahydrofuran (3.35 mL) and water (6.70 mL) and to the stirring solution was added lithium hydroxide hydrate (1.044 g, 24.87 mmol). The mixture was stirred at room temperature for 1.5 hours and then was diluted with water (20 mL) and washed with diethyl ether (20 mL). The aqueous layer was removed and its pH was adjusted to ~2 using 2M HCl (aq). The aqueous layer was then extracted with ethyl acetate (3 x 40 mL). The combined organics were washed with brine (40 mL), dried ($MgSO_4$), and concentrated to afford 0.817 g of title compound as a white solid. No further purification was performed. Waters TOF MS-ESI *m/z* $[M-H]^-$ 368.0. ^{1}H NMR (400 MHz, DMSO-d_6): δ 12.50 (s, 1H), 8.21 (s, 1H), 8.13 (s, 2H), 4.55-3.73 (m, 1H), 3.50-3.35 (m, 2H), 3.15-2.95 (m, 1H), 2.65-2.54 (m, 1H), 2.08-1.40 (m, 5H).

General procedure for acid library[95]

The following procedure was performed in a parallel reaction format. To each 8 mL vial was added *N*-(4-chlorophenyl)piperidine-3-carboxamide (0.150 mmol), followed by a 0.500 mL of a solution containing EDCI (0.3M) and DMAP (0.3M) in dichloromethane, varied carboxylic acid (0.10 mmol), anhydrous DMF (0.150 mL), and dichloromethane (0.250 mL). The solution was sonicated between each addition. The reaction mixture was capped and allowed to stir 48 hours at room temperature on an orbital shaker at 2,500 rpm. The reaction solution was diluted with dichloromethane (5 mL), and Amberlyst-15 (~300 mg) was added. The reaction mixture was allowed to stir on an orbital shaker 3,000 rpm overnight. The mixture was then filtered and concentrated. Water (3 mL) and dichloromethane (3 mL) were added to the vial. The vial was shaken and the layers allowed to separate for 30 minutes. The aqueous layer was then removed,

and the remaining organic layer was washed a second time with water (3 mL), and the layers were again allowed to separate for 30 minutes. The dichloromethane layer was removed and transferred to a clean vial and concentrated. The water wash and organic isolation was repeated. Organics were concentrated to afford title compounds below.

ESI-MS was performed in positive mode on an Agilent Technologies LC/MS system using a 1200 Series LC and 6130 Quadrupole LC/MS (Agilent Technologies, Santa Clara, CA, USA) in positive mode with 5–10 μL injection volume and a linear gradient of 10% Solvent D (0.02% TFA and 0.1% acetic acid in acetonitrile) in Solvent C (0.02% TFA and 0.1% acetic acid in water) to 90% Solvent D in Solvent C over 6 min with a hold at 90% for 7 min.

***N*-(4-chlorophenyl)-1-(3-(furan-2-yl)benzoyl)piperidine-3-carboxamide (203971).** 32 mg (0.078 mmol, 78% yield) of title compound as an orange-brown oil. ESI(+) *m/z* $[M+H]^+$ 409.0; [M+Na] 434.0; HPLC (gradient A): ret time = 7.52 min; purity = >95%. ^{1}H NMR (500 MHz, DMSO-d_6): 1.5:1.0 mixture of rotamers, δ 10.21 (rotamer 1, s), 9.90 (rotamer 2, s,1H), 7.85-7.24 (m, 9H), 7.05 (s, 1H), 6.62 (s, 1H), 4.63-4.20 (m, 1H), 3.73-3.49 (m, 1H), 3.17-2.91 (m, 2H), 2.68-2.56 (m, 1H), 2.01 (d, *J* = 9.1 Hz, 1H), 1.93-1.63 (m, 2H), 1.46 (s, 1H).

1-(3-benzoylbenzoyl)-*N*-(4-chlorophenyl)piperidine-3-carboxamide (203972). 31 mg (0.069 mmol, 69% yield) of title compound as a light brown oil. ESI(+) *m/z* $[M+H]^+$ 447.0; [M+Na] 469.0; HPLC (gradient A): ret time = 7.46 min; purity = >95%. ^{1}H NMR (500 MHz, DMSO-d_6): 1.5:1.0 mixture of rotamers, δ 10.17 (rotamer 1, s), 9.99 (rotamer 2, s, 1H), 7.88-7.21 (m, 13H), 4.58-4.13 (m, 1H), 3.75-3.53 (m, 1H), 3.19-2.93 (m, 2H), 2.64-2.54 (m, 1H), 2.01 (s, 1H), 1.89-1.61 (m, 2H), 1.57-1.33 (m, 1H).

1-(2-(3,5-bis(trifluoromethyl)phenyl)acetyl)-*N*-(4-chlorophenyl)piperidine-3-carboxamide (203960). 41 mg (0.083 mmol, 83% yield) of title compound as an amber glass. ESI(+) *m/z* $[M+H]^+$ 493.0; [M+23] 515.0; HPLC (gradient A): ret time = 8.19 min; purity = >95%. ^{1}H NMR (500 MHz, DMSO-d_6): δ 10.12 (d, *J* = 10.2 Hz, 2H), 8.02-7.88 (m, 3H), 7.69-7.55 (m, 2H), 7.40-7.32 (m, 2H), 4.46-4.16 (m, 1H), 4.10-3.95 (m, 3H),

3.16-3.06 (m, 1H), 2.82-2.70 (m, 1H), 2.45-2.38 (m, 1H), 2.09-1.91 (m, 1H), 1.83-1.63 (m, 2H), 1.50-1.30 (m, 1H).

***N*-(4-chlorophenyl)-1-(3-(thiazol-2-yl)benzoyl)piperidine-3-carboxamide (206115).** 40 mg (0.094 mmol, 94% yield) as a light brown oil. ESI(+) m/z $[M+H]^+$ 426.1; [M+23] 448.1; HPLC (gradient A): ret time = 6.88 min; purity = >95%. ^{1}H NMR (500 MHz, DMSO-d_6): 1.4:1.0 mixture of rotamers, δ 10.27 (rotamer 1, s), 10.07 (rotamer 2, s, 1H), 8.08-7.91 (m, 3H), 7.85 (s, 1H), 7.74-7.46 (m, 4H), 7.44-7.22 (m, 2H), 4.62-4.15 (m, 1H), 3.75-3.52 (m, 1H), 3.17-2.95 (m, 2H), 2.69-2.59 (m, 1H), 2.02 (d, *J* = 10.2 Hz, 1H), 1.93-1.66 (m, 2H), 1.58-1.36 (m, 1H).

***N*-(4-chlorophenyl)-1-(3-(3,3-dimethylbutanamido)benzoyl)piperidine-3-carboxamide (203966).** 38 mg (0.083 mmol, 83% yield) of title compound as a light brown solid. ESI(+) *m/z* [M+Na] 456.0; HPLC (gradient A): ret time = 7.35 min; purity = >95%. ^{1}H NMR (500 MHz, DMSO-d_6): δ 10.26-9.86 (m, 2H), 7.75 (s, 1H), 7.70-7.44 (m, 3H), 7.42-7.20 (m, 4H), 7.03 (d, *J* = 7.5 Hz, 1H), 4.57-4.23 (m, 1H), 3.77-3.50 (m, 1H), 3.13-2.89 (m, 2H), 2.19 (s, 2H), 2.01 (s, 1H), 1.89-1.58 (m, 3H), 1.43 (s, 1H), 1.02 (s, 9H).

***N*-(4-chlorophenyl)-1-(3-vinylbenzoyl)piperidine-3-carboxamide (203968).** 34 mg (0.071 mmol, 71% yield) of title compound as an off-white foam. ESI(+) *m/z* $[M+H]^+$ 369.0; [M+Na] 391.0; HPLC (gradient A): ret time = 7.31 min; purity = >95%. ^{1}H NMR (500 MHz, DMSO-d_6): 1.5:1.0 mixture of rotamers, δ 10.19 (rotamer 1, s), 10.00 (rotamer 2, s, 1H), 7.71-7.17 (m, 8H), 6.75 (s, 1H), 5.89 (d, *J* = 17.6 Hz, 1H), 5.38-5.25 (m, 1H), 4.60-4.20 (m, 1H), 3.72-3.43 (m, 1H), 3.13-2.90 (m, 2H), 2.62-2.53 (m, 1H), 2.07-1.57 (m, 4H), 1.43 (s, 1H).

***N*-(4-chlorophenyl)-1-(3-(2-methylthiazol-4-yl)benzoyl)piperidine-3-carboxamide (203975).** 17 mg (0.039 mmol, 39% yield) of title compound as an off-white solid. ESI(+) *m/z* $[M+H]^+$ 440.0; [M+Na] 462.0; HPLC (gradient A): ret time = 7.20 min; purity = >95%. ^{1}H NMR (500 MHz, DMSO-d_6): 1.4:1.0 mixture of rotamers, δ 10.22

(rotamer 1, s), 10.00 (rotamer 2, s, 1H), 8.12-7.24 (m, 9H), 4.67-4.19 (m, 1H), 3.74-3.53 (m, 1H), 3.18-2.90 (m, 2H), 2.72 (s, 3H), 2.66-2.55 (m, 1H), 2.11-1.94 (m, 1H), 1.93-1.63 (m, 2H), 1.55-1.35 (m, 1H).

***N*-(4-chlorophenyl)-1-(3-methylbenzoyl)piperidine-3-carboxamide (203977).** 40 mg (0.112 mmol, 112% yield). ESI(+) *m/z* $[M+H]^+$ 357.0; [M+Na] 379.0; HPLC (gradient A): ret time = 7.26; purity = >90%. ^{1}H NMR (500 MHz, DMSO-d_6): 2.0:1.0 mixture of rotamers, δ 10.22 (rotamer 1, s), 10.04 (rotamer 2, 1H), 7.80-7.44 (m, 2H), 7.44-7.11 (m, 5H), 6.60-6.56 (m, 1H), 4.60-4.16 (m, 1H), 3.70-3.50 (m, 1H), 3.13-2.91 (m, 2H), 2.40-2.24 (m, 3H), 2.07-1.61 (m, 3H), 1.51-1.30 (m, 1H).

***N*-(4-chlorophenyl)-1-(3-(methylthio)benzoyl)piperidine-3-carboxamide (203963).** 32 mg (0.082 mmol, 82% yield) of title compound as an off-white oil. ESI(+) *m/z* $[M+H]^+$ 389.0; [M+Na] 411.0; HPLC (gradient A): ret time = 7.26 min; purity = >95%. ^{1}H NMR (500 MHz, DMSO-d_6): 1.4:1.0 mixture of rotamers, δ 10.20 (rotamer 1, s), 10.02 (rotamer 2, s, 1H), 7.73-7.06 (m, 8H), 4.60-4.20 (m, 1H), 3.70-3.45 (m, 1H), 3.14-2.90 (m, 2H), 2.10-1.62 (m, 3H), 1.55-1.35 (m, 1H).

***N*-(4-chlorophenyl)-1-(3-(oxazol-5-yl)benzoyl)piperidine-3-carboxamide (203973).** 28 mg (0.068 mmol, 68% yield) of title compound as a yellowish solid. ESI(+) *m/z* $[M+H]^+$ 410.0; [M+Na] 432.0; HPLC (gradient A): ret time = 6.53 min; purity = >95%. ^{1}H NMR (500 MHz, DMSO-d_6): 1.4:1.0 mixture of rotamers, δ 10.21 (rotamer 1, s), 9.98 (rotamer 2, s, 1H), 8.53-7.19 (m, 10H), 4.63-4.17 (m, 1H), 3.70-3.48 (m, 1H), 3.17-2.93 (m, 2H), 2.66-2.54 (m, 1H), 2.01 (d, J = 12.9 Hz, 1H), 1.91-1.61 (m, 2H), 1.46 (s, 1H).

***N*-(4-chlorophenyl)-1-(3-(N,N-diethylsulfamoyl)benzoyl)piperidine-3-carboxamide (203967).** 34 mg (0.071 mmol, 71% yield) of title compound as a light brown oily solid. ESI(+) *m/z* $[M+H]^+$ 478.0; [M+Na] 500.0; HPLC (gradient A): ret time = 7.24 min; purity = >95%. ^{1}H NMR (500 MHz, DMSO-d_6): 1.2:1.0 mixture of rotamers, δ 10.02 (rotamer 1, s), 10.03 (rotamer 2, s, 1H), 7.92-7.81 (m, 1H), 7.78-7.60 (m, 4H), 7.58-7.49 (m, 1H), 7.34 (dd, J = 17.9, 9.4 Hz, 2H), 4.55-4.18 (m, 1H), 3.58-3.38 (m, 1H), 3.26-2.95

(m, 6H), 2.67-2.55 (m, 1H), 2.12-1.94 (m, 1H), 1.88-1.64 (m, 2H), 1.59-1.35 (m, 1H), 1.12-0.85 (m, 6H).

Methyl 3-(3-((4-chlorophenyl)carbamoyl)piperidine-1-carbonyl)benzoate (203969). 30 mg (0.075 mmol, 75% yield) of title compound as a light brown oil. ESI(+) *m/z* $[M+H]^+$ 401.0; [M+Na] 423.0; HPLC (gradient A): ret time = 6.86 min; purity = >90%. ^{1}H NMR (500 MHz, DMSO-d_6): 1.4:1.0 mixture of rotamers, δ 10.19 (rotamer 1, s), 9.96 (rotamer 2, s, 1H), 8.12-7.24 (m, 8H), 4.60-4.13 (m, 1H), 3.87 (s, 3H), 3.65-3.45 (m, 1H), 3.20-2.95 (m, 2H), 2.13-1.61 (m, 3H), 1.59-1.33 (m, 1H).

***N*-(4-chlorophenyl)-1-(3-(5-methyl-1,2,4-oxadiazol-3-yl)benzoyl)piperidine-3-carboxamide (203974).** 36 mg (0.085 mmol, 85% yield) of title compound as a light brown solid. ESI(+) *m/z* $[M+H]^+$ 425.0; [M+Na] 447.0; HPLC (gradient A): ret time = 6.89 min; purity = >95%. ^{1}H NMR (500 MHz, DMSO-d_6): 1.5:1.0 mixture of rotamers, δ 10.22 (rotamer 1, s), 9.97 (rotamer 2, s, 1H), 8.17-7.20 (m, 8H), 4.62-4.10 (m, 1H), 3.73-3.49 (m, 1H), 3.19-2.95 (m, 1H), 2.73-2.55 (m, 4H), 2.05-1.95 (m, 1H), 1.93-1.64 (m, 2H), 1.58-1.35 (m, 1H).

***N*-(4-chlorophenyl)-1-(3-methoxybenzoyl)piperidine-3-carboxamide (203979).** TOF MS-ESI *m/z* $[M+H]^+$ 373.0; [M+Na] 395.0. HPLC (gradient A): ret time = 6.99 min; purity = >95%. ^{1}H NMR (500 MHz, DMSO-d_6): 1.6:1.0 mixture of rotamers, δ 10.22 (rotamer 1, s), 10.03 (rotamer 2, s, 1H) 7.70 (m, 2H), 7.35 (s, 3H), 7.01 (s, 1H), 6.92 (d, *J* = 7.7 Hz, 1H), 6.90-6.87 (m, 1H), 4.59-4.21 (m, 1H), 3.77 (s, 3H), 3.67-3.47 (m, 1H), 3.12-2.87 (m, 2H), 2.07-1.61 (m, 3H), 1.55-1.31 (m, 1H).

***N*-(4-chlorophenyl)-1-(3-(methoxymethyl)benzoyl)piperidine-3-carboxamide (203962).** 37 mg (0.096 mmol, 96% yield) of title compound as an off-white foam. ESI(+) *m/z* $[M+H]^+$ 387.0; [M+Na] 409.0; HPLC (gradient A): ret time = 6.76 min; purity = >95%. ^{1}H NMR (500 MHz, DMSO-d_6): 1.4:1.0 mixture of rotamers, δ 10.20 (rotamer 1, s), 10.02 (rotamer 2, s, 1H), 7.72-7.24 (m, 8H), 4.60-4.20 (m, 3H), 3.70-3.48

(m, 1H), 3.30-3.23 (m, 3H), 3.13-2.88 (m, 2H), 2.63-2.53 (m, 1H), 2.08-1.62 (m, 3H), 1.55-1.32 (m, 1H).

***N*-(4-chlorophenyl)-1-(3-(methylsulfonamido)benzoyl)piperidine-3-carboxamide (203965).** 36 mg (0.083 mmol, 83% yield) of title compound as an off-white solid. ESI(+) *m/z* $[M+H]^+$ 436.0; [M+Na] 458.0; HPLC (gradient A): ret time = 6.2 min; purity = >95%. ^{1}H NMR (500 MHz, DMSO-d_6): 1.2:1.0 mixture of rotamers, δ 10.19 (rotamer 1, s), 9.99 (s, 1H), 9.93 (rotamer 2, s, 1H), 7.76-7.07 (m, 8H), 4.57-4.23 (m, 1H), 3.75-3.47 (m, 1H), 3.01 (s, 5H), 2.61-2.54 (m, 1H), 2.02 (s, 1H), 1.88-1.63 (m, 2H), 1.44 (s, 1H).

***N*-(4-chlorophenyl)-1-(3-cyanobenzoyl)piperidine-3-carboxamide (203961).** 22 mg (0.060 mmol, 60% yield) of title compound as an off-white oil. ESI(+) *m/z* $[M+H]^+$ 368.0; [M+Na] 390.0; HPLC (gradient A): ret time = 6.68 min; purity = >95%. ^{1}H NMR (500 MHz, DMSO-d_6): 1.2:1.0 mixture of rotamers, δ 10.22 (rotamer 1, s), 9.99 (rotamer 2, s, 1H), 8.02-7.23 (m, 8H), 4.58-4.14 (m, 1H), 3.60-3.40 (m, 1H), 3.16-2.93 (m, 2H), 2.65-2.52 (m, 1H), 2.00 (d, *J* = 8.1 Hz, 1H), 1.91-1.64 (m, 2H), 1.47 (s, 1H).

***N*-(4-chlorophenyl)-1-(3-(methylsulfonyl)benzoyl)piperidine-3-carboxamide (203970).** 39 mg (0.093 mmol, 93% yield) of title compound as a yellowish-brown oil. ESI(+) *m/z* $[M+H]^+$ 421.0; [M+Na] 443.0; HPLC (gradient A): ret time = 6.25 min; purity = >95%. ^{1}H NMR (500 MHz, DMSO-d_6): 1.4:1.0 mixture of rotamers, δ 10.20 (rotamer 1, s), 9.99 (rotamer 2, s, 1H), 8.06-7.87 (m, 2H), 7.79-7.47 (m, 4H), 7.42-7.27 (m, 2H), 4.59-4.19 (m, 1H), 3.64-3.42 (m, 1H), 3.31 (s, 3H), 3.19-2.95 (m, 2H), 2.67-2.52 (m, 1H), 2.02 (s, 1H), 1.91-1.37 (m, 3H).

1-(3-acetamidobenzoyl)-N-(4-chlorophenyl)piperidine-3-carboxamide (203964). 27 mg (0.068 mmol, 68% yield) of title compound as an off-white solid. ESI(+) *m/z* $[M+H]^+$ 400.0; [M+Na] 422.0; HPLC (gradient A): ret time = 6.08 min; purity = >95%. ^{1}H NMR (500 MHz, DMSO-d_6): δ 10.29-9.93 (m, 2H), 7.72 (s, 1H), 7.69-7.49 (m, 3H), 7.35 (bs,

3H), 7.02 (d, *J* = 7.6 Hz, 1H), 4.60-4.24 (m, 1H), 3.75-3.49 (m, 1H), 3.10-2.89 (m, 2H), 2.13-1.60 (m, 6H), 1.43 (s, 1H).

General procedure for aniline library[95]

The following procedure was performed in a parallel reaction format. To each 8 mL vial was added varied aniline (0.100 mmol), followed by a 0.500 mL of a solution containing EDCI (0.3M) and DMAP (0.3M) in dichloromethane, 1-(3,5-bis(trifluoromethyl)benzoyl)piperidine-3-carboxylic acid (0.055 g, 0.150 mmol), and anhydrous dichloromethane (0.500 mL). The solution was sonicated between each addition. The reaction mixture was capped and allowed to stir 48 hours at room temperature on an orbital shaker at 2,500 rpm. The reaction solution was diluted with dichloromethane (3 mL) and washed with saturated $NaHCO_3$ (2 mL). The vial was shaken and the layers allowed to separate for 30 minutes. The aqueous layer was then removed, and the remaining organic layer was washed 1M aqueous Hydrochloric acid (2 mL), and the layers were again allowed to separate for 30 minutes. The dichloromethane layer was removed and transferred to a clean vial and concentrated. Organics were dried ($MgSO_4$) and concentrated to afford title compounds below.

1-(3,5-bis(trifluoromethyl)benzoyl)-*N*-(3-phenoxyphenyl)piperidine-3-carboxamide (206114). 52 mg (0.097 mmol, 97% yield) of title compound as a white solid. ESI(+) *m/z* $[M+H]^+$ 537.2; [M+Na] 559.2. HPLC (gradient A): ret time = 8.44 min; purity = 89%. ^{1}H NMR (400 MHz, DMSO-d_6): 1.1:1.0 mixture of rotamers, δ 10.13 (rotamer 1, s), 9.90 (rotamer 2, s, 1H), 8.25-6.59 (m, 12H), 4.55-4.01 (m, 1H), 3.53-3.33 (m, 1H), 3.22-2.89 (m, 2H), 2.03-1.25 (m, 5H).

***N*-(3-benzylphenyl)-1-(3,5-bis(trifluoromethyl)benzoyl)piperidine-3-carboxamide (206108).** 56 mg (0.105 mmol, 105% yield) of title compound as a light purple solid. ESI(+) *m/z* $[M+H]^+$ 535.2; [M+Na] 557.2. HPLC (gradient A): ret time = 8.52 min; purity = 91%. ^{1}H NMR (400 MHz, DMSO-d_6): 1.2:1.0 mixture of rotamers, δ 10.02 (rotamer 1, s), 9.80 (rotamer 2, s, 1H), 8.29-7.91 (m, 4H), 7.52-7.07 (m, 7H), 6.91 (d, *J* =

16.7 Hz, 1H), 4.58-4.06 (m, 1H), 3.97-3.81 (m, 2H), 3.55-3.35 (m, 1H), 3.22-2.93 (m, 2H), 2.06-1.38 (m, 5H).

1-(3,5-bis(trifluoromethyl)benzoyl)-*N*-(3-(2-(pyridin-2-yl)ethoxy)phenyl)piperidine-3-carboxamide (206124). 18 mg (0.032 mmol, 32%) of title compound as a white solid. ESI(+) *m/z* $[M+H]^+$ 566.2; [M+Na] 588.2. HPLC (gradient A): ret time = 6.13 min; purity = >95%. ^{1}H NMR (400 MHz, DMSO-d_6): 1.2:1.0 mixture of rotamers, δ 10.02 (rotamer 1, s), 9.79 (rotamer 2, s, 1H), 8.54-8.47 (m, 1H), 8.27-8.14 (m, 1H), 8.10 (s, 2H), 7.73 (t, *J* = 7.6 Hz, 2H), 7.41-6.95 (m, 6H), 6.68-6.53 (m, 1H), 4.58-4.05 (m, 3H), 3.57-3.36 (m, 2H), 3.23-2.98 (m, 4H), 2.70-2.53 (m, 1H), 2.06-1.95 (m, 1H), 1.86-1.64 (m, 2H), 1.59-1.39 (m, 1H).

1-(3,5-bis(trifluoromethyl)benzoyl)-*N*-(3-(pyrrolidin-1-ylsulfonyl)phenyl)piperidine-3-carboxamide (206109). 54 mg (0.094 mmol, 94% yield) of title compound as a yellow solid. ESI(+) *m/z* $[M+H]^+$ 578.2; [M+Na] 600.2. HPLC (gradient A): ret time = 7.65 min; purity = 94%. ^{1}H NMR (400 MHz, DMSO-d_6): 1.1:1.0 mixture of rotamers, δ 10.44 (rotamer 1, s), 10.22 (rotamer 2, s, 1H), 8.37-7.39 (m, 7H), 4.59-4.01 (m, 1H), 3.71-3.37 (m, 2H), 3.13 (s, 5H), 2.78-2.53 (m, 2H), 2.14-1.98 (m, 1H), 1.92-1.42 (m, 6H).

1-(3,5-bis(trifluoromethyl)benzoyl)-*N*-(3-(2-methylthiazol-4-yl)phenyl)piperidine-3-carboxamide (206244). 22 mg (0.041 mmol, 41% yield) of title compound as a white solid. ESI(+) *m/z* $[M+H]^+$ 542.0; [M+Na] 564.0. HPLC (gradient A): ret time = 7.63 min; purity = >95%. ^{1}H NMR (400 MHz, DMSO-d_6): 1.1:1.0 mixture of rotamers, δ 10.17 (rotamer 1, s), 9.94 (rotamer 2, s, 1H), 8.28-8.02 (m, 4H), 7.87-7.75 (m, 1H), 7.64-7.44 (m, 2H), 7.38-7.22 (m, 1H), 4.58-4.04 (m, 1H), 3.57-3.34 (m, 1H), 3.21-2.96 (m, 2H), 2.76-2.52 (m, 4H), 2.01 (d, *J* = 10.9, 1H), 1.87-1.35 (m, 3H).

1-(3,5-bis(trifluoromethyl)benzoyl)-*N*-(3-ethylphenyl)piperidine-3-carboxamide (206102). 51 mg (0.108 mmol, 70% yield) of title compound as a light brown solid. ESI(+) *m/z* $[M+H]^+$ 473.2; [M+Na] 495.1. HPLC (gradient A): ret time = 8.15 min; purity = 92%. ^{1}H NMR (500 MHz, DMSO-d_6): 1.0:1.0 mixture of rotamers, δ 10.02

(rotamer 1, s), 9.80 (rotamer 2, s, 1H), 8.27-8.16 (m, 1H), 8.12 (s, 2H), 7.55-7.25 (m, 2H), 7.18 (dt, *J* = 29.5, 7.9 Hz, 1H), 6.95-6.82 (m, 1H), 4.58-4.05 (m, 1H), 3.55-3.38 (m, 1H), 3.25-2.99 (m, 2H), 2.68-2.52 (m, 3H), 2.06-1.97 (m, 1H), 1.73-1.38 (m, 3H), 1.15 (dq, *J* = 15.0, 7.4 Hz, 3H).

1-(3,5-bis(trifluoromethyl)benzoyl)-*N*-(3-vinylphenyl)piperidine-3-carboxamide (206248). ESI(+) *m/z* $[M+H]^+$ 471.0; [M+Na] 493.0. HPLC (gradient A): ret time = 6.05 min; purity = 82%. ^{1}H NMR (400 MHz, DMSO-d_6): 1.2:1.0 mixture of rotamers, δ 10.07 (rotamer 1, s), 9.85 (rotamer 2, s, 1H), 8.26-7.91 (m, 3H), 7.76-7.06 (m, 4H), 6.75-6.57 (m, 1H), 5.80-5.60 (m, 1H), 5.30-5.13 (m, 1H), 4.55-4.00 (m, 1H), 3.52-3.34 (m, 1H), 3.21-2.94 (m, 2H), 2.66-2.51 (m, 1H), 2.05-1.93 (m, 1H), 1.81-1.40 (m, 3H).

1-(3,5-bis(trifluoromethyl)benzoyl)-*N*-(3-(oxazol-5-yl)phenyl)piperidine-3-carboxamide (206243). ESI(+) *m/z* $[M+H]^+$ 512.0; [M+Na] 534.0. HPLC (gradient A): ret time = 7.19 min; purity = >95%. ^{1}H NMR (400 MHz, DMSO-d_6): 1.2:1.0 mixture of rotamers, δ 10.23 (rotamer 1, s), 10.09 (rotamer 2, s, 1H), 8.47-7.28 (m, 9H), 4.59-3.98 (m, 1H), 3.55-3.35 (m, 1H), 3.25-2.96 (m, 2H), 2.68-2.52 (m, 1H), 2.07-1.94 (m, 1H), 1.86-1.61 (m, 2H), 1.59-1.38 (m, 1H).

1-(3,5-bis(trifluoromethyl)benzoyl)-*N*-(3-(methylthio)phenyl)piperidine-3-carboxamide (206241). 19 mg (0.039 mmol, 39% yield) of title compound as a clear oil. ESI(+) *m/z* $[M+H]^+$ 491.0; [M+Na] 512.9. HPLC (gradient A): ret time = 7.93 min; purity = 81%. ^{1}H NMR (400 MHz, $CDCl_3$): 8.20-7.60 (m, 4H), 7.30-7.20 (m, 2H), 7.01 (d, *J* = 6.3 Hz, 1H), 4.60-4.20 (m, 1H), 3.82 (s, 1H), 3.70-3.25 (m, 2H), 2.67 (s, 1H), 2.48 (s, 3H), 2.25-1.50 (m, 4H).

Methyl 3-(1-(3,5-bis(trifluoromethyl)benzoyl)piperidine-3-carboxamido)benzoate (206110). 36 mg (0.072 mmol, 72% yield) of title compound as a light purple solid. ESI(+) *m/z* $[M+H]^+$ 503.1; [M+Na] 525.2. HPLC (gradient A): ret time = 7.63 min; purity = 90%. ^{1}H NMR (400 MHz, DMSO-d_6): 1.1:1.0 mixture of rotamers, δ 10.33 (rotamer 1, s), 10.09 (rotamer 2, s, 1H, 8.39-8.16 (m, 2H), 8.12 (s, 2H), 7.91-7.70 (m,

1H), 7.70-7.57 (m, 1H), 7.44 (dq, *J* = 14.3, 7.6 Hz, 1H), 4.60-4.00 (m, 1H), 3.90-3.79 (m, 3H), 3.51-3.38 (m, 1H), 3.29-2.97 (m, 2H), 2.76-2.60 (m, 1H), 2.10-1.98 (m, 1H), 1.88-1.65 (m, 2H), 1.63-1.43 (m, 1H).

1-(3,5-bis(trifluoromethyl)benzoyl)-*N*-(3-methoxyphenyl)piperidine-3-carboxamide (206242). 29 mg (0.061 mmol, 61% yield) of title compound as an amber oil. ESI(+) *m/z* $[M+H]^+$ 475.0; [M+Na] 497.0. HPLC (gradient A): ret time = 7.59 min; purity = 80%. ^{1}H NMR (400 MHz, DMSO-d_6): 1.1:1.0 mixture of rotamers, δ 10.07 (rotamer 1, s), 9.85 (rotamer 2, s, 1H), 8.30-8.17 (m, 1H), 8.11 (s, 2H), 8.09-7.96 (m, 1H), 7.38-6.97 (m, 3H), 6.61 (dd, *J* = 18.4, 6.8 Hz, 1H), 4.58-4.06 (m, 1H), 3.77-3.66 (m, 3H), 3.56-3.38 (m, 1H), 3.24-2.97 (m, 2H), 2.08-1.95 (m, 1H), 1.86-1.26 (m, 3H).

1-(3,5-bis(trifluoromethyl)benzoyl)-*N*-(3-cyanophenyl)piperidine-3-carboxamide (206104). 62 mg (0.132 mmol, 132% yield) of title compound as a light brown foam. ESI(+) *m/z* $[M+H]^+$ 470.1; [M+Na] 492.1. HPLC (gradient A): ret time = 7.43 min; purity = 93%. ^{1}H NMR (500 MHz, DMSO-d_6): 1.0:1.0 mixture of rotamers, δ 10.48 (rotamer 1, s), 10.25 (rotamer 2, s, 1H), 8.31-7.44 (m, 7H), 4.60-3.97 (m, 1H), 4.02 (s, 1H), 3.62-3.39 (m, 2H), 3.17-3.03 (m, 1H), 2.73-2.55 (m, 1H), 2.08-1.97 (m, 1H), 1.88-1.66 (m, 2H), 1.63-1.42 (m, 1H).

1-(3,5-bis(trifluoromethyl)benzoyl)-N-(3-(morpholinomethyl)phenyl)piperidine-3-carboxamide (206247). 31 mg (0.057 mmol, 57% yield) of title compound as a white solid. ESI(+) *m/z* $[M+H]^+$ 544.1; [M+Na] 566.1. HPLC (gradient A): ret time = 5.96 min; purity = >95%. ^{1}H NMR (400 MHz, DMSO-d_6): 1.1:1.0 mixture of rotamers, δ 10.08 (rotamer 1, s), 9.85 (rotamer 2, s, 1H), 8.30-8.16 (m, 1H), 8.12 (s, 2H), 7.64-7.37 (m, 2H), 7.22 (dt, *J* = 15.7, 7.4 Hz, 1H), 6.96 (dd, *J* = 17.8, 6.7 Hz, 1H), 4.59-4.05 (m, 1H), 3.56 (bs, 4H), 3.40 (d, *J* = 17.6 Hz, 3H), 3.25-2.97 (m, 2H), 2.74-2.59 (m, 1H), 2.45-2.23 (m, 4H), 2.09-1.95 (m, 4H), 1.89-1.63 (m, 1H), 1.63-1.38 (m, 1H).

1-(3,5-bis(trifluoromethyl)benzoyl)-*N*-(3-nitrophenyl)piperidine-3-carboxamide (206103). 59 mg, (0.121 mmol, 121% yield) of title compound as an amber oil. ESI(+) *m/z* $[M+H]^+$ 490.1; [M+Na] 512.1. HPLC (gradient A): ret time = 7.62 min; purity =

>95%. ^{1}H NMR (500 MHz, DMSO-d_6): 1.1:1.0 mixture of rotamers, δ 10.60 (rotamer 1, s), 10.35 (rotamer 2, s, 1H), 8.73-8.53 (m, 1H), 8.28-8.16 (m, 1H), 8.12 (s, 2H), 7.99-7.77 (m, 2H), 7.59 (dt, *J* = 30.8, 7.7 Hz, 1H), 4.60-3.95 (m, 1H), 3.62-3.38 (m, 2H), 3.17-3.04 (m, 1H), 2.73-2.56 (m, 1H), 2.11-1.97 (m, 1H), 1.88-1.64 (m, 2H), 1.64-1.43 (m, 1H).

***N*-(3-acetylphenyl)-1-(3,5-bis(trifluoromethyl)benzoyl)piperidine-3-carboxamide (206105).** 57 mg (0.117 mmol, 117% yield) of title compound as a light brown foam. ESI(+) *m/z* $[M+H]^+$ 487.1; [M+Na] 509.1. HPLC (gradient A): ret time = 7.25 min; purity = 92%. ^{1}H NMR (500 MHz, DMSO-d_6): 1.1:1.0 mixture of rotamers, δ 10.31 (rotamer 1, s), 10.07 (rotamer 2, s, 1H), 8.47-8.07 (m, 5H), 7.93-7.60 (m, 2H), 7.50-7.38 (m, 1H), 4.60-4.05 (m, 1H), 3.58-3.38 (m, 1H), 3.27-3.02 (m, 2H), 2.71-2.52 (m, 4H), 2.09-2.00 (m, 1H), 1.87-1.41 (m, 4H).

1-(3,5-bis(trifluoromethyl)benzoyl)-N-(3-(pyrrolidin-1-ylmethyl)phenyl)piperidine-3-carboxamide (206123). ESI(+) *m/z* $[M+H]^+$ 528.2; [M+Na] 550.2. HPLC (gradient A): ret time = 6.05 min; purity = >95%. ^{1}H NMR (400 MHz, DMSO-d_6): 1.2:1.0 mixture of rotamers, δ 10.01 (rotamer 1, s, 1H), 9.79 (rotamer 2, s), 8.21 (rotamer 1, s, 1H), 8.15 (rotamer 2, s), 8.08 (s, 2H), 7.65-7.33 (m, 2H), 7.25-7.10 (m, 1H), 7.00-6.88 (m, 1H), 4.60-4.00 (m, 1H), 3.60-3.35 (m, 4H), 3.20-2.95 (m, 2H), 2.70-2.55 (m, 1H), 1.98 (d, *J* = 9.5, 1H), 1.85-1.60 (m, 6H), 1.60-1.35 (m, 1H).

Methyl 5-(3-(1-(3,5-bis(trifluoromethyl)benzoyl)piperidine-3-carboxamido)phenyl)furan-2-carboxylate (206112). 25 mg (0.044 mmol, 44% yield) of title compound as a white solid. ESI(+) m/z $[M+H]^+$ 569.2; [M+Na] 591.2. HPLC (gradient A): ret time =8.00 min; purity = >95%. ^{1}H NMR (400 MHz, DMSO-d_6): 1.0:1.0 mixture of rotamers, δ 10.31 (rotamer 1, s), 10.07 (rotamer 2, s, 1H), 8.28-7.06 (m, 9H), 4.61-4.07 (m, 1H), 3.85 (s, 7H), 3.58-2.99 (m, 3H), 2.77-2.56 (m, 1H), 2.11-1.98 (m, 1H), 1.92-1.66 (m, 2H), 1.64-1.46 (m, 1H).

***N*-(3-(allyloxy)phenyl)-1-(3,5-bis(trifluoromethyl)benzoyl)piperidine-3-carboxamide (206240).** 37 mg (0.074 mmol, 74% yield) of title compound as an orange oil. ESI(+) m/z

$[M+H]^+$ 501.0; [M+Na] 523.0. HPLC (gradient A): ret time = 7.96 min; purity = 79%. TOF MS-ESI *m/z* $[M+H]^+$ 501.0; [M+Na] 523.0. ^{1}H NMR (400 MHz, DMSO-d_6): 1.2:1.0 mixture of rotamers, δ 10.03 (rotamer 1, s), 9.81 (rotamer 2, s, 1H), 8.28-7.93 (m, 3H), 7.41-6.93 (m, 3H), 6.64-6.52 (m, 1H), 6.08-5.90 (m, 1H), 5.43-5.28 (m, 1H), 5.26-5.16 (m, 1H), 4.53-4.40 (m, 2H), 4.15-3.33 (m, 2H), 3.21-2.94 (m, 2H), 1.97 (m, 1H), 1.82-1.40 (m, 3H).

***N*-(3-benzoylphenyl)-1-(3,5-bis(trifluoromethyl)benzoyl)piperidine-3-carboxamide (206111).** 41 mg (0.075 mmol, 75% yield) of title compound as a light brown solid. ESI(+) *m/z* $[M+H]^+$ 549.2; [M+Na] 571.2. HPLC (gradient A): ret time = 8.13 min; purity = 90%. ^{1}H NMR (400 MHz, DMS)-d_6) 1.2:1.0 mixture of rotamers, δ 10.34 (rotamer 1, s), 10.10 (rotamer 2, s, 1H), 8.29-7.33 (m, 12H), 4.60-4.05 (m, 1H), 3.48-3.35 (m, 1H), 3.24-2.98 (m, 2H), 2.75-2.60 (m, 1H), 2.08-1.97 (m, 1H), 1.88-1.65 (m, 2H), 1.65-1.40 (m, 1H).

1-(3,5-bis(trifluoromethyl)benzoyl)-*N*-(3-(4-methyl-4*H*-1,2,4-triazol-3-yl)phenyl)piperidine-3-carboxamide (206245). ESI(+) *m/z* $[M+H]^+$ 526.0; [M+Na] 548.0. HPLC (gradient A): ret time = 6.00 min; purity = >95%. ^{1}H NMR (500 MHz, DMSO-d_6): 1.1:1.0 mixture of rotamers, δ 10.28 (rotamer 1, s), 10.06 (rotamer 2, s, 1H), 8.58-8.51 (m, 1H), 8.26-8.14 (m, 1H), 8.09 (s, 2H), 8.05-7.89 (m, 1H), 7.79-7.59 (m, 1H), 7.51-7.33 (m, 2H), 4.52-4.05 (m, 1H), 3.82-3.61 (m, 2H), 3.47-3.35 (m, 1H), 3.22-3.00 (m, 2H), 2.69-2.53 (m, 1H), 2.07-1.97 (m, 1H), 1.84-1.63 (m, 2H), 1.59-1.40 (m, 1H).

1-(3,5-bis(trifluoromethyl)benzoyl)-N-(3-(2-oxopyrrolidin-1-yl)phenyl)piperidine-3-carboxamide (206113). 29 mg (0.055 mmol, 55% yield) of title compound as a white solid. ESI(+) *m/z* $[M+H]^+$ 528.2; [M+Na] 550.2. HPLC (gradient A): ret time = 7.02 min; purity = 94%. ^{1}H NMR (500 MHz, DMSO-d_6): 1.1:1.0 mixture of rotamers, δ 10.28 (rotamer 1, s), 10.06 (rotamer 2, s, 1H), 8.25-8.13 (m, 1H), 8.11-7.88 (m, 3H), 7.77-7.58 (m, 1H), 7.51-7.33 (m, 2H), 4.57-4.03 (m, 1H), 3.77-3.65 (m, 2H), 3.47-3.35 (m, 1H),

3.23-3.00 (m, 2H), 2.69-2.30 (m, 2H), 2.07-1.97 (m, 1H), 1.83-1.64 (m, 2H), 1.59-1.42 (m, 1H).

1-(3,5-bis(trifluoromethyl)benzoyl)-*N*-(3-((3-chloro-5-(trifluoromethyl)pyridin-2-yl)oxy)phenyl)piperidine-3-carboxamide (206125). 42 mg (0.066 mmol, 66% yield) of title compound as a white solid. ESI(+) *m/z* $[M+H]^+$ 640.1. HPLC (gradient A): ret time = 8.70 min; purity = >95%. ^{1}H NMR (400 MHz, DMSO-d_6): 1.1:1.0 mixture of rotamers, δ 10.27 (rotamer 1, s), 10.05 (rotamer 2, s, 1H), 8.59 (s, 1H), 8.55-8.46 (m, 1H), 8.27-8.15 (m, 1H), 8.13-8.07 (m, 2H), 7.67-7.53 (m, 1H), 7.47-7.23 (m, 4H), 6.92 (dd, *J* = 18.2, 6.1 Hz, 1H), 4.58-3.95 (m, 1H), 3.55-3.36 (m, 3H), 3.29-2.97 (m, 4H), 2.69-2.53 (m, 1H), 2.07-1.96 (m, 2H), 1.84-1.39 (m, 7H).

***tert*-butyl 3-(1-(3,5-bis(trifluoromethyl)benzoyl)piperidine-3-carboxamido)benzoate (206107).** 47 mg (0.086 mmol, 86% yield) of title compound as a white solid. ESI(+) *m/z* [M+Na] 567.2. HPLC (gradient A): ret time = 8.52 min; purity = 87%. ^{1}H NMR (400 MHz, DMSO-d_6): 1.1:1.0 mixture of rotamers, δ 10.28 (rotamer 1, s), 10.05 (rotamer 2, s, 1H), 8.30-7.96 (m, 4H), 7.91-7.73 (m, 1H), 7.64-7.32 (m, 2H), 4.60-4.03 (m, 1H), 3.60-3.37 (m, 1H), 3.24-3.01 (m, 2H), 2.72-2.54 (m, 1H), 2.12-1.19 (m, 13H).

***N*-(4-chlorophenyl)-1-(3-(thiophen-2-yl)benzoyl)piperidine-3-carboxamide (206455).** 29 mg (0.068 mmol, 93% yield) as an amber glass. ESI(+) m/z $[M+H]^+$ 425.0; [M+23] 447.0; HPLC (gradient A): ret time = 7.66 min; purity = >95%. ^{1}H NMR (500 MHz, DMSO-d_6): 1.4:1.0 mixture of rotamers, δ 10.25 (rotamer 1, s), 10.06 (rotamer 2, s, 1H), 7.99-7.11 (m, 11H), 4.64-4.19 (m, 1H), 3.75-3.51 (m, 1H), 3.18-2.93 (m, 2H), 2.68-2.54 (m, 1H), 2.12-1.64 (m, 3H), 1.59-1.36 (m, 1H).

***N*-(4-chlorophenyl)-1-(4-(furan-2-yl)benzoyl)piperidine-3-carboxamide (206119).** 31 mg (0.076 mmol, 76% yield). ESI(+) m/z $[M+H]^+$ 409.1; [M+23] 431.1; HPLC (gradient A): ret time = 7.38 min; purity = 99%. ^{1}H NMR (500 MHz, DMSO-d_6): 1.4:1.0 mixture of rotamers, δ 10.23 (rotamer 1, s), 10.06 (rotamer 2, s, 1H), 7.88-7.50 (m, 5H), 7.44 (d, *J*

= 8.3 Hz, 2H), 7.35 (bs, 2H), 7.04 (s, 1H), 6.63 (s, 1H), 4.60-4.20 (m, 1H), 3.78-3.53 (m, 1H), 3.15-2.90 (m, 2H), 2.63-2.53 (m, 1H), 2.01 (s, 1H), 1.89-1.62 (m, 2H), 1.46 (s, 1H).

1-(3,5-bis(trifluoromethyl)benzoyl)-*N*-(3-(furan-2-yl)phenyl)piperidine-3-carboxamide (206122). 23 mg (0.045 mmol, 45% yield) of title compound as a white solid. ESI(+) *m/z* $[M+H]^+$ 511.1; [M+Na] 533.1. HPLC (gradient A): ret time = 8.10 min; purity = 91%. ^{1}H NMR (400 MHz, $CDCl_3$): δ 8.40-7.76 (m, 5H), 7.55-7.30 (m, 4H), 6.67 (s, 1H), 6.46 (s, 1H), 4.30-4.20 (m, 1H), 3.85-3.25 (m, 3H), 2.70 (s, 1H), 2.27-1.50 (m, 4H).

***tert*-butyl 3-((3-(methylthio)phenyl)carbamoyl)piperidine-1-carboxylate.** Prepared using **43** according to Procedure D to afford 0.030 g (0.086 mmol, 86% yield) of title compound. No further purification was performed.

***N*-(3-(methylthio)phenyl)piperidine-3-carboxamide.** *tert*-butyl 3-((3-(methylthio)phenyl)carbamoyl)piperidine-1-carboxylate (0.028 g, 0.080 mmol) was dissolved in DCM (0.540 mL) and the solution was cooled to -10 °C. TFA (0.270 mL) was added to the cooled, stirring solution. The reaction mixture continued stirring at -10 °C for 45 minutes. The solution was added to a cooled 2M NaOH solution (10 mL). The mixture was then extracted with DCM (3 x 5 mL). The combined organics were dried ($MgSO_4$) and concentrated *in vacuo* to afford 0.010 g (0.040 mmol, 50% yield) of title compound as a brown oil. No further purification was performed.

1-(3-(furan-2-yl)benzoyl)-*N*-(3-(methylthio)phenyl)piperidine-3-carboxamide (206683). Prepared using *N*-(3-(methylthio)phenyl)piperidine-3-carboxamide according to Procedure B to afford 0.013 g (0.031 mmol, 77% yield) of title compound as a tan solid. No further purification was performed. ESI(+) *m/z* $[M+H]^+$ 421.0; [M+Na] 442.9. HPLC (gradient A): ret time = 7.35 min; purity = >90%. ^{1}H NMR (400 MHz, DMSO-d_6): 1.4:1.0 mixture of rotamers, δ 10.08 (rotamer 1, s), 9.88 (rotamer 2, s, 1H), 7.80-7.15 (m, 8H), 7.04 (s, 1H), 6.93 (s, 1H), 6.62 (s, 1H), 4.65-4.20 (m, 1H), 3.74-3.49 (m, 1H), 3.19-

2.96 (m, 2H), 2.64-2.54 (s, 1H), 2.44 (bs, 3H), 2.07-1.95 (m, 1H), 1.91-1.66 (m, 2H), 1.47 (s, 1H).

1-(3,5-bis(trifluoromethyl)benzoyl)-N-(3-(pyridin-2-yloxy)phenyl)piperidine-3-carboxamide. (206681). Prepared using 3-(pyridin-2-yloxy)aniline and **48** according to Procedure D. Crude material was purified using a Biotage FlashMaster Personal^{+} system (2.5% Methanolic ammonia/DCM) to afford 0.007 g (0.013 mmol, 13% yield) of title compound as a clear glass. ESI(+) *m/z* $[M+H]^+$ 537.9; [M+Na] 559.8. HPLC (gradient A): ret time = 7.51 min; purity = >95%. ^{1}H NMR (400 MHz, DMSO-d_6): 1.1:1.0 mixture of rotamers, δ 10.17 (rotamer 1, s), 9.95 (rotamer 2, s, 1H), 8.27-8.12 (m, 2H), 8.10 (s, 2H), 7.90-7.81 (m, 1H), 7.56-7.22 (m, 3H), 7.14 (s, 1H), 7.07-6.95 (m, 1H), 6.87-6.72 (m, 1H), 4.58-4.07 (m, 1H), 3.55-3.35 (m, 1H), 3.21-2.96 (m, 2H), 2.69-2.53 (m, 1H) 2.06-1.96 (m, 1H), 1.87-1.39 (m, 3H).

2-((3-nitrophenoxy)methyl)pyridine.[147]

3-(pyridin-2-ylmethoxy)aniline.[148] 2-((3-nitrophenoxy)methyl)pyridine (0.050 g, 0.217 mmol), iron powder (0.050 g, 0.890 mmol), and ammonium chloride (0.014 g, 0.261 mmol) were combined in a solution of methanol (1.41 mL), tetrahydrofuran (1.41 mL), and water (0.470 mL), and was refluxed for 3 hours. The resulting mixture was cooled to room temperature, diluted with methanol (5 mL), and filtered through a pad of celite. The filtrate was concentrated and triturated with dichloromethane. The triturated solid was discarded, and the filtrate was concentrated *in vacuo* to afford 0.035 g of title compound as a brown oil. No further purification was performed. ^{1}H NMR (400 MHz, DMSO-d_6): δ 8.56 (d, J = 4.5 Hz, 1H), 7.82 (t, J = 7.7 Hz, 1H), 7.46 (d, J = 7.9 Hz, 1H), 7.38-7.28 (m, 1H), 6.89 (dd, J = 8.7, 7.4 Hz, 1H), 6.21 (d, J = 1.7 Hz, 1H), 6.18-6.12 (m, 2H), 5.06 (s, 4H).

1-(3,5-bis(trifluoromethyl)benzoyl)-*N*-(3-(pyridin-2-ylmethoxy)phenyl)piperidine-3-carboxamide (208798). Prepared using 3-(pyridin-2-ylmethoxy)aniline and **48** according to Procedure D. Crude material was purified using a Biotage FlashMaster Personal^{+}

system (1-15% Methanolic ammonia/DCM) to afford 0.019 g (0.034 mmol, 27% yield) of title compound as an orangish-brown solid. ESI(-) *m/z* $[M-H]^-$ 550.0. HPLC (gradient A): ret time = 6.36 min; purity = >95%. ^{1}H NMR (400 MHz, DMSO-d_6): 1.1:1.0 mixture of rotamers, δ 10.06 (rotamer 1, s), 9.83 (rotamer 2, s, 1H), 8.57 (s, 1H), 8.27-8.15 (m, 1H), 8.10 (s, 2H), 7.83 (t, *J* = 6.4, 1H), 7.54-7.00 (m, 5H), 6.70 (d, *J* = 7.2, 1H), 5.13 (d, *J* = 13.8, 2H), 4.55-4.05 (m, 1H), 3.55-2.95 (m, 3H), 2.65-2.55 (m, 1H), 2.06-1.95 (m, 1H), 1.88-1.38 (m, 3H).

1-(3,5-bis(trifluoromethyl)benzoyl)-*N*-(5-chloropyridin-2-yl)piperidine-3-carboxamide (206101). Only base wash was performed. The crude material was purified using Biotage with 1% Methanolic ammonia in DCM to afford 19 mg (0.040 mmol, 40% yield) of title compound as a white solid. TLC R_f (5% Methanolic ammonia/DCM): 0.63. ESI(+) *m/z* $[M+H]^+$ 480.1; [M+Na] 502.1. HPLC (gradient A): ret time = 7.81 min; purity = >95%. ^{1}H NMR (500 MHz, DMSO-d_6): 1.1:1.0 mixture of rotamers, δ 10.86 (rotamer 1, s), 10.62 (rotamer 2, s, 1H), 8.47-7.99 (m, 5H), 7.97-7.82 (m, 1H), 4.55-3.98 (m, 1H), 3.63-3.37 (m, 2H), 3.31-3.05 (m, 2H), 2.89-2.66 (m, 1H), 2.10-1.93 (m, 1H), 1.90-1.63 (m, 2H), 1.58-1.37 (m, 1H).

1-(3,5-bis(trifluoromethyl)benzoyl)-*N*-(6-chloropyridin-3-yl)piperidine-3-carboxamide (206106). 28 mg (0.058 mmol, 58% yield) of title compound. ESI(+) *m/z* $[M+H]^+$ 480.1. HPLC (gradient A): ret time = 7.40 min; purity = >95%. ^{1}H NMR (500 MHz, DMSO-d_6) 1.1:1.0 mixture of rotamers, δ 10.46 (rotamer 1, s), 10.22 (rotamer 2, s, 1H), 8.70-8.48 (m, 1H), 8.31-7.91 (m, 4H), 7.46 (dd, *J* = 28.4, 8.7 Hz, 1H), 4.61-4.00 (m, 1H), 3.61-3.00 (m, 1H), 2.75-2.55 (m, 2H), 2.10-2.00 (m, 1H), 1.88-1.65 (m, 2H), 1.61-1.41 (m, 1H).

1-(3,5-bis(trifluoromethyl)benzoyl)-*N*-(pyridin-4-yl)piperidine-3-carboxamide (206682). Pyridin-4-amine (0.021 g, 0.220 mmol) was dissolved in DCM (2.00 mL) and was treated with EDC (0.058 g, 0.300 mmol), followed by DMAP (0.037 g, 0.300 mmol) and **48** (0.074 g, 0.200 mmol). The suspension was stirred overnight at room temperature. The reaction was then diluted with DCM to a volume of 10 mL and was washed with

saturated $NaHCO_3$ (5 mL). Organics were dried ($MgSO_4$) and concentrated *in vacuo*. Crude material was purified using a CombiFlash Retrieve system (0-5% Methanolic ammonia/DCM) to afford 0.028 g (0.063 mmol, 31% yield) of title compound as a clear glass. TLC R_f (5% Methanolic ammonia/DCM): 0.23. ESI(+) *m/z* $[M+H]^+$ 445.9. HPLC (gradient A): ret time = 5.70 min; purity = >90%. ^{1}H NMR (400 MHz, DMSO-d_6): 1.0:1.0 mixture of rotamers, δ 10.45 (rotamer 1, s), 10.21 (rotamer 2, s, 1H), 8.47-8.33 (m, 2H), 8.27-8.15 (m, 1H), 8.10 (s, 2H), 7.59 (s, 1H), 7.46 (s, 1H), 4.60-3.97 (m, 1H), 3.60-3.36 (m, 1H), 3.29-3.00 (m, 2H), 2.62-2.54 (m, 1H), 2.09-1.99 (m, 1H), 1.90-1.64 (m, 2H), 1.61-1.40 (m, 1H).

***N*-(6-chloropyridin-3-yl)-1-(3-(furan-2-yl)benzoyl)piperidine-3-carboxamide (206460).** 42 mg (0.102 mmol, 44% yield) of title compound as a light brown solid. Agilent ESI(+) *m/z* [M+Na] 432.0. HPLC (gradient A): ret time = 6.75 min; purity = >95%. ^{1}H NMR (400 MHz, DMSO-d_6): 1.4:1.0 mixture of rotamers, δ 10.44 (rotamer 1, s), 10.21 (rotamer 2, s, 1H), 8.75-8.43 (m, 1H), 8.20-7.93 (m, 1H), 7.77 (bs, 2H), 7.67 (s, 1H), 7.48 (bs, 2H), 7.28 (d, *J* = 7.4 Hz, 1H), 7.04 (s, 1H), 6.62 (s, 1H), 4.65-4.15 (m, 1H), 3.75-3.49 (m, 1H), 3.21-2.89 (m, 2H), 2.70-2.55 (m, 1H), 2.09-2.00 (m, 1H), 1.92-1.65 (m, 2H), 1.47 (s, 1H).

***tert*-butyl 3-((3-chloro-4-methoxyphenyl)carbamoyl)piperidine-1-carboxylate (206120).** Prepared using **28** according to Procedure D. Crude material was triturated with DCM to afford 0.009 g (0.024 mmol, 22% yield) of title compound as a white solid. ESI(+) m/z $[M+H]^+$ 381.1; [M+Na] 403.1. HPLC (gradient A): ret time = 7.11; purity = >95%. ^{1}H NMR (400 MHz, DMSO-d_6: δ 9.04 (s, 1H), 8.17 (s, 1H), 7.97-7.38 (m, 8H), 7.03 (s, 1H), 6.63 (s, 1H), 4.70 (s, 1H), 4.23 (t, *J* = 8.6 Hz, 1H), 3.80 (d, *J* = 10.8 Hz, 1H), 3.01 (dd, *J* = 17.8, 8.5 Hz, 1H), 2.64 (d, *J* = 17.9 Hz, 1H).

1-(3-(furan-2-yl)benzoyl)-*N*-(3-phenoxyphenyl)piperidine-3-carboxamide (206451). 20 mg (0.043 mmol, 67% yield) of title compound as a white solid. Agilent ESI(+) *m/z* $[M+H]^+$ 467.1. HPLC (gradient A): ret time = 8.00 min; purity = >90%. ^{1}H NMR (400 MHz, DMSO-d_6): 1.4:1.0 mixture of rotamers, δ 10.14 (rotamer 1, s), 9.94 (rotamer 2, s,

1H), 7.77 (s, 2H), 7.67 (s, 1H), 7.53-6.94 (m, 12H), 6.75-6.58 (m, 2H), 4.65-4.18 (m, 1H), 3.70-3.48 (m, 1H), 3.15-2.88 (m, 2H), 2.65-2.53 (m, 1H), 2.07-1.93 (m, 1H), 1.89-1.63 (m, 2H), 1.44 (bs, 1H).

***N*-(3-benzylphenyl)-1-(3-(furan-2-yl)benzoyl)piperidine-3-carboxamide (206450).** 15 mg (0.032 mmol, 67% yield) of title compound as a white solid. Agilent ESI(+) *m/z* $[M+H]^+$ 465.1; [M+Na] 487.1. HPLC (gradient A): ret time = 8.04 min; purity = >90%. ^{1}H NMR (400 MHz, DMSO-d_6): 1.6:1.0 mixture of rotamers, δ 10.00 (rotamer 1, s), 9.80 (rotamer 2, s, 1H), 7.82-7.65 (m, 3H), 7.54-7.11 (m, 10H), 7.05 (s, 1H), 6.92 (s, 1H), 6.61 (s, 1H), 4.62-4.20 (m, 1H), 3.98-3.80 (m, 2H), 3.71-3.48 (m, 1H), 3.15-2.85 (m, 2H), 2.65-2.55 (m, 1H), 2.10-1.93 (m, 1H), 1.88-1.62 (m, 2H), 1.44 (s, 1H).

(*R*)-1-(4-chlorophenyl)-4-hydroxypyrrolidin-2-one (50a).[106] (*R*)-4-hydroxypyrrolidin-2-one **49a** (0.102 g, 1.01 mmol) was added to a pressure tube containing Copper(I) iodide (0.032 g, 0.168 mmol), potassium phosphate (0.356 g, 1.68 mmol), and a stir bar. 1-chloro-4-iodobenzene (0.200 g, 0.839 mmol) dissolved in 1,4-dioxane (8.4 mL) was added, and the tube was purged with nitrogen. *trans*-1,2-diaminocyclohexane (0.030 mL, 0.252 mmol) was added to the pressure tube, and the tube was purged with nitrogen. The pressure tube was capped and stirred at 110 °C overnight. Crude material was combined with a two additional reactions and was purified by column chromatography (75-100% EtOAc/Hex) to afford 0.444 g (2.10 mmol, 63% yield) of title compound as a brown solid. TLC R_f (80% EtOAc/Hex): 0.23. ^{1}H NMR (400 MHz, DMSO-d_6): δ 7.70 (m, 2H), 7.42 (m, 2H), 5.37 (d, *J* = 3.8, 1H), 4.42-4.35 (m, 1H), 4.04 (dd, *J* = 10.5, 5.1, 1H), 3.61-3.55 (m, 1H), 2.84 (dd, *J* = 17.1, 6.1, 1H), 2.30 (dd, *J* = 17.1, 1.4, 1H).

(*R*)-1-(4-chlorophenyl)-5-oxopyrrolidin-3-yl 4-methylbenzenesulfonate (51a). Compound **50a** (0.410 g, 1.94 mmol), pyridine (3.13 mL, 38.7 mmol), and *p*-toluenesulfonyl chloride (1.11 g, 5.81 mmol) were mixed, and the reaction was allowed to stir overnight at room temperature under nitrogen. Water (30 mL) was added, and the water layer was extracted with ether (3 x 30 mL). The combined ether layers were then washed with water (2 x 30 mL), followed by saturated $NaHCO_3$ (2 x 30 mL), and then

brine (30 mL). The ether layer was dried ($MgSO_4$) and concentrated *in vacuo* to afford 0.643 g (1.76 mmol, 91% yield) of title compound as a brown solid. No further purification was performed. ^{1}H NMR (400 MHz, DMSO-d_6): δ 7.90-7.82 (m, 2H), 7.68-7.59 (m, 2H), 7.55-7.47 (m, 2H), 7.48-7.39 (m, 2H), 5.25 (ddt, *J* = 6.8, 5.4, 1.7 Hz, 1H), 4.21 (dd, *J* = 11.9, 5.2 Hz, 1H), 3.92-3.84 (m, 1H), 3.01 (dd, *J* = 17.9, 6.4 Hz, 1H), 2.54-2.46 (m, 1H), 2.44 (s, 3H).

(*S*)-4-azido-1-(4-chlorophenyl)pyrrolidin-2-one (52a). Compound **51a** (0.641 g, 1.75 mmol) was dissolved in DMSO (2.19 mL), and to the stirring solution was added sodium azide (0.570 g, 8.76 mmol). The mixture was stirred at room temperature for 5 hours. The mixture was diluted with water (25 mL) and was extracted with DCM (3 x 25 mL). Combined organics were washed with water (25 mL), dried ($MgSO_4$), and concentrated *in vacuo*. Crude material was purified using a Biotage SP1 system (7-40% EtOAc/Hex) to afford 0.073 g (0.308 mmol, 18% yield) of title compound as an amber oil. TLC R_f (30% EtOAc/Hex): 0.18. ^{1}H NMR (400 MHz, DMSO-d_6): δ 7.71-7.64 (m, 2H), 7.48-7.41 (m, 2H), 4.59 (tt, *J* = 5.9, 2.6 Hz, 1H), 4.17 (dd, *J* = 10.9, 5.8 Hz, 1H), 3.77 (dd, *J* = 10.9, 2.1 Hz, 1H), 3.00 (dd, *J* = 17.3, 7.0 Hz, 1H).

(*S*)-4-amino-1-(4-chlorophenyl)pyrrolidin-2-one (53a). Compound **52a** (0.071 g, 0.300 mmol) and Pd-C (6.39 mg, 6.00 µmol) were added to a flask, and the flask was evacuated and backfilled with nitrogen 3 times. Sparged methanol (1.50 mL) was then slowly added. A blanket of hydrogen was provided, and the reaction was stirred for 5 h. The reaction was then filtered through a plug of celite and was flushed using additional methanol. Organics were concentrated *in vacuo* to afford 0.059 g (0.280 mmol, 93% yield) of title compound as a brown opaque oil. No further purification was performed. ^{1}H NMR (400 MHz, DMSO-d_6): δ 7.71-7.64 (m, 2H), 7.48-7.40 (m, 2H), 4.59 (tt, *J* = 5.6, 2.6 Hz, 1H), 4.17 (dd, *J* = 10.9, 5.9 Hz, 1H), 3.77 (dd, *J* = 10.9, 2.1 Hz, 1H), 3.00 (dd, *J* = 17.3, 7.1 Hz, 1H), 2.54-2.47 (m, 1H).

(*S*)-*N*-(1-(4-chlorophenyl)-5-oxopyrrolidin-3-yl)-3,5-bis(trifluoromethyl)benzamide (206684). Compound **53a** (0.020 g, 0.095 mmol) was suspended in DCM (0.950 mL)

and was treated with DIPEA (0.025 ml, 0.142 mmol) followed by 3,5-bis(trifluoromethyl)benzoyl chloride (0.019 mL, 0.104 mmol). Upon treatment with the acid chloride, a sample was removed for HPLC, and the reaction appeared to have completed instantaneously. Therefore, the solution was diluted with DCM to a volume of 5 mL, and the organic layer was washed with 1 N HCl (5 mL) followed by $NaHCO_3$ (5 mL) and was then dried ($MgSO_4$) and concentrated *in vacuo* to afford 0.028 g of title compound as a white solid. No further purification was performed. ESI(+) *m/z* $[M+H]^+$ 450.9; [M+Na] 472.8. HPLC (gradient A): ret time = 7.84 min; purity = >95%. ^{1}H NMR (400 MHz, DMSO-d_6): δ 9.36 (d, *J* = 6.6 Hz, 1H), 8.51 (s, 2H), 8.33 (s, 1H), 7.78-7.69 (m, 2H), 7.49-7.40 (m, 2H), 4.72 (qt, *J* = 7.0, 3.8 Hz, 1H), 4.25 (dd, *J* = 10.4, 7.0 Hz, 1H), 3.83 (dd, *J* = 10.4, 2.8 Hz, 1H), 3.06 (dd, *J* = 17.4, 8.5 Hz, 1H), 2.64 (dd, *J* = 17.4, 3.4 Hz, 1H).

(*S*)-1-(4-chlorophenyl)-4-hydroxypyrrolidin-2-one (50b). (*S*)-4-hydroxypyrrolidin-2-one (**49b)** (0.102 g, 1.01 mmol) was added to a pressure tube containing copper(I) iodide (0.032 g, 0.168 mmol), potassium phosphate (0.356 g, 1.68 mmol), and a stir bar. 1-chloro-4-iodobenzene (0.200 g, 0.839 mmol) dissolved in 1,4-dioxane (8.4 mL) was added, and the tube was purged with nitrogen. *trans*-1,2-diaminocyclohexane (0.030 mL, 0.252 mmol) was added to the pressure tube, and the tube was purged with nitrogen. The pressure tube was capped and stirred at 110 °C overnight. Crude material was combined with a two additional reactions and was purified using a Biotage SP1 system (60-82% EtOAc/Hex) to afford 0.427 g (2.02 mmol, 60% yield) of title compound as a brown solid. TLC R_f (80% EtOAc/Hex): 0.23. ^{1}H NMR (400 MHz, DMSO-d_6): δ 7.70-7.63 (m, 2H), 7.42-7.35 (m, 2H), 5.34 (d, *J* = 3.8 Hz, 1H), 4.34 (dtt, *J* = 5.7, 3.8, 1.8 Hz, 1H), 4.00 (dd, *J* = 10.5, 5.1 Hz, 1H), 3.54 (d, *J* = 10.6 Hz, 1H), 2.79 (dd, *J* = 17.1, 6.1 Hz, 1H), 2.31-2.23 (m, 1H).

(*S*)-1-(4-chlorophenyl)-5-oxopyrrolidin-3-yl 4-methylbenzenesulfonate (51b). Compound **50b** (0.425 g, 2.01 mmol), Pyridine (3.25 mL, 40.2 mmol), and *p*-toluenesulfonyl chloride (1.15 g, 6.02 mmol) were mixed, and the reaction was allowed to stir overnight at room temperature under nitrogen. Water (35 mL) was added, and the

water layer was extracted with ether (3 x 35 mL). The combined ether layers were then washed with water (2 x 35 mL), followed by saturated $NaHCO_3$ (2 x 35 mL), and then brine (35 mL). The ether layer was dried ($MgSO_4$), filtered, and concentrated *in vacuo*. Crude material was purified using a Biotage SP1 system (12-45% EtOAc/Hex) to afford 0.244 g (0.667 mmol, 33% yield) of title compound as an amber oil. TLC R_f (50% EtOAc/Hex): 0.36. ^{1}H NMR (400 MHz, DMSO-d_6): δ 7.90-7.82 (m, 2H), 7.68-7.59 (m, 2H), 7.51 (d, *J* = 7.9 Hz, 2H), 7.48-7.39 (m, 2H), 5.29-5.20 (m, 1H), 4.21 (dd, *J* = 11.9, 5.2 Hz, 1H), 3.88 (d, *J* = 11.9 Hz, 1H), 3.01 (dd, *J* = 17.9, 6.3 Hz, 1H), 2.54-2.65 (m, 1H), 2.44 (s, 3H).

(*R*)-4-azido-1-(4-chlorophenyl)pyrrolidin-2-one (52b). Compound **51b** (0.242 g, 0.662 mmol) was dissolved in DMSO (0.827 mL), and to the stirring solution was added sodium azide (0.215 g, 3.31 mmol). The mixture was stirred at room temperature for 5 h. The mixture was diluted with water (20 mL) and was extracted with DCM (3 x 20 mL). Combined organics were washed with water (20 mL), dried ($MgSO_4$), and concentrated *in vacuo*. Crude material was purified using a Biotage SP1 system (7-40% EtOAc/Hex) to afford 0.073 g (0.308 mmol, 47% yield) of title compound as an amber oil. TLC R_f (30% EtOAc/Hex): 0.18. ^{1}H NMR (400 MHz, DMSO-d_6): δ 7.68-7.59 (m, 2H), 7.45-7.36 (m, 2H), 4.55 (ddt, *J* = 7.0, 5.5, 2.6 Hz, 1H), 4.13 (dd, *J* = 10.9, 5.9 Hz, 1H), 2.97 (dd, *J* = 17.3, 7.0 Hz, 1H), 2.51-2.43 (m, 1H).

(*R*)-4-amino-1-(4-chlorophenyl)pyrrolidin-2-one (53b). Compound **52b** (0.071 g, 0.300 mmol) and Pd-C (6.39 mg, 6.00 µmol) were added to a flask, and the flask was evacuated and backfilled with nitrogen 3 times. Sparged methanol (1.50 mL) was then slowly added. A blanket of hydrogen was provided, and the reaction was stirred for 5 h. The reaction was then filtered through a plug of celite and was flushed using additional methanol. Organics were concentrated *in vacuo* to afford 0.059 g (0.280 mmol, 93% yield) of title compound as a brown opaque oil. No further purification was performed. ^{1}H NMR (400 MHz, DMSO-d_6): δ 12.44 (s, 1H), 8.17 (s, 1H), 8.09 (s, 2H), 4.50-3.70-

3.76 (m, 1H), 3.45-3.31 (m, 2H), 3.11-2.90 (m, 1H), 2.58-2.50 (m, 1H), 2.03-1.84 (m, 1H), 1.78-1.43 (m, 3H).

(*R*)-*N*-(1-(4-chlorophenyl)-5-oxopyrrolidin-3-yl)-3,5-bis(trifluoromethyl)benzamide (206685). Compound **53b** (0.011 g, 0.052 mmol) was suspended in DCM (0.525 mL) and was treated with DIPEA (0.014 mL, 0.078 mmol) followed by 3,5-bis(trifluoromethyl)benzoyl chloride (10.35 µl, 0.057 mmol). Upon treatment with the acid chloride, a sample was removed for HPLC, and the reaction appeared to have completed instantaneously. Therefore, the solution was diluted with DCM to a volume of 5 mL, and the organic layer was washed with 1 N HCl (5 mL) followed by $NaHCO_3$ (5 mL) and was then dried ($MgSO_4$) and concentrated *in vacuo* to afford 0.015 g of title compound as a white solid. No further purification was performed. ESI(+) *m/z* $[M+H]^+$ 450.9; [M+Na] 472.8. HPLC (gradient A): ret time = 7.85 min; purity = >90%. ^{1}H NMR (400 MHz, DMSO-d_6): δ 9.36 (d, *J* = 6.7 Hz, 1H), 8.51 (s, 2H), 8.33 (s, 1H), 7.79-7.69 (m, 2H), 7.49-7.40 (m, 2H), 4.78-4.66 (m, 1H), 4.25 (dd, *J* = 10.4, 6.9 Hz, 1H), 3.83 (dd, *J* = 10.5, 2.7 Hz, 1H), 3.06 (dd, *J* = 17.4, 8.5 Hz, 1H), 2.64 (dd, *J* = 17.4, 3.4 Hz, 1H).

(*S*)-*N*-((*S*)-1-(4-chlorophenyl)-5-oxopyrrolidin-3-yl)-3,3,3-trifluoro-2-methoxy-2-phenylpropanamide (208802).[107] Compound **53a** (0.017 g, 0.081 mmol) was suspended in DCM (0.805 mL) and was treated with DIPEA (0.021 ml, 0.121 mmol) followed by (*R*)-3,3,3-trifluoro-2-methoxy-2-phenylpropanoyl chloride (0.015 ml, 0.081 mmol). A sample was removed for HPLC, and the reaction appeared to have completed instantaneously. Therefore, the solution was diluted with DCM to a volume of 5 mL and the organic layer was washed with 1 N HCl (5 mL) followed by $NaHCO_3$ (5 mL) and was dried ($MgSO_4$) and concentrated *in vacuo* to afford 0.015 g (0.035 mmol, 44% yield) of title compound as a white solid. HPLC (gradient A): ret time = 7.44 min; purity = >90%. ESI(+) *m/z* $[M+H]^+$ 426.9; [M+Na] 448.9. ^{1}H NMR (400 MHz, DMSO-d_6): δ 8.98 (d, *J* = 7.4 Hz, 1H), 7.69 (d, *J* = 9.0 Hz, 2H), 7.56-7.37 (m, 7H), 4.62 (s, 1H), 4.17 (dd, *J* = 10.1, 7.6 Hz, 1H), 3.71 (dd, *J* = 10.3, 3.7 Hz, 1H), 3.43 (s, 3H), 2.89 (dd, *J* = 17.3, 8.8 Hz, 1H), 2.44 (dd, *J* = 17.3, 4.5 Hz, 1H). ^{19}F NMR (400 MHz, DMSO): δ 68.51.

(*S*)-*N*-((*R*)-1-(4-chlorophenyl)-5-oxopyrrolidin-3-yl)-3,3,3-trifluoro-2-methoxy-2-phenylpropanamide (208805).[107] Prepared identically to **208802** using **53b**. ESI(+) *m/z* $[M+H]^+$ 426.9; [M+Na] 448.9. HPLC (gradient A): ret time = 7.41 min; purity = >90%. ^{1}H NMR (400 MHz, DMSO-d_6): δ 8.98 (d, *J* = 7.1, 1H), 7.73-7.67 (m, 2H), 7.55-7.40 (m, 7H), 4.63 (qt, *J* = 8.4, 4.3, 1H), 4.18 (dd, *J* = 10.2, 7.7 Hz, 1H), 3.72 (dd, *J* = 10.2, 3.9 Hz, 1H), 3.44 (s, 3H), 2.90 (dd, *J* = 17.3, 8.7 Hz, 1H), 2.45 (dd, *J* = 17.4, 4.6 Hz, 1H). ^{19}F NMR (400 MHz, DMSO-d_6): δ 68.50.

(*S*)-1-(*tert*-butoxycarbonyl)piperidine-3-carboxylic acid.[149]

(*S*)-*tert*-butyl 3-((4-chlorophenyl)carbamoyl)piperidine-1-carboxylate. Prepared according to Procedure C, but using 1.0 eq of (*S*)-1-(*tert*-butoxycarbonyl)piperidine-3-carboxylic acid and 1.1 eq of 4-chloro aniline to afford 0.054 g (0.159 mmol, 61% yield) of title compound. No further purification was performed. ^{1}H NMR (500 MHz, DMSO-d_6): δ 10.13 (s, 1H), 7.66-7.59 (m, 2H), 7.38-7.31 (m, 2H), 3.86 (d, *J* = 12.7 Hz, 1H), 3.12-2.72 (m, 1H), 2.43 (tt, *J* = 10.9, 3.9 Hz, 1H), 1.96-1.89 (m, 2H), 1.70 (d, *J* = 12.7 Hz, 1H), 1.61 (qd, *J* = 11.9, 3.6 Hz, 1H), 1.43-1.28 (m, 10H).

(*S*)-*N*-(4-chlorophenyl)piperidine-3-carboxamide, TFA salt. (*S*)-*tert*-butyl 3-((4-chlorophenyl)carbamoyl)piperidine-1-carboxylate (0.054 g, 0.159 mmol) was dissolved in DCM (1.30 mL), and to the stirring solution was added TFA (0.325 mL). Reaction was stirred for 45 minutes. Solution was concentrated *in vacuo* to afford 0.066 g (0.187 mmol, 117% yield) of title compound as a yellow oil. No further purification was performed. ^{1}H NMR (500 MHz, DMSO-d_6): δ 10.31 (s, 1H), 8.60 (s, 2H), 7.65-7.59 (m, 2H), 7.41-7.34 (m, 2H), 3.33 (d, *J* = 12.3 Hz, 1H), 3.20 (d, *J* = 12.4 Hz, 1H), 3.06 (tt, *J* = 11.6, 5.8 Hz, 1H), 2.98-2.87 (m, 1H), 2.85-2.75 (m, 1H), 2.08-1.97 (m, 1H), 1.89-1.78 (m, 1H), 1.72-1.59 (m, 2H).

(*S*)-N-(4-chlorophenyl)-1-(3-(furan-2-yl)benzoyl)piperidine-3-carboxamide (206116, Lot 380445). Prepared using (*S*)-*N*-(4-chlorophenyl)piperidine-3-carboxamide, TFA salt and 3-(furan-2-yl)benzoic acid according to Procedure C, but using 2.1 eq DIPEA. Crude

material was purified using a CombiFlash system (35-50% EtOAc/Hex) to afford 0.021 g (0.051 mmol, 27% yield) of title compound as a yellow oil. TLC R_f (50% EtOAc/Hex): 0.29. ESI(+) m/z $[M+H]^+$ 409.1; [M+23] 431.1. HPLC (gradient A): ret time = 7.50; purity = >95%. ^{1}H NMR (400 MHz, DMSO-d_6): 1.6:1.0 mixture of rotamers, δ 10.22 (rotamer 1, s), 10.01 (rotamer 2, s, 1H), 7.85-7.20 (m, 9H), 7.05 (s, 1H), 6.62 (s, 1H), 4.62-4.18 (m, 1H), 3.73-3.48 (m, 1H), 3.18-2.89 (m, 2H), 2.59 (s, 1H), 2.08-2.01 (m, 1H), 1.93-1.35 (m, 3H).

(*R*)-1-(*tert*-butoxycarbonyl)piperidine-3-carboxylic acid.[149]

(*R*)-*tert*-butyl 3-((4-chlorophenyl)carbamoyl)piperidine-1-carboxylate. Prepared according to Procedure C, but using 1.0 eq of (*R*)-1-(*tert*-butoxycarbonyl)piperidine-3-carboxylic acid and 1.1 eq of 4-chloro aniline to afford 0.054 g (0.159 mmol, 61% yield) of title compound. No further purification was performed. ^{1}H NMR (500 MHz, DMSO-d_6): δ 10.13 (s, 1H), 7.66-7.60 (m, 2H), 7.38-7.32 (m, 2H), 3.95-3.80 (m, 2H), 2.84-2.70 (m, 1H), 2.49-2.38 (m, 1H), 1.97-1.88 (m, 1H), 1.75-1.56 (m, 2H), 1.45-1.27 (m, 11H).

(*R*)-*N*-(4-chlorophenyl)piperidine-3-carboxamide, TFA salt. (*R*)-*tert*-butyl 3-((4-chlorophenyl)carbamoyl)piperidine-1-carboxylate (0.056 g, 0.165 mmol) was dissolved in DCM (1.30 mL), and to the stirring solution was added TFA (0.325 mL). Reaction was stirred for 45 minutes. Solution was concentrated *in vacuo* to afford 0.059 g (0.167 mmol, 101% yield) of title compound as a yellow oil. No further purification was performed. ^{1}H NMR (500 MHz, DMSO): δ 10.31 (s, 1H), 8.63 (bs, 2H), 7.65-7.57 (m, 2H), 7.41-7.35 (m, 2H), 3.33 (d, J = 12.5 Hz, 1H), 3.20 (d, J = 12.2 Hz, 1H), 3.11-3.02 (m, 1H), 2.92 (d, J = 6.3 Hz, 1H), 2.85-2.75 (m, 1H), 2.06-1.98 (m, 1H), 1.89-1.78 (m, 1H), 1.72-1.58 (m, 2H).

(*R*)-N-(4-chlorophenyl)-1-(3-(furan-2-yl)benzoyl)piperidine-3-carboxamide (206116, Lot 380439). Prepared using (*R*)-*N*-(4-chlorophenyl)piperidine-3-carboxamide, TFA salt and 3-(furan-2-yl)benzoic acid according to Procedure C, but using 2.1 eq DIPEA. Crude material was purified using a CombiFlash system (35-50% EtOAc/Hex) to afford 0.006 g

(0.015 mmol, 9% yield) of title compound as an opaque oil. TLC R_f (50% EtOAc/Hex):0.29. ESI(+) m/z $[M+H]^+$ 409.1; [M+23] 431.1. HPLC (gradient A): ret time = 7.50; purity = >90%. ^{1}H NMR (400 MHz, $CDCl_3$): δ 9.23 (s, 1H), 7.79-7.13 (m, 9H), 6.67 (d, *J* = 3.3 Hz, 1H), 6.49 (dd, *J* = 3.2, 1.8 Hz, 1H), 4.06 (s, 1H), 3.61-3.39 (m, 2H), 2.75-2.65 (m, 1H), 2.35-2.20 (m, 1H), 1.89 (s, 2H), 1.67-1.45 (m, 2H).

(*S*)-1-(3,5-bis(trifluoromethyl)benzoyl)piperidine-3-carboxylic acid. Prepared according to Procedure A to afford 0.402 g (1.09 mmol, 70% yield) of title compound as a white solid. ^{1}H NMR (400 MHz, DMSO-d_6): δ 12.44 (s, 1H), 8.17 (s, 1H), 8.09 (s, 2H), 4.50-3.70 (m, 1H), 3.45-3.31 (m, 2H), 3.11-2.90 (m, 1H), 2.58-2.50 (m, 1H), 2.03-1.84 (m, 1H), 1.78-1.43 (m, 3H).

(*S*)-1-(3,5-bis(trifluoromethyl)benzoyl)-*N*-(3-phenoxyphenyl)piperidine-3-carboxamide (206686). (*S*)-1-(3,5-bis(trifluoromethyl)benzoyl)piperidine-3-carboxylic acid (0.074 g, 0.200 mmol) was dissolved in THF (0.667 mL) and was treated with EDC (0.042 g, 0.220 mmol) followed by HOBt (0.034 g, 0.220 mmol), and was then stirred for 10 minutes. 3-phenoxyaniline (0.037 g, 0.200 mmol) was then added and stirring continued overnight at room temperature. The reaction was then diluted with EtOAc (10 mL) and was washed with saturated $NaHCO_3$ (5 mL), followed by a wash with 1N HCl (5 mL) and then brine (5 mL). Organics were dried ($MgSO_4$) and concentrated *in vacuo*. Crude material was purified using a Biotage Flashmaster Personal$^+$ system (25% EtOAc/Hex) to afford 0.021 g (0.039 mmol, 20% yield) of title compound as an off-white solid. TLC R_f (50% EtOAc/Hex): 0.43. ESI(+) *m/z* $[M+H]^+$ 536.9; [M+Na] 558.8. HPLC (gradient A): ret time = 8.36 min; purity = >95%. ^{1}H NMR (400 MHz, DMSO-d_6): 1.1:1.0 mixture of rotamers, δ 10.13 (rotamer 1, s), 9.91 (rotamer 2, s, 1H), 8.26-8.15 (m, 1H), 8.09 (s, 2H), 7.49-7.18 (m, 5H), 7.15 (t, *J* = 6.6 Hz, 1H), 7.08-6.92 (m, 2H), 6.75-6.63(m, 1H), 4.59-4.04 (m, 1H), 3.57-3.34 (m, 1H), 3.20-2.93 (m, 2H), 2.65-2.55 (s, 1H), 2.05-1.94 (m, 1H), 1.85-1.60 (m, 2H), 1.48 (s, 1H).

(*R*)-1-(3,5-bis(trifluoromethyl)benzoyl)piperidine-3-carboxylic acid. Prepared using Procedure A using 1.25 eq of amine to afford 0.310 g (1.14 mmol, 74% yield) of title

compound as a white solid. ^{1}H NMR (400 MHz, DMSO-d_6) δ 12.44 (s, 1H), 8.17 (s, 1H), 8.09 (s, 2H), 4.50-3.70 (m, 1H), 3.49-3.30 (m, 2H), 3.10-2.90 (m, 1H), 2.60-2.50 (m, 1H), 2.03-1.83 (m, 1H), 1.80-1.48 (m, 3H).

(*R*)-1-(3,5-bis(trifluoromethyl)benzoyl)-*N*-(3-phenoxyphenyl)piperidine-3-carboxamide (206687). (*R*)-1-(3,5-bis(trifluoromethyl)benzoyl)piperidine-3-carboxylic acid (0.074 g, 0.200 mmol) was dissolved in THF (0.670 mL) and was treated with EDC (0.042 g, 0.220 mmol) followed by HOBt (0.034 g, 0.220 mmol) and was then stirred for 10 minutes. 3-phenoxyaniline (0.037 g, 0.200 mmol) was then added and stirring continued overnight at room temperature. The reaction was then diluted with EtOAc (10 mL) and was washed with saturated $NaHCO_3$ (5 mL) followed by a wash with 1N HCl (5 mL) and then brine (5 mL). Organics were dried ($MgSO_4$) and concentrated *in vacuo*. Crude material was purified using a Biotage Flashmaster Personal$^+$ system (25% EtOAc/Hex) to afford 0.027 g (0.050 mmol, 25% yield) of title compound as a white solid. TLC R_f (50% EtOAc/Hex): 0.43. ESI(+) *m/z* $[M+H]^+$ 536.9; [M+Na] 558.9. HPLC (gradient A): ret time = 8.35 min; purity = >95%. ^{1}H NMR (400 MHz, DMSO-d_6): 1.1:1.0 mixture of rotamers, δ 10.13 (rotamer 1, s), 9.91 (rotamer 2, s, 1H), 8.27-8.15 (m, 1H), 8.09 (s, 2H), 7.47-7.20 (m, 5H), 7.15 (t, *J* = 7.1 Hz, 1H), 7.09-6.92 (m, 2H), 6.77-6.62 (m, 1H), 4.59-4.05 (m, 1H), 3.59-3.35 (m, 1H), 3.21-2.94 (m, 2H), 2.65-2.55 (m, 1H), 2.06-1.94 (m, 1H), 1.88-1.61 (m, 2H), 1.59-1.38 (m, 1H).

Diethyl 3,5-Pyridinedicarboxylate (56).[108]

3-carboxy-5-(ethyloxycarbonyl)pyridinium chloride (57).[109]

5-*tert*-Butoxycarbonylamino-nicotinic acid ethyl ester (58).[110]

5-*tert*-Butoxycarbonylamino-nicotinic acid (59).[110]

(3R,5S)-5-((tert-butoxycarbonyl)amino)piperidine-3-carboxylic acid (**60**). To a Parr reactor containing rhodium on aluminum oxide (0.065 g, 0.032 mmol), water (20.9 mL),

and ammonia (2.33 mL, 1.08 mmol) was **59** (0.279 g, 1.18 mmol). The mixture was placed on the Parr shaker at room temperature at ~40 psi for ~72 hours. The reaction was then filtered through a plug of celite and rinsed with water. The solvent was then removed *in vacuo* to afford 0.255 g (1.04 mmol, 89% yield) of title compound as a white solid. ^{1}H NMR (400 MHz, D_2O): δ 3.96-3.77 (m, 1H), 3.63-3.45 (m, 1H), 3.42-3.04 (m, 1H), 3.00-2.83 (m, 1H), 2.80-2.65 (m, 1H), 2.40-2.90 (m, 1H), 1.98-1.87 (m, 1H), 1.70-1.35 (m, 10H).

Chapter 4

1-(3,5-bis(trifluoromethyl)benzoyl)-*N*-(3-chloro-4-methoxyphenyl)piperidine-3-carboxamide (101331). Prepared using **48** according to Procedure C. Crude material was triturated using EtOAc to afford 0.201 g (0.413 mmol, 36% yield) of title compound as a light yellow solid. TOF MS-ESI *m/z* $[M+H]^+$ 509.0; [M+Na] 531.0. HPLC (gradient A): ret time = 7.72 min; purity = 99%. ^{1}H NMR (500 MHz, DMSO-d_6) 1.2:1.0 mixture of rotamers, δ 10.08 (rotamer 1, s), 9.85 (rotamer 2, s, 1H), 8.26-8.17 (m, 1H), 8.11 (s, 2H), 7.85-7.67 (m, 1H), 7.51-7.30 (m, 1H), 7.52-7.28 (m, 1H), 7.17-7.04 (m, 1H), 4.58-4.05 (m, 1H), 3.87-3.76 (m, 3H), 3.65-3.38 (m, 2H), 3.29-2.97 (m, 1H), 2.68-2.56 (m, 1H), 2.06-2.00 (m, 1H), 1.93-1.63 (m, 2H), 1.62-1.39 (m, 1H).

5-(3,5-bis(trifluoromethyl)benzamido)pentanoic acid. Prepared according to Procedure A to afford 0.392 g (1.10 mmol, 93% yield) of title compound as a white crystalline solid. TOF MS-ESI *m/z* $[M-H]^-$ 356.1. ^{1}H NMR (500 MHz, DMSO-d_6): δ 12.05 (bs, 1H), 8.97 (s, 1H), 8.50 (s, 2H), 8.31 (s, 1H), 3.40-3.28 (m, 2H), 2.35-2.23 (m, 2H), 1.57 (s, 4H).

***N*-(5-((3-chloro-4-methoxyphenyl)amino)-5-oxopentyl)-3,5-bis(trifluoromethyl)benzamide (101339).** Prepared using 5-(3,5-bis(trifluoromethyl)benzamido)pentanoic acid according to Procedure C. Crude material was triturated using EtOAc to afford 0.179 g (0.360 mmol, 34% yield) of title compound as a solid. TOF MS-ESI *m/z* [M+Na] 518.9. HPLC (gradient A): ret time = 7.62 min; purity = 99%. ^{1}H NMR (500 MHz, DMSO-d_6): δ 9.90 (s, 1H), 8.98 (t, *J* = 5.4 Hz, 1H), 8.50 (s, 2H), 8.32 (s, 1H), 7.78 (d, *J* = 2.5 Hz, 1H), 7.41 (dd, *J* = 8.9 Hz, 2.5 Hz, 1H),

7.08 (d, *J* = 9.0 Hz, 1H), 3.80 (s, 3H), 3.38-3.31 (m, 2H), 2.33 (t, *J* = 7.1 hz, 2H), 1.74-1.53 (m, 4H).

1-(3,5-bis(trifluoromethyl)benzoyl)-*N*-(4-chloro-3-methoxyphenyl)piperidine-3-carboxamide (101341). Prepared using **48** according to Procedure C. Crude material was purified Combiflash (25-60% EtOAc/Hex) to afford 0.207 g (0.407 mmol, 49% yield) of title compound. TLC R_f (50% EtOAc/Hex): 0.23. TOF MS-ESI *m/z* $[M-H]^-$ 375.9. HPLC (gradient A): ret time = 7.93 min; purity = 99%. ^{1}H NMR (500 MHz, DMSO-d_6): 1.1:1.0 mixture of rotamers, δ 10.23 (rotamer 1, s), 10.00 (rotamer 2, s, 1H), 8.28-8.18 (m, 1H), 8.12 (s, 2H), 7.60-7.46 (m, 1H), 7.40-7.00 (m, 2H), 4.60-4.00 (m, 1H), 3.90-3.75 (m, 3H), 3.55-3.00 (m, 3H), 2.72-2.58 (m, 1H), 2.09-2.00 (m, 1H), 1.90-1.64 (m, 2H), 1.62-1.42 (m, 1H).

***N*-(5-((4-chloro-3-methoxyphenyl)amino)-5-oxopentyl)-3,5-bis(trifluoromethyl)benzamide (101337).** Prepared using 5-(3,5-bis(trifluoromethyl)benzamido)pentanoic acid according to Procedure C. Crude material was triturated using EtOAc to afford 0.104 g (0.209 mmol, 20% yield) of title compound as a light brown solid. TOF MS-ESI *m/z* [M+Na] 518.9. HPLC (gradient A): ret time = 7.78 min; purity = 99%. ^{1}H NMR (500 MHz, DMSO-d_6): δ 10.04 (s, 1H), 8.99 (t, *J* = 5.4 Hz, 1H), 8.51 (s, 2H), 8.32 (s, 1H), 7.53 (d, *J* = 2.1 Hz, 1H), 7.31 (d, *J* = 8.6 Hz, 1H), 7.16 (dd, *J* = 8.6 Hz, 2.2 Hz, 1H), 3.81 (s, 3H), 3.39-3.35 (m, 2H), 2.37 (t, *J* = 7.1 Hz, 2H), 1.63 (m, 4H).

***tert*-butyl (2-(2-(2-hydroxyethoxy)ethoxy)ethyl)carbamate.**[121]

1-(3,5-bis(trifluoromethyl)benzoyl)-*N*-(3-chloro-4-hydroxyphenyl)piperidine-3-carboxamide (67). *N*,*N*-Carbonyldiimidazole (CDI) (0.102 g, 0.627 mmol) was dissolved in dry THF (0.780 mL) with stirring at room temperature under nitrogen. Compound **48** (0.231 g, 0.627 mmol) was carefully added and the reaction mixture was stirred for 10 minutes. After CO_2 evolution stopped, 4-amino-2-chlorophenol (0.075 g, 0.522 mmol) was added and stirring was continued for 10 minutes at room temperature

and was then heated to 62 °C. Upon reaching temperature, nitrogen was removed and tube was capped. Heating continued overnight. ^{1}H NMR (500 MHz, MeOD): δ 8.15-8.03 (m, 3H), 7.70-7.46 (m, 1H), 7.31-7.06 (m, 1H), 6.90-6.78 (m, 1H), 4.65-4.15 (m, 1H), 3.68-3.48 (m, 1H), 3.40-3.20 (m, 1H), 2.70-2.48 (m, 1H), 2.11-2.04 (m, 1H), 1.98-1.47 (m, 3H).

2,2-dimethyl-4-oxo-3,8,11-trioxa-5-azatridecan-13-yl methanesulfonate (68).[121, 150]

2-chlorophenoxy)ethoxy)ethoxy)ethyl)carbamate (69).[120] Compound **68** (0.019 g, 0.058 mmol) was dissolved in DMF (1.05 mL) and to the stirring solution were added **67** (0.026 g, 0.053 mmol) and cesium carbonate (0.094 g, 0.289 mmol). The purple mixture was heated at 75 °C for 8 hours. Cesium carbonate was filtered off and rinsed with dichloromethane. Filtrate was concentrated *in vacuo* to afford 0.033 g (0.045 mmol, 85% yield) of title compound. Compound was used without further purification.

***N*-(5-((3-chloro-4-hydroxyphenyl)amino)-5-oxopentyl)-3,5-bis(trifluoromethyl)benzamide.**[145] To a stirring solution 5-(3,5-bis(trifluoromethyl)benzamido)pentanoic acid (0.357 g, 1.00 mmol) and 4-amino-2-chlorophenol (0.172 g, 1.20 mmol) in DMF (2.00 mL) was added EDC (0.230 g, 1.200 mmol). The mixture was allowed to stir overnight at room temperature. After stirring, DMF was removed *in vacuo*, and ten milliliters of water were added. The water layer was then extracted with EtOAc (3 x 30 mL). Combined organics were washed with brine (30 mL), dried ($MgSO_4$), and concentrated to afford 0.566 g of an oil. The oil was triturated with dichloromethane, and the solid was filtered and dried *in vacuo* to afford 0.263 g (0.545 mmol, 55% yield) of title compound as an off-white solid. ^{1}H NMR (500 MHz, MeOD): δ 8.44 (s, 2H), 8.15 (s, 1H), 7.61-7.59 (m, 1H), 7.24-7.21 (m, 1H), 6.86-6.82 (m, 1H), 3.49-3.43 (m, 2H), 3.49-3.43 (m, 2H), 2.44-2.38 (m, 2H), 1.82-1.67 (m, 4H).

***tert*-Butyl (2-(2-(2-(4-(5-(3,5-bis(trifluoromethyl)benzamido)pentanamido)-2-chlorophenoxy)ethoxy)ethoxy)ethyl)carbamate.** Compound **68** (0.012 g, 0.036 mmol)

and cesium carbonate (0.059 g, 0.182 mmol) were added to *N*-(5-((3-chloro-4-hydroxyphenyl)amino)-5-oxopentyl)-3,5-bis(trifluoromethyl)benzamide (0.016 g, 0.033 mmol) in DMF (0.663 mL). The mixture was heated at 75 °C overnight. The cesium carbonate was filtered off and the DMF was removed *in vacuo* to afford 0.035 g (0.049 mmol, 151% yield) of title compound. Compound was used without further purification. . ^{1}H NMR (500 MHz, MeOD) δ 8.44 (s, 2H), 8.14 (s, 1H), 7.98 (s, 1H), 7.69 (d, *J* = 2.6 Hz, 1H), 7.37 (dd, *J* = 8.8, 2.6 Hz, 1H), 7.02 (d, *J* = 8.9 Hz, 1H), 4.19-4.14 (m, 2H), 3.89-3.84 (m, 2H), 3.76-3.71 (m, 2H), 3.65-3.61 (m, 2H), 3.54-3.50 (m, 2H), 3.49-3.44 (m, 2H), 3.24-3.19 (m, 2H), 2.45-2.39 (m, 2H), 1.83-1.66 (m, 4H), 1.41 (s, 9H).

***N*-(5-((4-(2-(2-(2-aminoethoxy)ethoxy)ethoxy)-3-chlorophenyl)amino)-5-oxopentyl)-3,5-bis(trifluoromethyl)benzamide (203882).** A solution of DCM (0.327 mL) and TFA (0.163 mL) (2:1) was added to a vial containing *tert*-butyl (2-(2-(2-(4-(5-(3,5-bis(trifluoromethyl)benzamido)pentanamido)-2-chlorophenoxy)ethoxy)ethoxy)ethyl)carbamate (0.035 g, 0.049 mmol). The mixture was stirred for 1 hour and 45 minutes at room temperature and was concentrated *in vacuo*. Crude material was purified using a CombiFlash system (5-10% Methanolic ammonia/DCM) to afford 0.016 g (0.026 mmol, 69% yield) of title compound as a white solid. TLC R_f (10% Methanolic ammonia/DCM): 0.20. ^{1}H NMR (500 MHz, MeOD) δ 8.44 (s, 2H), 8.14 (s, 2H), 7.75-7.65 (m, 1H), 7.45-7.29 (m, 1H), 7.09-6.95 (m, 1H), 4.23-4.07 (m, 2H), 3.96-3.85 (m, 2H), 3.82-3.62 (m, 8H), 3.50-3.42 (m, 2H), 3.17-3.03 (m, 2H), 2.47-2.37 (m, 2H), 1.84-1.63 (m, 4H).

***N*-(4-(2-(2-(2-aminoethoxy)ethoxy)ethoxy)-3-chlorophenyl)-1-(3,5-bis(trifluoromethyl)benzoyl)piperidine-3-carboxamide (203883).** A solution of DCM (0.716 ml) and TFA (0.358 ml) were added to a vial containing **69** (0.078 g, 0.107 mmol). The mixture was stirred for 1.5 h at room temperature and was then concentrated. Crude material was purified using a CombiFlash system (5% Methanolic ammonia/DCM) to afford 0.034 g (0.046 mmol, 43% yield) of title compound as a yellow gummy solid. TLC R_f (10% Methanolic ammonia/DCM): 0.43. ^{1}H NMR (500 MHz, DMSO-d_6): 1.1:1.0 mixture of rotamers, δ 10.09 (rotamer 1, s), 9.86 (rotamer 2, s,

1H), 8.27-8.16 (m, 1H), 8.11 (s, 2H), 7.84-7.68 (m, 1H), 7.49-7.26 (m, 1H), 7.17-7.04 (m, 1H), 4.51 (d, *J* = 13.2 Hz, 1H), 4.12 (d, *J* = 15.6 Hz, 2H), 3.80-3.71 (m, 2H), 3.65-3.57 (m, 2H), 3.54-3.40 (m, 4H), 3.37 (s, 2H), 3.23-2.97 (m, 2H), 2.64 (s, 2H), 2.06-1.99 (m, 1H), 1.85-1.64 (m, 2H), 1.60-1.41 (m, 1H).

1-(3,5-bis(trifluoromethyl)benzoyl)-*N*-(3-chloro-4-(2-(2-(2-(5-(2-oxohexahydro-1*H*-thieno[3,4-*d*]imidazol-4-yl)pentanamido)ethoxy)ethoxy)ethoxy)phenyl)piperidine-3-carboxamide (203602). Compound **203883** (0.018 g, 0.024 mmol) was dissolved in anhydrous DMF (0.600 mL), and the clear solution was stirred for 10 minutes at room temperature. Biotin-OSu (0.010 g, 0.029 mmol) was added, and the reaction solution continued stirring overnight at room temperature. The reaction was concentrated *in vacuo* and crude material was purified using a CombiFlash system (5-10% MeOH/DCM) to afford 0.020 g (0.023 mmol, 96% yield) of title compound as a white solid. TLC R_f (10% Methanolic ammonia/DCM): 0.31. TOF MS-ESI *m/z* $[M+H]^+$ 851.9; [M+Na] 873.9. NMR was difficult to decipher due to rotamers, therefore heat experiment was conducted, increasing temperature to 30, 40, and then 50 °C. Rotamers coalesced to show desired product. 1H NMR (500 MHz, DMSO-d_6, 50 °C): δ 9.80 (s, 1H), 8.15 (s, 1H), 8.07 (s, 2H), 7.73 (s, 1H), 7.61 (s, 1H), 7.38 (s, 1H), 7.10 (d, *J* = 8.9 Hz, 1H), 6.21 (d, *J* = 11.1 Hz, 2H), 4.34-4.27 (m, 1H), 4.18-4.09 (m, 3H), 3.80-3.73 (m, 2H), 3.66-3.60 (m, 2H), 3.58-3.52 (m, 2H), 3.47-3.40 (m, 3H), 3.35-3.05 (under water peak, 2H), 2.84 (dd, *J* = 12.4, 5.2 Hz, 2H), 2.12-2.05 (m, 4H), 1.85-1.72 (m, 3H), 1.69-1.59 (m, 2H), 1.58-1.43 (m, 4H), 1.39-1.29 (m, 3H).

***tert*-butyl (2-(2-(2-(4-(5-(3,5-bis(trifluoromethyl)benzamido)pentanamido)-2-chlorophenoxy)ethoxy)ethoxy)ethyl)carbamate.**[120] Cesium carbonate (0.186 g, 0.570 mmol) and *N*-(5-((3-chloro-4-hydroxyphenyl)amino)-5-oxopentyl)-3,5-bis(trifluoromethyl)benzamide (0.050 g, 0.104 mmol) were added to a solution of **68** (0.037 g, 0.114 mmol) in DMF (2.08 ml). The mixture was stirred for 18 h at room temperature under nitrogen. After stirring overnight, the reaction was checked by TLC, which indicated the reaction had not completed. Therefore it was heated at 75 °C for 3 hours and re-checked by TLC, which indicated the reaction was complete. The cesium

carbonate was filtered off and resulting filtrate was concentrated *in vacuo* to afford 0.070 g (0.098 mmol, 95% yield) of title compound. Compound was used without further purification. ^{1}H NMR (500 MHz, MeOD) δ 8.44 (s, 2H), 8.14 (s, 1H), 7.98 (s, 1H), 7.69 (d, *J* = 2.6 Hz, 1H), 7.37 (dd, *J* = 8.8, 2.6 Hz, 1H), 7.02 (d, *J* = 8.9 Hz, 1H), 4.19-4.14 (m, 2H), 3.89-3.84 (m, 2H), 3.76-3.71 (m, 2H), 3.65-3.61 (m, 2H), 3.54-3.50 (m, 2H), 3.49-3.44 (m, 2H), 3.24-3.19 (m, 2H), 2.45-2.39 (m, 2H), 1.83-1.66 (m, 4H), 1.41 (s, 9H).

***N*-(5-((4-(2-(2-(2-aminoethoxy)ethoxy)ethoxy)-3-chlorophenyl)amino)-5-oxopentyl)-3,5-bis(trifluoromethyl)benzamide.** A solution of dichloromethane (0.327 ml) and TFA (0.163 mL) was added to a vial containing *tert*-butyl (2-(2-(2-(4-(5-(3,5-bis(trifluoromethyl)benzamido)pentanamido)-2-chlorophenoxy)ethoxy)ethoxy)ethyl)carbamate (0.035 g, 0.049 mmol). The mixture was stirred for 1 hour and 45 minutes at room temperature. The reaction was concentrated and dried using high vacuum to yield 0.035 g (0.048 mmol, 98% yield) of title compound as a yellow oil. Compound was used without further purification. ^{1}H NMR (500 MHz, MeOD) δ 8.44 (s, 2H), 8.14 (s, 2H), 7.75-7.65 (m, 1H), 7.45-7.29 (m, 1H), 7.09-6.95 (m, 1H), 4.23-4.07 (m, 2H), 3.96-3.85 (m, 2H), 3.82-3.62 (m, 8H), 3.50-3.42 (m, 2H), 3.17-3.03 (m, 2H), 2.47-2.37 (m, 2H), 1.84-1.63 (m, 4H).

***N*-(5-((3-chloro-4-(2-(2-(2-(5-(2-oxohexahydro-1*H*-thieno[3,4-*d*]imidazol-4-yl)pentanamido)ethoxy)ethoxy)ethoxy)phenyl)amino)-5-oxopentyl)-3,5-bis(trifluoromethyl)benzamide (203600).** *N*-(5-((4-(2-(2-(2-aminoethoxy)ethoxy)ethoxy)-3-chlorophenyl)amino)-5-oxopentyl)-3,5-bis(trifluoromethyl)benzamide (0.037 g, 0.051 mmol) was dissolved in anhydrous DMF (1.3 mL) and DIPEA (0.009 mL, 0.051 mmol) was added to the stirring solution. The solution continued for 10 minutes and Biotin-OSu (0.017 g, 0.051 mmol) was added. The mixture continued stirring overnight at room temperature under nitrogen. The solution was concentrated *in vacuo*. Crude material was purified by column chromatography (10-15% MeOH/DCM) followed by trituration with $CHCl_3$ to afford 0.017 g (0.020 mmol, 39% yield) of title compound as an off-white solid. TLC R_f (10% MeOH/DCM): 0.32. TOF MS-ESI *m/z* $[M+H]^+$ 839.9; [M+Na] 861.9. ^{1}H NMR (500

MHz, DMSO-d_6): δ 9.91 (s, 1H), 8.98 (t, *J* = 5.4 Hz, 1H), 8.50 (s, 2H), 8.31 (s, 1H), 7.83 (t, *J* = 5.6 Hz, 1H), 7.80-7.77 (m, 1H), 7.41-7.36 (m, 1H), 7.11-7.08 (m, 1H), 6.42 (s, 1H), 6.36 (s, 1H), 4.32-4.27 (m, 1H), 4.14-4.08 (m, 3H), 3.77-3.73 (m, 2H), 3.63-3.59 (m, 2H), 3.55-3.50 (m, 2H), 3.42-3.38 (m, 2H), 3.18 (q, *J* = 6.0 Hz, 2H), 3.11-3.05 (m, 1H), 2.84-2.77 (m, 1H), 2.59-2.53 (m, 1H), 2.36-2.29 (m, 2H), 2.08-2.02 (m, 2H), 1.70-1.19 (m, 12H). HPLC (gradient A): ret time = 6.55 min; purity = 99%.

***tert*-butyl 3-((4-chloro-3-methoxyphenyl)carbamoyl)piperidine-1-carboxylate.** Prepared using **43** according to Procedure D, but using 1.5 eq of aniline. Crude material was purified using a CombiFlash system (35% EtOAc/Hex) to afford 0.139 g (0.377 mmol, 86% yield) of title compound as a clear oil. TLC R_f (50% EtOAc/Hex): 0.48. ^{1}H NMR (500 MHz, $CDCl_3$): δ 8.61 (bs, 1H), 7.62 (d, *J* = 2.4 Hz, 1H), 7.28-7.23 (m, 1H), 6.93 (s, 1H), 3.89 (s, 3H), 3.83-3.18 (m, 1H), 2.52 (s, 1H), 2.12 (s, 1H), 1.90 (s, 1H), 1.63 (s, 1H), 1.47 (s, 10H).

***N*-(4-chloro-3-methoxyphenyl)piperidine-3-carboxamide.** *tert*-butyl 3-((4-chloro-3-methoxyphenyl)carbamoyl)piperidine-1-carboxylate (134 mg, 0.363 mmol) was dissolved in DCM (2.40 mL) and placed in an ice bath at approximately -5 °C. TFA (1.20 mL) was slowly added and the solution continued to stir at -5 °C for 1 hour. The solution was poured into 20 mL of cooled 2M NaOH. The mixture was extracted with DCM (3 x 20 mL), and the combined organic layers were dried ($MgSO_4$) and concentrated *in vacuo* to afford 0.073 g (0.272 mmol, 75% yield) of title compound as a yellow solid. No further purification was performed. ^{1}H NMR (500 MHz, $CDCl_3$): δ 10.75 (s, 1H), 7.67 (d, *J* = 2.4 Hz, 1H), 7.28-7.23 (m, 1H), 6.94-6.82 (m, 1H), 3.92 (s, 3H), 3.36-3.22 (m, 1H), 3.13-3.05 (m, 1H), 2.95 (dd, *J* = 12.0, 3.2 Hz, 1H), 2.81-2.72 (m, 1H), 2.59-2.53 (m, 1H), 2.20-1.99 (m, 2H), 1.85-1.71 (m, 2H), 1.65-1.52 (m, 1H).

***N*-(3-chloro-4-methoxyphenyl)piperidine-3-carboxamide (206117).** Prepared using *N*-(4-chloro-3-methoxyphenyl)piperidine-3-carboxamide according to Procedure D, but using 1.1 eq of EDC and DMAP. Crude material was triturated with DCM to afford 0.011 g (0.023 mmol, 17% yield) of title compound as a white solid. ESI(+) m/z $[M+H]^+$

477.2; [M+23] 499.1. HPLC (gradient A): ret time = 7.36; purity = >95%. ^{1}H NMR (400 MHz, DMSO-d_6): 1.3:1.0 mixture of rotamers, δ 10.21 (rotamer 1, s), 10.01 (rotamer 2, s, 1H), 7.91-7.00 (m, 12H), 4.62-4.13 (m, 1H), 3.89-3.72 (m, 3H), 3.72-3.53 (m, 1H), 3.20-2.91 (m, 2H), 2.66-2.55 (m, 1H), 2.01 (s, 1H), 1.92-1.64 (m, 2H), 1.59-1.32 (m, 1H).

***tert*-butyl 3-((3-chloro-4-methoxyphenyl)carbamoyl)piperidine-1-carboxylate.** Prepared using **43** according to Procedure D, but using 1.5 eq of aniline. Crude material was purified using a CombiFlash system (35% EtOAc/Hex) to afford 0.139 g (0.377 mmol, 86% yield) of title compound as a clear oil. TLC R_f (50% EtOAc/Hex): 0.48. ^{1}H NMR (500 MHz, $CDCl_3$): δ 8.41 (s, 1H), 7.67 (s, 1H), 7.44 (dd, *J* = 8.8, 2.6 Hz, 1H), 6.85 (d, *J* = 8.8 Hz, 1H), 3.90-3.10 (m, 7H), 2.49 (s, 1H), 2.11 (s, 1H), 1.89 (s, 1H), 1.63 (s, 1H), 1.54-1.43 (m, 10H).

***N*-(3-chloro-4-methoxyphenyl)piperidine-3-carboxamide.** *tert*-butyl 3-((3-chloro-4-methoxyphenyl)carbamoyl)piperidine-1-carboxylate (134 mg, 0.363 mmol) was dissolved in DCM (2.40 mL) and placed in an ice bath at approximately -5 °C. TFA (1.20 mL) was slowly added and the solution continued to stir at -5 °C for 1 hour. The solution was poured into 20 mL of cooled 2M NaOH. The mixture was extracted with DCM (3 x 20 mL), and the combined organic layers were dried ($MgSO_4$) and concentrated *in vacuo* to afford 0.063 g (0.234 mmol, 64% yield) of title compound as a light brown solid. No further purification was performed. ^{1}H NMR (500 MHz, $CDCl_3$): δ 10.60 (s, 1H), 7.60 (d, *J* = 2.5 Hz, 1H), 7.50-7.48 (m, 1H), 6.87 (d, *J* = 8.8 Hz, 1H), 3.88 (s, 3H), 3.29-3.23 (m, 1H), 3.11-3.05 (m, 1H), 2.92 (dd, *J* = 11.9, 3.3 Hz, 1H), 2.73 (td, *J* = 10.9, 3.1 Hz, 1H), 2.53 (p, *J* = 3.6 Hz, 1H), 2.12-2.01 (m, 1H), 1.87 (s, 1H), 1.82-1.69 (m, 2H), 1.63-1.50 (m, 1H).

1-(3-benzoylbenzoyl)-*N*-(3-chloro-4-methoxyphenyl)piperidine-3-carboxamide (206118). Prepared using *N*-(3-chloro-4-methoxyphenyl)piperidine-3-carboxamide according to Procedure D, but using 1.1 eq of EDC and DMAP. Crude material was using a CombiFlash system (65% EtOAc/Hex) to afford 0.040 g (0.084 mmol, 73% yield) of title compound as a yellow solid. ESI(+) m/z $[M+H]^+$ 477.2; [M+23] 499.2. HPLC

(gradient A): ret time = 7.17; purity = >95%. ^{1}H NMR (400 MHz, DMSO-d_6): 1.3:1.0 mixture of rotamers, δ 10.06 (rotamer 1, s), 9.87 (rotamer 2, s, 1H), 7.90-7.29 (m, 11H), 7.16-7.00 (m, 1H), 4.60-4.15 (m, 1H), 3.81 (s, 3H), 3.70-3.50 (m, 1H), 3.21-2.90 (m, 2H), 1.99 (bs, 1H), 1.90-1.65 (m, 2H), 1.58-1.30 (m, 1H).

***tert*-butyl (4-chloro-3-hydroxyphenyl)carbamate (81).**[126]

***tert*-butyl (4-chloro-3-(prop-2-yn-1-yloxy)phenyl)carbamate (82).** To a mixture of **81** (0.144 g, 0.591 mmol) and potassium carbonate (0.245 g, 1.773 mmol) in dioxane (1.45 mL) was added 3-bromoprop-1-yne (0.111 ml, 1.477 mmol). The reaction mixture was then heated to 80 °C for 48 h in a sealed tube. The reaction mixture was concentrated and was diluted with water (10 mL). The aqueous layer was extracted with dichloromethane (3 x 10 mL). The organics were washed with water (2 x 10 mL), dried ($MgSO_4$) and concentrated. Crude material was purified using a 12 g SiliaSep cartridge and was separated using a Biotage unit. Eight milliliter fractions were collected at 20 mL/min using a threshold of 20 mAU for collection. Gradient employed 100% Hexanes for 3 CVs; ramping 0-20% over 15 CVs; and holding at 20% for 5 CVs. Fractions 4-8 (R_f: 0.35 in 20% Ethyl acetate in Hexanes) were combined and concentrated to yield 0.108 g of title compound as a white solid. ^{1}H NMR (400 MHz, DMSO-d_6): δ 9.51 (s, 1H), 7.44 (d, J = 1.9 Hz, 1H), 7.29 (d, J = 8.7 Hz, 1H), 7.06 (dd, J = 8.7, 1.9 Hz, 1H), 4.81 (d, J = 2.3 Hz, 2H), 3.63 (t, J = 2.3 Hz, 1H), 1.47 (s, 9H).

4-chloro-3-(prop-2-yn-1-yloxy)aniline (83). Compound **82** (0.105 g, 0.373 mmol) was dissolved in dichloromethane (2.50 mL) and cooled to -10 °C. TFA (1.25 mL) was added slowly to the cooled solution. The solution was stirred at -5 °C for 45 minutes and was then poured into 10 mL of cooled 2M NaOH. The cooled basic solution was extracted with dichloromethane (3 x 10 mL), and the combined organics were dried ($MgSO_4$) and concentrated to afford 0.064 g (0.352 mmol) of title compound as a yellow solid. No further purification was performed. ^{1}H NMR (400 MHz, DMSO-d_6): δ 6.99 (d, J = 8.5 Hz, 1H), 6.38 (d, J = 2.1 Hz, 1H), 6.17 (dd, J = 8.5, 2.2 Hz, 1H), 5.29 (s, 2H), 4.75 (d, J = 2.0 Hz, 2H), 3.61 (s, 1H).

***tert*-butyl 3-((4-chloro-3-(prop-2-yn-1-yloxy)phenyl)carbamoyl)piperidine-1-carboxylate (84).** Compound **83** (0.061 g, 0.336 mmol) was dissolved in dichloromethane (3.36 mL), and to the stirring solution was added EDC (0.097 g, 0.504 mmol) followed by DMAP (0.062 g, 0.504 mmol) and **43** (0.085 g, 0.369 mmol). The mixture was stirred at room temperature under nitrogen overnight. Additional dichloromethane (6.7 mL) was added to the solution, and it was washed with saturated aqueous $NaHCO_3$ (10 mL), 1M HCl (10 mL), and then brine (10 mL) and was dried ($MgSO_4$) and concentrated to afford 0.109 g (0.277 mmol, 83% yield) of title compound as a white solid. No further purification was performed. ^{1}H NMR (400 MHz, DMSO-d_6): δ 10.16 (s, 2H), 7.60 (d, *J* = 1.7 Hz, 3H), 7.34 (d, *J* = 8.6 Hz, 2H), 7.23 (dd, *J* = 8.7, 1.8 Hz, 3H), 4.84 (d, *J* = 1.7 Hz, 6H), 4.15-3.80 (m, 2H), 3.66-3.63 (m, 1H), 3.10-2.70 (m, 2H), 2.44 (tt, *J* = 10.8, 3.8 Hz, 1H), 1.97-1.87 (m, 1H), 1.77-1.53 (m, 2H), 1.43-1.30 (m, 10H).

***N*-(4-chloro-3-(prop-2-yn-1-yloxy)phenyl)piperidine-3-carboxamide (85).** Compound **84** (0.107 g, 0.272 mmol) was dissolved in dichloromethane (1.82 mL) and cooled to -5 °C. TFA (0.910 mL) was added slowly to the cooled solution. Solution was stirred at -5 °C. After 1 hour, the solution was poured into 5 mL of cooled 2M NaOH. The cooled basic solution was extracted with dichloromethane (3 x 5 mL), and the organic layers were combined, dried ($MgSO_4$), and concentrated to afford 0.050 g (0.171 mmol, 63% yield) of title compound as a white solid. No further purification was performed. ^{1}H NMR (400 MHz, DMSO-d_6): δ 10.11 (s, 1H), 7.65-7.57 (m, 1H), 7.33 (d, *J* = 8.6 Hz, 1H), 7.22 (dd, *J* = 8.6, 1.7 Hz, 1H), 4.83 (d, *J* = 1.8 Hz, 2H), 3.64 (s, 1H), 3.06-2.99 (m, 1H), 2.90-2.83 (m, 1H), 2.66-2.57 (m, 6H), 2.48-2.38 (m, 2H), 1.92-1.83 (m, 1H), 1.68-1.50 (m, 2H), 1.45-1.33 (m, 1H).

1-(3-benzoylbenzoyl)-*N*-(4-chloro-3-(prop-2-yn-1-yloxy)phenyl)piperidine-3-carboxamide (206454). Prepared using **43** and **85** according to Procedure D. Crude material was purified using a Biotage FlashMaster Personal$^+$ system (30-100% EtOAc/Hex) to afford 0.049 g (0.098 mmol, 58% yield) of title compound as a white

solid. TLC R_f (50% EtOAc/Hex): 0.18. Agilent ESI(+) *m/z* $[M+H]^+$ 501.0; [M+Na] 523.0. HPLC (gradient A): ret time = 7.40 min; purity = >95%. ^{1}H NMR (400 MHz, DMSO-d_6): 1.4:1.0 mixture of rotamers, δ 10.22 (rotamer 1, s), 10.02 (rotamer 2, s, 1H), 7.98-7.44 (m, 10H), 7.40-7.03 (m, 2H), 4.87-4.75 (m, 1H), 4.58-4.14 (m, 1H), 3.76-3.49 (m, 2H), 3.17-2.83 (m, 2H), 1.98 (s, 1H), 1.89-1.60 (m, 2H), 1.57-1.31 (m, 1H).

1-(3-benzoylbenzoyl)-*N*-(4-chloro-3-(2-(prop-2-yn-1-yloxy)ethoxy)phenyl)piperidine-3-carboxamide (206558). Agilent ESI(+) *m/z* $[M+H]^+$ 545.0; [M+Na] 567.0. HPLC (gradient A): ret time = 7.46 min; purity = >95%. ^{1}H NMR (400 MHz, DMSO-d_6): 1.4:1.0 mixture of rotamers, δ 10.16 (rotamer 1, s), 9.97 (rotamer 2, s, 1H), 7.92-7.02 (m, 12H), 4.52 (d, *J* = 9.5 Hz, 1H), 4.32-4.20 (m, 2H), 4.13 (bs, 2H), 3.81 (s, 3H), 3.73-3.53 (m, 1H), 3.48-3.44 (m, 1H), 3.21-2.88 (m, 2H), 2.65-2.55 (m, 1H), 2.09 (s, 1H), 1.90-1.65 (m, 2H), 1.60-1.32 (m, 1H).

***N*-(3-benzoylphenyl)-1-(3-methoxy-5-(trifluoromethyl)benzoyl)piperidine-3-carboxamide (206448).** Waters ESI(+) *m/z* $[M+H]^+$ 511.3; [M+Na] 533.3. HPLC (gradient A): ret time = 7.71 min; purity = >95%. ^{1}H NMR (400 MHz, DMSO-d_6): 1.3:1.0 mixture of rotamers, δ 10.31 (rotamer 1, s), 10.10 (rotamer 2, s, 1H), 8.10-7.18 (m, 12H), 4.58-4.10 (m, 1H), 3.93-3.75 (m, 3H), 3.63-3.40 (m, 1H), 3.17-2.93 (m, 2H), 2.70-2.55 (m, 1H), 2.08-1.97 (m, 1H), 1.90-1.65 (m, 2H), 1.57-1.35 (m, 1H).

***N*-(3-benzoylphenyl)-1-(3-(prop-2-yn-1-yloxy)-5-(trifluoromethyl)benzoyl)piperidine-3-carboxamide (206559).** Agilent ESI(+) *m/z* $[M+H]^+$ 535.1; [M+Na] 557.0. HPLC (gradient A): ret time = 7.74 min; purity = 95%. ^{1}H NMR (400 MHz, DMSO-d_6): 1.6:1.0 mixture of rotamers, δ 10.28 (rotamer 1, s), 10.06 (rotamer 2, s, 1H), 8.11-7.22 (m, 12H), 5.00-4.85 (m, 1H), 4.55-4.08 (m,1H), 3.71-3.34 (m, 2H), 3.17-2.88 (m, 2H), 2.62-2.51 (m, 1H), 2.02-1.97 (m, 1H), 1.87-1.60 (m, 2H), 1.43 (s, 1H).

***N*-(3-azido-4-chlorophenyl)-1-(3-methoxy-5-(trifluoromethyl)benzoyl)piperidine-3-carboxamide (206449).** Agilent ESI(+) *m/z* $[M+H]^+$ 482.0; [M+Na] 504.0. HPLC (gradient A): ret time = 8.01 min; purity = >95%. ^{1}H NMR (400 MHz, DMSO-d_6): 1.3:1.0 mixture of rotamers, δ 10.35 (rotamer 1, s), 10.13 (rotamer 2, s, 1H), 8.00-7.66 (m, 1H), 7.50-7.12 (m, 5H), 4.58-4.00 (m, 1H), 3.90-3.77 (m, 3H), 3.63-3.69 (m, 1H), 3.09 (d, *J* = 37.6 Hz, 2H), 2.70-2.55 (m, 1H), 2.07-1.96 (m, 1H), 1.91-1.65 (m, 2H), 1.60-1.37 (m, 1H).

Methyl 3-hydroxy-5-(trifluoromethyl)benzoate (96). 3-hydroxy-5-(trifluoromethyl)benzoic acid (**95**) (0.220 g, 1.067 mmol) was dissolved in methanol (1.60 mL) and was cooled to 0 °C. Thionyl chloride (0.117 ml, 1.601 mmol) was added slowly. Following addition, the bath was allowed to warm to room temperature. The reaction continued stirring at room temperature overnight. The reaction was concentrated *in vacuo* and was dissolved in ethyl acetate (5 mL). The organic layer was then washed with saturated $NaHCO_3$ (5 mL), followed by brine (5 mL). The organic layer was then dried ($MgSO_4$), filtered, and concentrated to afford 0.193 g (0.877 mmol, 82% yield) of title compound as an off-white solid. No further purification was performed. ^{1}H NMR (400 MHz, DMSO-d_6): δ 10.61 (s, 1H), 7.61-7.54 (m, 2H), 7.28 (t, *J* = 2.0 Hz, 1H), 3.84 (s, 3H).

Methyl 3-(prop-2-yn-1-yloxy)-5-(trifluoromethyl)benzoate (97). To a mixture of **96** (0.181 g, 0.822 mmol) in dioxane (2.05 mL) was added 3-bromoprop-1-yne (0.155 ml, 2.06 mmol). The reaction mixture was then heated to 80 °C in a sealed tube. After stirring overnight, the reaction mixture was concentrated and was diluted with water (10 mL). The aqueous layer was extracted with DCM (3 x 10 mL). The combined organics were washed with water (10 mL), dried ($MgSO_4$), and concentrated *in vacuo* to afford 0.154 g (0.596 mmol, 73% yield) of title compound as a yellow oil. No further purification was performed. ^{1}H NMR (400 MHz, DMSO-d_6): δ 7.85-7.76 (m, 2H), 7.63 (t, *J* = 2.0 Hz, 1H), 5.03 (d, *J* = 2.3 Hz, 2H), 3.90 (s, 3H), 3.67 (t, *J* = 2.3 Hz, 1H).

3-(prop-2-yn-1-yloxy)-5-(trifluoromethyl)benzoic acid (98). A solution of sodium hydroxide (0.061 g, 1.521 mmol), Methanol (1.20 mL), and Water (0.400 mL) was added to a vial containing **97** (0.151 g, 0.585 mmol). The reaction was stirred for 3 hours and was then concentrated *in vacuo*. Residue was acidified using 2N HCl (5 mL). The aqueous layer was extracted with DCM (3 x 5 mL). The combined organics were dried ($MgSO_4$) and concentrated to afford 0.107 g (0.438 mmol, 75% yield) of title compound as a white solid. No further purification was performed. ^{1}H NMR (400 MHz, DMSO-d_6): δ 13.59 (s, 1H), 7.83-7.75 (m, 2H), 7.59 (t, *J* = 2.0 Hz, 1H), 5.01 (d, *J* = 2.3 Hz, 3H), 3.66 (t, *J* = 2.3 Hz, 1H).

***N*-(4-chloro-3-nitrophenyl)acetamide (107).**[151]

***N*-(3-amino-4-chlorophenyl)acetamide (108).**[151]

***N*-(3-azido-4-chlorophenyl)acetamide (109).**[151]

3-azido-4-chloroaniline (110).[151]

***tert*-butyl 3-((3-azido-4-chlorophenyl)carbamoyl)piperidine-1-carboxylate.** Compound **110** (0.075 g, 0.445 mmol) was dissolved in dichloromethane (4.45 mL), and to the stirring solution was added EDC (0.128 g, 0.667 mmol) followed by DMAP (0.082 g, 0.667 mmol) and **43** (0.112 g, 0.489 mmol). The mixture was stirred at room temperature under nitrogen overnight. Additional dichloromethane (5.55 mL) was added to the solution, and it was washed with saturated aqueous $NaHCO_3$ (10 mL), 1M HCl (10 mL), and then brine (10 mL). Organics were dried ($MgSO_4$) and concentrated to afford 0.149 g (0.392 mmol, 88% yield) of title compound as a fluffy yellow solid. No further purification was performed**.** ^{1}H NMR (400 MHz, DMS)-d_6): δ 10.28 (s, 1H), 7.86 (d, *J* = 2.0 Hz, 1H), 7.42 (d, *J* = 8.7 Hz, 1H), 7.33 (dd, *J* = 8.8, 2.1 Hz, 1H), 4.15-3.77 (m, 2H), 3.12-2.73 (m, 2H), 2.44 (tt, *J* = 10.5, 3.6 Hz, 1H), 1.97-1.88 (m, 1H), 1.77-1.54 (m, 2H), 1.39 (s, 10H).

***N*-(3-azido-4-chlorophenyl)piperidine-3-carboxamide (112).** Compound **111** (0.148 g, 0.390 mmol) was dissolved in dichloromethane (2.60 mL) and cooled to -5 °C. TFA (1.30 mL) was added slowly to the cooled solution. Solution was stirred at -5 °C for 1 hour and was then poured into 10 mL of cooled 2M NaOH. The cooled basic solution was extracted with dichloromethane (3 x 10 mL), and the organic layers were combined, dried ($MgSO_4$), and concentrated *in vacuo* to afford 0.094 g (0.336 mmol, 86% yield) of title compound as an orange solid. No further purification was performed. ^{1}H NMR (400 MHz, DMSO-d_6): δ 10.21 (s, 1H), 7.87 (d, *J* = 1.4 Hz, 1H), 7.40 (d, *J* = 8.7 Hz, 1H), 7.33 (dd, *J* = 8.8, 2.0 Hz, 1H), 3.06-2.98 (m, 1H), 2.89-2.81 (m, 1H), 2.65-2.54 (m, 1H), 2.50-2.35 (m, 2H), 1.93-1.83 (m, 1H), 1.66-1.49 (m, 2H), 1.45-1.30 (m, 1H).

***N*-(3-azido-4-chlorophenyl)-1-(3-(prop-2-yn-1-yloxy)-5-(trifluoromethyl)benzoyl)piperidine-3-carboxamide (206569).** Prepared using **112** and **98** according to Procedure D. Crude material was purified using a Biotage FlashMaster Personal$^+$ (40% EtOAc/Hex) to afford 0.055 g (0.109 mmol, 42% yield) of title compound as a pale yellow solid HPLC (gradient A): ret time = 8.01 min; purity = >95%. ESI(+) *m/z* [M+Na] 527.9. ^{1}H NMR (400 MHz, DMSO-d_6): 1.5:1.0 mixture of rotamers, δ 10.36 (rotamer 1, s), 10.14 (rotamer 2, s, 1H), 7.90-7.72 (m, 1H), 7.51-7.12 (m, 5H), 5.06-4.88 (m, 2H), 4.63-4.06 (m, 1H), 3.73-3.35 (m, 2H), 3.20-2.92 (m, 2H), 2.65-2.52 (m, 1H), 2.09-1.99 (m, 1H), 1.90-1.64 (m, 2H), 1.47 (s, 1H).

1-(3-azido-5-(trifluoromethyl)benzoyl)-*N*-(4-chloro-3-(prop-2-yn-1-yloxy)phenyl)piperidine-3-carboxamide (206452). Agilent ESI(+) *m/z* [M+H]$^+$ 506.0; [M+Na] 528.0. HPLC (gradient A): ret time = 7.75 min; purity = >90%. ^{1}H NMR (400 MHz, DMSO-d_6): 1.2:1.0 mixture of rotamers, δ 10.24 (rotamer 1, s), 10.02 (rotamer 2, s, 1H), 7.68-6.99 (m, 6H), 4.90-4.75 (m, 2H), 4.58-4.07 (m, 1H), 3.58-3.40 (m, 2H), 3.21-2.89 (m, 2H), 2.74-2.54 (m, 1H), 2.03 (s, 1H), 1.88-1.64 (m, 2H), 1.46 (bs, 1H).

***tert*-butyl (5-((3-benzoylphenyl)amino)-5-oxopentyl)carbamate (115).** 5-((tert-butoxycarbonyl)amino)pentanoic acid (0.050 g, 0.230 mmol)was dissolved in dichloromethane (2.3 mL) and was treated with EDC (0.066 g, 0.345 mmol) followed by

DMAP (0.042 g, 0.345 mmol) then (3-aminophenyl)(phenyl)methanone (0.045 g, 0.230 mmol). The reaction was stirred overnight at room temperature. The reaction was then diluted with additional DCM to a volume of 5 mL. Organics were washed with 1N HCl (5 mL) followed by saturated $NaHCO_3$ (5 mL) and was dried ($MgSO_4$) and concentrated *in vacuo* to afford 0.080 g of light brown solid. No further purification was performed. ^{1}H NMR (400 MHz, $CDCl_3$): δ 7.80-7.15 (m, 9H), 3.03-2.87 (m, 2H), 2.26-2.11 (m, 2H), 1.60-1.45 (m, 2H), 1.40-1.25 (m, 2H).

5-amino-*N*-(3-benzoylphenyl)pentanamide (116). Compound **115** was dissolved in dichloromethane (1.35 mL) and the solution was cooled to approximately -10 °C. To the cooled stirring solution was added TFA (0.675 mL). The reaction mixture continued stirring at -7 °C for 45 minutes. The solution was added to a cooled 2M NaOH solution (10 mL). The mixture was then extracted with additional dichloromethane (3 x 5 mL). The organics were combined, dried ($MgSO_4$), and concentrated *in vacuo* to afford 0.039 g (0.132 mmol, 65% yield) of title compound. ^{1}H NMR (400 MHz, DMSO-d_6): δ 10.23 (s, 1H), 8.07 (s, 1H), 7.90 (d, J = 8.2, 1H), 7.76-7.65 (m, 3H), 7.60-7.33 (m, 4H), 2.72-2.60 (m, 2H), 2.38-2.29 (m, 2H), 1.68-1.57 (m, 2H), 1.54-1.40 (m, 2H).

5-amino-*N*-(3-benzoylphenyl)pentanamide (117). Compound **116** (0.080 g, 0.202 mmol) was dissolved in DCM (1.35 mL) and the solution was cooled to approximately -10 °C. To the cooled stirring solution was added TFA (0.675 mL). The reaction mixture continued stirring at -7 °C and the reaction's progression was monitored by TLC, which indicated completion after 45 minutes. Therefore, the solution was added to a cooled 2M NaOH solution (10 mL). The mixture was then extracted with additional DCM (3 x 5 mL). The combined organics were dried ($MgSO_4$) and concentrated *in vacuo* to afford 0.039 g (0.132 mmol, 65% yield) of title compound. ^{1}H NMR (400 MHz, DMSO-d_6): δ 10.23 (s, 1H), 8.07 (s, 1H), 7.90 (d, J = 8.2, 1H), 7.76-7.65 (m, 3H), 7.60-7.33 (m, 4H), 2.72-2.60 (m, 2H), 2.38-2.29 (m, 2H), 1.68-1.57 (m, 2H), 1.54-1.40 (m, 2H).

***N*-(5-((3-benzoylphenyl)amino)-5-oxopentyl)-3-(prop-2-yn-1-yloxy)-5-(trifluoromethyl)benzamide (208797)**. Prepared using **117** and **98** according to

Procedure D, but using 0.10 mmol of each to afford 0.017 g (0.033 mmol, 40% yield) of title compound as a white solid. No further purification was performed. ESI(+) *m/z* $[M+H]^+$ 522.9; [M+Na] 544.9. HPLC (gradient A): ret time = 7.53 min; purity = >90%. ^{1}H NMR (400 MHz, DMSO-d_6): δ 10.13 (s, 1H), 8.70 (t, *J* = 5.5 Hz, 1H), 8.01 (t, *J* = 1.7 Hz, 1H), 7.94-7.87 (m, 1H), 7.80 (s, 1H), 7.76-7.71 (m, 3H), 7.71-7.65 (m, 1H), 7.60-7.54 (m, 2H), 7.52-7.44 (m, 1H), 7.39 (dt, *J* = 7.7, 1.2 Hz, 1H), 4.98 (d, *J* = 2.4 Hz, 2H), 3.64 (t, *J* = 2.3 Hz, 1H), 3.30-3.27 (m, 2H), 3.22 (s, 2H), 2.36 (t, *J* = 7.1 Hz, 2H), 1.69-1.52 (m, 4H).

(3,5-bis(trifluoromethyl)phenyl)(4-((4-chlorophenyl)amino)piperidin-1-yl)methanone (102441). Compound **22** (0.124 g, 0.366 mmol) was dissolved in 1,2-dichloroethane (1.3 mL) and was treated with 4-chloroaniline (0.047 g, 0.366 mmol) followed by Sodium triacetoxyborohydride (0.109 g, 0.512 mmol) and Acetic acid (0.021 mL, 0.366 mmol). The mixture was stirred overnight at room temperature. Reaction was then basified to pH ~9 using 2M NaOH and the aqueous layer was extracted with ether (3 x 10 mL). Combined extracts were washed with brine (20 mL), dried, and concentrated. Crude material was purified using flash chromatography (5-80% EtOAc/Hex) to afford 0.044 g (0.098 mmol, 27% yield) of title compound as a clear oil. TLC R_f (50% EtOAc/Hex): 0.74. TOF MS-ESI *m/z* $[M+H]^+$ 451.1; [M+Na] 473.1. HPLC (gradient A): ret time = 7.96 min; purity = 99%. ^{1}H NMR (500 MHz, d_6-DMSO): δ 8.22 (s, 1H), 8.12 (s, 2H), 7.08 (d, *J* = 8.7 Hz, 2H), 6.61 (d, *J* = 8.8 Hz, 2H), 5.74 (d, *J* = 7.8 Hz, 1H), 4.34 (d, *J* = 12.2 Hz, 1H), 3.55-3.05 (m, 5H), 2.06-1.78 (m, 2H), 1.45-1.28 (m, 2H).

Bibliography

1. O'Callaghan, K.; Kuliopulos, A.; Covic, L., Turning Receptors On and Off with Intracellular Pepducins: New Insights into G-protein-coupled Receptor Drug Development. *Journal of Biological Chemistry 287* (16), 12787-12796.

2. Liu, J. J.; Horst, R.; Katritch, V.; Stevens, R. C.; Wüthrich, K., Biased Signaling Pathways in beta-2-Adrenergic Receptor Characterized by ^{19}F-NMR. *Science 335* (6072), 1106-1110.

3. Bridges, T. M.; Lindsley, C. W., G-Protein-Coupled Receptors: From Classical Modes of Modulation to Allosteric Mechanisms. *ACS Chemical Biology* **2008,** *3* (9), 530-541.

4. Dorsam, R. T.; Gutkind, J. S., G-protein-coupled receptors and cancer. *Nat Rev Cancer* **2007,** *7* (2), 79-94.

5. Huang, J.-H.; Cao, D.-S.; Yan, J.; Xu, Q.-S.; Hu, Q.-N.; Liang, Y.-Z., Using core hydrophobicity to identify phosphorylation sites of human G protein-coupled receptors. *Biochimie 94* (8), 1697-1704.

6. Juneja, J.; Casey, P. J., Role of G12 proteins in oncogenesis and metastasis. *Br J Pharmacol* **2009,** *158* (1), 32-40.

7. Murray, F.; Yuan, J. X. J.; Insel, P. A.; Garcia, J. G. N.; West, J. B.; Hales, C. A.; Rich, S.; Archer, S. L., Receptor-Mediated Signal Transduction and Cell Signaling

Textbook of Pulmonary Vascular Disease. Springer US: pp 245-260.

8. Riobo, N. A.; Manning, D. R., Receptors coupled to heterotrimeric G proteins of the G12 family. *Trends in Pharmacological Sciences* **2005,** *26* (3), 146-154.

9. Even-Ram, S.; Uziely, B.; Cohen, P.; Grisaru-Granovsky, S.; Maoz, M.; Ginzburg, Y.; Reich, R.; Vlodavsky, I.; Bar-Shavit, R., Thrombin receptor overexpression in malignant and physiological invasion processes. *Nat Med* **1998,** *4* (8), 909-14.

10. Chay, C. H.; Cooper, C. R.; Gendernalik, J. D.; Dhanasekaran, S. M.; Chinnaiyan, A. M.; Rubin, M. A.; Schmaier, A. H.; Pienta, K. J., A functional thrombin receptor (PAR1) is expressed on bone-derived prostate cancer cell lines. *Urology* **2002,** *60* (5), 760-765.

11. Kelly, P.; Stemmle, L. N.; Madden, J. F.; Fields, T. A.; Daaka, Y.; Casey, P. J., A Role for the G12 Family of Heterotrimeric G Proteins in Prostate Cancer Invasion. *Journal of Biological Chemistry* **2006,** *281* (36), 26483-26490.

12. Cuttitta, F.; Carney, D. N.; Mulshine, J.; Moody, T. W.; Fedorko, J.; Fischler, A.; Minna, J. D., Bombesin-like peptides can function as autocrine growth factors in human small-cell lung cancer. *Nature* **1985,** *316* (6031), 823-826.

13. Corral, R. S.; Iniguez, M. A.; Duque, J.; Lopez-Perez, R.; Fresno, M., Bombesin induces cyclooxygenase-2 expression through the activation of the nuclear factor of activated T cells and enhances cell migration in Caco-2 colon carcinoma cells. *Oncogene* **2006,** *26* (7), 958-969.

14. Zheng, R.; Iwase, A.; Shen, R.; Goodman, O. B., Jr.; Sugimoto, N.; Takuwa, Y.; Lerner, D. J.; Nanus, D. M., Neuropeptide-stimulated cell migration in prostate cancer cells is mediated by RhoA kinase signaling and inhibited by neutral endopeptidase. *Oncogene* **2006,** *25* (44), 5942-5952.

15. Kang, J.; Ishola, T. A.; Baregamian, N.; Mourot, J. M.; Rychahou, P. G.; Evers, B. M.; Chung, D. H., Bombesin induces angiogenesis and neuroblastoma growth. *Cancer Letters* **2007,** *253* (2), 273-281.

16. Levine, L.; Lucci Iii, J. A.; Pazdrak, B.; Cheng, J. Z.; Guo, Y. S.; Townsend Jr, C. M.; Hellmich, M. R., Bombesin stimulates nuclear factor ÎºB activation and expression of proangiogenic factors in prostate cancer cells. *Cancer Research* **2003,** *63* (13), 3495-3502.

17. Bian, D.; Mahanivong, C.; Yu, J.; Frisch, S. M.; Pan, Z. K.; Ye, R. D.; Huang, S., The G12/13-RhoA signaling pathway contributes to efficient lysophosphatidic acid-stimulated cell migration. *Oncogene* **2005,** *25* (15), 2234-2244.

18. Cai, Q.; Zhao, Z.; Antalis, C.; Yan, L.; Del Priore, G.; Hamed, A. H.; Stehman, F. B.; Schilder, J. M.; Xu, Y., Elevated and secreted phospholipase A2 activities as new potential therapeutic targets in human epithelial ovarian cancer. *The FASEB Journal*.

19. Peyruchaud, O.; Leblanc, R.; David, M., Pleiotropic activity of lysophosphatidic acid in bone metastasis. *Biochimica et Biophysica Acta (BBA) - Molecular and Cell Biology of Lipids* (0).

20. Sawada, K.; Morishige, K.-i.; Tahara, M.; Kawagishi, R.; Ikebuchi, Y.; Tasaka, K.; Murata, Y., Alendronate Inhibits Lysophosphatidic Acid-induced Migration of Human Ovarian Cancer Cells by Attenuating the Activation of Rho. *Cancer Research* **2002,** *62* (21), 6015-6020.

21. Hwang, Y. S.; Hodge, J. C.; Sivapurapu, N.; Lindholm, P. F., Lysophosphatidic acid stimulates PC-3 prostate cancer cell matrigel invasion through activation of RhoA and NF-κB activity. *Molecular Carcinogenesis* **2006,** *45* (7), 518-529.

22. Rathinam, R.; Berrier, A.; Alahari, S. K., Role of Rho GTPases and their regulators in cancer progression. *Front Biosci* **2012,** *17*, 2561-71.

23. Ridley, A. J., Historical overview of Rho GTPases. *Methods Mol Biol 827*, 3-12.

24. Narumiya, S.; Tanji, M.; Ishizaki, T., Rho signaling, ROCK and mDia1, in transformation, metastasis and invasion. *Cancer Metastasis Rev* **2009,** *28* (1-2), 65-76.

25. Benitah, S. A.; Valeron, P. F.; van Aelst, L.; Marshall, C. J.; Lacal, J. C., Rho GTPases in human cancer: an unresolved link to upstream and downstream transcriptional regulation. *Biochim Biophys Acta* **2004,** *1705* (2), 121-32.

26. Whitehead, I. P.; Zohn, I. E.; Der, C. J., Rho GTPase-dependent transformation by G protein-coupled receptors. *Oncogene* **2001,** *20* (13), 1547-55.

27. Pertz, O., Spatio-temporal Rho GTPase signaling - where are we now? *Journal of Cell Science* **2010,** *123* (11), 1841-1850.

28. Karlsson, R.; Pedersen, E. D.; Wang, Z.; Brakebusch, C., Rho GTPase function in tumorigenesis. *Biochimica et Biophysica Acta (BBA) - Reviews on Cancer* **2009,** *1796* (2), 91-98.

29. Ellenbroek, S. I.; Collard, J. G., Rho GTPases: functions and association with cancer. *Clin Exp Metastasis* **2007,** *24* (8), 657-72.

30. Vega, F. M.; Ridley, A. J., Rho GTPases in cancer cell biology. *FEBS Lett* **2008,** *582* (14), 2093-101.

31. Kjoller, L.; Hall, A., Signaling to Rho GTPases. *Exp Cell Res* **1999,** *253* (1), 166-79.

32. Hall, A., The cytoskeleton and cancer. *Cancer Metastasis Rev* **2009,** *28* (1-2), 5-14.

33. Vega, F. M.; Ridley, A. J., Rho GTPases in cancer cell biology. *Febs Letters* **2008,** *582* (14), 2093-2101.

34. Heasman, S. J.; Ridley, A. J., Mammalian Rho GTPases: new insights into their functions from in vivo studies. *Nat Rev Mol Cell Biol* **2008,** *9* (9), 690-701.

35. Rossman, K. L.; Der, C. J.; Sondek, J., GEF means go: Turning on Rho GTPases with guanine nucleotide-exchange factors. *Nature Reviews Molecular Cell Biology* **2005,** *6* (2), 167-180.

36. Chen, Z.; Guo, L.; Hadas, J.; Gutowski, S.; Sprang, S. R.; Sternweis, P. C., Activation of p115-RhoGEF requires direct association of G-alpha13 and the Dbl-homology domain. *Journal of Biological Chemistry*.

37. Siehler, S., Regulation of RhoGEF proteins by G12/13-coupled receptors. *British Journal of Pharmacology* **2009,** *158* (1), 41-49.

38. Evelyn, C. R. High-Throughput Screening for Small-Molecule Inhibitors of the Ga12/13/RhoA Signaling Pathway. University of Michigan, Ann Arbor, 2009.

39. Knöll, B.; Beck, H., The cytoskeleton and nucleus: the role of actin as a modulator of neuronal gene expression. *e-Neuroforum* **2011,** *2* (1), 1-5.

40. Yamana, N.; Arakawa, Y.; Nishino, T.; Kurokawa, K.; Tanji, M.; Itoh, R. E.; Monypenny, J.; Ishizaki, T.; Bito, H.; Nozaki, K.; Hashimoto, N.; Matsuda, M.; Narumiya, S., The Rho-mDia1 Pathway Regulates Cell Polarity and Focal Adhesion Turnover in Migrating Cells through Mobilizing Apc and c-Src. *Molecular and Cellular Biology* **2006,** *26* (18), 6844-6858.

41. Parri, M.; Chiarugi, P., Rac and Rho GTPases in cancer cell motility control. *Cell Commun Signal* **2010,** *8*, 23.

42. Baugher, P. J., Rac1 and Rac3 isoform activation is involved in the invasive and metastatic phenotype of human breast cancer cells. *Breast cancer research : BCR* **2005,** *7* (6), R965-74.

43. Pan, Y.; Bi, F.; Liu, N.; Xue, Y.; Yao, X.; Zheng, Y.; Fan, D., Expression of seven main Rho family members in gastric carcinoma. *Biochemical and Biophysical Research Communications* **2004,** *315* (3), 686-691.

44. Kamai, T.; Yamanishi, T.; Shirataki, H.; Takagi, K.; Asami, H.; Ito, Y.; Yoshida, K.-I., Overexpression of RhoA, Rac1, and Cdc42 GTPases Is Associated with Progression in Testicular Cancer. *Clinical Cancer Research* **2004,** *10* (14), 4799-4805.

45. Huang, M., RhoB in cancer suppression. *Histology and histopathology* **2006,** *21* (2), 213-8.

46. Jiang, K.; Sun, J.; Cheng, J.; Djeu, J. Y.; Wei, S.; Sebti, S. d., Akt Mediates Ras Downregulation of RhoB, a Suppressor of Transformation, Invasion, and Metastasis. *Molecular and Cellular Biology* **2004,** *24* (12), 5565-5576.

47. Dietrich, K. A.; Schwarz, R.; Liska, M.; Grass, S.; Menke, A.; Meister, M.; Kierschke, G.; Langle, C.; Genze, F.; Giehl, K., Specific induction of migration and invasion of pancreatic carcinoma cells by RhoC, which differs from RhoA in its localisation and activity. *Biological Chemistry* **2009,** *390* (10), 1063-1077.

48. Vega, F. M.; Fruhwirth, G.; Ng, T.; Ridley, A. J., RhoA and RhoC have distinct roles in migration and invasion by acting through different targets. *The Journal of Cell Biology* **2011,** *193* (4), 655-665.

49. Sequeira, L.; Dubyk, C. W.; Riesenberger, T. A.; Cooper, C. R.; van Golen, K. L., Rho GTPases in PC-3 prostate cancer cell morphology, invasion and tumor cell diapedesis. *Clin Exp Metastasis* **2008,** *25* (5), 569-79.

50. Yao, H.; Dashner, E. J.; van Golen, C. M.; van Golen, K. L., RhoC GTPase is required for PC-3 prostate cancer cell invasion but not motility. *Oncogene* **2005,** *25* (16), 2285-2296.

51. Hakem, A.; Sanchez-Sweatman, O.; You-Ten, A.; Duncan, G.; Wakeham, A.; Khokha, R.; Mak, T. W., RhoC is dispensable for embryogenesis and tumor initiation but essential for metastasis. *Genes Dev* **2005,** *19* (17), 1974-9.

52. Clark, E. A.; Golub, T. R.; Lander, E. S.; Hynes, R. O., Genomic analysis of metastasis reveals an essential role for RhoC. *Nature* **2000,** *406* (6795), 532-5.

53. Mardilovich, K.; Olson, M. F.; Baugh, M., Targeting Rho GTPase signaling for cancer therapy. *Future Oncol* **2012,** *8* (2), 165-77.

54. Street, C. A.; Bryan, B. A., Rho kinase proteins--pleiotropic modulators of cell survival and apoptosis. *Anticancer Res* **2011,** *31* (11), 3645-57.

55. Imamura, F.; Mukai, M.; Ayaki, M.; Akedo; Hitoshi, Y-27632, an Inhibitor of Rho-associated Protein Kinase, Suppresses Tumor Cell Invasion via Regulation of Focal Adhesion and Focal Adhesion Kinase. *Cancer Sci* **2000,** *91* (8), 811-816.

56. Abe, H.; Kamai, T.; Tsujii, T.; Nakamura, F.; Mashidori, T.; Mizuno, T.; Tanaka, M.; Tatsumiya, K.; Furuya, N.; Masuda, A.; Yamanishi, T.; Yoshida, K.-I., Possible role of the RhoC/ROCK pathway in progression of clear cell renal cell carcinoma. *Biomedical Research* **2008,** *29* (3), 155-161.

57. Kamai, T.; Tsujii, T.; Arai, K.; Takagi, K.; Asami, H.; Ito, Y.; Oshima, H., Significant Association of Rho/ROCK Pathway with Invasion and Metastasis of Bladder Cancer. *Clinical Cancer Research* **2003,** *9* (7), 2632-2641.

58. Breitenlechner, C.; Gaßel, M.; Hidaka, H.; Kinzel, V.; Huber, R.; Engh, R. A.; Bossemeyer, D., Protein Kinase A in Complex with Rho-Kinase Inhibitors Y-27632, Fasudil, and H-1152P: Structural Basis of Selectivity. *Structure (London, England : 1993)* **2003,** *11* (12), 1595-1607.

59. Hahmann, C.; Schroeter, T., Rho-kinase inhibitors as therapeutics: from pan inhibition to isoform selectivity. *Cellular and Molecular Life Sciences 67* (2), 171-177.

60. Muehlich, S.; Hampl, V.; Khalid, S.; Singer, S.; Frank, N.; Breuhahn, K.; Gudermann, T.; Prywes, R., The transcriptional coactivators megakaryoblastic leukemia 1/2 mediate the effects of loss of the tumor suppressor deleted in liver cancer 1. *Oncogene*.

61. Medjkane, S.; Perez-Sanchez, C.; Gaggioli, C.; Sahai, E.; Treisman, R., Myocardin-related transcription factors and SRF are required for cytoskeletal dynamics and experimental metastasis. *Nat Cell Biol* **2009,** *11* (3), 257-68.

62. Evelyn, C. R.; Wade, S. M.; Wang, Q.; Wu, M.; Iniguez-Lluhi, J. A.; Merajver, S. D.; Neubig, R. R., CCG-1423: a small-molecule inhibitor of RhoA transcriptional signaling. *Molecular Cancer Therapeutics* **2007,** *6* (8), 2249-2260.

63. Evelyn, C. R.; Bell, J. L.; Ryu, J. G.; Wade, S. M.; Kocab, A.; Harzdorf, N. L.; Hollis Showalter, H. D.; Neubig, R. R.; Larsen, S. D., Design, synthesis and prostate cancer cell-based studies of analogs of the Rho/MKL1 transcriptional pathway inhibitor, CCG-1423. *Bioorganic & Medicinal Chemistry Letters* **2010,** *20* (2), 665-672.

64. Burton, P. S.; Conradi, R. A.; Ho, N. F.; Hilgers, A. R.; Borchardt, R. T., How structural features influence the biomembrane permeability of peptides. *J Pharm Sci* **1996,** *85* (12), 1336-40.

65. Lipinski, C. A.; Lombardo, F.; Dominy, B. W.; Feeney, P. J., Experimental and computational approaches to estimate solubility and permeability in drug discovery and development settings. *Advanced Drug Delivery Reviews* **1997,** *23* (1-3), 3-25.

66. Mann, A., Conformational Restriction and/or Steric Hindrance in Medicinal Chemistry. In *Practice of Medicinal Chemistry*, 2nd ed.; Wermuth, C. G., Ed. Elsevier: London, 2003; pp 233-250.

67. Veber, D. F.; Johnson, S. R.; Cheng, H.-Y.; Smith, B. R.; Ward, K. W.; Kopple, K. D., Molecular Properties That Influence the Oral Bioavailability of Drug Candidates. *Journal of Medicinal Chemistry* **2002,** *45* (12), 2615-2623.

68. Lima, L. M.; Barreiro, E. J., Bioisosterism: a useful strategy for molecular modification and drug design. *Curr Med Chem* **2005,** *12* (1), 23-49.

69. Orelli, L. R.; Garcia, M. B.; Niemevz, F.; Perillo, I. A., Selective monoformylation of 1,3-diaminopropane derivatives. *Synthetic Communications* **1999,** *29* (11), 1819-1833.

70. Liu, A. P.; Wang, X. G.; Ou, X. M.; Huang, M. Z.; Chen, C.; Liu, S. D.; Huang, L.; Liu, X. P.; Zhang, C. L.; Zheng, Y. Q.; Ren, Y. G.; He, L. A.; Yao, J. R., Synthesis and fungicidal activities of novel bis(trifluoromethyl)phenyl-based strobilurins. *Journal of Agricultural and Food Chemistry* **2008,** *56* (15), 6562-6566.

71. Tellitu, I.; Urrejola, A.; Serna, S.; Moreno, I.; Herrero, M. T.; Dominguez, E.; SanMartin, R.; Correa, A., On the Phenyliodine(III)-bis(trifluoroacetate)-mediated olefin amidohydroxylation reaction. *European Journal of Organic Chemistry* **2007,** (3), 437-444.

72. Ishihara, M.; Togo, H., An efficient preparation of 2-imidazolines and imidazoles from aldehydes with molecular iodine and (diacetoxyiodo)benzene. *Synlett* **2006,** (2), 227-230.

73. Simoni, D.; Romagnoli, R.; Giannini, G.; Alloati, D.; Pisano, C. Preparation of combretastatin derivatives with cytotoxic activity. WO2005007635A2, 2005.

74. Jeddeloh, M. R.; Holden, J. B.; Nouri, D. H.; Kurth, M. J., A library of 3-aryl-4,5-dihydroisoxazole-5-carboxamides. *Journal of Combinatorial Chemistry* **2007,** *9* (6), 1041-1045.

75. Simoni, D.; Roberti, M.; Invidiata, F. P.; Rondanin, R.; Baruchello, R.; Malagutti, C.; Mazzali, A.; Rossi, M.; Grimaudo, S.; Capone, F.; Dusonchet, L.; Meli, M.; Raimondi, M. V.; Landino, M.; D'Alessandro, N.; Tolomeo, M.; Arindam, D.; Lu, S.; Benbrook, D. M., Heterocycle-containing retinoids. Discovery of a novel isoxazole arotinoid possessing potent apoptotic activity in multidrug and drug-induced apoptosis-resistant cells. *Journal of Medicinal Chemistry* **2001,** *44* (14), 2308-2318.

76. Rostovtsev, V. V.; Green, L. G.; Fokin, V. V.; Sharpless, K. B., A stepwise huisgen cycloaddition process: copper(I)-catalyzed regioselective "ligation" of azides and terminal alkynes. *Angew Chem Int Ed Engl* **2002,** *41* (14), 2596-9.

77. Freire, E., Isothermal titration calorimetry: controlling binding forces in lead optimization. *Drug Discovery Today: Technologies* **2004,** *1* (3), 295-299.

78. Herradura, P. S.; Josyula, V. P. V. N.; Renslo, A. R. Preparation of diazepine oxazolidinones as antibacterial agents. 2005-IB3559

2006056877, 20051117., 2006.

79. Jia, Z. J.; Wu, Y. H.; Huang, W. R.; Zhang, P. L.; Clizbe, L. A.; Goldman, E. A.; Sinha, U.; Arfsten, A. E.; Edwards, S. T.; Alphonso, M.; Hutchaleelaha, A.; Scarborough, R. M.; Zhu, B. Y., 1-(2-Naphthyl)-1H-pyrazole-5-carboxylamides as potent factor Xa inhibitors. Part 2: A survey of P4 motifs. *Bioorganic & Medicinal Chemistry Letters* **2004,** *14* (5), 1221-1227.

80. Klapars, A.; Huang, X. H.; Buchwald, S. L., A general and efficient copper catalyst for the amidation of aryl halides. *Journal of the American Chemical Society* **2002,** *124* (25), 7421-7428.

81. Kim, T.-S.; Bellon, S.; Booker, S.; D'Angelo, N.; Dominguez, C.; Fellows, I.; Lee, M.; Liu, L.; Rainbeau, E.; Siegmund, A. C.; Tasker, A.; Xi, N.; Cheng, Y. Preparation of substituted heterocycles for treating HGF mediated diseases. WO2006060318A2, 2006.

82. Mylari, B. L.; Zembrowski, W. J.; Beyer, T. A.; Aldinger, C. E.; Siegel, T. W., Orally Active Aldose Reductase Inhibitors - Indazoleacetic, Oxopyridazineacetic, and Oxopyridopyridazineacetic Acid-Derivatives. *Journal of Medicinal Chemistry* **1992,** *35* (12), 2155-2162.

83. Sasaki, T.; Ueda, H., Synthetic experiments on 4-aminohydrocarbostyril and its derivatives. *Proc. Imp. Acad. (Tokyo)* **1939,** *15*, 315-20.

84. Yang, W.-Y.; Breiner, B.; Kovalenko, S. V.; Ben, C.; Singh, M.; LeGrand, S. N.; Sang, Q.-X. A.; Strouse, G. F.; Copland, J. A.; Alabugin, I. V., C-Lysine Conjugates: pH-Controlled Light-Activated Reagents for Efficient Double-Stranded DNA Cleavage with Implications for Cancer Therapy. *Journal of the American Chemical Society* **2009,** *131* (32), 11458-11470.

85. Maruoka, H.; Okabe, F.; Yamagata, K., Synthesis of substituted 3-pyrrolidinecarbonitriles. *Journal of Heterocyclic Chemistry* **2007,** *44* (1), 201-203.

86. Van Berkom, L. W. A.; de Gelder, R.; Scheeren, H. W., 6-spiro-1,4-diazepane-2,5-diones by head-to-tail N1/C2 amide bond formation. *European Journal of Organic Chemistry* **2005,** (5), 907-917.

87. Soledade, M.; Pedras, C.; Jha, M., Concise syntheses of the cruciferous phytoalexins brassilexin, sinalexin, wasalexins, and analogues: Expanding the scope of the Vilsmeier formylation. *Journal of Organic Chemistry* **2005,** *70* (5), 1828-1834.

88. Borch, R. F.; Bernstein, M. D.; Durst, H. D., Cyanohydridoborate anion as a selective reducing agent. *Journal of the American Chemical Society* **1971,** *93* (12), 2897-2904.

89. Gerspacher, M.; La Vecchia, L.; Mah, R.; von Sprecher, A.; Anderson, G. P.; Subramanian, N.; Hauser, K.; Bammerlin, H.; Kimmel, S.; Pawelzik, V.; Ryffel, K.; Ball, H. A., Dual neurokinin NK1/NK2 antagonists: N-[(R,R)-(E)-1-arylmethyl-3-(2-oxo-azepan-3-yl)carbamoyl]allyl-N-methyl-3,5-bis(trifluoromethyl)benzamides and 3-[Nâ€²-3,5-bis(trifluoromethyl)benzoyl-N-arylmethyl-Nâ€²-methylhydrazino]-N-[(R)-2-oxo-azepan-3-yl]propionamides. *Bioorganic & Medicinal Chemistry Letters* **2001,** *11* (23), 3081-3084.

90. Wu, P.-L.; Peng, S.-Y.; Magrath, J., 1-Acyl-2-alkylhydrazines by the Reduction of Acylhydrazones. *Synthesis* **1995,** *1995* (4), 435-438.

91. Parikh, J. R.; Doering, W. V. E., Sulfur Trioxide in Oxidation of Alcohols by Dimethyl Sulfoxide. *Journal of the American Chemical Society* **1967,** *89* (21), 5505-5507.

92. Wipf, P.; Venkatraman, S.; Miller, C. P., A New Synthesis of Alpha-Methylserine by Nucleophilic Ring-Opening of N-Sulfonyl Aziridines. *Tetrahedron Letters* **1995,** *36* (21), 3639-3642.

93. AbdelMagid, A. F.; Carson, K. G.; Harris, B. D.; Maryanoff, C. A.; Shah, R. D., Reductive amination of aldehydes and ketones with sodium triacetoxyborohydride. Studies on direct and indirect reductive amination procedures. *Journal of Organic Chemistry* **1996,** *61* (11), 3849-3862.

94. Bunnelle, W. H.; Daanen, J. F.; Ryther, K. B.; Schrimpf, M. R.; Dart, M. J.; Gelain, A.; Meyer, M. D.; Frost, J. M.; Anderson, D. J.; Buckley, M.; Curzon, P.; Cao, Y. J.; Puttfarcken, P.; Searle, X.; Ji, J. G.; Putman, C. B.; Surowy, C.; Toma, L.; Barlocco, D., Structure-activity studies and analgesic efficacy of N-(3-pyridinyl)-Bridged bicyclic diamines, exceptionally potent agonists at nicotinic acetylcholine receptors. *Journal of Medicinal Chemistry* **2007,** *50* (15), 3627-3644.

95. Lawrence, R. M.; Biller, S. A.; Fryszman, O. M.; Poss, M. A., Automated Synthesis and Purification of Amides: Exploitation of Automated Solid Phase Extraction in Organic Synthesis. *Synthesis* **1997,** *1997* (5), 553-558.

96. Kerns, E. H.; Di, L., *Drug-like properties : concepts, structure design and methods : from ADME to toxicity optimization*. Academic Press: Amsterdam ; Boston, 2008; p xix, 526 p., [2] p. of plates.

97. Winiwarter, S.; Bonham, N. M.; Ax, F.; Hallberg, A.; LennernÃ¤s, H.; KarlÃ©n, A., Correlation of Human Jejunal Permeability (in Vivo) of Drugs with Experimentally and Theoretically Derived Parameters. A Multivariate Data Analysis Approach. *Journal of Medicinal Chemistry* **1998,** *41* (25), 4939-4949.

98. Sundaresan, V.; Abrol, R., Biological chiral recognition: The substrate's perspective. *Chirality* **2005,** *17* (S1), S30-S39.

99. Burke, D.; Henderson, D. J., Chirality: a blueprint for the future. *British Journal of Anaesthesia* **2002,** *88* (4), 563-576.

100. Easson, L. H.; Stedman, E., Studies on the relationship between chemical constitution and physiological action: Molecular dissymmetry and physiological activity. *Biochem. J.* **1933,** *27* (4), 1257-0.

101. Mesecar, A. D.; Koshland, D. E., Structural biology: A new model for protein stereospecificity. *Nature* **2000,** *403* (6770), 614-615.

102. Sundaresan, V.; Abrol, R., Towards a general model for protein–substrate stereoselectivity. *Protein Science* **2002,** *11* (6), 1330-1339.

103. Bentley, R., Diastereoisomerism, contact points, and chiral selectivity: a four-site saga. *Archives of Biochemistry and Biophysics* **2003,** *414* (1), 1-12.

104. Ariëns, E. J., Stereochemistry, a basis for sophisticated nonsense in pharmacokinetics and clinical pharmacology. *European Journal of Clinical Pharmacology* **1984,** *26* (6), 663-668.

105. Pfeiffer, C. C., Optical Isomerism and Pharmacological Action, a Generalization. *Science* **1956,** *124* (3210), 29-31.

106. Strieter, E. R.; Blackmond, D. G.; Buchwald, S. L., The role of chelating diamine ligands in the Goldberg reaction: A kinetic study on the copper-catalyzed amidation of aryl iodides. *Journal of the American Chemical Society* **2005,** *127* (12), 4120-4121.

107. Allen, D. A.; Tomaso, A. E.; Priest, O. P.; Hindson, D. F.; Hurlburt, J. L., Mosher Amides: Determining the Absolute Stereochemistry of Optically-Active Amines. *Journal of Chemical Education* **2008,** *85* (5), 698.

108. Speelman, J. C.; Kellogg, R. M., Behavior of Pyridinium Salts Obtained from Derivatives of Pyridinedicarboxylic Acids in Basic Solutions - Addition of Hydroxide or Alkoxide to Form 1,2-Dihydropyridine Intermediates. *Journal of Organic Chemistry* **1990,** *55* (2), 647-653.

109. Leger, S.; Deschenes, D.; Fortin, R.; Isabel, E.; Powell, D. Preparation of [1,3]thiazolo[4,5-d]pyrimidine derivatives as inhibitors of stearoyl-coenzyme a delta-9 desaturase. WO2008141455A1, 2008.

110. Astles, P. C.; Eastwood, P. R.; Houille, O.; Levell, J.; Pauls, H.; Czekaj, M.; Liang, G.; Gong, Y.; Pribish, J.; Neuenschwander, K. Preparation of (hetero)arylacyl-piperidinyl-benzylamines for use as tryptase inhibitors. WO2001090101A1, 2001.

111. Jacobsen, P.; Schaumburg, K.; Larsen, J. J.; Krogsgaard-Larsen, P., Syntheses of some aminopiperidinecarboxylic acids related to nipecotic acid. *Acta Chem. Scand., Ser. B* **1981,** *B35* (4), 289-94.

112. Leslie, B. J.; Hergenrother, P. J., Identification of the cellular targets of bioactive small organic molecules using affinity reagents. *Chemical Society Reviews* **2008,** *37* (7), 1347-1360.

113. Kim, Y. K.; Chang, Y.-T., Tagged library approach facilitates forward chemical genetics. *Molecular BioSystems* **2007,** *3* (6), 392-397.

114. Mano, N.; Sato, K.; Goto, J., Specific Affinity Extraction Method for Small Molecule-Binding Proteins. *Analytical Chemistry* **2006,** *78* (13), 4668-4675.

115. Sakamoto, S.; Hatakeyama, M.; Ito, T.; Handa, H., Tools and methodologies capable of isolating and identifying a target molecule for a bioactive compound. *Bioorganic & Medicinal Chemistry 20* (6), 1990-2001.

116. Burdine, L.; Kodadek, T., Target Identification in Chemical Genetics: The (Often) Missing Link. *Chemistry & Biology* **2004,** *11* (5), 593-597.

117. Sato, S.-i.; Murata, A.; Shirakawa, T.; Uesugi, M., Biochemical Target Isolation for Novices: Affinity-Based Strategies. *Chemistry & Biology 17* (6), 616-623.

118. Sato, S.-i.; Kwon, Y.; Kamisuki, S.; Srivastava, N.; Mao, Q.; Kawazoe, Y.; Uesugi, M., Polyproline-Rod Approach to Isolating Protein Targets of Bioactive Small Molecules:â€‰ Isolation of a New Target of Indomethacin. *Journal of the American Chemical Society* **2007,** *129* (4), 873-880.

119. Kumar, A.; Narasimhan, B.; Kumar, D., Synthesis, antimicrobial, and QSAR studies of substituted benzamides. *Bioorganic & Medicinal Chemistry* **2007,** *15* (12), 4113-4124.

120. Cozzi, F.; Annunziata, R.; Benaglia, M.; Cinquini, M., Soluble-polymer-supported synthesis of beta-lactams on a modified poly(ethylene glycol). *Chemistry-a European Journal* **2000,** *6* (1), 133-138.

121. Luc Lebeau, P. O., Charles Mioskowski,, Synthesis of New Phospholipids Linked to Steroid-Hormone Derivatives Designed for Two-Dimensional Crystallization of Proteins. *Helvetica Chimica Acta* **1991,** *74* (8), 1697-1706.

122. Dorman, G.; Prestwich, G. D., Benzophenone Photophores in Biochemistry. *Biochemistry* **1994,** *33* (19), 5661-5673.

123. Dorm·n, G.; Prestwich, G. D., Using photolabile ligands in drug discovery and development. *Trends in Biotechnology* **2000,** *18* (2), 64-77.

124. A. Fleming, S., Chemical reagents in photoaffinity labeling. *Tetrahedron* **1995,** *51* (46), 12479-12520.

125. Deseke, E.; Nakatani, Y.; Ourisson, G., Intrinsic Reactivities of Amino Acids towards Photoalkylation with Benzophenone − A Study Preliminary to Photolabelling of the Transmembrane Protein Glycophorin A. *European Journal of Organic Chemistry* **1998,** *1998* (2), 243-251.

126. Dhanak, D.; Knight, S. D. Sulfonamide derivative urotensin-II receptor antagonists, preparation, pharmaceutical compositions, and therapeutic use. WO2001045694A1, 2001.

127. Sundberg, R. J.; Suter, S. R.; Brenner, M., Photolysis of 0-substituted aryl azides in diethylamine. Formation and autoxidation of 2-diethylamino-1H-azepine intermediates. *Journal of the American Chemical Society* **1972,** *94* (2), 513-520.

128. Sydnes, M. O.; Doi, I.; Ohishi, A.; Kuse, M.; Isobe, M., Determination of Solvent-Trapped Products Obtained by Photolysis of Aryl Azides in 2,2,2-Trifluoroethanol. *Chemistry – An Asian Journal* **2008,** *3* (1), 102-112.

129. McInnes, C., Virtual screening strategies in drug discovery. *Current Opinion in Chemical Biology* **2007,** *11* (5), 494-502.

130. Willett, P., Similarity-based virtual screening using 2D fingerprints. *Drug Discovery Today* **2006,** *11* (23â€“24), 1046-1053.

131. Walters, W. P.; Stahl, M. T.; Murcko, M. A., Virtual screening--an overview. *Drug Discovery Today* **1998,** *3* (4), 160-178.

132. Bajorath, J., Molecular Similarity Methods and QSAR Models as Tools for Virtual Screening. In *Drug Discovery Handbook*, John Wiley & Sons, Inc.: 2005; pp 87-122.

133. Acharya, C.; Coop, A.; Polli, J. E.; Mackerell, A. D., Jr., Recent advances in ligand-based drug design: relevance and utility of the conformationally sampled pharmacophore approach. *Curr Comput Aided Drug Des 7* (1), 10-22.

134. Yang, S.-Y., Pharmacophore modeling and applications in drug discovery: challenges and recent advances. *Drug Discovery Today 15* (11-12), 444-450.

135. Zhao, H., Scaffold selection and scaffold hopping in lead generation: a medicinal chemistry perspective. *Drug Discovery Today* **2007,** *12* (3-4), 149-155.

136. Güner, O. F.; Henry, D. R., Metric for analyzing hit lists and pharmacophores. In *Pharmacophore perception, development and use in drug design*, Güner, O. F., Ed. International University Line: La Jolla, 2000; pp 193-212.

137. Venkatraman, V.; Perez-Nueno, V. I.; Mavridis, L.; Ritchie, D. W., Comprehensive comparison of ligand-based virtual screening tools against the DUD data set reveals limitations of current 3D methods. *J Chem Inf Model 50* (12), 2079-93.

138. Jin, W. Z.; Goldfine, A. B.; Boes, T.; Henry, R. R.; Ciaraldi, T. P.; Kim, E. Y.; Emecan, M.; Fitzpatrick, C.; Sen, A.; Shah, A.; Mun, E.; Vokes, M.; Schroeder, J.; Tatro, E.; Jimenez-Chillaron, J.; Patti, M. E., Increased SRF transcriptional activity in human and mouse skeletal muscle is a signature of insulin resistance. *Journal of Clinical Investigation* **2011,** *121* (3), 918-929.

139. Ong, S. E.; Schenone, M.; Margolin, A. A.; Li, X.; Do, K.; Doud, M. K.; Mani, D. R.; Kuai, L.; Wang, X.; Wood, J. L.; Tolliday, N. J.; Koehler, A. N.; Marcaurelle, L. A.; Golub, T. R.; Gould, R. J.; Schreiber, S. L.; Carr, S. A., Identifying the proteins to which small-molecule probes and drugs bind in cells. *Proc Natl Acad Sci U S A* **2009,** *106* (12), 4617-22.

140. Slater, R. A.; Howson, W.; Swayne, G. T. G.; Taylor, E. M.; Reavill, D. R., Design and Synthesis of a Series of Combined Vasodilator Beta-Adrenoceptor Antagonists Based on 6-Arylpyridazinones. *Journal of Medicinal Chemistry* **1988,** *31* (2), 345-351.

141. Laitar, D. S.; Mathison, C. J. N.; Davis, W. M.; Sadighi, J. P., Copper(I) complexes of a heavily fluorinated beta-diketiminate ligand: Synthesis, electronic properties, and intramolecular aerobic hydroxylation. *Inorganic Chemistry* **2003,** *42* (23), 7354-7356.

142. Warrier, M.; Lo, M. K.; Monbouquette, H.; Garcia-Garibay, M. A., Photocatalytic reduction of aromatic azides to amines using CdS and CdSe nanoparticles. *Photochem Photobiol Sci* **2004,** *3* (9), 859-63.

143. Kuroda, N.; Hird, N.; Cork, D. G., Further development of a robust workup process for solution-phase high-throughput library synthesis to address environmental and sample tracking issues. *Journal of Combinatorial Chemistry* **2006,** *8* (4), 505-512.

144. Jia, Z. J.; Wu, Y.; Huang, W.; Zhang, P.; Clizbe, L. A.; Goldman, E. A.; Sinha, U.; Arfsten, A. E.; Edwards, S. T.; Alphonso, M.; Hutchaleelaha, A.; Scarborough, R. M.; Zhu, B.-Y., 1-(2-Naphthyl)-1H-pyrazole-5-carboxylamides as potent factor Xa inhibitors. Part 2: A survey of P4 motifs. *Bioorganic & Medicinal Chemistry Letters* **2004,** *14* (5), 1221-1227.

145. Kim, K. H.; Lee, H. S.; Kim, J. N., Synthesis of 3,4-disubstituted 2(1H)-quinolinones via intramolecular Friedel-Crafts reaction of N-arylamides of Baylis-Hillman adducts. *Tetrahedron Letters* **2009,** *50* (11), 1249-1251.

146. Ife, R. J.; Catchpole, K. W.; Durant, G. J.; Ganellin, C. R.; Harvey, C. A.; Meeson, M. L.; Owen, D. A. A.; Parsons, M. E.; Slingsby, B. P.; Theobald, C. J., Non-Basic Histamine H-1-Antagonists .1. Synthesis and Biological Evaluation of Some Substituted 2-(2-Pyridylaminoalkylamino) Pyrimidones and Related-Compounds. *European Journal of Medicinal Chemistry* **1989,** *24* (3), 249-258.

147. Kakizuka, A.; Hori, S.; Shudo, T.; Fuchigami, T. Preparation of 2-(arylazo or heteroarylazo)-4-aminonaphthalene-1-sulfonic acid derivatives as regulators of vasolin-containing protein (VCP). WO2012014994A1.

148. Betebenner, D. A.; Maring, C. J.; Rockway, T. W.; Cooper, C. S.; Anderson, D. D.; Wagner, R.; Zhang, R.; Molla, A.; Mo, H.; Pilot-Matias, T. J.; Masse, S. V.; Carrick, R. J.; He, W.; Lu, L. Antiviral compounds, their preparation, pharmaceutical compositions, and use in therapy. WO2008133753A2, 2008.

149. Cumming, J. N.; Huang, Y.; Li, G.; Iserloh, U.; Stamford, A.; Strickland, C.; Voigt, J. H.; Wu, Y.; Pan, J.; Guo, T.; Hobbs, D. W.; Le, T. X. H.; Lowrie, J. F. Preparation of cyclic amine BACE-1 inhibitors having a heterocyclic substituent. WO2005014540A1, 2005.

150. Cuthbertson, A.; Glaser, M.; Morrison, M.; Solbakken, M.; Arukwe, J.; Karlsen, H.; Wiggen, U.; Champion, S.; Kindberg, G. M., Radiosynthesis and biodistribution of cyclic RGD peptides conjugated with novel [F-18]fluorinated aldehyde-containing prosthetic groups. *Bioconjugate Chem* **2008,** *19* (4), 951-957.

151. Lamotte, H.; Degeilh, F.; Neau, P.; Ripoche, P.; Rousseau, B., Synthesis of N-(3-Azido-4-Chlorophenyl)-N'-[H-3-Methyl] Thiourea, an Efficient Photoaffinity Probe for the Urea Carrier. *Journal of Labelled Compounds & Radiopharmaceuticals* **1994,** *34* (3), 289-295.